

For Reference

NOT TO BE TAKEN FROM THIS ROOM

Ex libris
UNIVERSITATIS
ALBERTAENSIS





Digitized by the Internet Archive
in 2020 with funding from
University of Alberta Libraries

<https://archive.org/details/Peppard1971>

THE UNIVERSITY OF ALBERTA

AUTOMATIC AND MANUAL OPTIMAL CONTROL
OF PERSONAL-VEHICLE SYSTEMS

by



LLOYD E. PEPPARD

A THESIS

SUBMITTED TO THE FACULTY OF GRADUATE STUDIES AND RESEARCH
IN PARTIAL FULFILMENT OF THE REQUIREMENTS FOR THE DEGREE
OF DOCTOR OF PHILOSOPHY

DEPARTMENT OF ELECTRICAL ENGINEERING

EDMONTON, ALBERTA

FALL, 1971

UNIVERSITY OF ALBERTA

FACULTY OF GRADUATE STUDIES AND RESEARCH

The undersigned certify that they have read, and recommend to the Faculty of Graduate Studies and Research for acceptance, a thesis entitled AUTOMATIC AND MANUAL OPTIMAL CONTROL OF PERSONAL-VEHICLE SYSTEMS submitted by Lloyd E. Peppard in partial fulfilment of the requirements for the degree of Doctor of Philosophy.

Date.....*Sept 17, 1971*.....

ABSTRACT

One possible solution to the automobile traffic congestion and high accident rates prevalent in urban areas is the development of an automated personal-vehicle system. Research which has been carried out into this and related topics is reviewed in the first part of this thesis.

The requirements of an automatic longitudinal control system for personal vehicles are outlined and several previously-developed controllers are examined. Optimal control theory is then used to design feedback controllers for two and three-vehicle type vehicle-following systems. Dynamic behaviour of these systems corresponding to different performance criteria is studied by means of analogue simulation.

The criterion for asymptotic stability of a string of vehicles is presented and it is shown that all of the optimal systems developed in this thesis are asymptotically stable. Effects of a time delay on string stability are also investigated.

A simulated vehicle-following experiment using the human operator as a link in the automatic system is capable of only slightly sub-optimal performance and has the advantage of yielding the implementation of the vehicle-following system economically feasible.

ACKNOWLEDGMENT

The author wishes to gratefully acknowledge the encouragement and valuable discussions relating to the work in this thesis provided by Professor V. Gourishankar. Assistance received from other members of the staff and students in the Department of Electrical Engineering is also acknowledged.

The work described in this thesis was carried out under support from the National Research Council of Canada whose assistance is gratefully acknowledged.

The author also wishes to thank Miss Shirley Swift for her accurate work in typing the manuscript.

TABLE OF CONTENTS

	Page
CHAPTER 1 INTRODUCTION	1
1.1 The Role of Transportation in Modern Society	2
1.2 The Requirements of an Automatic Longitudinal Control System for the Personal Vehicle	4
1.3 Background (A General Survey of Related Research)	6
1.4 Scope of the Thesis	25
References	27
CHAPTER 2 AUTOMATIC OPTIMAL CAR-FOLLOWING SYSTEMS	34
2.1 The Limitations of Conventional Traffic Flow	34
2.2 Velocity and Position Feedback in Automatic Car-Following Systems	36
2.3 A Two-Vehicle Optimal Car-Following Unit	41
2.4 A Three-Vehicle Optimal Car-Following Unit	77
2.5 Comparison of the Two and Three- Vehicle Systems	87
References	95

	Page
CHAPTER 3	
ASYMPTOTIC STABILITY OF OPTIMALLY- CONTROLLED STRINGS OF VEHICLES	96
3.1 Introduction	96
3.2 Asymptotic Stability of Three Classical Car-Following Feedback Systems	99
3.3 Asymptotic Stability of an Optimally- Controlled Vehicle String Using the Two-Vehicle Basic Unit	101
3.4 Asymptotic Stability of an Optimally- Controlled Vehicle String Using the Three-Vehicle Basic Unit	106
3.5 Effects of a Time Lag on Asymptotic Behaviour	125
3.6 Summary	128
References	132
Appendix 3-1 A Necessary and Sufficient Condition for Asymptotic Stability of Vehicle Strings	133
Appendix 3-2	136
Appendix 3-3	141
CHAPTER 4	
THE ROLE OF THE HUMAN OPERATOR IN A SEMI- AUTOMATIC CAR-FOLLOWING SYSTEM	142
4.2 Adaptive and Optimization Character- istics of the Human Operator	144

	Page
4.3 Effects of Display and Controller Characteristics on Human Operator Tracking Performance	146
4.4 A Simulated Car-Following Experiment With the Human Operator	157
4.5 Proposal of a Semi-Automatic Car- Following System	167
References	172
Appendix 4-1 Tabulation of Experimental Results	173
CHAPTER 5 CONCLUSIONS AND SUGGESTIONS FOR FUTURE RESEARCH	178
5.1 Summary of Results and Conclusions	178
5.2 Suggestions for Future Research	181

LIST OF FIGURES

		Page
FIGURE 1.1	Normalized Flow vs. Normalized Concentration for (a) Greenshields' Equation and (b) Greenberg's Equation ($c = 17.2$ m.p.h. and $k_j = 228$ cars per mi.)	11
FIGURE 1.2	Block Diagram of the Human Operator Performing Compensatory Tracking	21
FIGURE 1.3	Block Diagram of an Optimal Control Model of the Human Operator	24
FIGURE 2.1	Block Diagram of a "Relative-Motion Feedback" Car-Following System Described in the Text	37
FIGURE 2.2	Two-Vehicle Basic Car-Following Unit	41
FIGURE 2.3	Linearization of the Drag Force About the Scheduled Velocity v_s	44
FIGURE 2.4	Block Diagram of Two-Vehicle Optimal Feedback System	52
FIGURE 2.5	Analogue Simulation Diagram for Two-Vehicle Car-Following System	54
FIGURE 2.6	Analogue Simulation Diagram for Generation of Pseudo-Random Signal	56
FIGURE 2.7	Position and Velocity Error Response of the $(n+1)$ th Vehicle for a Step Change in Position Error of the n th Vehicle (System 1a)	57
FIGURE 2.8	Position and Velocity Error Response of the $(n+1)$ th Vehicle for a Step Change in Position Error of the n th Vehicle (Systems 2a, 2c and 2d)	58
FIGURE 2.9	Position and Velocity Error Response of the $(n+1)$ th Vehicle for a Step Change in Position Error of the n th Vehicle (System 4c)	60
FIGURE 2.10	Position and Velocity Error Response of the $(n+1)$ th Vehicle for a Step Change in Position Error of the n th Vehicle (System 5d)	61

FIGURE 2.11	Position and Velocity Error Response of the $(n+1)$ th Vehicle for a Step Change in Position Error of the n th Vehicle (Systems 6c and 6d)	63
FIGURE 2.12	Position and Velocity Error Response of the $(n+1)$ th Vehicle for a Step Change in Position Error of the n th Vehicle (Systems 7b and 7c)	64
FIGURE 2.13	Pseudo-Random Signals Used for the Position and Velocity Errors of the n th Vehicle for Test 2	65
FIGURE 2.14	Results of Test 2 for System 2a	67
FIGURE 2.15	Results of Test 2 for System 2c	68
FIGURE 2.16	Results of Test 2 for System 2d	69
FIGURE 2.17	Results of Test 2 for System 3a	70
FIGURE 2.18	Results of Test 2 for System 3c	71
FIGURE 2.19	Results of Test 2 for System 3d	72
FIGURE 2.20	Results of Test 2 for System 4c	73
FIGURE 2.21	Results of Test 2 for System 6d	74
FIGURE 2.22	Results of Test 2 for System 7b	76
FIGURE 2.23	Three-Vehicle Basic Car-Following Unit	78
FIGURE 2.24	Block Diagram of Three-Vehicle Optimal Feedback System	83
FIGURE 2.25	Analogue Simulation Diagram for Three-Vehicle Car-Following System	84
FIGURE 2.26	Position Error Response of the n th Vehicle (Systems 1a, 1b and 1c) to an Initial Offset in Position Error	86
FIGURE 2.27	Velocity Error Response of the n th Vehicle (Systems 1a, 1b and 1c) to an Initial Offset in Velocity Error	88
FIGURE 2.28	Velocity Error Response of the n th Vehicle (Systems 2a, 2b and 2c) to an Initial Offset in Velocity Error	89

		Page
FIGURE 2.29	Position Error Response of the nth Vehicle (Systems 3a, 3b and 3c) to an Initial Offset in Position Error	90
FIGURE 2.30	Velocity Error Response of the nth Vehicle (Systems 3a, 3b and 3c) to an Initial Offset in Position Error	91
FIGURE 2.31	Position Error Response of the nth Vehicle to Offsets in the Position Errors of the (n-1)th and (n+1)th Vehicles	93
FIGURE 3.1	A Simplified Block Diagram of the Two-Vehicle Basic Unit	102
FIGURE 3.2	Block Diagram of a Four-Vehicle String Based on the Two-Vehicle Unit	103
FIGURE 3.3	Signal Flow Graph for an Optimally-Controlled Two-Vehicle Unit	103
FIGURE 3.4	Magnitude of $G(j\omega)$ vs. Frequency for Two-Vehicle System Type 2	107
FIGURE 3.5	Magnitude of $G(j\omega)$ vs. Frequency for Two-Vehicle System Type 4	108
FIGURE 3.6	A Simplified Block Diagram of the Three-Vehicle Basic Unit	110
FIGURE 3.7	Block Diagram of a Four-Vehicle String Based on the Three-Vehicle Unit	111
FIGURE 3.8	Signal Flow Graph for a String of Four Vehicles Based on the Three-Vehicle Basic Unit	112
FIGURE 3.9	Reduced Block Diagram for the Four-Vehicle String Based on the Three-Vehicle Unit	113
FIGURE 3.10	Signal Flow Graph for an r-Vehicle String Based on the Three-Vehicle Unit	113
FIGURE 3.11	Position Errors for a Five-Vehicle String (System 1a) When the Leading Vehicle Undergoes a Step Position Error Change	117

FIGURE 3.12	Velocity Errors for a Five-Vehicle String (System 1a) When the Leading Vehicle Undergoes a Step Position Error Change	118
FIGURE 3.13	Position Errors for a Five-Vehicle String (System 1b) When the Leading Vehicle Undergoes a Step Position Error Change	119
FIGURE 3.14	Velocity Errors for a Five-Vehicle String (System 1b) When the Leading Vehicle Undergoes a Step Position Error Change	120
FIGURE 3.15	Position Errors for a Five-Vehicle String (System 1c) When the Leading Vehicle Undergoes a Step Position Error Change	121
FIGURE 3.16	Velocity Errors for a Five-Vehicle String (System 1c) When the Leading Vehicle Undergoes a Step Position Error Change	122
FIGURE 3.17	Position Errors for a Five-Vehicle String (Systems 1a and 3c) When the Leading Vehicle Undergoes a Step Position Error Change	123
FIGURE 3.18	Velocity Errors for a Five-Vehicle String (System 3c) When the Leading Vehicle Undergoes a Step Position Error Change	124
FIGURE 3.19	Block Diagram of Four-Vehicle String with Time Delays in the Control Paths	126
FIGURE 3.20	Position Error Response of the Second Vehicle in a Four-Vehicle String for Various Time Delays (System 1a)	127
FIGURE 3.21	Position Error Response of a Four-Vehicle String for a 2.5 Second Time Delay (System 1a)	127
FIGURE 3.22	Position Error Response of the Second Vehicle in a Four-Vehicle String for Various Time Delays (System 3c)	129
FIGURE 3.23	Position Error Response of a Four-Vehicle String for a 1.625 Second Time Delay (System 3c)	129

	Page
FIGURE A3-2.1 Signal Flow Graph Required to Calculate $G'(s)$	137
FIGURE A3-2.2 Signal Flow Graph Required to Calculate $\Gamma_1(s)$ and $\Gamma_2(s)$	137
FIGURE A3-2.3 Signal Flow Graph Required to Calculate $\Gamma_3(s)$ and $\Gamma_4(s)$	138
FIGURE A3-2.4 Signal Flow Graph for a Four-Vehicle String	139
FIGURE 4.1(a) Scope Display in Which Tracking Error is Proportional to Displacement of Dot From Zero	147
FIGURE 4.1(b) Meter Display in Which Tracking Error is Proportional to Displacement of Needle From Zero	147
FIGURE 4.2(a) Lever Controller	148
FIGURE 4.2(b) Knob Controller	148
FIGURE 4.3 Block Diagram for the Tracking Experiments Described in Section 4.3	150
FIGURE 4.4 Tracking Performance of Subjects A and B Using the Oscilloscope Display and Knob Controller	152
FIGURE 4.5 Tracking Performance of Subjects A and B Using the Meter Display and Knob Controller	152
FIGURE 4.6 Tracking Error Time Response of Subject B for Various Oscilloscope Display Magnifications	153
FIGURE 4.7 Tracking Performance of Subject A for Varying Knob Controller Sensitivity	155
FIGURE 4.8 Tracking Performance of Subject B for Varying Lever Controller Sensitivity	156
FIGURE 4.9 Tracking Performance of Subject B Using the Meter Display and Lever Controller	156

		Page
FIGURE 4.10	Block Diagram of the Simulated Car-Following Experiment Described in Section 4.4	159
FIGURE 4.11	Variation in Mean Squared Headway Deviation With Display Weighting Factor	160
FIGURE 4.12	Variation in Mean Squared Relative Velocity With Display Weighting Factor	160
FIGURE 4.13	Variation in Mean Squared Control Error With Display Weighting Factor	161
FIGURE 4.14	Operator and Optimal Controller Performance for $\phi = 0$	162
FIGURE 4.15	Operator and Optimal Controller Performance for $\phi = 2$	163
FIGURE 4.16	Operator and Optimal Controller Performance for $\phi = 16$	164
FIGURE 4.17	Control Errors as a Function of Time Near the Critical Value of ϕ	165
FIGURE 4.18	Diagram of Proposed Semi-Automatic Car-Following System	170
FIGURE 4.19	Overall View of Equipment Used in Tracking Experiments Reported in This Chapter	171

LIST OF TABLES

		Page
Table 1.1	A Classification of Transportation According to Distance Travelled	2
Table 1.2	Experimental Values for Optimum Velocity (c) and α_o of the Reciprocal Spacing Law	12
Table 2.1	A Summary of the Notation Used for the Motional Variables of the Two-Vehicle Unit	43
Table 2.2	Tabulation of Feedback Gains for the Two-Vehicle Unit	53
Table 2.3	Tabulation of Feedback Gains for the Three-Vehicle Unit	85
Table 3.1	Tabulation of ζ and ω_b for a String of Vehicles Based on the Two-Vehicle Unit	105
Table 4.1	Average Relative Mean Squared Errors for each Set of Four Runs Taken for a Particular Value of	161

CHAPTER 1

INTRODUCTION

1.1 The Role of Transportation in Modern Society

It is generally agreed that transportation is one of the many social and technological problems which will require a major expenditure of human and economic effort in the closing decades of the twentieth century. Until now, the development of new methods of transporting people and goods has not kept pace with the social changes which have taken place in most industrialized countries since 1900. The growing urbanization of the population of these countries has been the main cause of the decreased efficiency of existing modes of transportation. For instance it is estimated^{[1]*} that by 1990, 85% of the population of the United States will live in essentially urban areas. It should immediately be realized that in certain areas of that country, and others including Canada, this percentage will be even greater.

Gibson^[1] has divided transportation into four categories according to distance travelled with corresponding methods for moving people most efficiently. These are shown in Table 1.1. The latter two modes have received considerable attention and will in the near future be highly developed. This will result in short terminal-to-terminal transit times over long distances. The additional departure

* Numbers in [] refer to references listed at the end of the Chapter. References are listed in the order in which they appear in the text.

Distance (miles)	Mode	Average Speed (m.p.h.)
50 to 150	personal vehicle	50
75 to 750	high speed ground transportation (HSGT)	250
50 to 2500	jet plane	500
2000 to 6000	super-sonic transport (SST)	1500

Table 1.1 A Classification of Transportation
According to Distance Travelled

point-to-terminal and terminal-to-destination times will however remain relatively long unless the former two modes of transportation become more highly developed. Thus the two most important links in the overall global transportation system outlined in Table 1.1 are the development of a computer-controlled, hybrid, personal-vehicle system for intracity travel and a high speed ground transportation system (HSGT) for intercity movement. At the present time substantial effort is being made to develop HSGT systems which are technologically and economically feasible. Examples of such modern HSGT systems are San Francisco's BART system^[2], Japan's New Tokaido Line^[3] and those envisioned by several major cities around the world.

For several reasons, HSGT systems do not appear to be a complete solution to the traffic congestion problem in urban areas.

From the human standpoint, the desirability of a personal vehicle with its intrinsic convenience and flexibility cannot be denied. Unfortunately, the present-day automobile is not suited to the task of transporting large numbers of people in high-density urban areas. It is still best suited to recreational motoring for which it was originally conceived. In fact, Michaels^[4] has estimated that a single HSGT guideway is capable of a passenger flow rate which would be 15 times that of a single lane of automobile roadway. In addition, the automobile has shown itself to be relatively unsafe compared to other modes of transportation and to be the cause of much of the air and other pollution experienced in many areas. Despite these disadvantages it has been estimated^[5] that 90% of the passenger miles accumulated in the United States in 1966 was attributable to the private automobile. Hence it would appear that efforts should be directed toward the development of a personal vehicle which would have increased safety features and would cause less traffic congestion and pollution without sacrificing the attractive aspects of the automobile such as flexibility and privacy.

The problem of pollution is best solved by the elimination of the internal combustion engine used in today's automobiles. Great difficulty has been experienced in developing an alternative propulsion unit which is as compact, serviceable and which exhibits the desirable dynamic properties of the conventional engine. If a system were envisioned in which the vehicles received power from the roadway in some form, then a more satisfactory personal vehicle could be developed. The problems of reducing congestion and increasing safety of

travel are mutually opposed. If congestion is to be reduced, traffic flow rates must be increased (by increasing the average vehicle speed and concentration). This however, is likely to result in reduced safety of travel, especially in the case of the conventional automobile. Hence some form of automatic longitudinal control of the personal vehicle will be required to increase its efficiency without sacrificing safety. This subject will be pursued in some detail later in this thesis (Chapters 2 and 3).

It is also important to recognize that as a first step in improving longitudinal control of automobiles, driver-aids might be provided to supply more accurate information about the state of adjacent vehicles (such as position and velocity) to the vehicle operator. This type of system might be termed a semi-automatic or a driver-aided system. This type of system will also be considered later in this thesis (Chapter 4).

1.2 The Requirements of an Automatic Longitudinal Control System for the Personal Vehicle

The personal vehicle introduced in the previous section could take several forms depending on the requirements imposed by the environment in which it would be used. It is evident that in order to be useful under a variety of conditions the vehicle should be capable of being controlled both manually and automatically.

Regardless of the exact form of the personal-vehicle system, several requirements pertaining to its longitudinal control are fundamental. We shall assume that the vehicles operate on a single lane of roadway and that some form of lateral and steering control is provided either automatically or manually. The following set of requirements

are similar to those given by Fenton and Bender^[6] but have been somewhat enlarged upon here.

1. The system must be capable of maintaining a particular separation between adjacent vehicles. We shall term the distance from a particular point on one vehicle to the same point on the adjacent vehicle (say, the distance between the front bumpers) the headway. In order to achieve a high traffic flow rate, the headway should be made as small as possible for some fixed velocity. The requirement to maintain a scheduled headway is closely related to the requirement of maintaining zero relative velocity between adjacent vehicles.
2. Each vehicle in a string of vehicles must be stable with respect to the motion of the vehicle directly ahead. That is, bounded perturbations in the motion of one vehicle must result in bounded perturbations in the motion of the vehicle directly behind. We shall term this requirement that of *local stability*.
3. Perturbations in the motion of any vehicle in a string must be attenuated as they propagate down the string. We shall term this requirement that of *asymptotic stability*.
4. The application of large accelerating and decelerating forces to the vehicles must be limited in the interest of passenger comfort. In any case the magnitude of these forces must not exceed the capabilities of the vehicle.

The above descriptive statement of requirements will be put into mathematical form when the design of an automatic vehicle-following system is formulated in Chapter 2.

1.3 Background (A General Survey of Related Research)

Before attempting to outline the scope of this thesis, it will be useful to review in a general way the work done so far in the areas of HSGT systems, traffic models, car-following systems and studies related to the human operator as part of a vehicular control system. Further reference to certain of the above areas of research will be made in later chapters when deemed useful.

i) High Speed Ground Transportation Systems

Many of the techniques and results developed for the automatic longitudinal control of HSGT systems are applicable to the control of a more tightly coupled personal-vehicle system. Other aspects of HSGT systems will not be discussed here but can be found in the literature^[2,3,7].

The use of modern control theory to design longitudinal HSGT control systems was initiated in the United States in 1964 at the Massachusetts Institute of Technology (M.I.T.) under a directive from and supported by the United States Department of Commerce^[8]. These studies included many aspects of HSGT systems such as vehicle aerodynamics, propulsion, vehicle-guideway interactions, human factors, scheduling, network configuration, computer control, communications, and dynamics and control of vehicle groups. It is the last-mentioned category which has application to the work reported in this thesis.

An early result reported by researchers Athans and Levine at M.I.T. was concerned with the design of an optimal error regulator for a string of high-speed trains^[9,10]. The requirements of a control system for a string of trains travelling on a single, straight, level

guideway were put in the form of a quadratic cost functional and the feedback gains for the optimal error regulator solved for by use of optimal linear regulator theory. The resulting system when simulated appeared to perform in the desired manner. A scheme for merging two train systems was also investigated^[11]. This scheme made use of the optimal feedback system developed earlier for single guideway use. These error-regulating systems required the continuous transmission of the velocity and position of each vehicle to every other vehicle in the system. To simplify the communication system somewhat, sub-optimal forms of the original regulator (in which data was transmitted only between adjacent vehicles) were studied^[12]. This resulted in a reduction in the number of feedback loops required. Simulation studies indicated that the performance of the sub-optimal system was only slightly inferior to that of the optimal system. With the idea of further reducing the communication system requirements, Levis and Athans developed an optimal sampled-data control system for high-speed trains^[13]. In this system, the position and velocity of each vehicle is measured once every T seconds. The accelerating and decelerating forces applied to each vehicle are held constant during the sampling period. In general, there is a trade-off between the size of sampling period (which governs channel capacity, band-width, etc. of the communication system) and system performance.

Anderson and Powney^[14,15] have investigated the optimal sampled-data control of high-speed trains in the presence of state measurement noise and random disturbances. Use was made of the discrete form of the Kalman estimator together with an optimal sampled-

data feedback system similar to that used by Athans and Levis.

Peppard and Gourishankar^[16] have considered the addition to the cost functional of a term penalizing the system for excessive jerk or time rate of change of acceleration. The resulting system was shown to exhibit a smoother change in acceleration which is desirable for passenger comfort.

Melzer and Kuo^[17] have developed a general theory for the optimal control of linear systems comprised of infinite identical objects. The method has been applied to the case of an infinite number of trains and the structure for the control system obtained.

The research described up to this point has centred around the concept of using a *linear* optimal control system to regulate the position and velocity of each vehicle in the HSGT system. This approach requires the use of a quadratic cost functional since other forms of performance index would result in a *nonlinear* controller. A wider range of problems associated with HSGT systems is considered by Hajdu *et al.*^[18] including headway and speed control, merging, station control, and emergency procedures.

ii) Car Following and Traffic Flow Models

In order to successfully design an automatic motion control system for strings of personal vehicles, it is necessary to understand the nature of present-day traffic flow especially with regard to its limitations in the areas of flow rates and safety of travel. The study of the motion of closely-grouped strings of automobiles when no passing is permitted (single-lane traffic) can be made in two ways:

1. For long strings of vehicles, measurements can be made of the concentration (cars per unit length of roadway) and the flow rate (cars per unit time past a point on the roadway). If these measurements are made over sufficient distances (say $\frac{1}{4}$ mile) and sufficient time (say the time required for $\frac{1}{4}$ mile length of vehicles to pass a given point), a steady-state flow vs. density relation can be determined. Generally the flow rate will be zero for zero concentration and for the "jam" or bumper-to-bumper concentration, reaching a maximum for some intermediate concentration. The optimum velocity at which the maximum flow rate occurs is also of interest. From the experimental data, equations relating flow and density can be empirically postulated.
2. The second approach to the study of traffic flow is by use of car-following models. Car following is a term applied to the mode of traffic flow in which the motion of each vehicle in a string is determined by the motion of the vehicle immediately ahead. Car-following models can be tested either experimentally or by deriving the steady-state flow vs. density relation corresponding to a particular model. This relation should agree with the measurements made on actual traffic flow.

Two equations relating traffic flow and concentration which have been proposed are the following:

Greenshields' equation:

$$q = 2ck(1 - k/k_j)^{[19]} \quad (1.1)$$

Greenberg's equation:

$$q = ck \ln(k_j/k) \quad [20] \quad (1.2)$$

where q is the flow rate, c is the optimum speed at which q is a maximum, k is the concentration and k_j is the jam concentration. These two relationships are plotted in Figure 1.1 for values of $c = 17.2$ m.p.h. and $k_j = 228$ cars per mile. From experimental data taken by Greenshields^[19] and by Edie and Foote in the tunnels of New York City^[21], Greenberg's equation seems to give the best description of traffic flow.

In a car-following law, each vehicle in a string of vehicles is assumed to follow a differential-difference equation. Such a law was first proposed by Pipes^[22]. Extensions to this law by Chandler, Herman and Montroll^[23] and Gazis, Herman and Potts^[24] have resulted in a car-following law of the form

$$\ddot{z}_{n+1}(t + T) = \alpha[\dot{z}_n(t) - \dot{z}_{n+1}(t)] \quad (1.3)$$

where $\dot{z}_n(t)$ and $\dot{z}_{n+1}(t)$ are the velocities of the n th and $(n+1)$ th cars in the string, $\ddot{z}_{n+1}(t + T)$ is the acceleration of the $(n+1)$ th car at time t plus a time lag T and α is a proportionality coefficient which can either be a constant or a function of the position of the two vehicles (i.e. $\alpha = \text{constant}$ or $\alpha = \alpha_o / (z_n - z_{n+1})$). The latter value makes (1.3) nonlinear and yields a reciprocal spacing car-following model. Car-following experiments have shown the reciprocal spacing model to give the best agreement with the collected data. The assumption of $\alpha = \text{constant}$ is not very realistic since it yields a car-following law which is independent of spacing between vehicles.

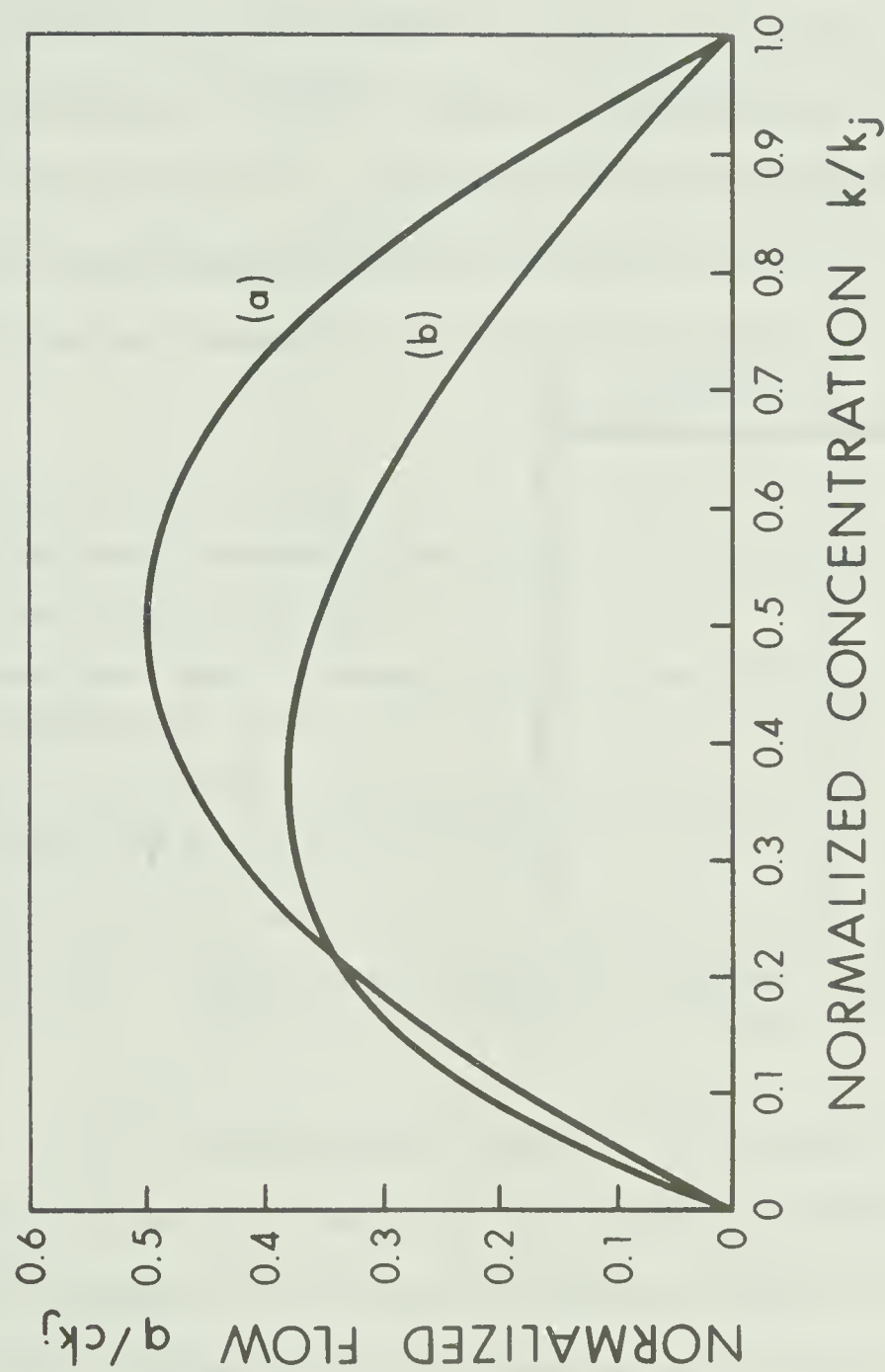


FIGURE 1.1 Normalized Flow vs. Normalized Concentration for (a) Greenshield's Equation and (b) Greenberg's Equation ($c = 17.2$ m.p.h. and $k_j = 228$ cars per mi.)

The traffic flow vs. density relation derived from the reciprocal spacing car-following model is

$$q = \alpha_o k \ln(k_j/k) \quad (1.4)$$

which is identical with Greenberg's law if α_o is set equal to c , the speed for maximum flow^[24]. Table 1.2 shows values of c obtained by Edie^[25] and values of α_o calculated from this data and from car-following experiments carried out by Gazis *et al.*^[24].

	α_o (m.p.h.)	c (m.p.h.)
Lincoln Tunnel (Edie)	20	17
Holland Tunnel (Edie)	18	15
Queens Tunnel (Edie)	22	25
GM Test Track (Gazis <i>et al.</i>)	27	-

Table 1.2 Experimental Values for Optimum Velocity (c) and α_o of the Reciprocal Spacing Law

It is interesting to observe at this point that the car-following law not only describes the *microscopic* movements of individual vehicles in the string but also by implication the *macroscopic* relationship between flow and concentration for the entire string.

The above car-following laws also give values of α and T for which a vehicle in a string will become unstable relative to the motion of the vehicle directly ahead (local instability) and for which a disturbance propagating down a string of vehicles will not be damped

out (asymptotic instability). The constant- α and the reciprocal spacing laws have been examined in this light by Herman, Montroll, Potts and Rothery^[26] and by Komitani and Susaki^[27].

For the constant- α model the condition for local stability is $\alpha T < 1/e$ and for asymptotic stability is $\alpha T < 1/2$. A typical value for the time lag T has been found to be about 1.5 seconds. Numerical analysis of the reciprocal spacing model indicates that traffic obeying this car-following law would exhibit slightly greater local and asymptotic stability.

Several other methods of modelling traffic flow have been proposed. Lee^[28] has introduced the idea of a memory function to describe the way in which a driver of a vehicle processes the information which he receives from the lead vehicle. Cosgriff^[29] has used an asymptotic approximation to a car-following law as well as introduced the use of frequency-domain (transfer function) techniques to analyze asymptotic stability. Unwin and Duckstein^[30] have used a phase plane analysis to study the stability of a reciprocal spacing type car-following model.

Gazis^[31] has suggested a variational formulation of a car-following model in which the driver attempts to minimize a function of the form

$$W = \int \{ [v - F(y)]^2 + \lambda a^2 + \mu (v - v_d)^2 \} dt \quad (1.5)$$

where $v = F(y)$ gives the desired relationship between the velocity v and the spacing y , a is the vehicle acceleration, v_d is the desired velocity and λ and μ are weighting factors. This approach seems

promising in the light of recent research into the nature of the human operator as an optimal controller. This work will be discussed further later in this chapter.

iii) Automatic Car-Following Systems

Essentially, two approaches have been taken in the development of methods to improve the characteristics of a string of automobiles. In each case the object has been to increase the flow rate on a roadway and at the same time to increase the safety of travel. One approach has been directed toward developing methods to aid the driver in his task of longitudinal control. The methods include the design of devices to collect and display information on the relative motion between the driver's vehicle and that directly ahead, as well as new control devices. The above techniques, which will be referred to as driver aids, constitute an intermediate stage between the conventional automobile and a fully-automatic vehicle. Considerable work has also been done in designing and testing fully-automatic longitudinal control systems for automobiles. Some of the more important results of this latter approach will be reviewed here.

All the systems developed so far have been designed to meet the requirements outlined in section 1.2. Hajdu *et al.*^[18] have outlined three alternative feedback schemes which will result in an automatic linear controller for regulating the position and velocity of a string of vehicles. These alternatives are:

1. Relative velocity and relative position feedback.
2. Actual velocity and relative position feedback.
3. Actual velocity and actual position feedback (measured with respect to a fixed reference).

Alternative 3 is generally undesirable since no information on the state of the vehicle directly ahead is transmitted to the following vehicle. Consequently, emergency stopping procedures could not be implemented. Alternative 1 results in a control law of the form

$$\ddot{z}_{n+1} = K_v(\dot{z}_n - \dot{z}_{n+1}) + K_d(z_n - z_{n+1} - \hat{h}) \quad (1.6)$$

where z_n and z_{n+1} are the positions of the n th (lead) and $(n+1)$ th (following) vehicles respectively, h is the desired headway and K_v and K_d are feedback gains. It can be shown that a sinusoidal disturbance in the motion of the n th vehicle will result in an increased amplitude of disturbance in the motion of the $(n+1)$ th vehicle for frequencies $\omega < (2K_d)^{\frac{1}{2}}$. This would result in asymptotic instability of a string of vehicles governed by (1.6).

Alternative 2 would result in a control law of the form

$$\ddot{z}_{n+1} = K_v(v_{n+1} - \dot{z}_{n+1}) + K_d(z_n - z_{n+1} - \hat{h}) \quad (1.7)$$

where v_{n+1} is an on-board velocity reference for the following vehicle. A string of vehicles based on control law (1.7) will be asymptotically stable for $K_v^2 \geq 2K_d$. In general a combination of alternatives 1 and 2 will result in a stable system for the proper choice of the gains K_v and K_d .

Fenton and Bender^[6,32] have considered a system with a control law

$$\ddot{z}_{n+1} = K_v(\dot{z}_n - \dot{z}_{n+1}) + K_d(\Delta h - k_1\dot{z}_n - k_2\dot{z}_{n+1}) \quad (1.8)$$

for which they have determined the conditions for asymptotic stability.

They also showed that in order to achieve high traffic flow rates, operation near the limit for asymptotic stability would be required. This is due to the vehicle time constant τ which is defined as the time required for the vehicle to reach 63.2% of its final velocity value for a command step change in velocity. This was found to range from 8 to 40 seconds. The necessary condition for asymptotic stability was shown to be $(k_1 + k_2) \geq 0.787 \tau$ and hence for operation with small intervehicular spacing (i.e. $(k_1 + k_2) < 1$), it would be necessary to reduce τ to 1 second or less. The system governed by (1.8) was tested in an actual vehicle for various values of K_v , K_d and $k = k_1 + k_2$. It was concluded that in order to achieve high flow densities and to simplify the nature of the control system, it was desirable to use only relative velocity feedback information ($K_d = 0$). The headway would then be fixed by other factors such as string velocity. When headway feedback was used, it was found that a very responsive vehicle was required and the resulting changes in velocity were detrimental to passenger comfort.

The preceding results can also be found in [33] which is a collection of results of the work done at Ohio State University concerning longitudinal control systems for automobiles. Reference to specific sections of this report will be made in later chapters of this thesis.

The longitudinal control systems developed at Ohio State University were tested by Bender and Fenton by using sinusoidal and other deterministic disturbances in the motion of the lead vehicle. In practice, disturbances generated within a string of vehicles are

stochastic in nature. The nature of the "noise" associated with vehicles attempting to maintain a constant velocity has been investigated by Montroll^[34]. Roeca^[35] has studied the response of queues of automatically controlled vehicles to various types of random disturbances. Controllers were designed to optimize queue response to these disturbances.

The results reported above do not indicate methods to measure vehicle-spacing or methods of transmitting position and velocity information between vehicles. Although this area of investigation is not related to the main topic of this thesis, it is useful to be aware that the type of detection scheme employed will to some extent govern the type of control system used and vice-versa. For example, if the headway detection is by means of sensors placed at fixed intervals along the guideway, a control system requiring continuous headway information could not be implemented.

While the automatic systems described above indicate considerable improvement in the performance of a car-following system as against the conventional automobile, these schemes cannot be implemented overnight or in a single sweep. The transition to automatic systems must be gradual and compatible at all times with the present roadway system. Hence several intermediate steps between the conventional automobile and the fully-automated personal vehicle must be developed. Even the fully-automatic vehicle will be required to operate in a manual mode on roads with light traffic. For this reason, several investigators have attempted to improve the performance of the human operator while driving a vehicle in the car-following mode.

Fenton^[36] has pointed out that the first step in the transition from the conventional automobile to an automatically controlled system of vehicles is the elimination of the accelerator-brake pedal system which is not optimal from a human-factors viewpoint. Fenton^[37] and Fenton and Montano^[38] have tested a control stick with a built-in tactile aiding device to control steering, acceleration and braking in a simulated car-following situation. The aiding device is in the form of a "finger" mounted in the head of the control stick. The outward-inward movement of the finger supplies the driver with information about headway or a linear combination of headway and relative velocity. Results indicated a substantial reduction in relative velocity and headway variance particularly for the case when both headway and relative velocity information are supplied to the driver. The above results were gained from a simulated car-following situation and were compared with those obtained using a conventional automobile. The use of a control stick appears to have the following advantages:

1. Difficulties involved in manual-to-automatic driving control and vice-versa are minimized.
2. The effective human reaction time for braking is sizeably reduced.
3. A driver aid (the tactile finger mentioned above) can be readily incorporated into the control device.

The main disadvantage of such a controller is the lack of public acceptance and this must be weighed rather heavily.

Other types of displays such as audible and visual types can be used to supply information to the driver of a conventional

automobile. Bierley^[39] used meters to supply visual information about headway or headway plus relative velocity to the driver. It was found that the latter type of display resulted in a reduced headway variability in actual car-following experiments.

The simplest form of driver aid which is currently in use is the tail-light system on the conventional automobile. Safford, Rockwell and Banasik^[40,41,42] have investigated the effect of additional information supplied to the driver of a following vehicle by the addition of lights to the rear of the leading vehicle. Effects of various colours have also been considered. Results indicate that almost any change from the current rear lighting system results in an improvement in the performance of the driver.

Krenek and Rockwell^[43] have studied the effects of changes in the automobile dynamics on a driver's longitudinal control performance. Results from actual driving tests indicate that performance can be significantly improved by matching a particular operator to a specific carburettor-accelerator linkage characteristic.

iv) The Human Operator in a Control System

The development of driver-aids as reported in the previous section has been based largely on experimental research. Since most of the experiments have been performed under actual driving conditions, the results are at once meaningful and implementable. However, it is possible that better aids could be developed by using known information concerning the characteristics of the human operator engaged in tracking tasks. A brief description of several proposed models of the human operator performing a tracking task follows.

1. Describing-function model

A continuous describing-function model of the human operator performing a compensatory tracking task is based on the assumption that the nonlinear response of the human operator can be approximated by a linear equation plus a "remnant". In compensatory tracking the operator attempts to reduce to zero the difference between a forcing function and the output of the controlled element as shown in Figure 1.2. The remnant includes all components of the operator's response which are not linearly correlated with the input. Typical of the large amount of significant research done in determining the form of the describing function model is the work of McRuer *et al.*^[44]. The Laplace transform model representing the linear portion of the operator's response in tracking systems is most often expressed in the form

$$H(s) = \frac{K e^{-\tau s} (1 + T_L s)}{(1 + T_N s)(1 + T_I s)} \quad (1.9)$$

where K = operator gain

τ = reaction time delay

T_L = lead time constant

T_N = neuromuscular lag time constant

T_I = compensatory lag time constant

This model is only a description of the input-output characteristics of the human operator and does not attempt to describe human processes. The time delay τ is 0.15 sec. \pm .03 sec. for most compensatory tracking. The neuromuscular lag T_N varies with the dynamic characteristics of the limb in relation to the controller and on the

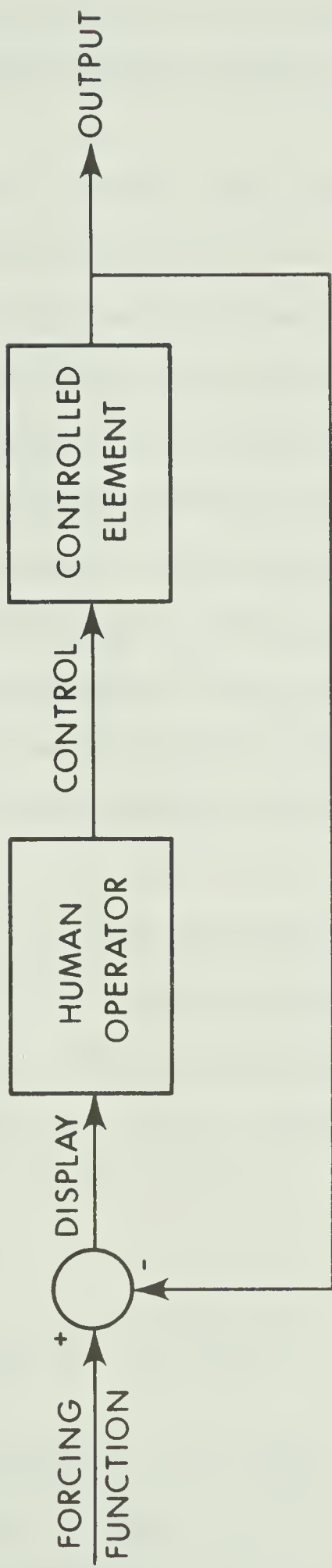


FIGURE 1.2 Block Diagram of the Human Operator Performing Compensatory Tracking

bandwidth of the signal received by the operator. Observed values range from 0.1 sec. (high bandwidth signals) to 0.5 sec. (low bandwidth signals).

The remainder of terms in $H(s)$ represent the operator's compensation for the characteristics of the controlled element and the forcing function. These terms thus vary widely from system to system and may change with time as the result of human operator learning, adaption, etc. The gain K is the human operator's primary adjustment coefficient and when tracking random-appearing signals is nearly inversely proportional to the input bandwidth (gain-bandwidth product ≈ 1.5 Hz.). As indicated above, the nature of $H(s)$ depends to a large extent on the dynamics of the controlled element. Elkind and Miller^[45] have studied the adaptive characteristics of the human operator when the controlled system is time varying.

2. Sampled-data model

Evidence of a sampling behaviour in tracking records led several investigators^[46,47] to attempt to model the human operator as a sampled-data system. Observed intermittency in the operator's response is of the order of 2 to 3 Hz. Bekey^[46] has proposed the inclusion in the linear transfer function (1.9) of a first-order hold circuit of the form

$$\left[(T_p s + 1) / T_p \right] \left[(1 - e^{-T_p s}) / s \right]^2 \quad (1.10)$$

where T_p is the sampling period. The output is initially proportional to the input at the previous sampling period and changes in proportion to the rate of change between the preceding two samples. The outputs

from this discrete model appear to approximate experimental data more closely over a wider range of input frequencies than the describing-function model described earlier. Bekey^[48] has considered an adaptive sampled-data model in which the sampling rate and gain are adjustable.

3. Optimal control models

These models assume that in a tracking task the human operator performs in a near-optimum manner with respect to some performance criterion. Blank and Schumacher^[49] represented the operator by a linear optimal feedback system with a quadratic performance index. Various optimal controllers were simulated and their performance compared with that of the human operator performing compensatory tracking. The transfer function for the optimal feedback system chosen to represent the operator was shown to approximate that given by (1.9). Another approach used by Obermayer and Muckler^[50] involved the determination of the performance index to which the system described by (1.9) is optimal. The model obtained by this inverse optimal control problem approach does not take into account the instrument-sampling behaviour, the time delay and observation limitations of the human operator.

Baron, Kleinman and Levison^[51,52,53] have proposed a mathematical model of the human operator which includes descriptions for instrument monitoring and information processing by the operator. A block diagram of the optimal model discussed in [53] is shown in Figure 1.3.

The controlled element dynamics are non-time-varying and the output of this plant is governed by the output from the manipulator

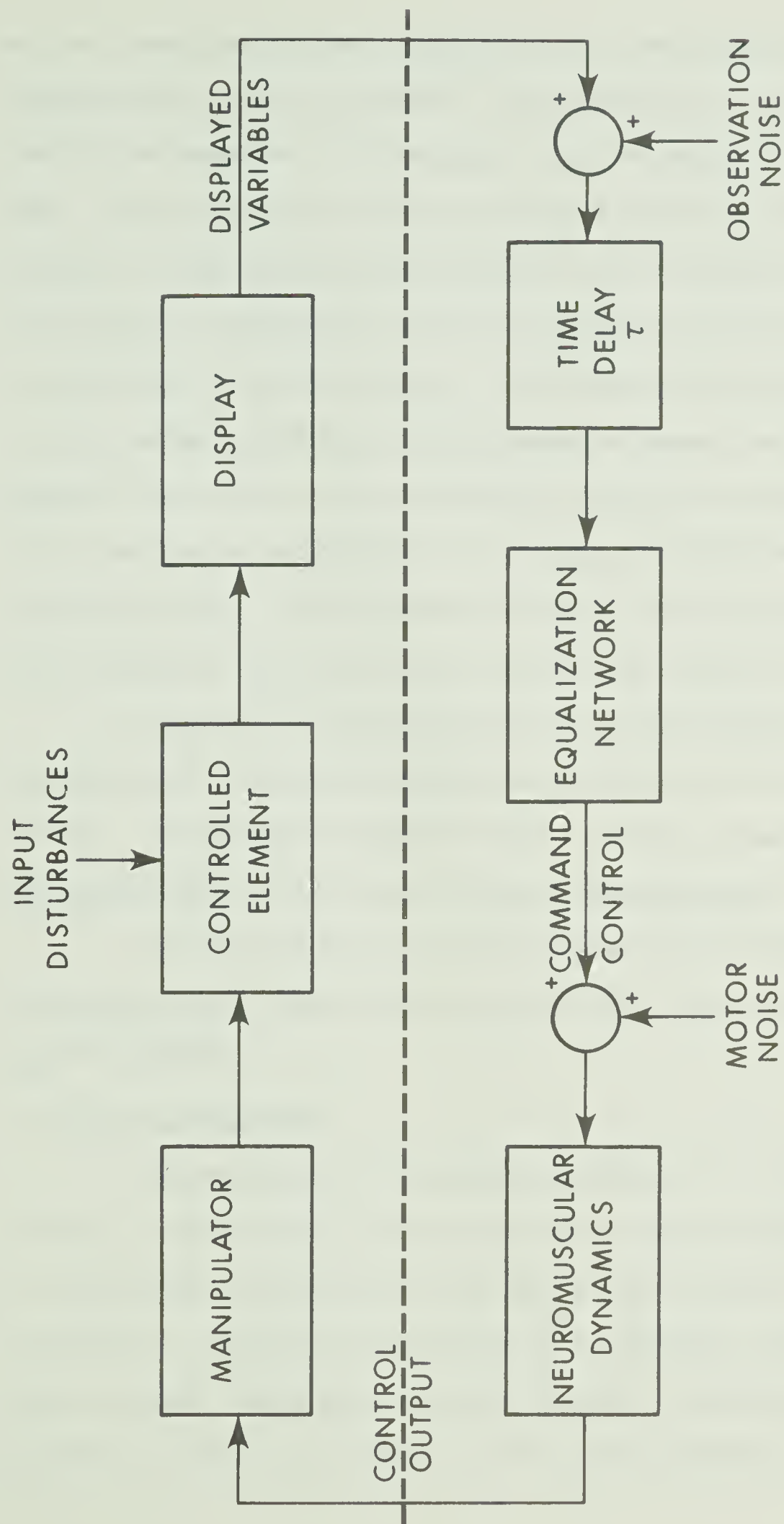


FIGURE 1.3 Block Diagram of an Optimal Control Model of the Human Operator

and the input disturbances. The latter are considered to be random (Gaussian white noise) in nature. The limitations of the human operator are modelled by a time delay τ and an additive observation noise. The equalization network includes a Kalman estimator for providing a least mean squared estimate of the displayed states in the presence of observation noise and a least mean squared predictor to compensate for the time delay τ . Also included in this block is a linear optimal controller which produces a command control output. Effects of motor noise and neuromuscular dynamics are imposed on this control before the manipulator is activated to produce an input to the controlled element. The mathematical details of the development of the components of the equalization network are described by Kleinman^[54].

Wierenga^[55] has investigated an optimal pilot model based on the above block diagram by considering the inverse filter and control problem. The frequency response of the resulting system was found to give good agreement with that determined experimentally.

Several good review articles concerning the human operator as an element in a control system can be found in the literature^[56,57,58,59].

1.4 Scope of the Thesis

The purpose of the preceding discussion was intended to put the topic of this thesis into perspective as far as the general field of automatically and manually-controlled ground transportation systems is concerned. Also, the requirements of an automatic longitudinal vehicle control system were presented in order to show the direction in which the bulk of the research in this area has been directed.

In Chapter 2, car-following behaviour of traffic and car-following models of traffic flow will be summarized. Relative velocity and headway feedback type automatic systems will be discussed with emphasis placed on the stability characteristics of vehicle strings. The optimal control approach to car following will then be introduced and compared with the more classical approach discussed earlier. Optimal control systems for two and three-vehicle type car-following will be developed and their dynamic behaviour examined and compared.

In Chapter 3, asymptotic stability of vehicle strings will be defined and the conditions for such stability obtained. Asymptotic stability of two and three-vehicle type strings will be examined in the frequency and time domains. The effect of a transport time lag on asymptotic stability will also be considered.

In Chapter 4, a semi-automatic (or driver-aided) form of the optimal system previously developed will be discussed. Experimental results obtained from simulated car-following situations will be presented. Comparison of the performance of the automatic and driver-aided systems will be made.

A summary of results and conclusions as well as suggestions for future research will be presented in Chapter 5.

REFERENCES

1. J.E. Gibson, "National Goals in Transportation", Proc. I.E.E.E., Vol. 56, No. 4, pp. 380-384, April 1968.
2. B.R. Stokes, "BART: The New Look in Rapid Transit", Proc. I.E.E.E., Vol. 56, No. 4, pp. 616-624, April 1968.
3. M. Fujii, "New Tokaido Line", Proc. I.E.E.E., Vol. 56, No. 4, pp. 625-645, April 1968.
4. E.L. Michaels, "Today's Need for Balanced Urban Transit Systems", I.E.E.E. Spectrum, Vol. 4, pp. 87-91, December 1967.
5. W.W. Seifert, "The Status of Transportation", Proc. I.E.E.E., Vol. 56, No. 4, pp. 385-395, April 1968.
6. R.E. Fenton and J.G. Bender, "A Study of Automatic Car Following", I.E.E.E. Trans. Vehicular Technology, Vol. VT-18, pp. 134-140, November 1969.
7. Y. Shirai and Y. Ishihara, "Teito Rapid Transit Authority's Automatic Train Operation", Proc. I.E.E.E., Vol. 56, No. 4, pp. 605-615, April 1968.
8. R.J. Hansen, "Planning for High-Speed Ground Transportation", Proc. I.E.E.E., Vol. 56, No. 4, pp. 472-486, April 1968.
9. W.S. Levine, "On the Linear Optimal Control of a String of Moving Vehicles", M.Sc. Thesis, M.I.T., May 1965.
10. W.S. Levine and M. Athans, "On the Optimal Error Regulation of a String of Moving Vehicles", I.E.E.E. Trans. Auto. Control, Vol. AC-11, pp. 355-361, July 1966.

11. M. Athans, "Applications of Optimal Control to High-Speed Ground Transportation Problems", Sixth Allerton Conference on Circuit and System Theory, Monticello, Ill., Oct. 1968.
12. M. Athans, W.S. Levine and A.H. Levis, "On the Optimal and Sub-optimal Position and Velocity Control of a String of High-Speed Moving Trains", ESL-R-291, Electronic Systems Laboratory, M.I.T., Cambridge, Mass. November 1966.
13. A.H. Levis and M. Athans, "On the Optimal Sampled Data Control of Strings of Vehicles", Transportation Science, Vol. 1, pp. 362-382.
14. E.T. Powner, J.H. Anderson and G.H. Qualtrough, "Optimal Digital Computer Control of Cascaded Vehicles in High-Speed Transportation Systems", Transportation Research, Vol. 3, pp. 101-113, 1969.
15. J.H. Anderson and E.T. Powner, "Optimal Digital Computer Control of Cascaded Vehicles in High-Speed Transportation Systems in the Presence of Measurement Noise and Stochastic Input Disturbances", Transportation Research, Vol. 4, pp. 185-198, 1970.
16. L.E. Peppard and V. Gourishankar, "Optimal Control of a String of Moving Vehicles", I.E.E.E., Trans. Auto.Control, Vol. AC-15, pp. 386-387, June 1970.
17. S.M. Melzer and B.C. Kuo, "Optimal Regulation of Systems Described by a Countably Infinite Number of Objects", to be published.

18. L.P. Hajdu, K.W. Gardiner, H. Tamura and G.L. Pressman, "Design and Control Considerations for Automated Ground Transportation Systems", Proc. I.E.E.E., Vol. 56, No. 4, pp. 493-513, April 1968.
19. B.D. Greenshields, "A Study of Traffic Capacity", Proc. Highway Research Board, Vol. 14, p. 468, 1935.
20. H. Greenberg, "An Analysis of Traffic Flow", Ops. Res., Vol. 7, pp. 79-85, 1959.
21. L.C. Edie and R.S. Foote, "Traffic Flow in Tunnels", Proc. Highway Research Board, Vol. 37, pp. 334-444, 1958.
22. L.A. Pipes, "An Operational Analysis of Traffic Dynamics", J. Appl. Phys., Vol. 24, pp. 274-281, 1953.
23. R.E. Chandler, R. Herman and E.W. Montroll, "Traffic Dynamics: Studies in Car Following", Ops. Res., Vol. 6, pp. 165-184, 1958.
24. D.C. Gazis, R. Herman and R.B. Potts, "Car-Following Theory of Steady-State Traffic Flow", Ops. Res., Vol. 7, pp. 499-505, 1959.
25. L.C. Edie, "Car-Following and Steady-State Theory for Non-Congested Traffic", Ops. Res., Vol. 9, pp. 66-76, 1961.
26. R. Herman, E.W. Montroll, R.B. Potts and R.W. Rothery, "Traffic Dynamics: Analysis of Stability in Car Following", Ops. Res., Vol. 7, pp. 86-106, 1959.
27. E. Kometani and T. Sasaki, "On the Stability of Traffic Flow", J. Ops. Res. (Japan), Vol. 2, pp. 11-26, 1958.

28. G. Lee, "A Generalization of Linear Car-Following Theory", *Ops. Res.*, Vol. 14, pp. 595-606, 1966.
29. R.L. Cosgriff, "The Asymptotic Approach to Traffic Dynamics", *I.E.E.E. Trans. Systems Science and Cybernetics*, Vol. SSC-5, pp. 361-368, October 1969.
30. E.A. Unwin and L. Duckstein, "Stability of Reciprocal-Spacing Type Car-Following Models", *Transp. Sc.*, Vol. 1, No. 2, pp. 95-108, 1967.
31. D.C. Gazis, "Control Problems in Automobile Traffic", *Proc. I.B.M. Scientific Computing Symposium (Control Theory and Applications)*, pp. 171-187, 1964.
32. R.E. Fenton and J.G. Bender, "A Study of Automatic Car Following", *Nineteenth I.E.E.E. VTG Conference*, San Francisco, December 1968.
33. "Theory and Design of Longitudinal Control Systems for Automobiles", *Ohio State University Report PB 172 996*, September 1965.
34. E.W. Montroll, "Acceleration Noise and Clustering Tendency of Vehicular Traffic", in *"Theory of Traffic Flow"*, Elsevier Publ. Co., 1961, pp. 147-157.
35. W. Roeca, "Design of an Automobile Controller for Optimum Traffic Response to Stochastic Disturbances", *Ph.D. Thesis*, Ohio State University, Columbus, Ohio, 1965.
36. R.E. Fenton, "Automatic Vehicular Guidance and Control - A State of the Art Survey", *I.E.E.E. Trans. Vehicular Technology*, Vol. VT-19, pp. 153-161, February 1970.

37. R.E. Fenton, "An Improved Man-Machine Interface for the Driver-Vehicle System", I.E.E.E. Trans. Human Factors, Vol. HFE-7, pp. 150-157, December 1966.
38. R.E. Fenton and W.B. Montano, "An Intervehicular Spacing Display for Improved Car-Following Performance", I.E.E.E. Trans. Man-Machine Systems, Vol. MMS-9, pp. 29-35, June 1968.
39. R.L. Bierley, "Investigation of an Intervehicle Spacing Display", Highway Research Record, No. 25, pp. 58-75, 1963.
40. R.R. Safford, R.H. Rockwell and R.C. Banasik, "The Effects of Automotive Rear Signal System Characteristics on Driving Performance", Ohio State University Internal Report obtained by private communication.
41. T.H. Rockwell and R.C. Banasik, "Experimental Highway Testing of Alternative Vehicle Rear Lighting Systems", The Ohio State University Research Foundation, Columbus, Ohio, 1968.
42. T.H. Rockwell, R.R. Safford, R.C. Banasik and F.L. Brachman, "An Index and Bibliography of Literature Pertinent to Vehicle Rear Lighting", Ohio State University, Systems Research Group, April 1968.
43. R.F. Krenek and T.H. Rockwell, "Aiding by Longitudinal Control Dynamics Changes in the Automobile", Ohio State University, Systems Research Group, Report No. EES 277B-2, June 1968.
44. D.T. McRuer, D. Graham, E. Krendel and W. Reisener, "Human Pilot Dynamics in Compensatory Systems", Wright-Patterson AFB, AFFDL-TR-65-15, July, 1965.

45. J.I. Elkind and D.C. Miller, "Adaptive Characteristics of the Human Controller of Time Varying Systems", Wright-Patterson AFB, AFFDL-TR-66-60, December 1967.
46. G.A. Bekey, "The Human Operator as a Sampled Data System", I.R.E. Trans. Human Factors in Electronics, Vol. HFE-3, pp. 43-51, September 1962.
47. G.W. Lange, "Representation of the Human Operator as a Sampled Data System", Proc. I.E.E., Vol. 115, No. 2, February 1968.
48. G.A. Bekey, "Adaptive Control Models of the Human Operator", pp. 203-217 in "Adaptive Control Systems", MacMillan Co., 1963.
49. G.L. Blank and P.J. Schumacker, "The Human Operator as an Optimal Controller", Sixth Allerton Conference on Circuit and System Theory, Monticello, Ill., October 1968.
50. R.W. Obermayer and F.A. Muckler, "On the Inverse Optimal Control Problem in Manual Control Systems", I.E.E.E. Int. Convention Record 1965, Part 6 (Human Factors), New York, March 1965.
51. S. Baron and D.L. Kleinman, "The Human Operator as an Optimal Controller and Information Processor", I.E.E.E. Trans. Man-Machine Systems, Vol. MMS-10, pp. 9-17, March 1969.
52. S. Baron and D.L. Kleinman, "The Human as an Optimal Controller and Information Processor", NASA Report CR-1151, September 1968.

53. D.L. Kleinman, S. Baron and W.H. Levison, "An Optimal Model of Human Response", Automatica, Vol. 6, pp. 357-383, 1969.
54. D.L. Kleinman, "Optimal Control of Linear Systems with Time Delay and Observation Noise", I.E.E.E. Trans. Auto. Control, Vol. AC-14, pp. 524-527, October 1969.
55. R.D. Wierenga, "An Evaluation of a Pilot Model Based on Kalman Filtering and Optimal Control", I.E.E.E. Trans. Man-Machine Systems, Vol. MMS-10, pp. 108-117, December 1969.
56. R.G. Costello and T.J. Higgins, "An Inclusive Classified Bibliography Pertaining to Modeling the Human Operator as an Element in an Automatic Control System", I.E.E.E. Trans. Human Factors in Electronics, Vol. HFE-7, pp. 174-181, December 1966.
57. D. McRuer and D.H. Weir, "Theory of Manual Vehicular Control", I.E.E.E. Trans. Man-Machine Systems, Vol. MMS-10, pp. 257-289, December 1969.
58. J.I. Elkind, "A Survey of the Development of Models for the Human Controller", pp. 623-645, in "Progress in Astronautics and Aeronautics", Vol. 13, 1964.
59. C.R. Kelley, "Manual and Automatic Control", John Wiley and Sons Inc., 1968.

CHAPTER 2

AUTOMATIC OPTIMAL CAR-FOLLOWING SYSTEMS

2.1 The Limitations of Conventional Traffic Flow

In Chapter 1 it was shown that once the motion of an individual vehicle in a string with respect to the vehicle directly ahead is described by a mathematical model, then the flow vs. density characteristics of the string of vehicles can accurately be predicted. In other words, the microscopic properties of the individual vehicles in the string determine its macroscopic behaviour. The above is true only if each vehicle in the string is exhibiting car-following behaviour (that is, its motion is affected only by that of the preceding vehicle). If a gap between two vehicles becomes large enough, the coupling between them will become negligible and the motion of the trailing vehicle will be governed by factors other than the motion of the leading vehicle such as the maximum allowable speed, the road conditions, etc.

The car-following models discussed in Chapter 1 are based on the idea that a driver of a vehicle responds to a stimulus according to the relation

$$\text{Driver response} = \text{Driver sensitivity} \times \text{Stimulus}$$

The reciprocal spacing model of Gazis, Herman and Potts^[1] is given by

$$\ddot{z}_{n+1}(t+T) = \left[\frac{\alpha_0}{z_n(t) - z_{n+1}(t)} \right] \left[\dot{z}_n(t) - \dot{z}_{n+1}(t) \right] \quad (2.1)$$

where $z_n(t)$ and $z_{n+1}(t)$ are the positions of the n th (leading) and $(n+1)$ th (trailing) vehicles respectively, T is a time lag and dots denote differentiation with respect to time. The response of the driver is thus in the form of an acceleration; the sensitivity varies inversely with the spacing between vehicles; and the stimulus is the relative velocity between the two vehicles.

It has been shown^[2,3] that the condition for the local stability of a vehicle string using the linear car-following model

$$\ddot{z}_{n+1}(t+T) = \alpha[\dot{z}_n(t) - \dot{z}_{n+1}(t)] \quad (2.2)$$

is $\alpha T < 1/e$ where α and T are defined earlier and e is the Napierian base. For the nonlinear model of (2.1), the condition for local stability of the vehicle string can be assumed to be very nearly the same. An approximate value of the lower limit for the headway between adjacent vehicles in a locally stable string is obtained by equating the sensitivity terms in (2.1) and (2.2) with $\alpha T = 1/e$. This minimum headway is then

$$z_n(t) - z_{n+1}(t) = \frac{\alpha_0}{\alpha} = \alpha_0 T e \quad (2.3)$$

From Chapter 1 we recall typical values for α_0 and T to be 20 m.p.h. and 1.5 seconds respectively which when substituted into (2.3) yields a minimum headway of 44 feet. Allowing say 14 feet for the length of each vehicle, this would correspond to a separation of about 30 feet between vehicles. Thus it is evident that both the flow rate and safety of travel are limited by the driver's sensitivity and the effective time lag T . Two main objectives in designing an automatic car-following system are thus to regulate the motion of a string of vehicles

so that intervehicular spacing can be small (this would increase the flow rate) and to ensure that the string is stable under this condition (this would increase the safety of travel). Depending on the propulsion-guideway system employed, an automatic system could also be made to reduce the air and noise pollution to levels lower than now existing (for example, if an electric propulsion system was employed).

2.2 Velocity and Position Feedback in Automatic Car-Following Systems

Before discussing the nature of the optimal feedback system proposed in this thesis, it is useful to look at some general characteristics of automatic car-following systems. As was shown in Chapter 1 there are two basic alternatives as far as the feedback of information from one vehicle to another is concerned. The first of these we shall term a "relative-motion feedback" type system which results in a control law of the form

$$\ddot{z}_{n+1} = K_v(\dot{z}_n - \dot{z}_{n+1}) + K_d(z_n - z_{n+1} - \hat{h}) \quad (2.4)$$

where z_n and z_{n+1} are the positions of two adjacent vehicles in a string of vehicles, \hat{h} is the desired headway (front bumper-to-front bumper distance) and K_v and K_d are gain factors. The subscript n refers to the leading vehicle and $n+1$ to the trailing vehicle. The resulting feedback system is shown in Figure 2.1.

By differentiating (2.4) with respect to time and taking the Laplace transform we get (for zero initial conditions for the variables)

$$s^3 Z_{n+1}(s) = s^2 K_v [Z_n(s) - Z_{n+1}(s)] + s K_d [Z_n(s) - Z_{n+1}(s)] \quad (2.5)$$

From (2.5) we obtain the transfer function

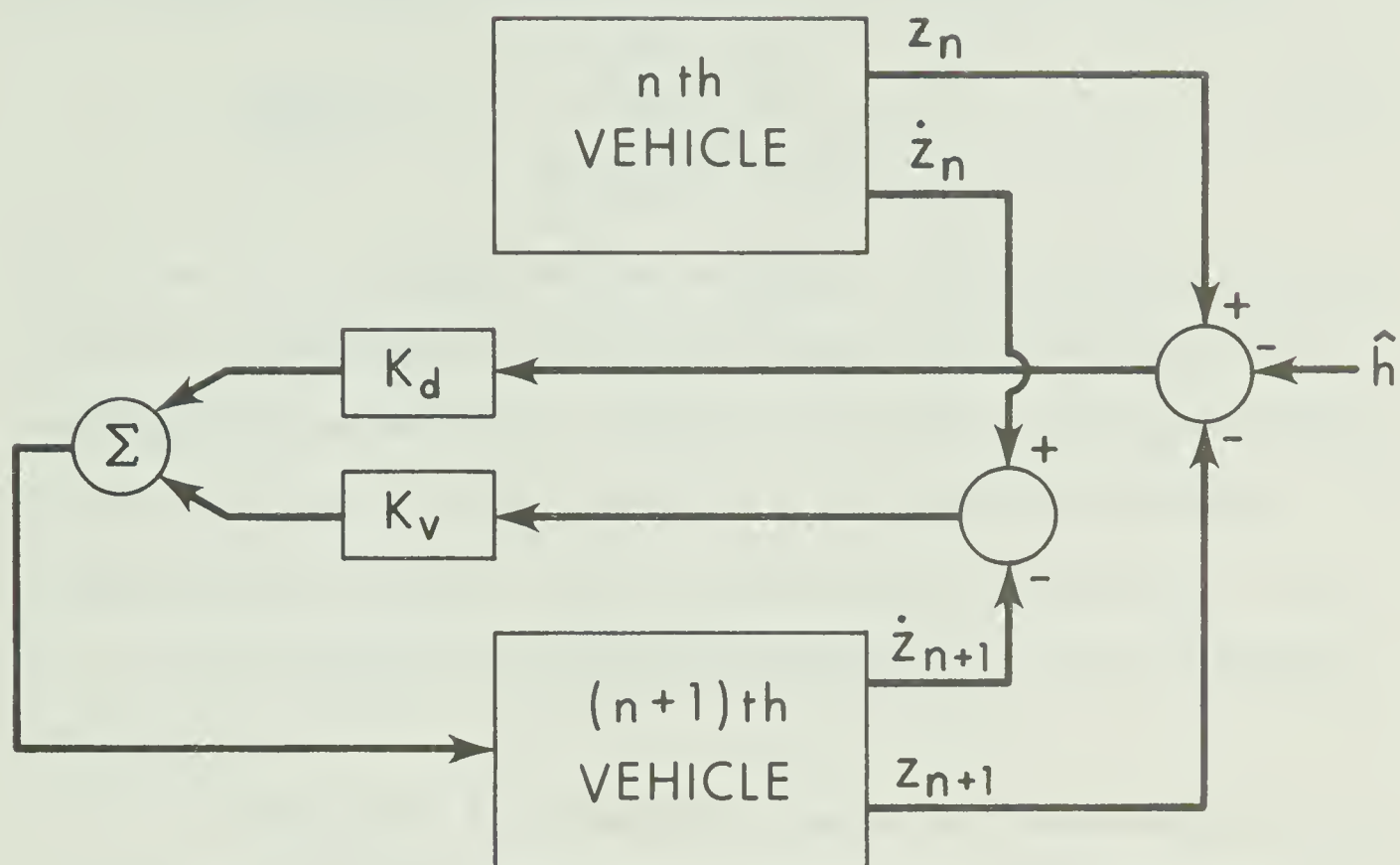


FIGURE 2.1 Block Diagram of a "Relative-Motion Feedback" Car-Following System Described in the Text

$$\frac{Z_{n+1}(s)}{Z_n(s)} = \frac{s(K_d + K_v s)}{s(s^2 + K_v s + K_d)} \quad (2.6)$$

For frequency response studies we let $s = j\omega$ and write (2.6) as

$$\frac{|Z_{n+1}(\omega)|}{|Z_n(\omega)|} = \left[\frac{K_d^2 + K_v^2 \omega^2}{(K_d^2 - \omega^2)^2 + K_v^2 \omega^2} \right]^{\frac{1}{2}} \quad (2.7)$$

Note that if the leading vehicle undergoes a periodic disturbance in position, the magnitude of this disturbance will be amplified by the trailing vehicle for $0 < \omega < (2K_d)^{\frac{1}{2}}$. If all pairs of adjacent vehicles in the string exhibited such behaviour, the system would become asymptotically unstable. For the special cases for which $K_d = 0$ and $K_v = 0$, the system will be asymptotically stable for all frequencies of disturbance.

Alternative 2 of Chapter 1, namely the scheme which involves the feedback of relative position only, results in a control law of the form

$$\ddot{z}_{n+1} = K_v(v_s - \dot{z}_{n+1}) + K_d(z_n - z_{n+1} - \hat{h}) \quad (2.8)$$

where v_s is a fixed on-board velocity reference for the trailing vehicle

For this case, the transfer function corresponding to (2.6) is

$$\frac{Z_{n+1}(s)}{Z_n(s)} = \frac{K_d}{s^2 + K_v s + K_d} \quad (2.9)$$

which can be written in the standard form

$$\frac{Z_{n+1}(s)}{Z_n(s)} = \frac{\omega_o^2}{s^2 + 2\zeta\omega_o s + \omega_o^2} \quad (2.10)$$

where ω_o is the resonant frequency and ζ is the damping factor. In this case the system will be asymptotically stable for periodic disturbances in the motion of the leading vehicle for

$$\zeta = \frac{K_v}{2(K_d)^{1/2}} \geq 0.7072 \quad (2.11)$$

The control law tested by Fenton and Bender^[4] is

$$\ddot{z}_{n+1} = K_v(\dot{z}_n - \dot{z}_{n+1}) + K_d(\Delta h - k_1\dot{z}_n - k_2\dot{z}_{n+1}) \quad (2.12)$$

where Δh is the incremental change in the headway between vehicles ($\Delta h = z_n - z_{n+1} - \hat{h}$). For this system, the transfer function is given by

$$\frac{Z_{n+1}(s)}{Z_n(s)} = \frac{K_d + s(K_v - K_d k_1)}{s^2 + s(K_v + K_d k_2) + K_d} \quad (2.13)$$

which can be written as

$$\frac{Z_{n+1}(s)}{Z_n(s)} = \frac{(\frac{1}{\beta\omega_o}s + 1)}{\frac{s^2}{\omega_o^2} + \frac{2\zeta}{\omega_o}s + 1} \quad (2.14)$$

$$\text{where } \omega_o^2 = K_d, \quad \beta\omega_o = \frac{K_d}{K_v - K_d k_1} \quad \text{and} \quad \frac{2\zeta}{\omega_o} = \frac{K_v + K_d k_2}{K_d}.$$

It can be shown that this system will exhibit asymptotic stability for periodic disturbances in the motion of the leading vehicle for

$$[\zeta^2 - (\frac{1}{2\beta})^2]^{1/2} \geq 0.7072 \quad (2.15)$$

This is clearly an improvement over the control law in alternative 1 where asymptotic stability was frequency-dependent.

The above examples of control strategies for an automatic car-following system give some indication of the effect of velocity and/or position feedback on the behaviour of a controlled vehicle in a system of two vehicles in a car-following mode. In the remaining sections of this chapter a different approach will be presented to determine the control strategy and nature of the feedback information supplied to the controlled vehicle. This approach will involve the solution of an "optimal control problem". The performance index to be minimized will be chosen so as to reflect the requirements outlined in Chapter 1 for an ideal personal-vehicle control system.

The optimal control problem will be formulated in two ways. First, a string of vehicles will be considered to consist of overlapping units of two vehicles each. In each unit, the trailing vehicle will be the "controlled vehicle" and the leading vehicle will be the "controlling vehicle" in the sense that changes in its motion will affect the trailing vehicle but not vice-versa. An optimal controller will be derived for the trailing vehicle of this two-vehicle unit and the dynamic performance of the unit will be studied for a variety of cost functionals to evaluate the merits of several different feedback schemes.

The optimal control problem will then be formulated using a basic unit of three consecutive vehicles in a string. The middle vehicle will be the "controlled vehicle" in this case. Its motion will be affected by the motion of the vehicles directly ahead and behind. The optimal controller for the middle vehicle will be derived and the dynamic performance of the three-vehicle unit will be studied and compared with that of the two-vehicle unit.

The application of the control strategies developed for both the two and three-vehicle units to a string of many vehicles will be pursued in the following chapter. The asymptotic stability characteristics of these strings will also be considered at that time.

2.3 A Two-Vehicle Optimal Car-Following Unit

2.3.1 Mathematical Development

The following will describe the design of an optimal controller for a basic unit consisting of two adjacent vehicles in a string (say the n th and $(n+1)$ th vehicles).

The n th vehicle is the "leading" vehicle and the $(n+1)$ th is the "following" vehicle. The basic unit is shown in Figure 2.2 .

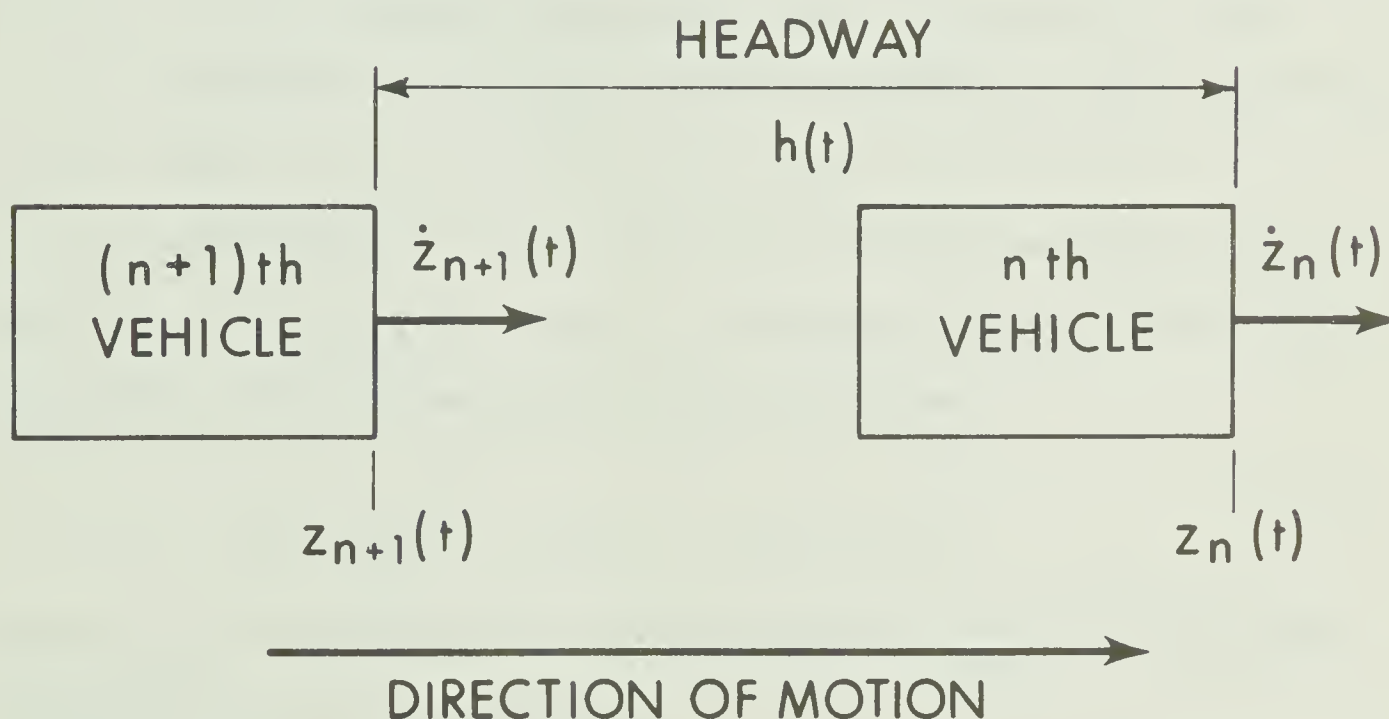


FIGURE 2.2 Two-Vehicle Basic Car-Following Unit

The following assumptions apply to the two vehicles in question:

1. Both vehicles have identical dynamics (weight, drag, acceleration and deceleration characteristics).
2. Both vehicles are operating on a single lane of straight and level roadway. (Since we are attempting to control only longitudinal motion we must assume some other system is available for lateral control).
3. The two vehicles are operating under steady state conditions and undergo small perturbations in velocity about a desired velocity v_s .
4. The motion of the leading vehicle is random in nature (zero-mean, Gaussian, white noise) and is the result of driver inattentiveness, road surface irregularities, wind variations, etc.

The notation to be used for the motional variables of the two vehicles is outlined in Table 2.1. The motion of the $(n+1)$ th vehicle is described by the following differential equation:

$$m_{n+1} \ddot{z}_{n+1}(t) = f_{n+1}(t) - d_{n+1}(\dot{z}_{n+1}; t) \quad (2.16)$$

where m_{n+1} is the mass of the $(n+1)$ th vehicle, $f_{n+1}(t)$ is the applied force and d_{n+1} is the drag force.

The drag force on a vehicle is generally a function of the square of the vehicle velocity plus some rolling friction as given by

$$d(\dot{z}; t) = f_r + \mu_d \dot{z}^2(t) \quad (2.17)$$

Variable	nth (leading) vehicle	(n+1)th (following) vehicle
position	$z_n(t)$	$z_{n+1}(t)$
velocity	$\dot{z}_n(t)$	$\dot{z}_{n+1}(t)$
scheduled velocity	v_s	v_s
scheduled position at time t	$\hat{z}_n(t) = v_s t + \hat{z}_n(0)$	$\hat{z}_{n+1}(t) = v_s t + \hat{z}_{n+1}(0)$
scheduled headway	$\hat{h} = \hat{z}_n(0) - \hat{z}_{n+1}(0)$	

Table 2.1 A Summary of the Notation Used for the Motional Variables of the Two-Vehicle Unit

where f_r is the rolling friction and μ_d is the drag coefficient. Since we have assumed that variations from the scheduled velocity v_s are small, we can linearize the drag force about v_s according to the following relation:

$$d_{n+1}(\dot{z}_{n+1}; t) = d_{n+1}(v_s) + \bar{\mu}[\dot{z}_{n+1}(t) - v_s] \quad (2.18)$$

where $\bar{\mu}$ is a linear drag coefficient. This linearization is illustrated in Figure 2.3.

We proceed now to define the "error" states of the (n+1)th vehicle.

$$x_{n+1,1}(t) = z_{n+1}(t) - \hat{z}_{n+1}(t) \quad (2.19)$$

$$x_{n+1,2}(t) = \dot{x}_{n+1,1}(t) = \dot{z}_{n+1}(t) - v_s \quad (2.20)$$

We can now rewrite (2.16) as

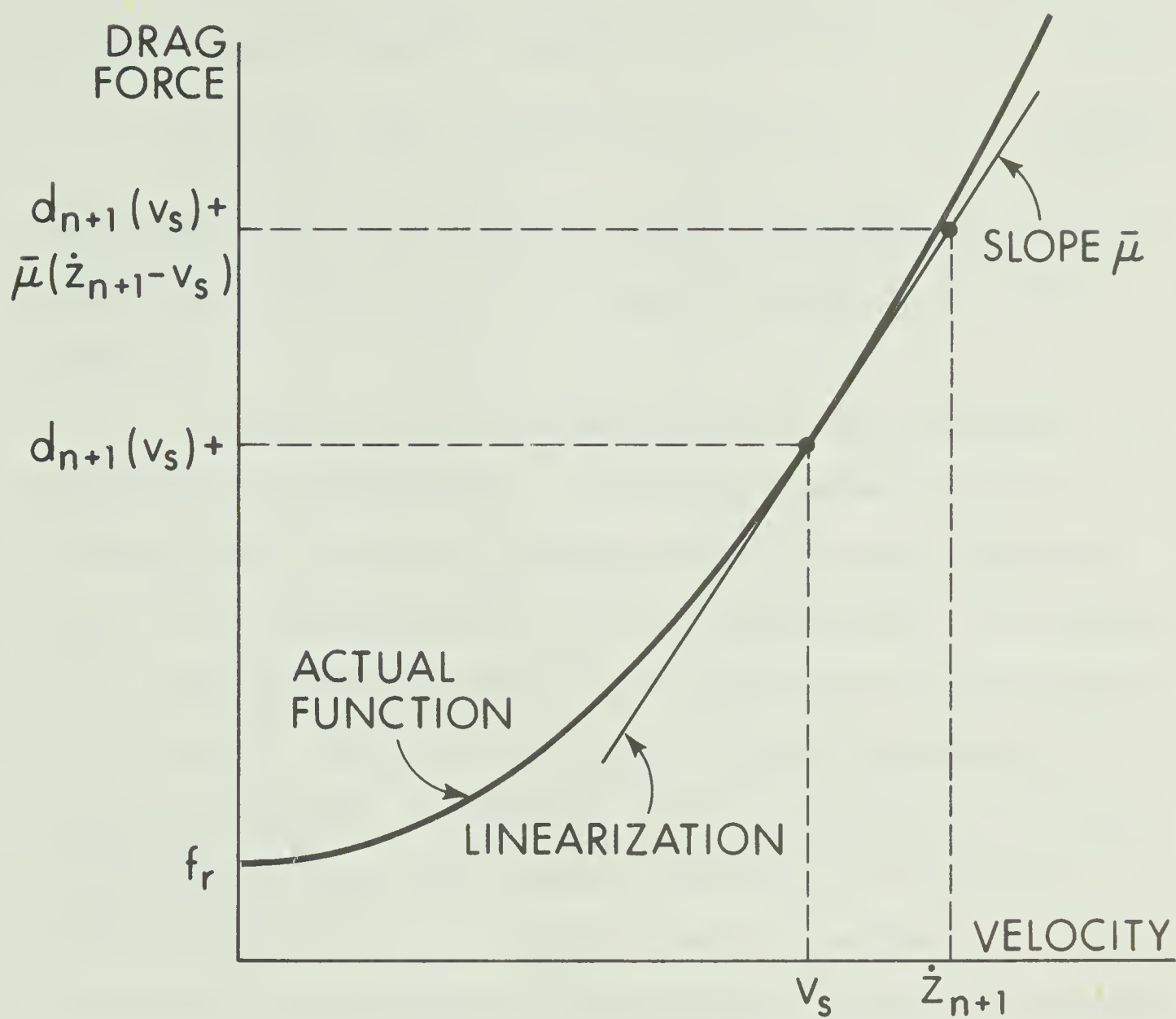


FIGURE 2.3 Linearization of the Drag Force About the Scheduled Velocity v_s

$$m_{n+1} \ddot{z}_{n+1}(t) = [f_{n+1}(t) - d_{n+1}(v_s)] - \bar{\mu} [\dot{z}_{n+1}(t) - v_s] \quad (2.21)$$

Setting $u_{n+1}(t) = f_{n+1}(t) - d_{n+1}(v_s)$, we can write

$$m_{n+1} \dot{x}_{n+1,2}(t) = u_{n+1}(t) - \bar{\mu} x_{n+1,2}(t) \quad (2.22)$$

We can term $u_{n+1}(t)$, the difference between the applied force and the drag force at velocity v_s , as the "control" applied to the $(n+1)$ th vehicle.

The term $u_{n+1}(t)$ represents the force that is actually applied to the $(n+1)$ th vehicle. In practice, however, it must be remembered that a propulsion system is present on each vehicle and $u_{n+1}(t)$ is the desired output of this propulsion system. The dynamics of the $(n+1)$ th vehicle as used in this thesis do not include the propulsion system. The input received by the propulsion system is in practice say $u'_{n+1}(t)$. For purposes of this discussion, we will assume that either the input-output transfer function of the propulsion system is unity (i.e. $u_{n+1} = u'_{n+1}$) or equal to σ so that $u_{n+1} = \sigma u'_{n+1}$. In any case, in the remainder of this discussion we shall be concerned with u_{n+1} only.

Equations similar to (2.19) and (2.22) can be written for the n th vehicle. The state equations for the two-vehicle unit can then be written as

$$\begin{aligned} \dot{x}_{n1}(t) &= x_{n2}(t) \\ \dot{x}_{n2}(t) &= -\frac{\bar{\mu}}{m} x_{n2}(t) + \frac{u_n(t)}{m} \\ \dot{x}_{n+1,1}(t) &= x_{n+1,2}(t) \\ \dot{x}_{n+1,2}(t) &= -\frac{\bar{\mu}}{m} x_{n+1,2}(t) + \frac{u_{n+1}(t)}{m} \end{aligned} \quad (2.23)$$

which when written in matrix form become

$$\dot{\underline{x}}(t) = \underline{A} \underline{x}(t) + \underline{B} \underline{u}(t) \quad (2.24)$$

where

$$\underline{A} = \begin{bmatrix} 0 & 1 & 0 & 0 \\ 0 & -\frac{\mu}{m} & 0 & 0 \\ 0 & 0 & 0 & 1 \\ 0 & 0 & 0 & -\frac{\mu}{m} \end{bmatrix} \quad \underline{B} = \begin{bmatrix} 0 & 0 \\ \frac{1}{m} & 0 \\ 0 & 0 \\ 0 & \frac{1}{m} \end{bmatrix}$$

$$\underline{x} = \begin{bmatrix} x_{n1} \\ x_{n2} \\ x_{n+1,1} \\ x_{n+1,2} \end{bmatrix} \quad \text{and} \quad \underline{u} = \begin{bmatrix} u_n \\ u_{n+1} \end{bmatrix} \quad (2.25)$$

The objectives of an automatic car-following system as outlined in Chapter 1 can now be put in the form of a quadratic cost functional of the form

$$J = \int_0^{\infty} \{ \alpha [x_{n1}(t) - x_{n+1,1}(t)]^2 + \beta [x_{n2}(t) - x_{n+1,2}(t)]^2 \\ + \rho_1 x_{n1}^2(t) + \rho_2 x_{n2}^2(t) + \rho_3 x_{n+1,1}^2(t) + \rho_4 x_{n+1,2}^2(t) \\ + \gamma_1 u_n^2(t) + \gamma_2 u_{n+1}^2(t) \} dt \quad (2.26)$$

where $\alpha, \beta, \rho_1, \rho_2, \rho_3, \rho_4, \gamma_1$ and γ_2 are non-negative weighting factors. This cost functional can be interpreted as follows:

1. Since the term $(x_{n1} - x_{n+1,1}) = z_n(t) - z_{n+1}(t) - [\hat{z}_n(t) - \hat{z}_{n+1}(t)] = h(t) - \hat{h}$ where $h(t)$ is the headway

- at time t , the inclusion of the first term in (2.26) penalizes the system for deviations of the actual headway from the desired headway.
2. The term $(x_{n2} - x_{n+1,2}) = \dot{z}_n(t) - \dot{z}_{n+1}(t)$ which is the relative velocity between the two vehicles. Thus the inclusion of the second term in (2.26) penalizes the system for deviations from zero of the relative velocity.
 3. The next four terms in (2.26) serve to penalize the system for deviations of the position and velocity of both vehicles from their desired values.
 4. The last two terms are the square of the forces applied to the two vehicles and hence are proportional to the energy input to the respective vehicles. Thus the inclusion of these two terms in (2.26) serves to penalize the system for application of large accelerating and decelerating forces which could result in passenger discomfort.

The cost functional (2.26) can be rewritten as

$$J = \int_0^{\infty} [\underline{x}^T(t) \underline{Q} \underline{x}(t) + \underline{u}^T(t) \underline{R} \underline{u}(t)] dt \quad (2.27)$$

where T denotes matrix transpose and

$$\underline{Q} = \begin{bmatrix} \alpha + \rho_1 & 0 & -\alpha & 0 \\ 0 & \beta + \rho_2 & 0 & -\beta \\ -\alpha & 0 & \alpha + \rho_3 & 0 \\ 0 & -\beta & 0 & \beta + \rho_4 \end{bmatrix} \quad \text{and} \quad \underline{R} = \begin{bmatrix} \gamma_1 & 0 \\ 0 & \gamma_2 \end{bmatrix} \quad (2.28)$$

\underline{Q} and \underline{R} will be chosen to be positive definite matrices. The objective is to find the control $\underline{u}^*(t)$ which minimizes (2.27) subject to (2.24). Here the initial value $\underline{x}(0)$ is assumed to be known but $\underline{x}(\infty)$ is unspecified.

It is useful to examine the engineering significance of the infinite time interval of the cost functional. Since the final time is not specified, the cost expression does not include a terminal cost term. The terminal time is set equal to ∞ for the following reasons: First, we wish to ensure that the state will remain near zero after an initial transient interval and, second, we wish to avoid specifying an arbitrarily large terminal time.

We can now proceed to use linear regulator theory of optimal control to derive $\underline{u}^*(t)$. This well-known theory has been used by Levine and Athans^[5] and Peppard and Gourishankar^[6] to design optimal controllers for high-speed trains. A detailed exposition of this theory can be found in most textbooks on optimal control such as [7]. The theory is summarized here for the convenience of the reader.

Given the controllable* linear time-invariant system

$$\dot{\underline{x}}(t) = \underline{A} \underline{x}(t) + \underline{B} \underline{u}(t) \quad (2.29)$$

and the cost functional

$$J = \frac{1}{2} \int_0^{\infty} [\underline{x}^T(t) \underline{Q} \underline{x}(t) + \underline{u}^T(t) \underline{R} \underline{u}(t)] dt \quad (2.30)$$

where $\underline{u}(t)$ is not constrained, \underline{Q} and \underline{R} are positive definite matrices, then a unique optimal control exists and is given by

* For a definition of controllability see [7], p. 200.

$$\underline{u}^*(t) = - \underline{R}^{-1} \underline{B}^T \hat{\underline{K}} \underline{x}(t) \quad (2.31)$$

where $\hat{\underline{K}}$ is the constant positive definite matrix which is the solution to the matrix algebraic equation

$$-\hat{\underline{K}}\underline{A} - \underline{A}^T \hat{\underline{K}} + \hat{\underline{K}}\underline{B}\underline{R}^{-1} \underline{B}^T \hat{\underline{K}} - \underline{Q} = \underline{0} \quad (2.32)$$

The minimum cost J^* is given by

$$J^*[\underline{x}(t)] = \frac{1}{2} [\underline{x}^T(t) \hat{\underline{K}} \underline{x}(t)] \quad (2.33)$$

For the two-vehicle car-following unit, the optimal control vector $\underline{u}^*(t)$ can be found for a particular form of cost functional (2.27) and specific values of \underline{A} and \underline{B} in (2.24).

2.3.2 Dynamic Performance

In this subsection the results of a study of the dynamic performance of the optimally-controlled two-vehicle basic unit will be reported. This study was carried out by simulating the optimal system on the PACE 231 analogue computer of the University of Alberta, Electrical Engineering Department for a variety of cost functionals obtained by assigning different values to the weighting factors in the cost functional (2.26).

In this study, each vehicle was assumed to have a weight of 3220 lbs. and a linear drag coefficient $\bar{\mu}$ of 1.7 lbf./ft./sec. These values were chosen to be both reasonable and convenient.

The following seven different general forms of cost functional (2.26) were examined. These will be referred to as systems type 1 to 7.

$$\text{Type 1: } J_1 = \int_0^{\infty} [\alpha(x_{n1} - x_{n+1,1})^2 + 100u_n^2 + 0.1u_{n+1}^2] dt \quad (2.34)$$

$$\begin{aligned} \text{Type 2: } J_2 = \int_0^{\infty} & [\alpha(x_{n1} - x_{n+1,1})^2 + (x_{n2} - x_{n+1,2})^2 + 100u_n^2 \\ & + 0.1u_{n+1}^2] dt \end{aligned} \quad (2.35)$$

$$\text{Type 3: } J_3 = \int_0^{\infty} [\beta(x_{n2} - x_{n+1,2})^2 + 100u_n^2 + 0.1u_{n+1}^2] dt \quad (2.36)$$

$$\begin{aligned} \text{Type 4: } J_4 = \int_0^{\infty} & [(x_{n1} - x_{n+1,1})^2 + \beta(x_{n2} - x_{n+1,2})^2 + 100u_n^2 \\ & + 0.1u_{n+1}^2] dt \end{aligned} \quad (2.37)$$

$$\begin{aligned} \text{Type 5: } J_5 = \int_0^{\infty} & [\alpha(x_{n1} - x_{n+1,1})^2 + \beta(x_{n2} - x_{n+1,2})^2 + 100u_n^2 \\ & + 0.1u_{n+1}^2] dt \end{aligned} \quad (2.38)$$

$$\begin{aligned} \text{Type 6: } J_6 = \int_0^{\infty} & [(x_{n1} - x_{n+1,1})^2 + (x_{n2} - x_{n+1,2})^2 + 100u_n^2 \\ & + 0.1u_{n+1}^2 + \rho_4 x_{n+1,2}^2] dt \end{aligned} \quad (2.39)$$

$$\begin{aligned} \text{Type 7: } J_7 = \int_0^{\infty} & [(x_{n1} - x_{n+1,1})^2 + (x_{n2} - x_{n+1,2})^2 + 100u_n^2 \\ & + 0.1u_{n+1}^2 + \rho_3 x_{n+1,1}^2] dt \end{aligned} \quad (2.40)$$

It should be noted that in all the above cost functionals, the expenditure of control energy, $u_n^2(t)$, by the leading vehicle is penalized 1000 times more heavily than that by the following vehicle. This is to ensure that the two-vehicle unit behaves in a true car-following manner in the sense that only the following vehicle reacts to the motion of the leading vehicle and not vice-versa. This is

equivalent to saying that for all the systems studied, $u_n^*(t) = 0$.

Instead of solving the algebraic Riccati equation (2.32) directly, the corresponding differential equation

$$-\underline{K}(t)\underline{A} - \underline{A}^T \underline{K}(t) + \underline{K}(t)\underline{B}\underline{R}^{-1}\underline{B}^T \underline{K}(t) - \underline{Q} = \dot{\underline{K}}(t) \quad (2.41)$$

was solved for each of the cost functionals shown above. This was done on the IBM 360/67 digital computer at the University of Alberta. The IBM subroutine RKGS (Fourth-order Runge-Kutta) was used. The solution $\hat{\underline{K}}$ of (2.32) was taken to be the steady-state solution of (2.41) with initial condition $\underline{K}(0) = \underline{0}$.

The optimal control strategy can then be found from (2.31) which can be rewritten as

$$\underline{u}^*(t) = - \underline{L}^* \underline{x}^*(t) \quad (2.42)$$

where $\underline{L}^* = - \underline{R}^{-1} \underline{B}^T \hat{\underline{K}}$. The optimal feedback system is shown in Figure 2.4. The optimal feedback gains L_1^* , L_2^* , L_3^* and L_4^* are given by

$$\begin{aligned} L_1^* &= - \frac{\hat{k}_{34}}{m\gamma_2}, & L_2^* &= - \frac{\hat{k}_{44}}{m\gamma_2} \\ L_3^* &= - \frac{\hat{k}_{14}}{m\gamma_2}, & L_4^* &= - \frac{\hat{k}_{24}}{m\gamma_2} \end{aligned} \quad (2.43)$$

Table 2.2 gives a listing of these gains for variations in the weighting factors in each of the seven cost functionals.

The analogue simulation diagram is shown in Figure 2.5.

Each of the seven systems corresponding to the various feedback gains given in Table 2.2 was subjected to two tests as described below:

* This fact could be taken into account in the problem formulation by defining suitable state variables.

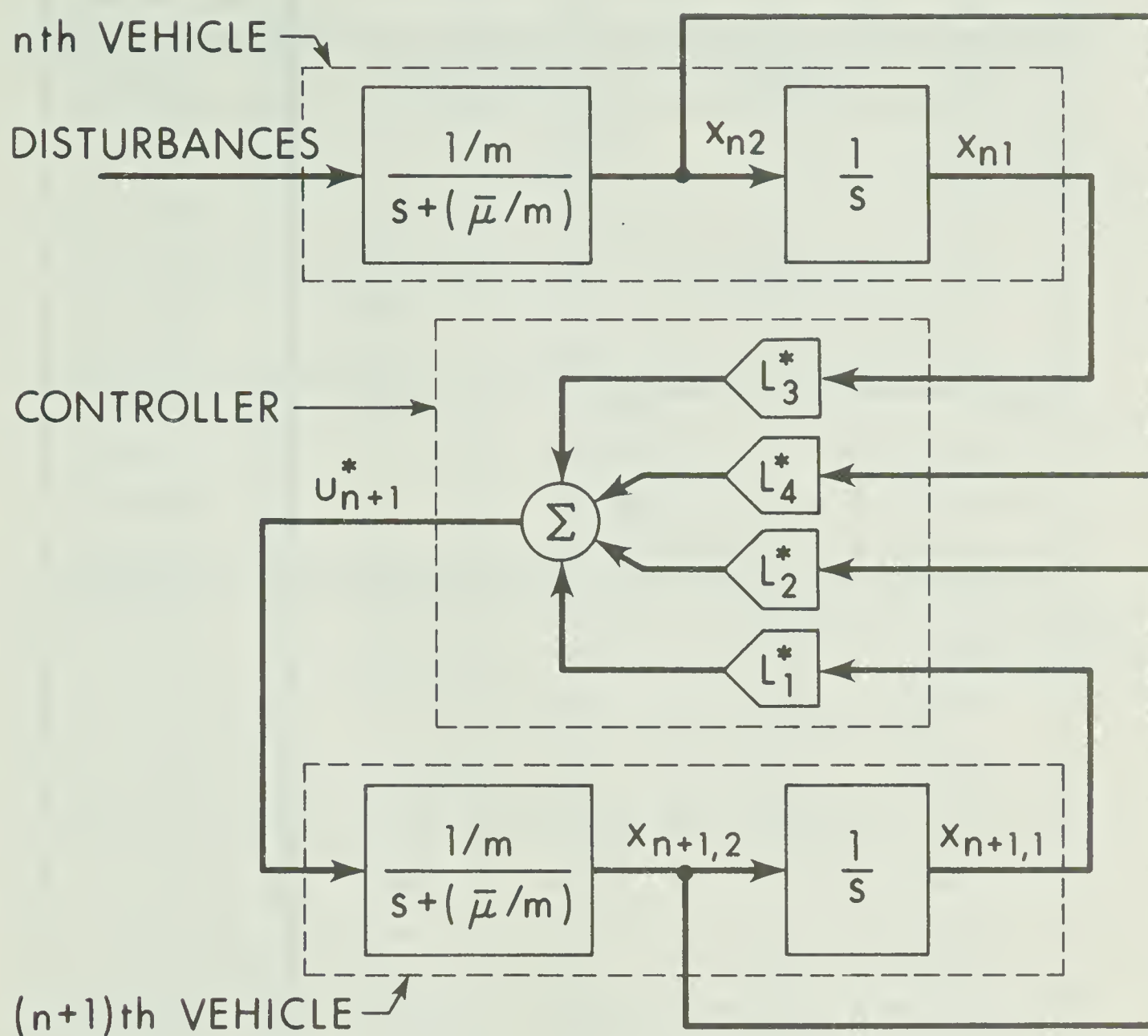


FIGURE 2.4 Block Diagram of Two-Vehicle Optimal Feedback System

System Type	L_1^*	L_2^*	L_3^*	L_4^*
1a($\alpha=1$)	-3.161	-23.49	3.161	23.49
2a($\alpha=1$)	-3.161	-23.69	3.161	23.69
2b($\alpha=5$)	-7.067	-36.05	7.067	36.05
2c($\alpha=10$)	-9.995	-43.13	9.995	43.13
2d($\alpha=100$)	-31.76	-78.05	31.76	78.05
2e($\alpha=500$)	-70.74	-117.2	70.74	117.2
2f($\alpha=900$)	-94.87	-136.0	94.87	136.0
3a($\beta=1$)	0	-1.890	0	1.890
3b($\beta=5$)	0	-5.570	0	5.570
3c($\beta=10$)	0	-8.440	0	8.440
3d($\beta=100$)	0	-29.95	0	29.95
4a($\beta=1$)	-3.161	-23.69	3.161	23.69
4b($\beta=100$)	-3.161	-38.43	3.161	38.43
4c($\beta=1000$)	-3.160	-101.4	3.160	101.4
4d($\beta=1600$)	-3.160	-125.8	3.160	125.8
4e($\beta=10^5$)	-1.768	-998.0	1.768	998.0
5a($\alpha=\beta=1$)	-3.161	-23.69	3.161	23.69
5c($\alpha=\beta=10$)	-9.995	-44.13	9.995	44.13
5d($\alpha=\beta=100$)	-31.61	-83.84	31.61	83.84
5e($\alpha=\beta=1000$)	-99.95	-171.4	99.95	171.4
6a($\rho_4=0$)	-3.161	-23.69	3.161	23.69
6b($\rho_4=20$)	-3.159	-27.35	3.159	26.34
6c($\rho_4=100$)	-3.143	-38.80	3.143	33.61
6d($\rho_4=1000$)	-2.771	-101.1	2.771	48.13
7a($\rho_3=0$)	-3.161	-23.69	3.161	23.69
7b($\rho_3=.5$)	-3.872	-26.35	2.544	16.20
7c($\rho_3=2$)	-5.477	-31.59	1.800	9.684
7d($\rho_3=10$)	-10.49	-44.24	0.9455	3.787
7e($\rho_3=50$)	-22.58	-65.60	0.4412	1.245

Table 2.2 Tabulation of Feedback Gains for the Two-Vehicle Unit

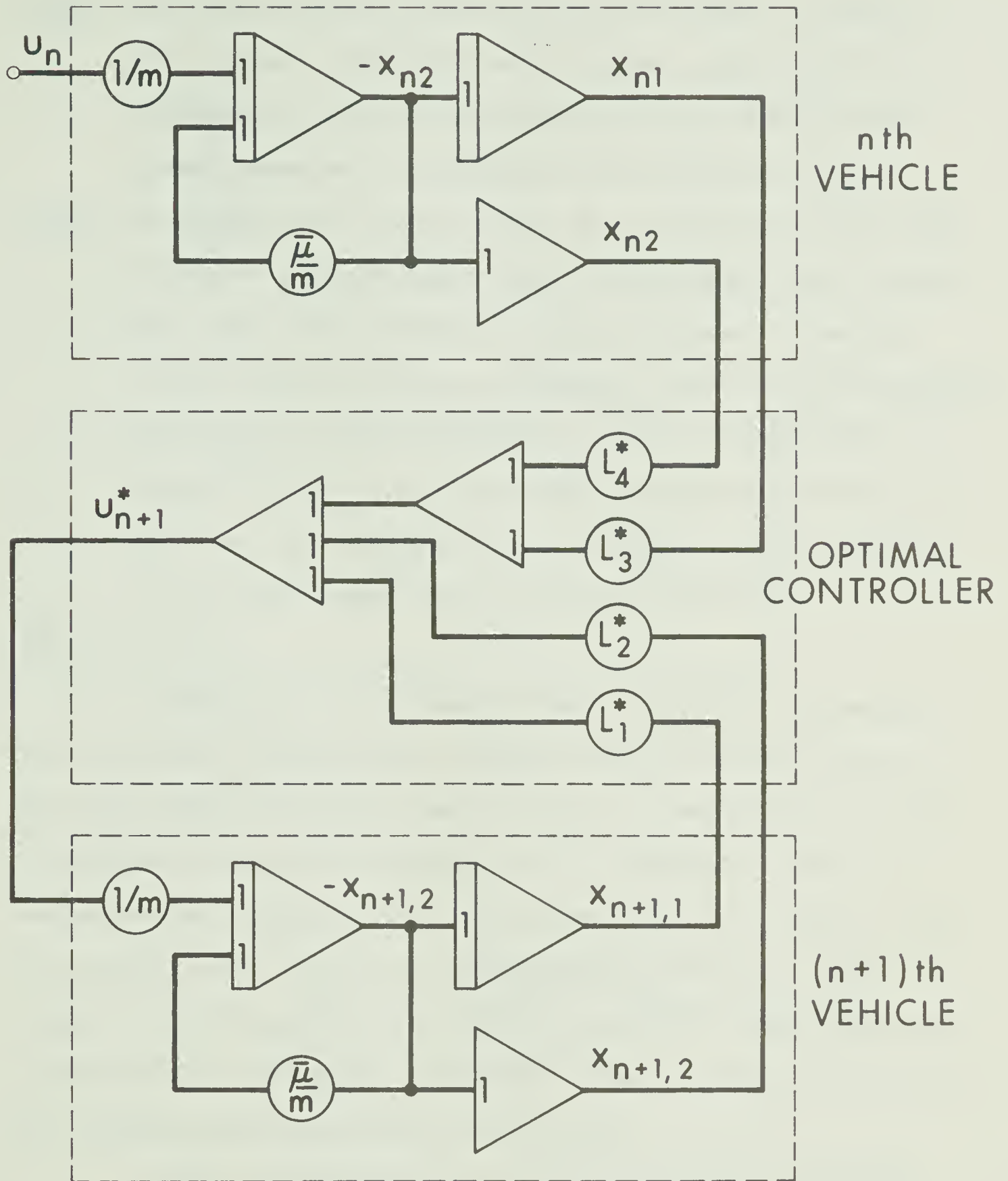


FIGURE 2.5 Analogue Simulation Diagram For Two-Vehicle Car-Following System

Test 1 The position error of the lead vehicle was made to undergo a step change. Although not very realistic, this type of perturbation is useful in determining the local stability and dynamic behaviour of the system under extreme conditions.

Test 2 The position and velocity errors of the lead vehicle were made to vary in a pseudo-random manner. The velocity error for the lead vehicle was generated by adding sinusoids of frequency 0.1 Hz., 0.07 Hz., 0.04 Hz., 0.015 Hz. and 0.005 Hz. The position error varied as the integral of this sum. A test duration of 60 sec. was used. The pseudo-random signals were identical for each test. The analogue simulation diagram for the generation of the pseudo-random signal is given in Figure 2.6.

Results of Test 1

Systems type 1 and 2 exhibit nearly identical step response as can be seen by comparing the feedback gains for systems 1a and 2a. The gains become essentially identical for $\alpha > 1$ and hence gain values for system 1 are not given except for $\alpha = 1$. Figure 2.7 shows the variation with respect to time t of the position error, $x_{n+1,1}(t)$, and the velocity error, $x_{n+1,2}(t)$ of the following vehicle for a unit step change in $x_{n1}(t)$ ($x_{n2}(t) = 0$ for all t) for system 1a. The steady-state headway error is zero which is desirable. This is a result of the headway deviation term in the cost functional J_{1a} .

Figure 2.8 shows the step response of system 2 for headway deviation weightings of $\alpha = 1, 10$ and 100 . The effect of increasing α is to shorten the rise time of $x_{n+1,1}(t)$ at the expense of increasing the maximum velocity error and acceleration or deceleration required of

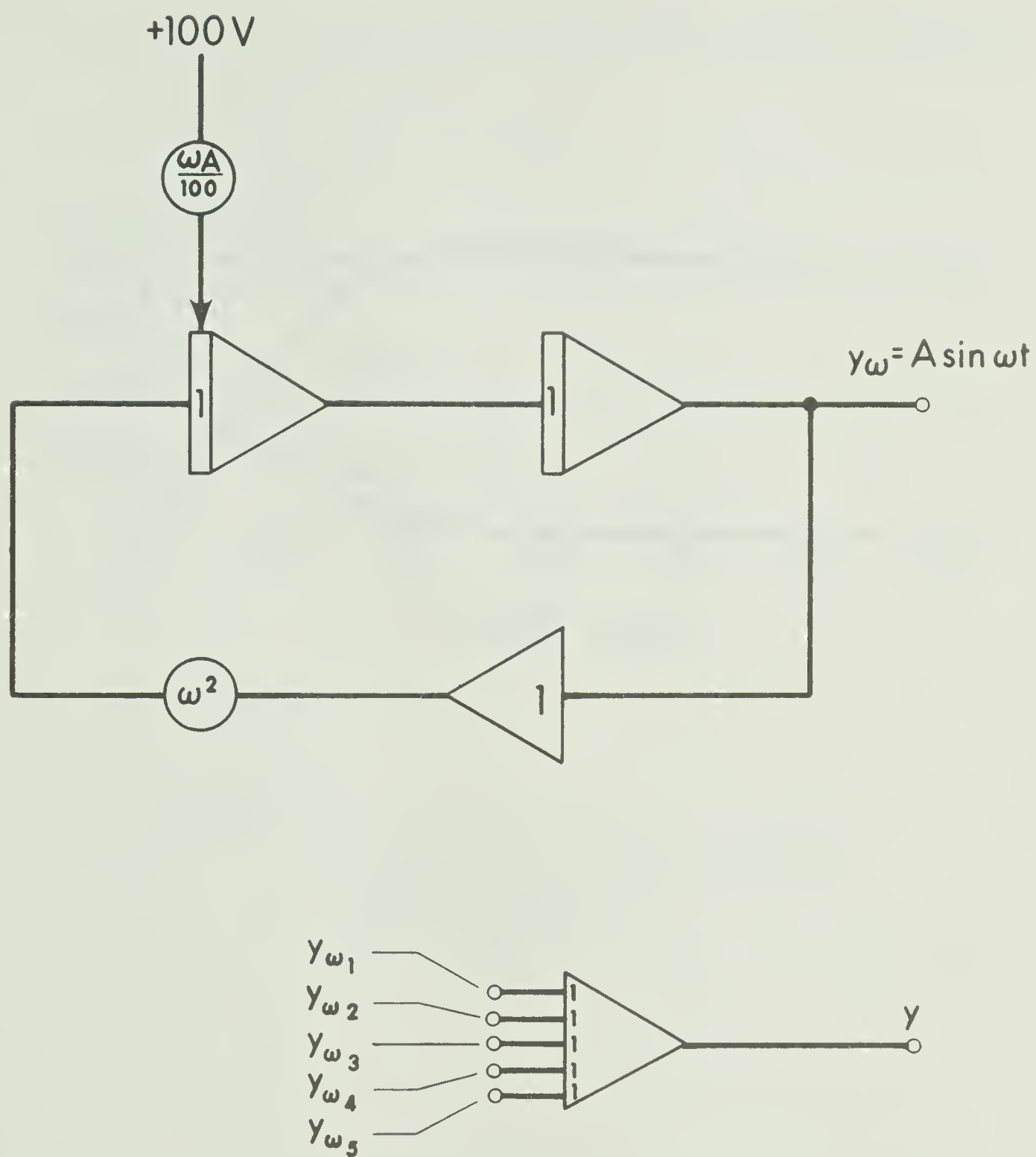


FIGURE 2.6 Analogue Simulation Diagram for Generation of Pseudo-Random Signal

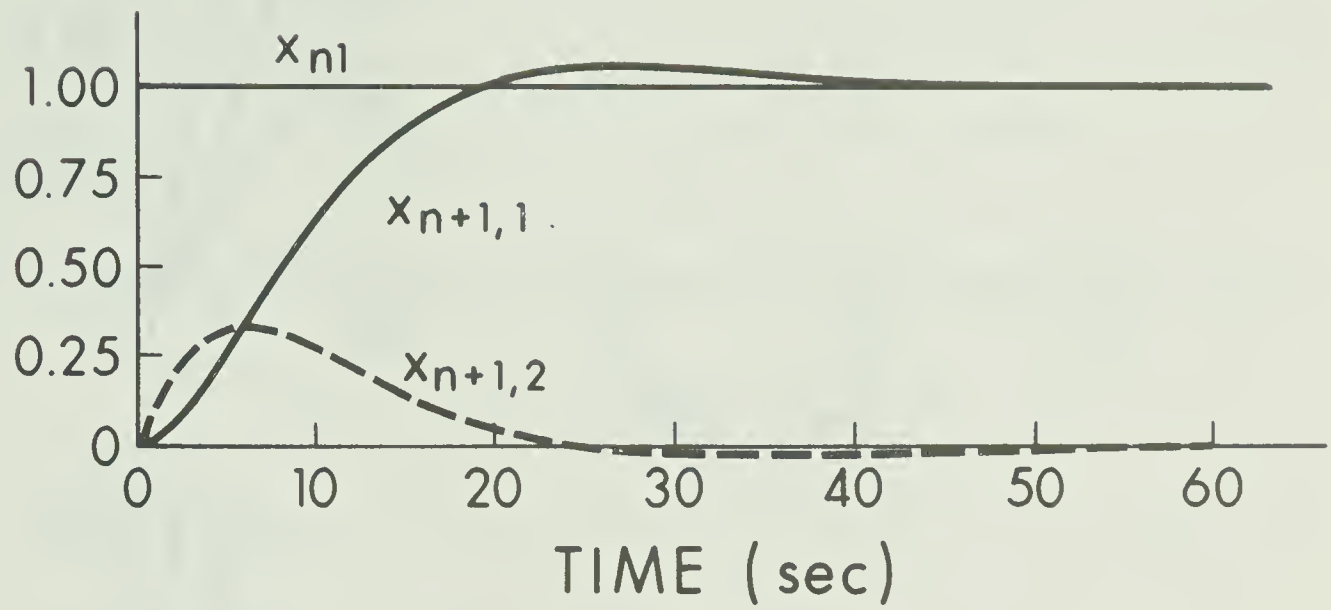


FIGURE 2.7 Position and Velocity Error Response of the (n+1)th Vehicle for a Step Change in Position Error of the nth Vehicle (System 1a)

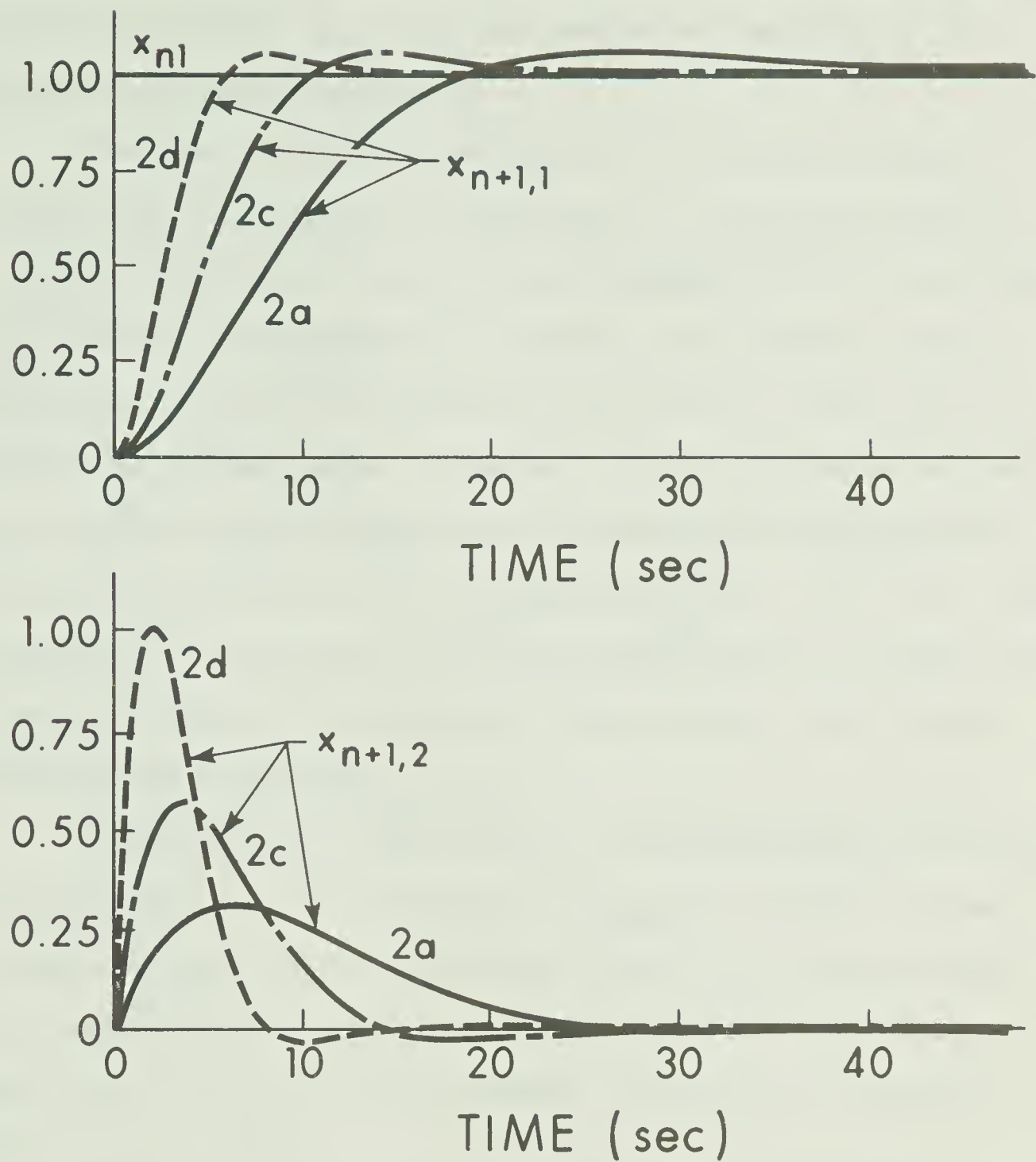


FIGURE 2.8 Position and Velocity Error Response of the (n+1)th Vehicle for a Step Change in Position Error of the nth Vehicle (Systems 2a, 2c and 2d)

the following vehicle. The actual values of relative velocity between vehicles and the force on the $(n+1)$ th vehicle are dependent on the magnitude of the step change in x_{n1} .

We have seen that the inclusion of the relative velocity term $(x_{n2} - x_{n+1,2})^2$ in the cost functional J_{1a} has little effect on the position error step response of the following vehicle. This is due to the fact that zero headway error implies a zero relative velocity between vehicles. That the converse is not true can be seen from the values of the feedback gains for system 3. In this system we are penalizing only for relative velocity error. Hence there is no feedback of position information to the following vehicle ($L_1^* = L_3^* = 0$). This is equivalent to saying that the following vehicle will be unaware of a deviation in headway from the desired value as long as the relative velocity of the two vehicles is zero.

In system type 4, the effect of large weighting on the relative velocity term in the cost functional is examined. The effect is only noticeable for very large β at which point due to the limiting effect on the maximum value of $x_{n+1,2}(t)$, the position error step response becomes very slow and more heavily damped. This effect is shown in Figure 2.9 for $\beta = 1000$.

For system type 5 weighting on both the headway deviation and relative velocity terms in the cost functional was varied equally. This produced the same effect as reducing the weighting on the following vehicle control energy for system 2a. Figure 2.10 shows the step response of the following vehicle for $\alpha = \beta = 100$. The response is nearly identical to that of system 2d in which $\alpha = 100, \beta = 1$.

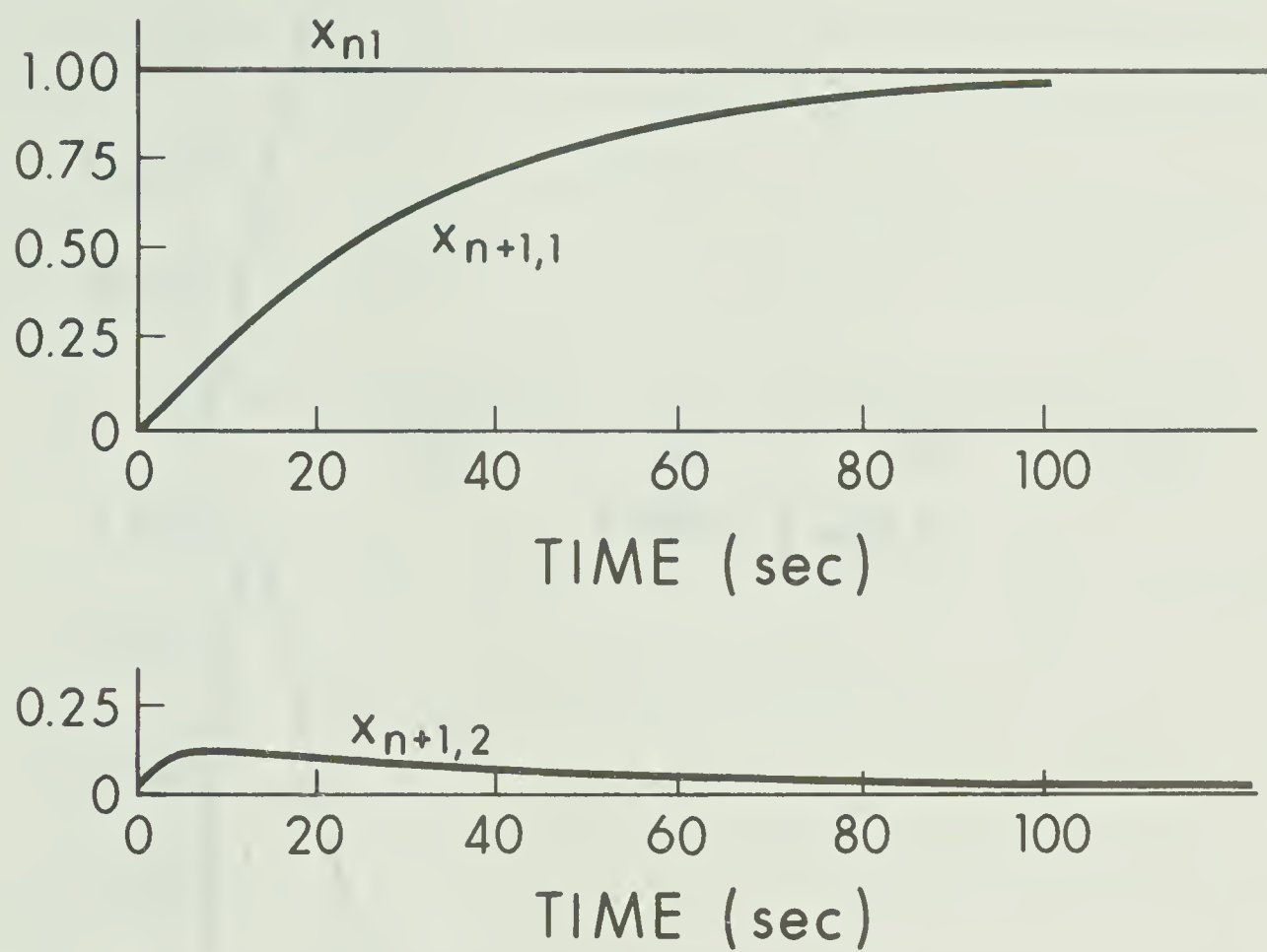


FIGURE 2.9 Position and Velocity Error Response of the (n+1)th Vehicle for a Step Change in Position Error of the nth Vehicle (System 4c)

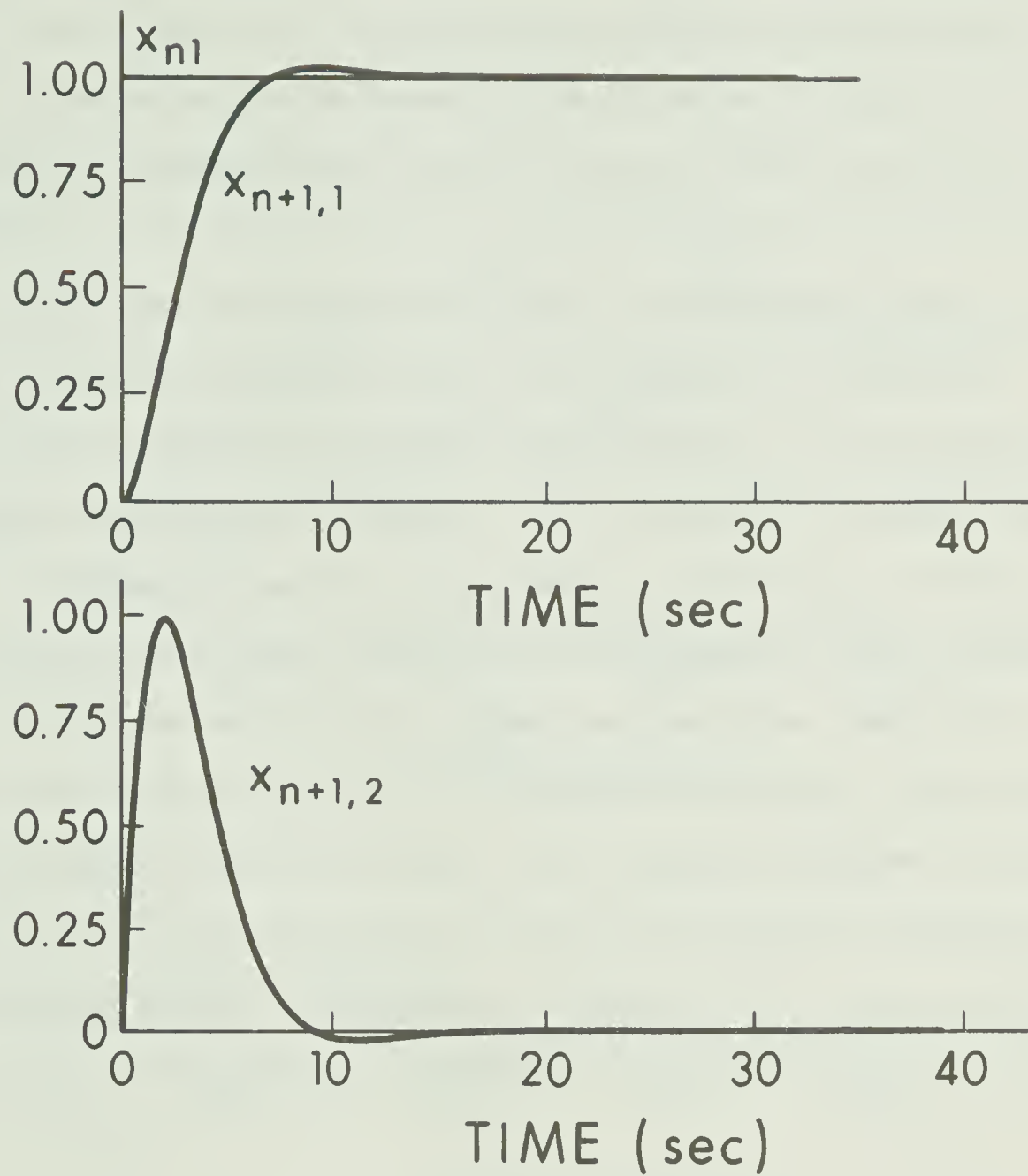


FIGURE 2.10 Position and Velocity Error Response of the (n+1)th Vehicle for a Step Change in Position Error of the nth Vehicle (System 5d)

The cost functional for system 6 is essentially that of system 2a with the addition of the term $\rho_4 x_{n+1,2}^2(t)$. From Figure 2.11, it can be seen that this additional penalty on velocity error of the following vehicle produces an effect similar to that of increasing the weighting on the relative velocity term in the case of system 4.

The cost functional for system 7 is identical to that of system 2a with the addition of the term $\rho_3 x_{n+1,1}^2(t)$. From Figure 2.12 it can be seen that the effect of increasing ρ_3 is to increase the steady-state headway deviation. This, in general, is undesirable.

In summarizing the above comments on the results of test 1, it can be said that three elements of system behaviour can be affected by cost functional manipulation. These are rise time, damping and steady-state headway deviation. It can also be seen that these elements can be altered in more than one way. The responses obtained for the various forms of cost functional J_2 (or J_1) are generally desirable from the point of view of smoothness of response, zero steady-state headway error and adjustable rise time.

Results of Test 2

The test signals used for $x_{n2}(t)$ and $x_{n1}(t)$ for this test are shown in Figure 2.13. The remaining figures in this subsection show the variation with respect to time of $x_{n1}(t)$, $x_{n+1,1}(t)$, $x_{n1}(t) - x_{n+1,1}(t)$, $x_{n2}(t)$, $x_{n+1,2}(t)$, $x_{n2}(t) - x_{n+1,2}(t)$ and $u_{n+1}(t)$. The duration of the test was 60 seconds.

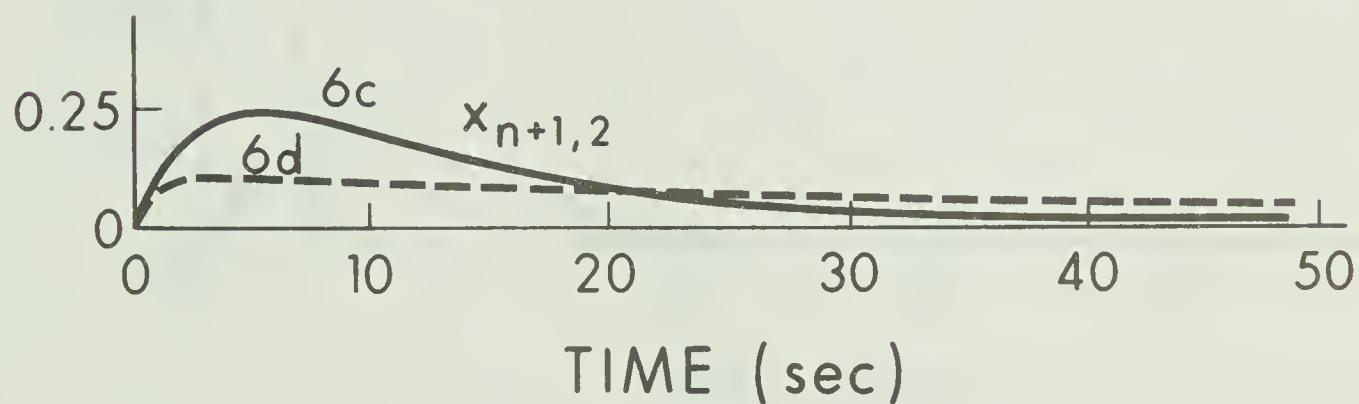
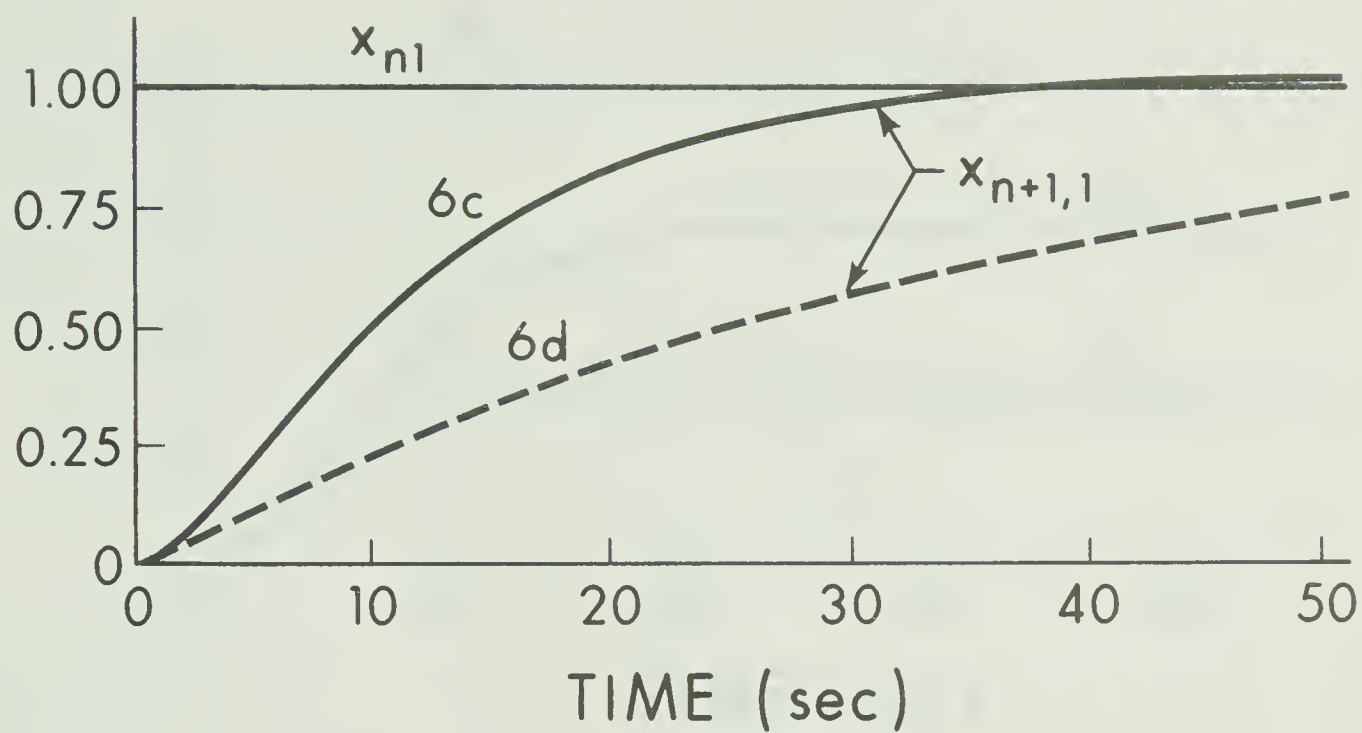


FIGURE 2.11 Position and Velocity Error Response of the $(n+1)$ th Vehicle for a Step Change in Position Error of the n th Vehicle (Systems δ_c and δ_d)

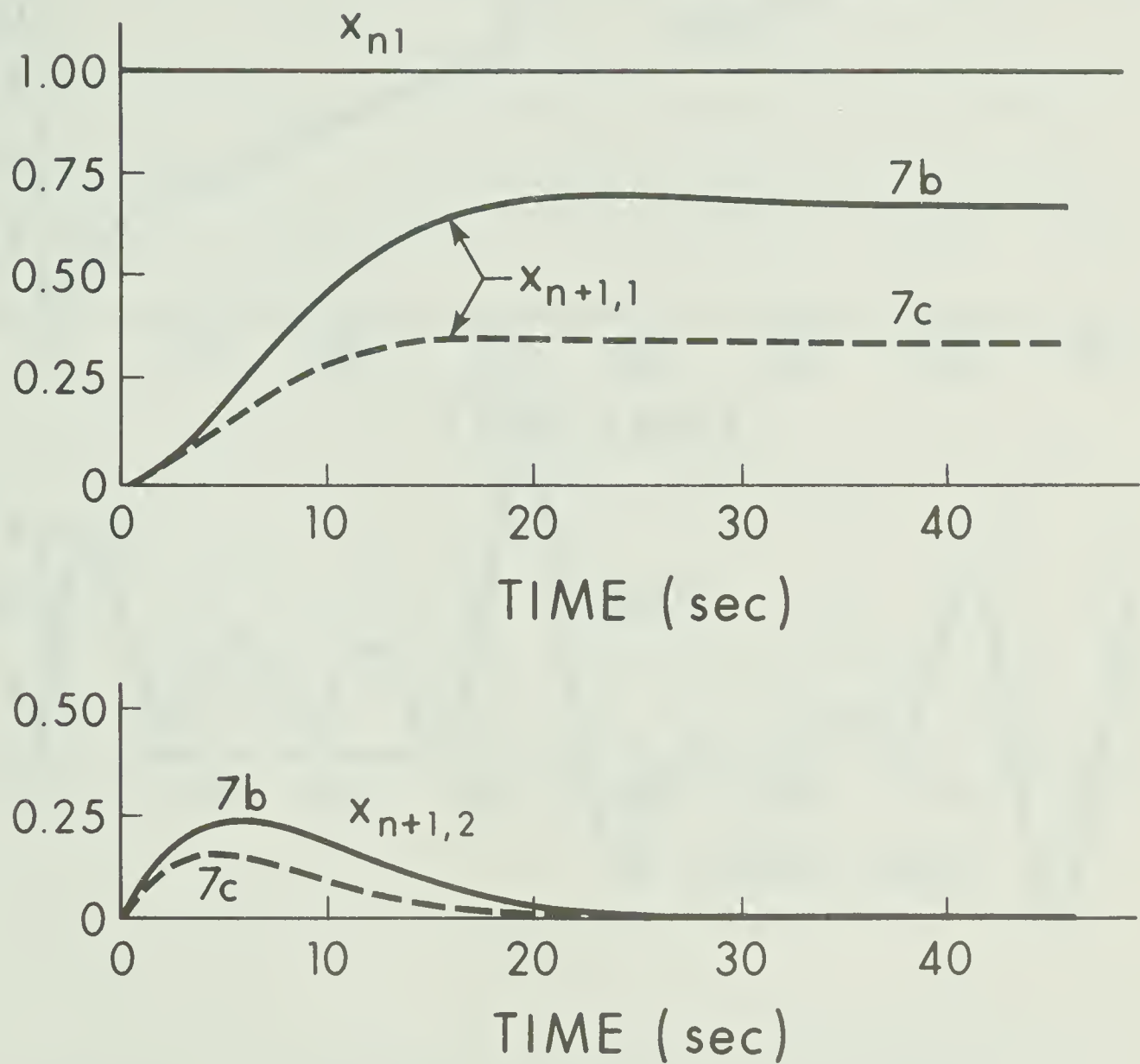


FIGURE 2.12 Position and Velocity Error Response of the (n+1)th Vehicle for a Step Change in Position Error of the nth Vehicle (Systems 7b and 7c)

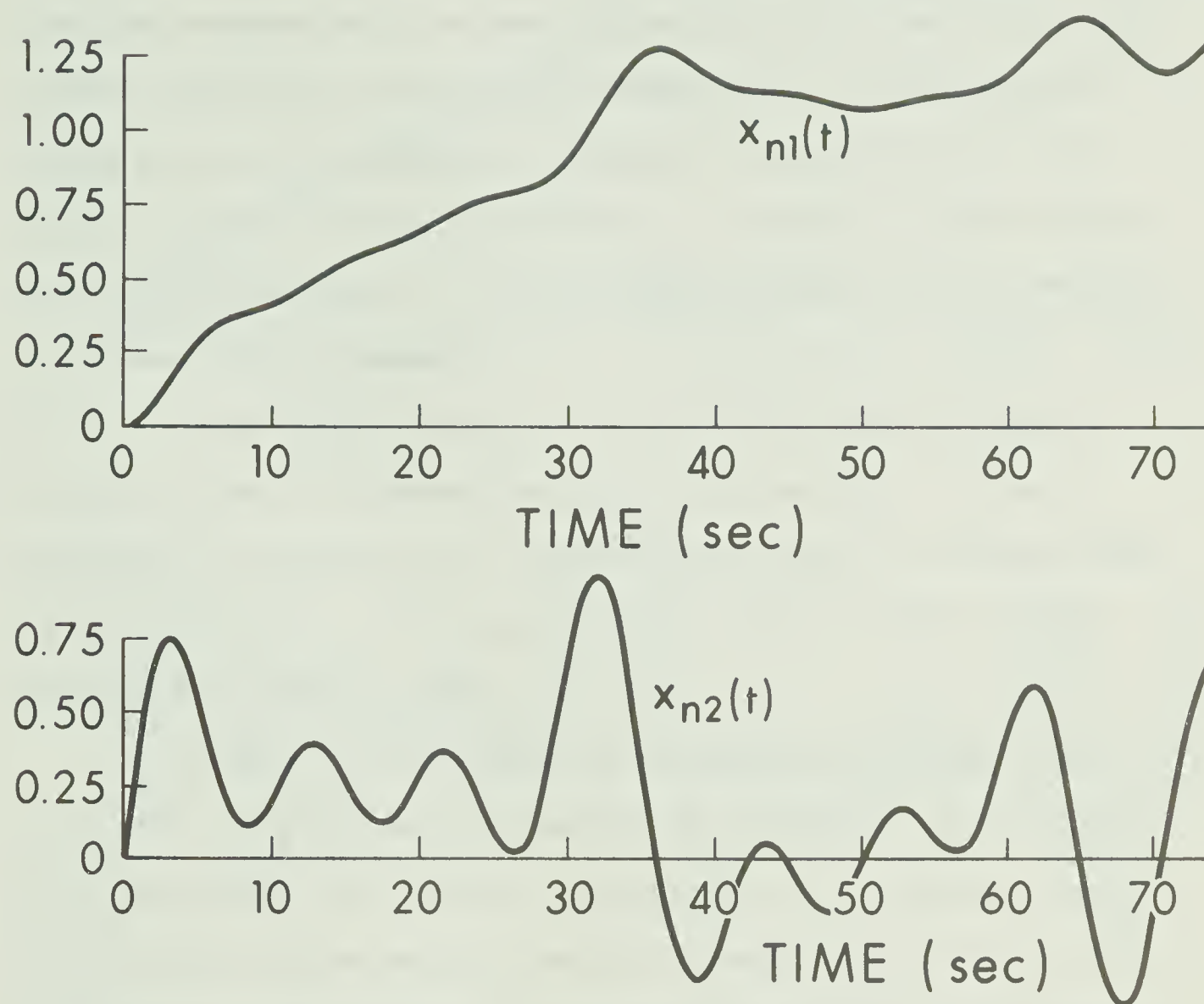


FIGURE 2.13 Pseudo-Random Signals Used for the Position and Velocity Errors of the n th Vehicle for Test 2

Figures 2.14, 2.15 and 2.16 show the results for systems 2a, 2c and 2d respectively ($\alpha = 1, 10$ and 100). As in the case of the step response tests on these systems, it can be seen that better headway regulation results as the headway error is penalized more and more but at the expense of increased peak velocity error and control force on the following vehicle. It should be noted however that better regulation of relative velocity between the two vehicles does result for increased α .

Results for systems 3a, 3c and 3d are shown in Figures 2.17, 2.18 and 2.19 respectively ($\beta = 1, 10$ and 100). It can be seen that a large value of β must be used in order to achieve proper headway regulation. The behaviour for $\beta = 100$ is similar to that exhibited by system 2 with $\alpha = 1, \beta = 1$.

Figure 2.20 illustrates the behaviour of system 4c with $\beta = 1000$. Although the step response of this system did not appear to be as desirable as that of system 2a ($\beta = 1$), its headway regulation and relative velocity control are much more effective when the system is subjected to a low frequency variation in the motion of the lead vehicle.

Figure 2.21 (system 6d) shows the effect of the addition to the cost functional of a larger weighting on the velocity error of the following vehicle as compared to system 2a. Velocity error $x_{n+1,2}(t)$ is reduced throughout the run but headway regulation deteriorates significantly.

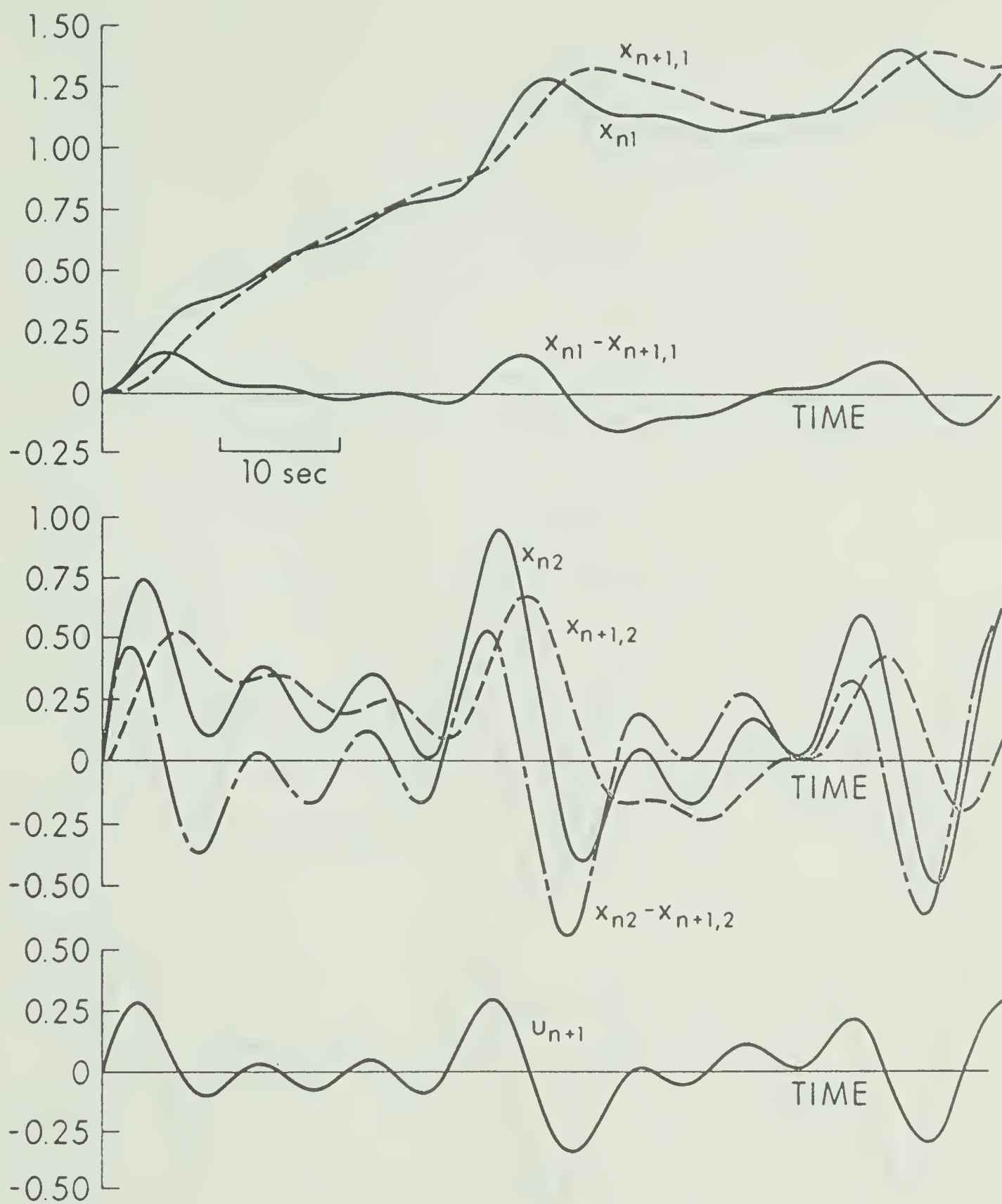


FIGURE 2.14 Results of Test 2 for System 2a

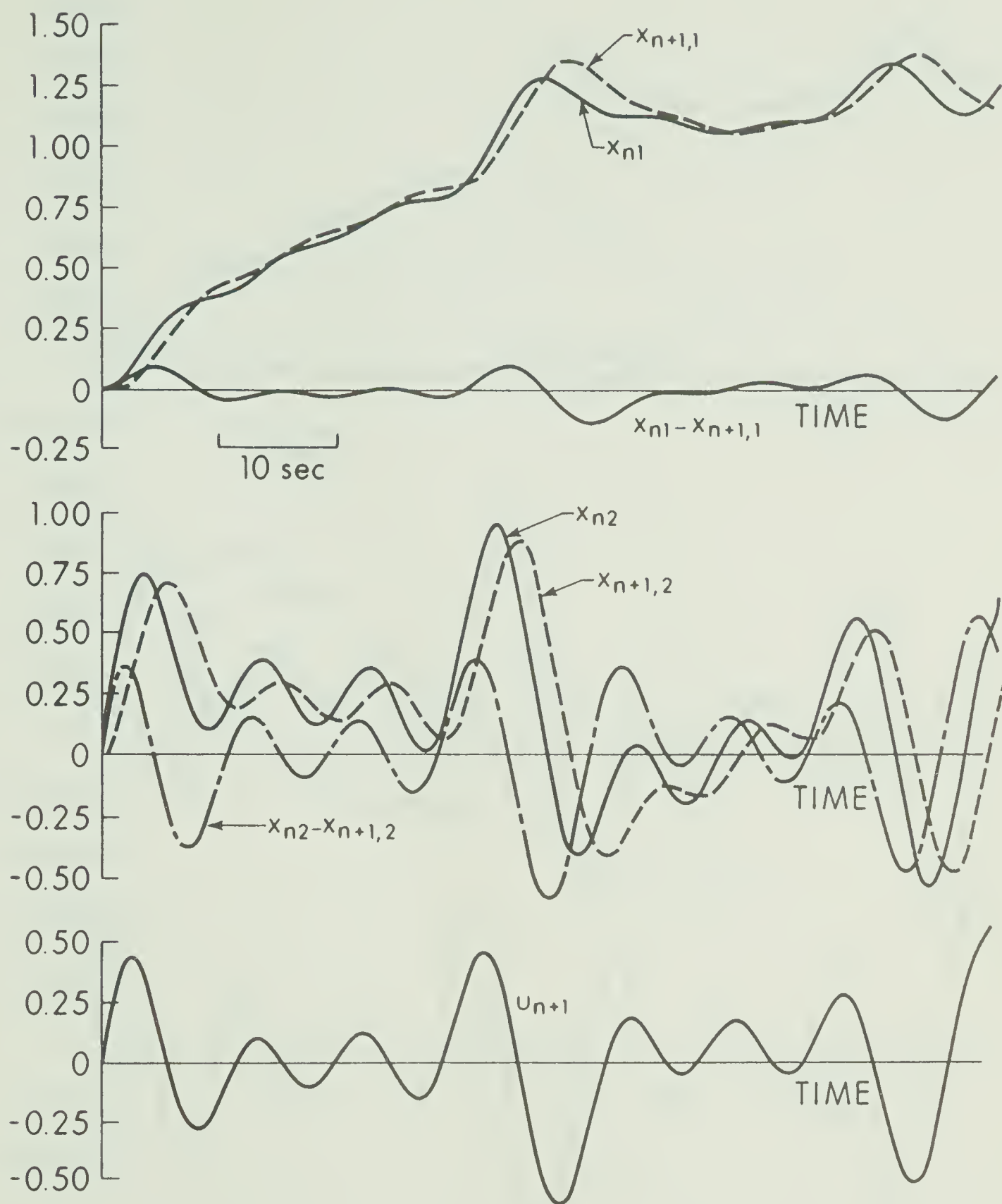


FIGURE 2.15 Results of Test 2 for System 2c

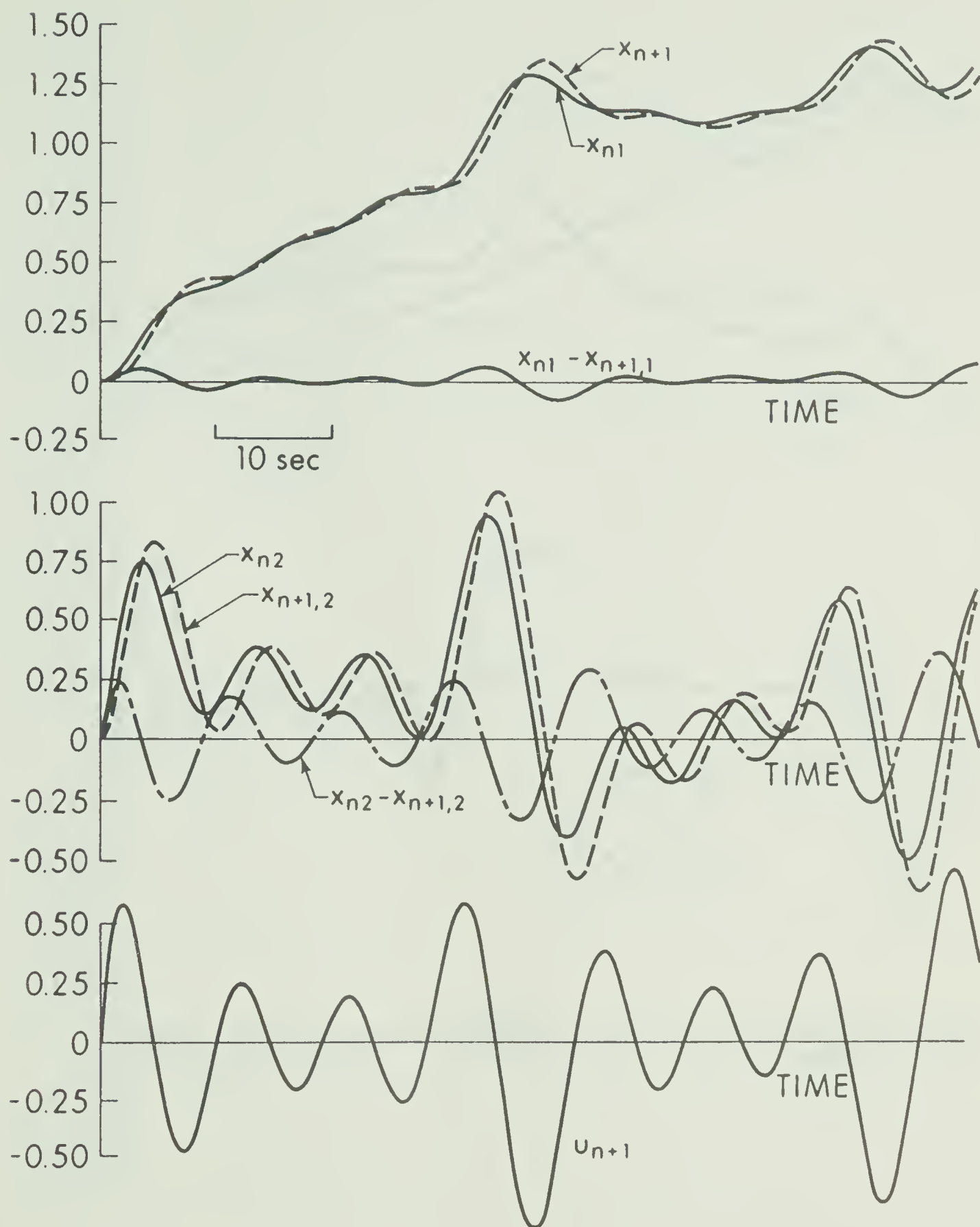


FIGURE 2.16 Results of Test 2 for System 2d

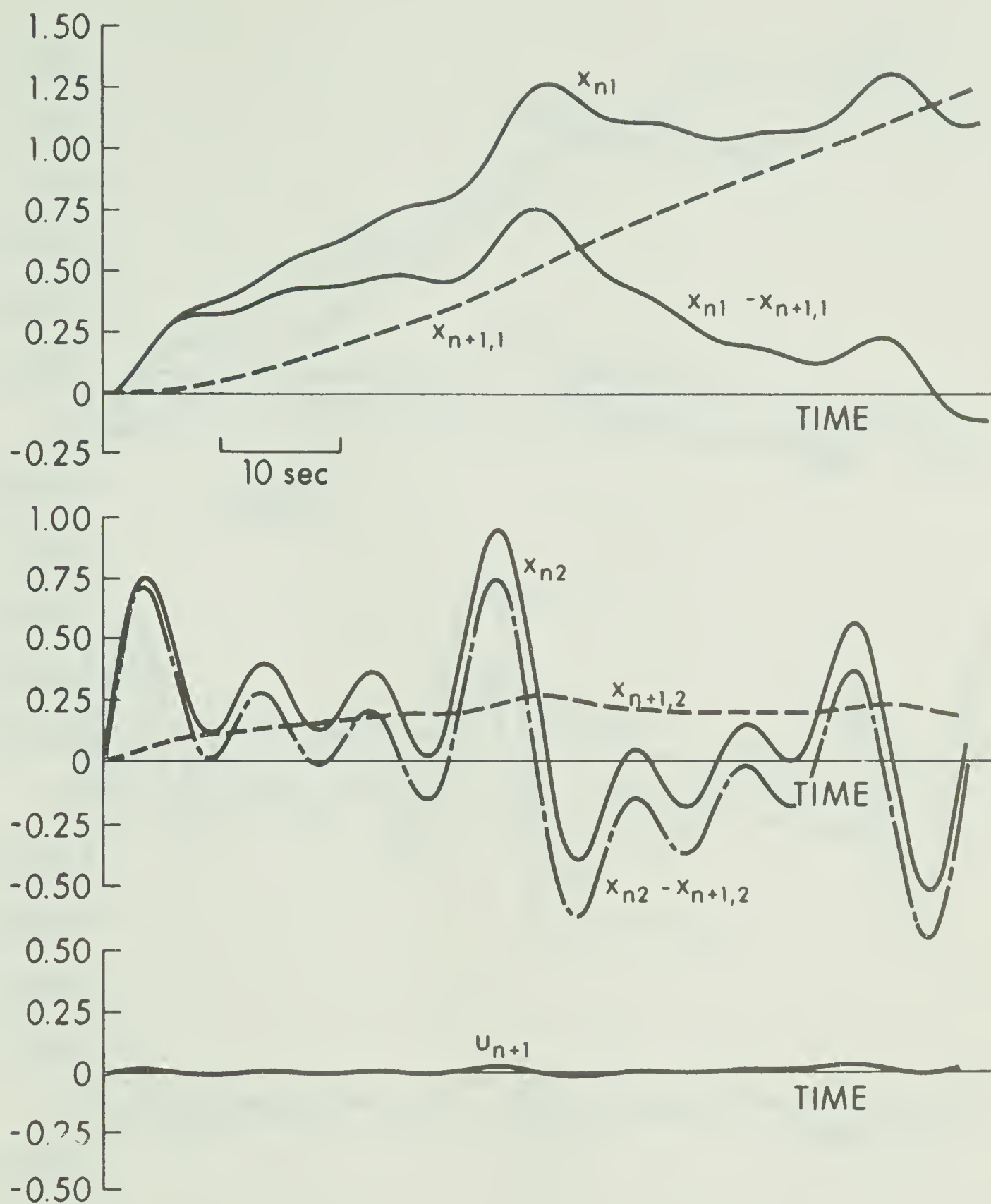


FIGURE 2.17 Results of Test 2 for System 3a

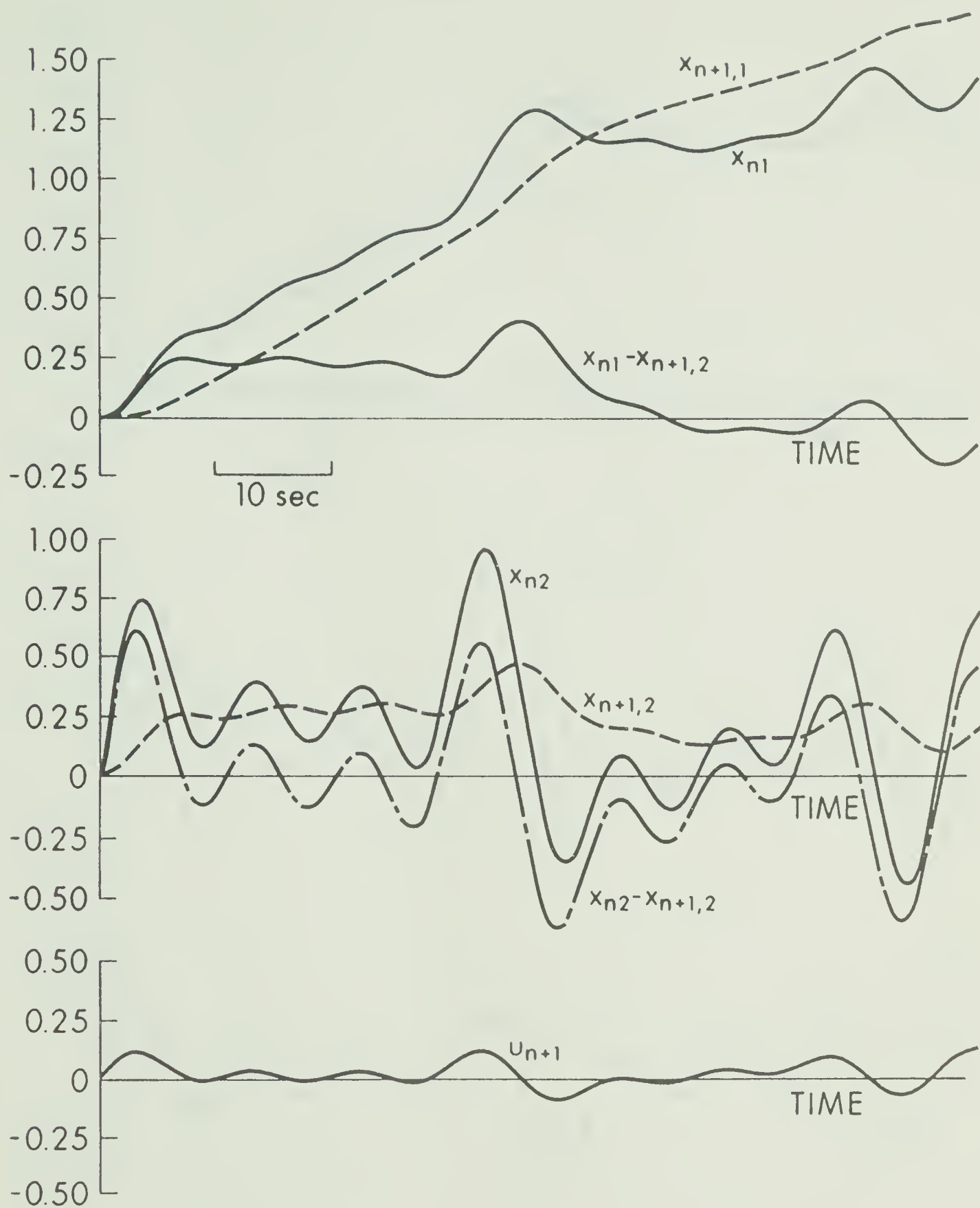


FIGURE 2.18 Results of Test 2 for System 3c

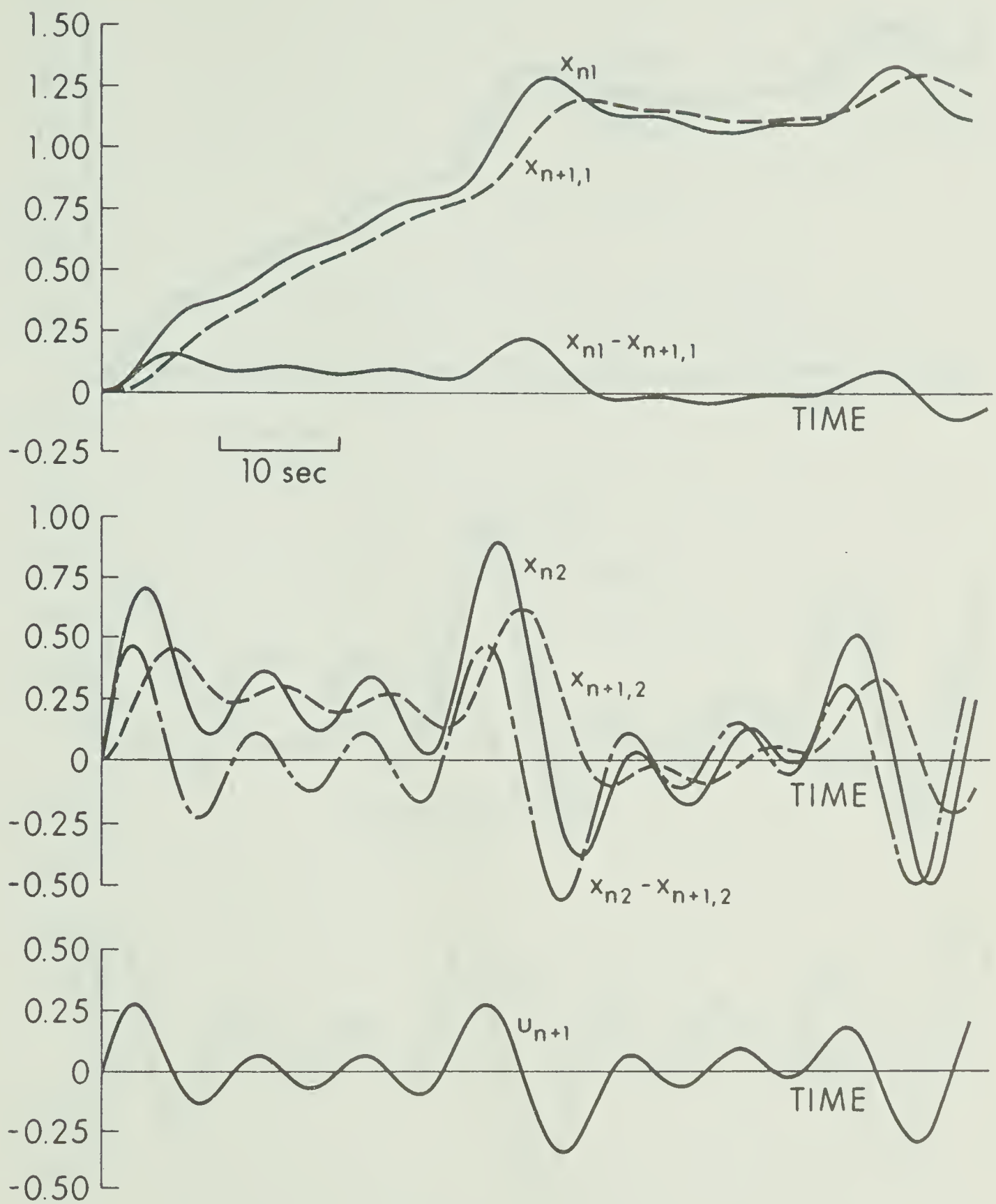


FIGURE 2.19 Results of Test 2 for System 3d

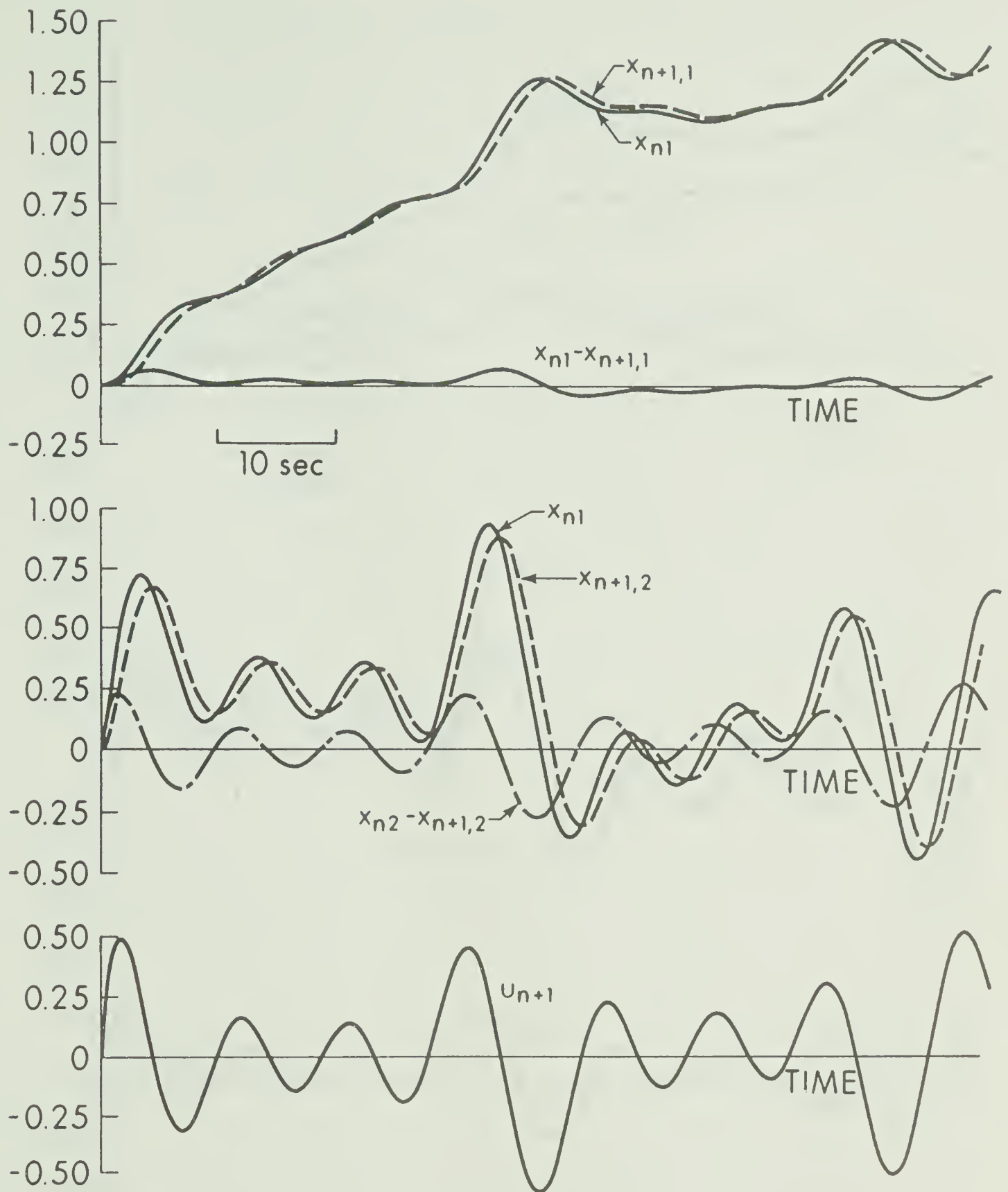


FIGURE 2.20 Results of Test 2 for System 4c

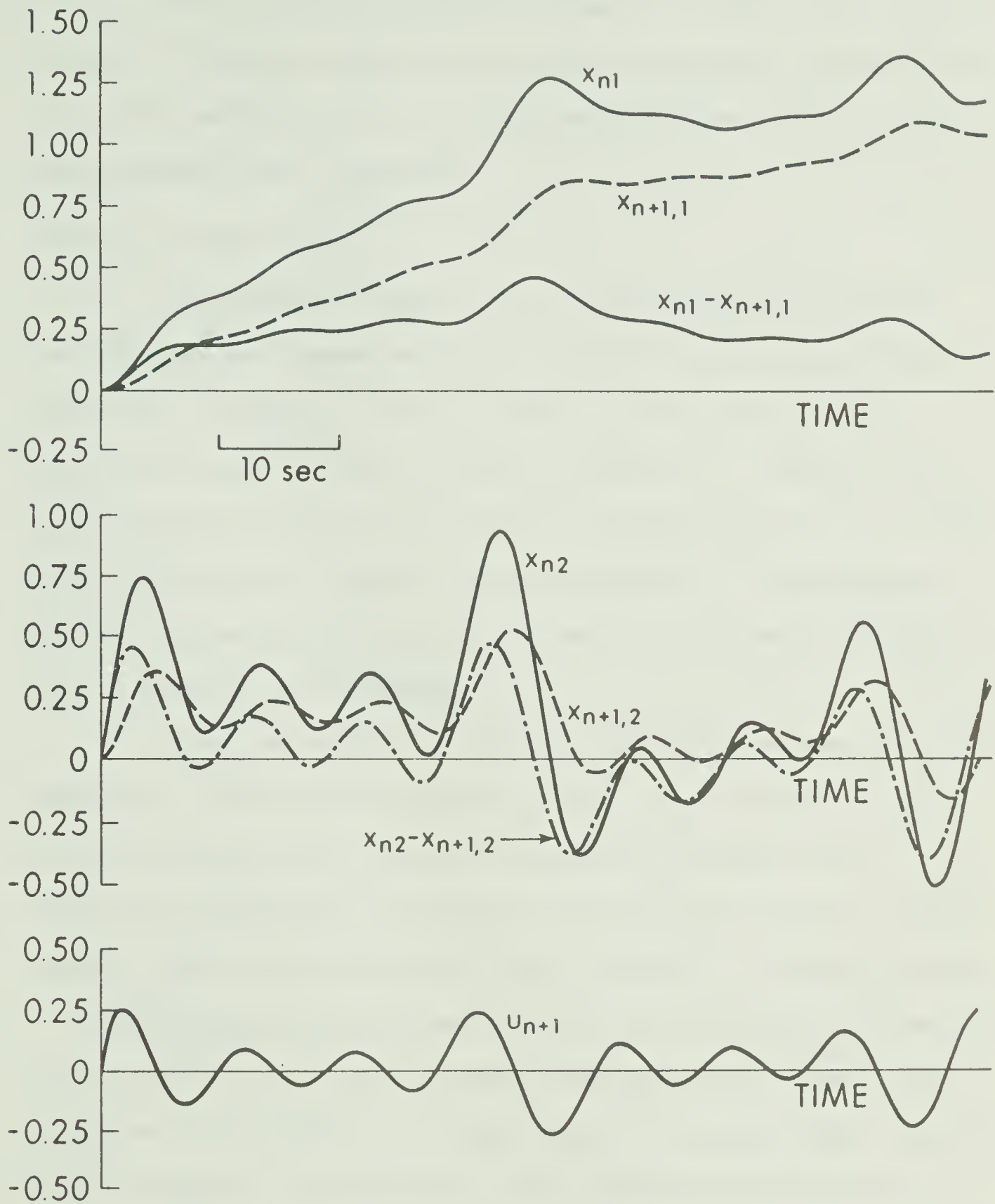


FIGURE 2.21 Results of Test 2 for System 6d

The behaviour of system 7b is shown in Figure 2.22. As in the case of the step response test, it can be seen that the penalization of the position error of the following vehicle results in degraded headway error regulation.

Summary of Tests 1 and 2

The results of tests 1 and 2 on the two-vehicle optimal car-following unit emphasize the fact that it is difficult to devise a desirable performance index for such a system purely from the qualitative specifications (as given in Chapter 1). The use of two quite different testing procedures on a simulated model of the system gives a great deal of insight into the dependence of car-following behaviour on the nature of cost functional or performance criterion used to evaluate its performance.

From the various cost functionals considered here, it seems undesirable to penalize the system for position or velocity errors of the following vehicle (refer to results for systems 6 and 7). It also appears undesirable to penalize the system for non-zero relative velocity while neglecting headway error (system 3). The exact values of weighting factors for systems 2, 4 or 5 to be chosen in the design of an automatic car-following system would depend on the exact specifications of the system. As stated earlier, the above tests indicate only the nature of the behaviour of the optimally-controlled two-vehicle unit and do not indicate how a string of many vehicles optimally controlled by the same strategy will behave in an asymptotic sense. This will be discussed in Chapter 3.

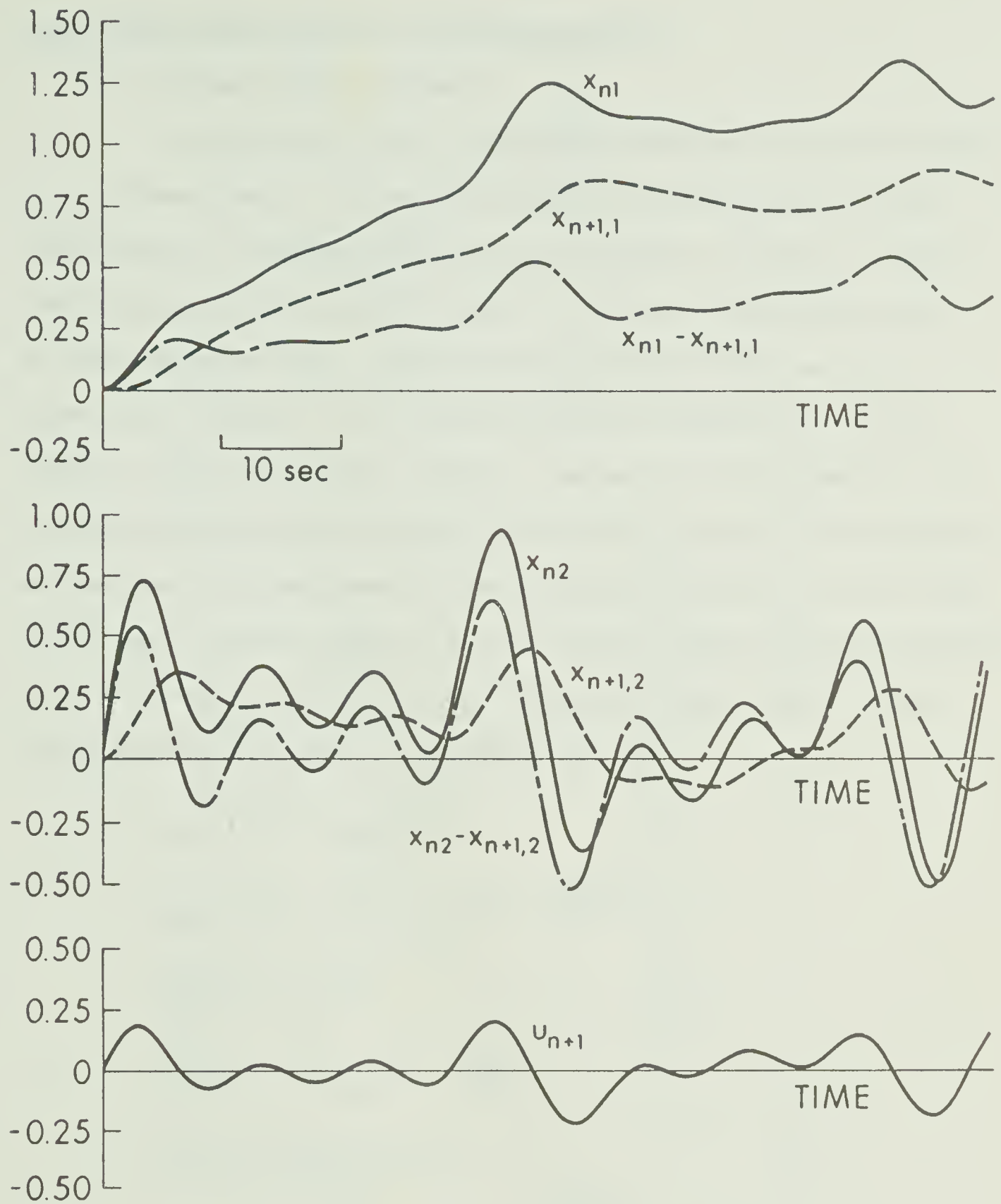


FIGURE 2.22 Results of Test 2 for System 7b

2.4 A Three-Vehicle Optimal Car-Following Unit

2.4.1 Mathematical Development

In this section the car-following problem will be formulated in a different way. A string of automatically-controlled vehicles travelling on a straight roadway will be assumed to consist of overlapping units of three vehicles each. A typical three-vehicle unit is shown in Figure 2.23. The $(n-1)$ th and $(n+1)$ th vehicles will be termed the "trailing" and "leading" vehicles respectively. The n th vehicle is the "controlled" vehicle. The motion of this vehicle will be affected by both the vehicle ahead and that behind. The assumptions and mathematical development of the equations of motion for the three-vehicle unit parallel those of the two-vehicle unit described in Section 2.3. The state equations for the three-vehicle unit can be written (using the same notation as in Section 2.3) as

$$\begin{aligned}
 \dot{x}_{n-1,1}(t) &= x_{n-1,2}(t) \\
 \dot{x}_{n-1,2}(t) &= -\frac{\bar{\mu}}{m} x_{n-1,2}(t) + \frac{u_{n-1}(t)}{m} \\
 \dot{x}_{n1}(t) &= x_{n2}(t) \\
 \dot{x}_{n2}(t) &= -\frac{\bar{\mu}}{m} x_{n2}(t) + \frac{u_n(t)}{m} \\
 \dot{x}_{n+1,1}(t) &= x_{n+1,2}(t) \\
 \dot{x}_{n+1,2}(t) &= -\frac{\bar{\mu}}{m} x_{n+1,2}(t) + \frac{u_{n+1}(t)}{m}
 \end{aligned} \tag{2.44}$$

which as before can be written in matrix form as

$$\underline{\dot{x}}(t) = \underline{A} \underline{x}(t) + \underline{B} \underline{u}(t) \tag{2.45}$$

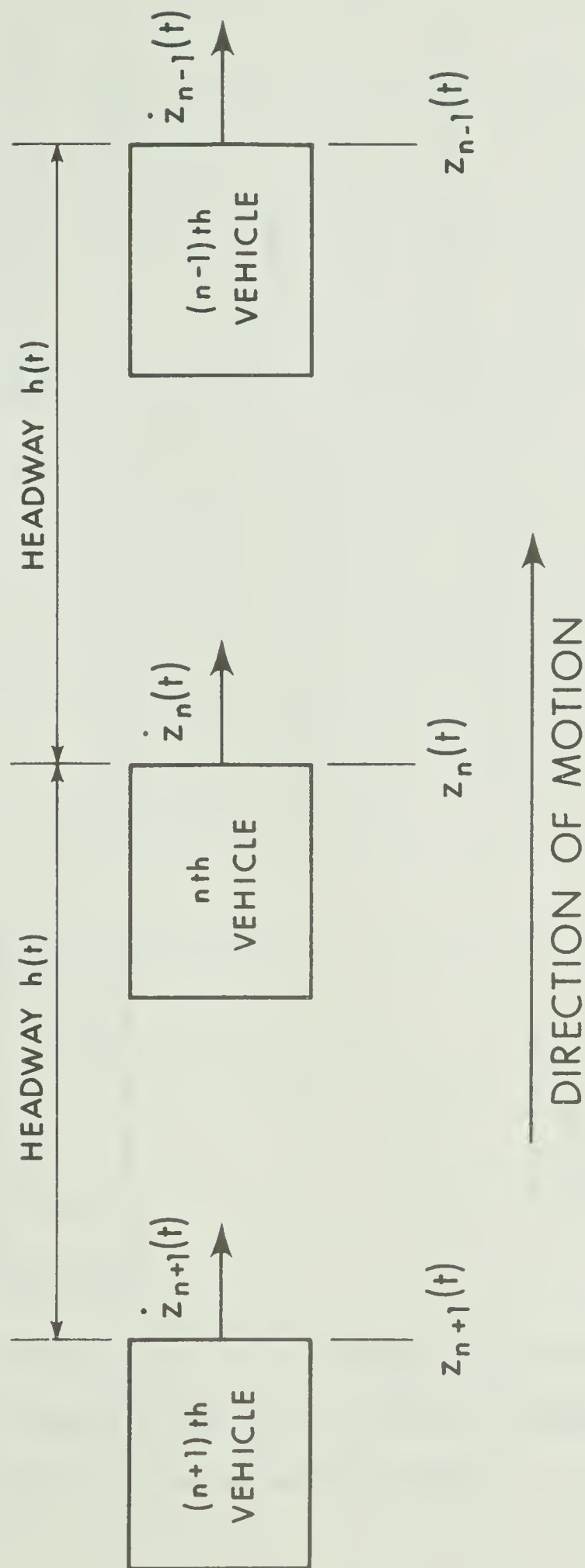


FIGURE 2.23 Three-Vehicle Basic Car-Following Unit

where

$$\underline{A} = \begin{bmatrix} 0 & 1 & 0 & 0 & 0 & 0 \\ 0 & -\frac{\mu}{m} & 0 & 0 & 0 & 0 \\ 0 & 0 & 0 & 1 & 0 & 0 \\ 0 & 0 & 0 & -\frac{\mu}{m} & 0 & 0 \\ 0 & 0 & 0 & 0 & 0 & 1 \\ 0 & 0 & 0 & 0 & 0 & -\frac{\tilde{\mu}}{m} \end{bmatrix} \quad (2.46)$$

$$\underline{B} = \begin{bmatrix} 0 & 0 & 0 \\ \frac{1}{m} & 0 & 0 \\ 0 & 0 & 0 \\ 0 & \frac{1}{m} & 0 \\ 0 & 0 & 0 \\ 0 & 0 & \frac{1}{m} \end{bmatrix} \quad (2.47)$$

$$\underline{x} = \begin{bmatrix} x_{n-1,1} \\ x_{n-1,2} \\ x_{n1} \\ x_{n2} \\ x_{n+1,1} \\ x_{n+1,2} \end{bmatrix} \quad \text{and} \quad \underline{u} = \begin{bmatrix} u_{n-1} \\ u_n \\ u_{n+1} \end{bmatrix} \quad (2.48)$$

The objectives of an automatic car-following system given in Chapter 1 can again be put in the form of a quadratic cost functional which is similar to that of equation (2.26).

$$\begin{aligned}
J = \int_0^{\infty} \left\{ \alpha_1 [x_{n+1,1}(t) - x_{n1}(t)]^2 + \alpha_2 [x_{n1}(t) - x_{n-1,1}(t)]^2 \right. \\
+ \beta_1 [x_{n+1,2}(t) - x_{n2}(t)]^2 + \beta_2 [x_{n2}(t) - x_{n-1,2}(t)]^2 \\
+ \rho_1 x_{n1}^2(t) + \rho_2 x_{n2}^2(t) + \gamma_1 u_{n+1}^2(t) + \gamma_2 u_n^2(t) \\
\left. + \gamma_3 u_{n-1}^2(t) \right\} dt \quad (2.49)
\end{aligned}$$

The philosophy underlying the choice of this cost functional as a performance index is the same as that for the two-vehicle unit. In this case, the system is penalized for headway and velocity deviations from desired values between the n th vehicle and that ahead and behind. In order to ensure that the n th vehicle reacts to the motion of the leading and trailing vehicles but not vice-versa, the control forces $u_{n-1}(t)$ and $u_{n+1}(t)$ must be made zero. This condition can be very nearly approximated by setting $\gamma_1 = \gamma_3 \gg \gamma_2$ in cost functional (2.49).

Equation (2.49) can be written in the form of (2.27), namely

$$J = \int_0^{\infty} [\underline{x}^T \underline{Q} \underline{x} + \underline{u}^T \underline{R} \underline{u}] dt \quad (2.50)$$

where

$$\underline{Q} = \begin{bmatrix} \alpha_1 & 0 & -\alpha_1 & 0 & 0 & 0 \\ 0 & \beta_1 & 0 & -\beta_1 & 0 & 0 \\ -\alpha_1 & 0 & \alpha_1 + \alpha_2 + \rho_1 & 0 & -\alpha_2 & 0 \\ 0 & -\beta_1 & 0 & \beta_1 + \beta_2 + \rho_2 & 0 & -\beta_2 \\ 0 & 0 & -\alpha_2 & 0 & \alpha_2 & 0 \\ 0 & 0 & 0 & -\beta_2 & 0 & \beta_2 \end{bmatrix} \quad (2.51)$$

$$\text{and } \underline{R} = \begin{bmatrix} \gamma_1 & 0 & 0 \\ 0 & \gamma_2 & 0 \\ 0 & 0 & \gamma_3 \end{bmatrix} \quad (2.52)$$

We are now in a position to solve for the optimal control $\underline{u}^*(t)$ which minimizes (2.49) for particular values for the matrices of \underline{A} , \underline{B} , \underline{Q} and \underline{R} .

2.4.2 Dynamic Performance

In this subsection the results of a study of the dynamic performance of the optimally-controlled three-vehicle basic unit will be reported. The optimal system was simulated using a PACE 231 analogue computer for a variety of weighting factors in the cost functional (2.49). As in the two-vehicle study, each vehicle was assumed to weigh 3220 lbs. and have a linear drag coefficient $\bar{\mu}$ of 1.7 lbf./ft./sec. The following three basic cost functionals were investigated.

Type 1 (Headway Type):

$$J_1 = \int_0^{\infty} [\alpha_1(x_{n+1,1} - x_{n1})^2 + \alpha_2(x_{n1} - x_{n-1,1})^2 + 10^4 u_{n+1}^2 + 0.1 u_n^2 + 10^4 u_{n-1}^2] dt \quad (2.53)$$

Type 2 (Velocity Type):

$$J_2 = \int_0^{\infty} [\beta_1(x_{n+1,2} - x_{n2})^2 + \beta_2(x_{n2} - x_{n-1,2})^2 + 10^4 u_{n+1}^2 + 0.1 u_n^2 + 10^4 u_{n-1}^2] dt \quad (2.54)$$

Type 3 (Combined):

$$J_3 = \int_0^{\infty} [\alpha_1(x_{n+1,1} - x_{n1})^2 + \alpha_2(x_{n1} - x_{n-1,1})^2 + \beta_1(x_{n+1,2} - x_{n2})^2 + \beta_2(x_{n2} - x_{n-1,2})^2 + 10^4 u_{n+1}^2 + 0.1 u_n^2 + 10^4 u_{n-1}^2] dt \quad (2.55)$$

The expenditure of control energy $u_{n+1}^2(t)$ and $u_{n-1}^2(t)$ by the trailing and leading vehicles was penalized in all cases a factor of 10^5 times greater than that by the "controlled" vehicle. This approximates the condition

$$\underline{u}^*(t) = u_n^*(t) \quad (2.56)$$

As a result of (2.56), only the controlled vehicle will react to disturbances in the motion of any of the three vehicles.

The optimal control strategy for the three-vehicle unit is obtained by solving an algebraic Riccati equation as in the two-vehicle case. The resulting control for the n th vehicle is of the form.

$$\begin{aligned} u_n^*(t) = & L_1^* x_{n+1,1}(t) + L_2^* x_{n+1,2}(t) \\ & + L_3^* x_{n1}(t) + L_4^* x_{n2}(t) \\ & + L_5^* x_{n-1,1}(t) + L_6^* x_{n-1,2}(t) \end{aligned} \quad (2.57)$$

The closed loop optimal control system for the three-vehicle unit is shown in Figure 2.24. Table 2.3 gives the values of the optimal feedback gains for the three groups of cost functionals given by (2.53), (2.54) and (2.55). The analogue simulation diagram for the closed loop system is shown in Figure 2.25.

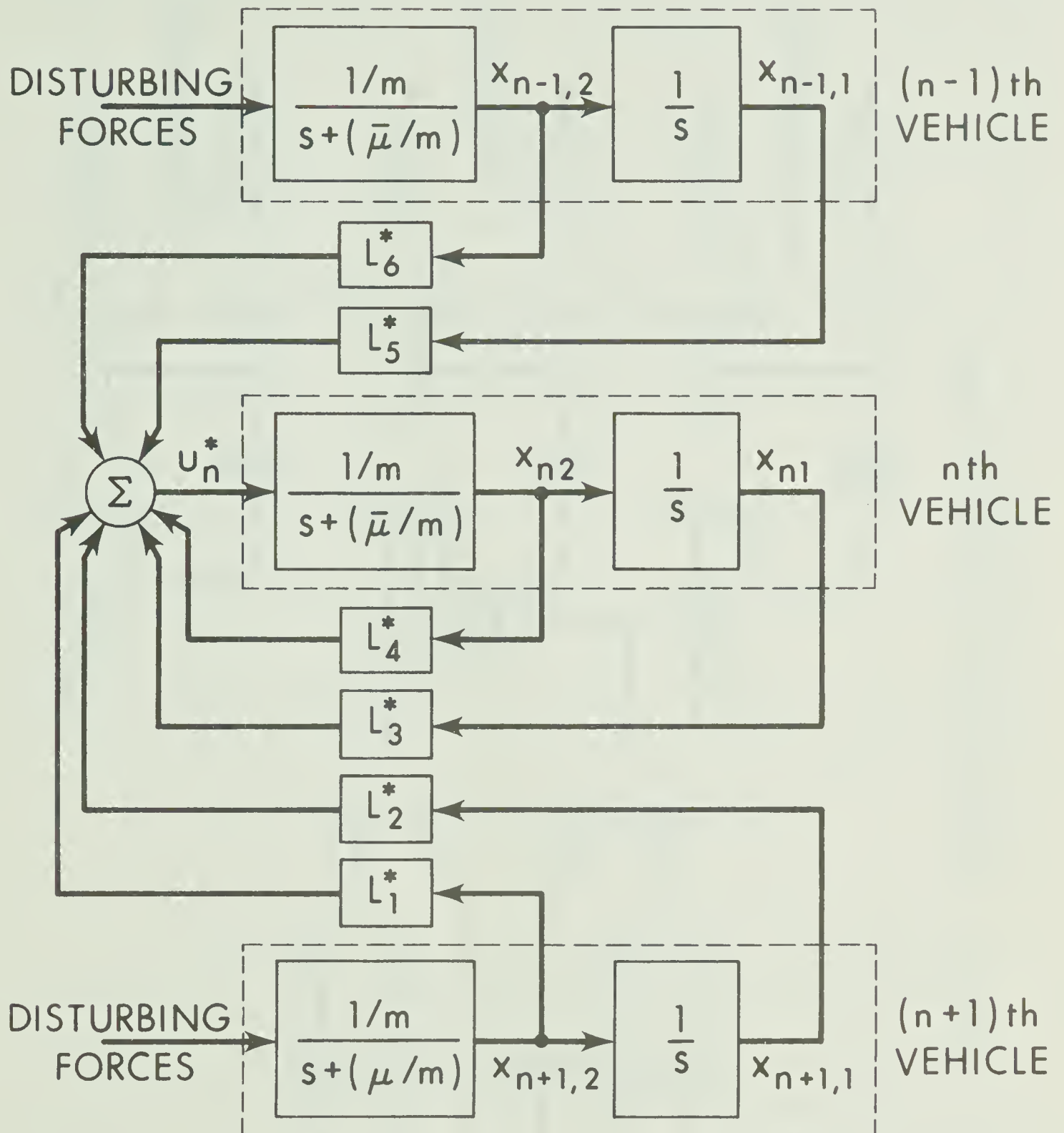


FIGURE 2.24 Block Diagram of Three-Vehicle Optimal Feedback System

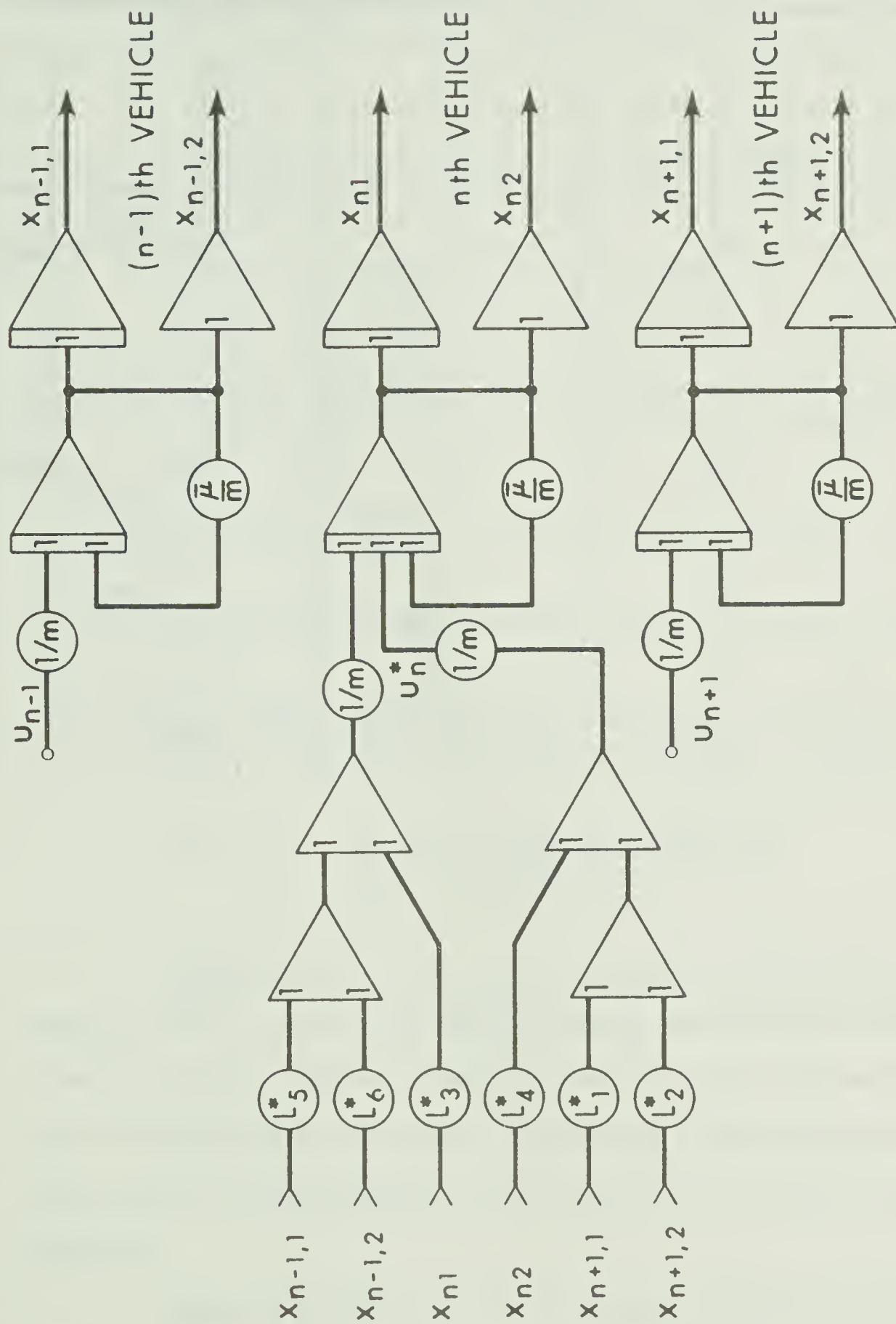


FIGURE 2.25 Analogue Simulation Diagram for Three-Vehicle Car-Following System

1	$\alpha_1 = \alpha_2$	L_1^*	L_2^*	L_3^*	L_4^*	L_5^*	L_6^*
a	1	2.236	14.13	-4.472	-28.25	2.236	14.13
b	10	7.071	25.75	-14.14	-51.51	7.071	25.75
c	100	22.36	46.44	-44.72	-92.89	22.36	46.44
2	$\beta_1 = \beta_2$						
a	1	0	1.542	0	-3.084	0	1.542
b	10	0	6.272	0	-12.54	0	6.272
c	100	0	21.53	0	-43.05	0	21.53
3							
a	$\alpha_1 = \alpha_2 = 1$ $\beta_1 = \beta_2 = 1$	2.236	14.29	-4.472	-28.59	2.236	14.29
b	$\alpha_1 = \alpha_2 = 1$ $\beta_1 = \beta_2 = 10$	2.236	15.71	-4.472	-31.43	2.236	15.71
c	$\alpha_1 = \alpha_2 = 1$ $\beta_1 = \beta_2 = 100$	2.236	26.06	-4.472	-52.13	2.236	26.06

Table 2.3 Tabulation of Feedback Gains for the Three-Vehicle Unit

Figures 2.26 to 2.30 show the results of simulating the n th vehicle to have, first, an initial offset in position error and, second, an initial offset in velocity error. These figures thus give some indication as to the manner in which the controlled vehicle restores itself to the equilibrium position from an initial offset condition.

Figure 2.26 shows the position error for the n th vehicle as a function of time for three systems of type 1. As was the case with the two-vehicle unit, increased weighting on the headway deviation

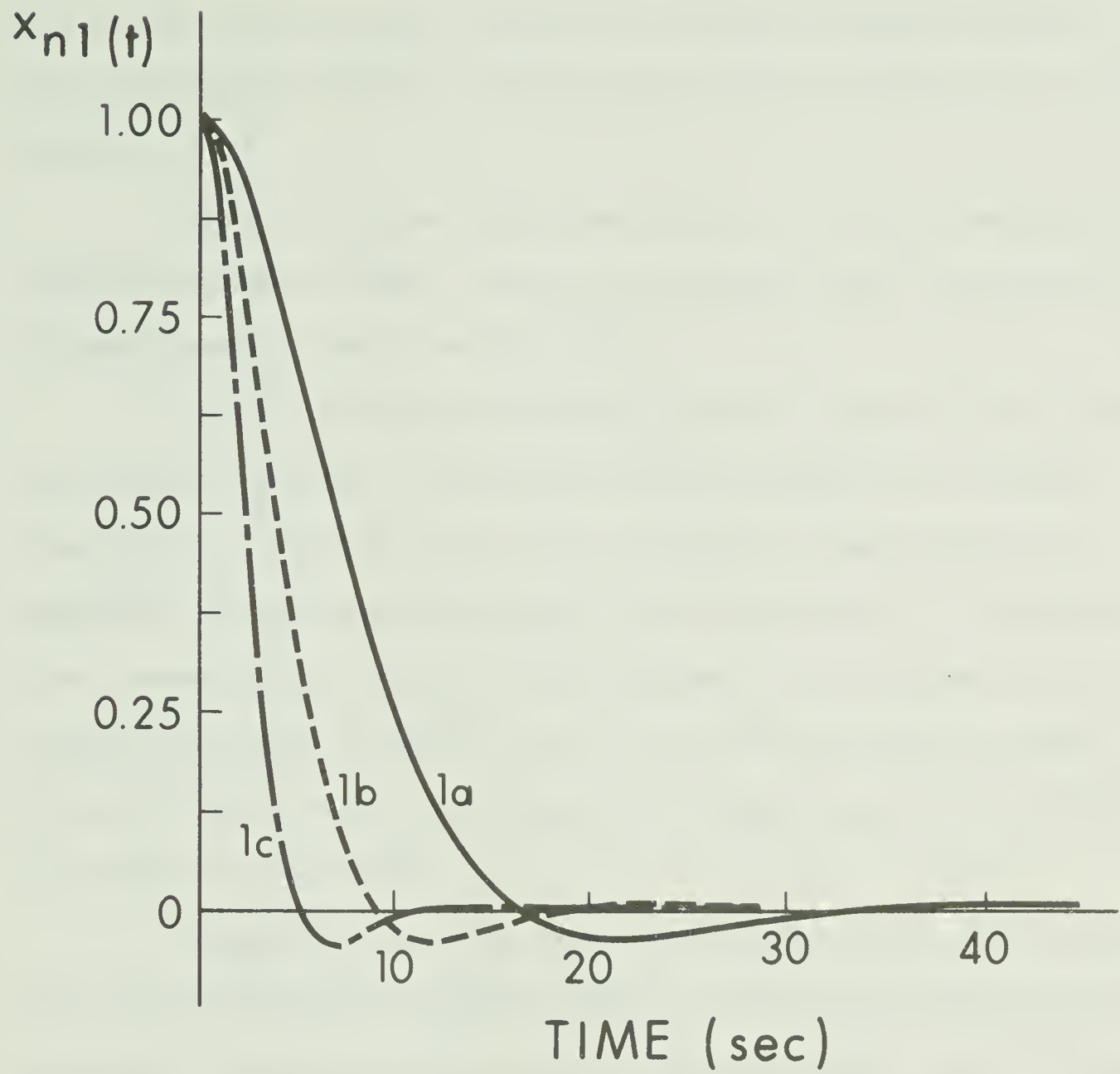


FIGURE 2.26 Position Error Response of the nth Vehicle (Systems 1a, 1b and 1c) to an Initial Offset in Position Error

term in the cost functional results in a reduced transient response time accompanied by higher velocity and greater expenditure of control energy.

Figure 2.27 shows the velocity error of the n th vehicle for an initial positive offset. Again, the response time is shortened by increased penalization of headway error.

Figure 2.28 shows the velocity error of the n th vehicle for three systems of type 2. Comparison with the same test on system 1 (Figure 2.27) indicates that system 2 exhibits a greater degree of damping while retaining the variable rise time feature. It should be noted, however, that like two-vehicle system 3, this system will not respond to position errors as long as the relative velocity between vehicles is zero. This is the result of feedback gains L_1^* , L_3^* and L_5^* being zero (see Table 2.3).

Figures 2.29 and 2.30 show the position and velocity errors respectively for three systems of type 3. System 3a is nearly identical to system 1a (as was system 1a to 2a in the two-vehicle case). Increased weighting on the relative velocity term in the cost functional has the effect of slowing the position error response and reducing the peak value of velocity exhibited by the n th vehicle.

2.5 Comparison of the Two and Three-Vehicle Systems

From examination of the simulation results for the two and three-vehicle systems, several observations can be made:

1. The structure of the cost functional for both systems was the same and thus one would expect the systems to exhibit similar dynamic behaviour for similar weighting factors in the cost

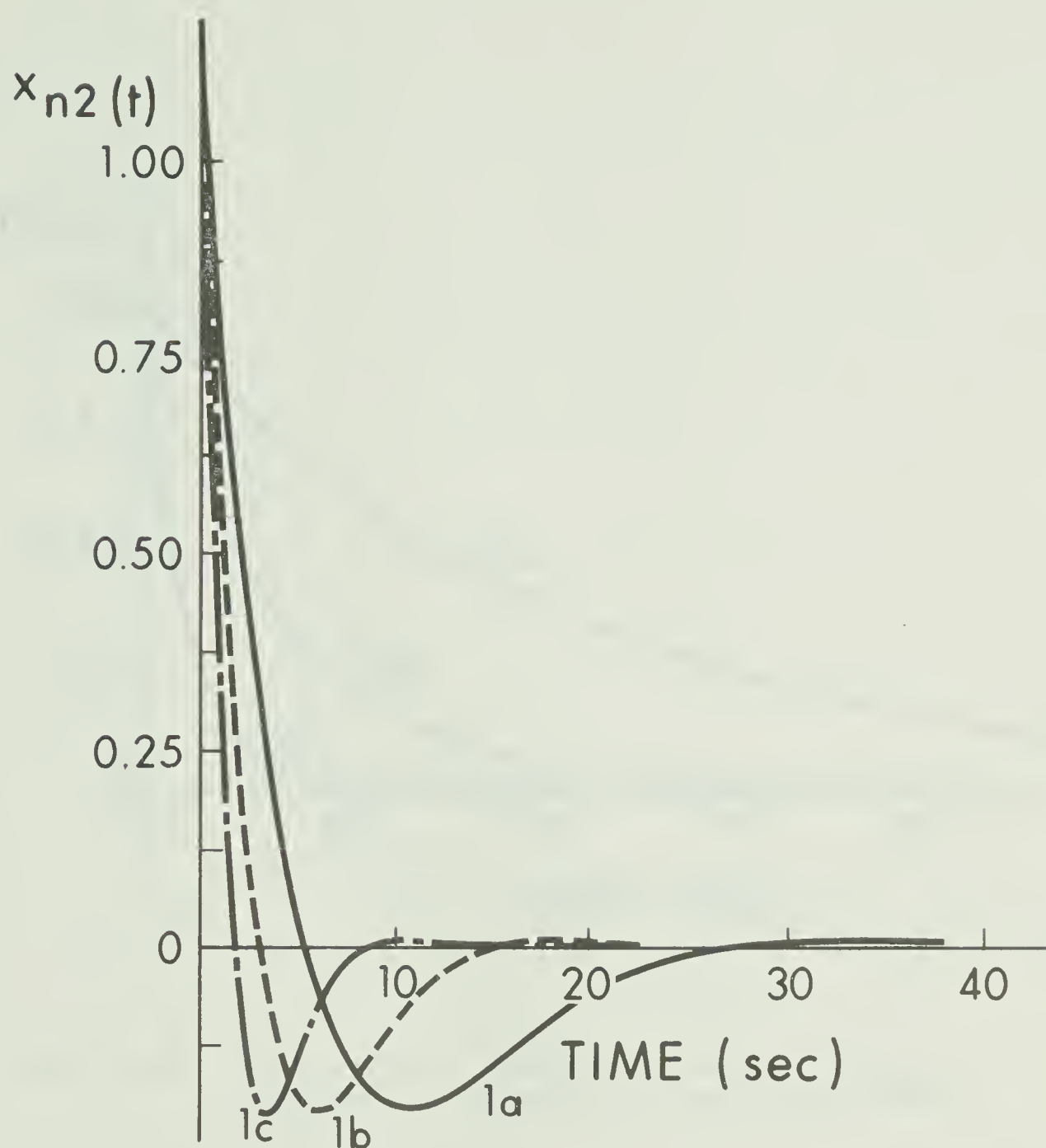


FIGURE 2.27 Velocity Error Response of the n th Vehicle (Systems 1a, 1b and 1c) to an Initial Offset in Velocity Error

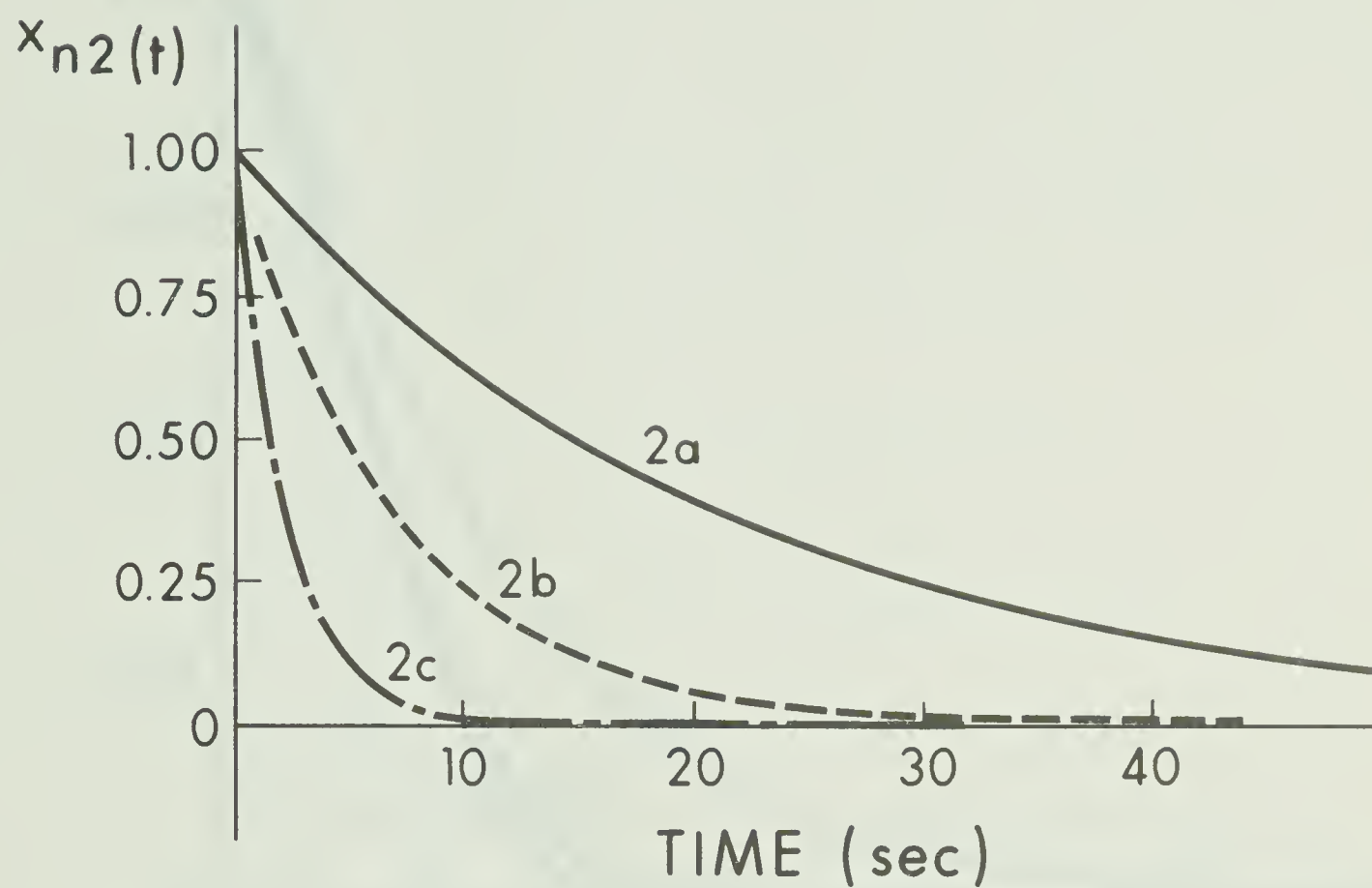


FIGURE 2.28 Velocity Error Response of the n th Vehicle (Systems 2a, 2b and 2c) to an Initial Offset in Velocity Error

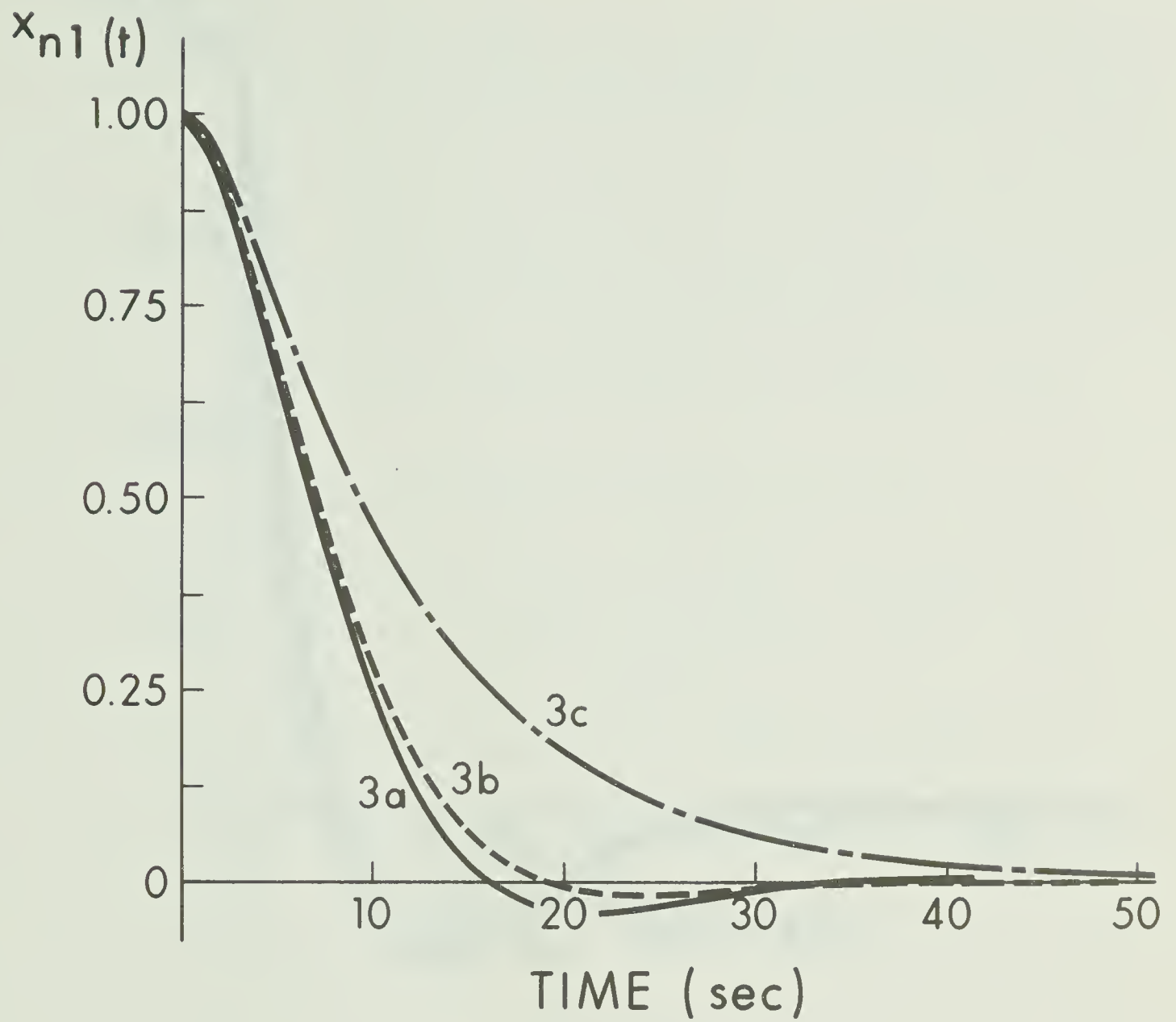


FIGURE 2.29 Position Error Response of the nth Vehicle (Systems 3a, 3b and 3c) to an Initial Offset in Position Error

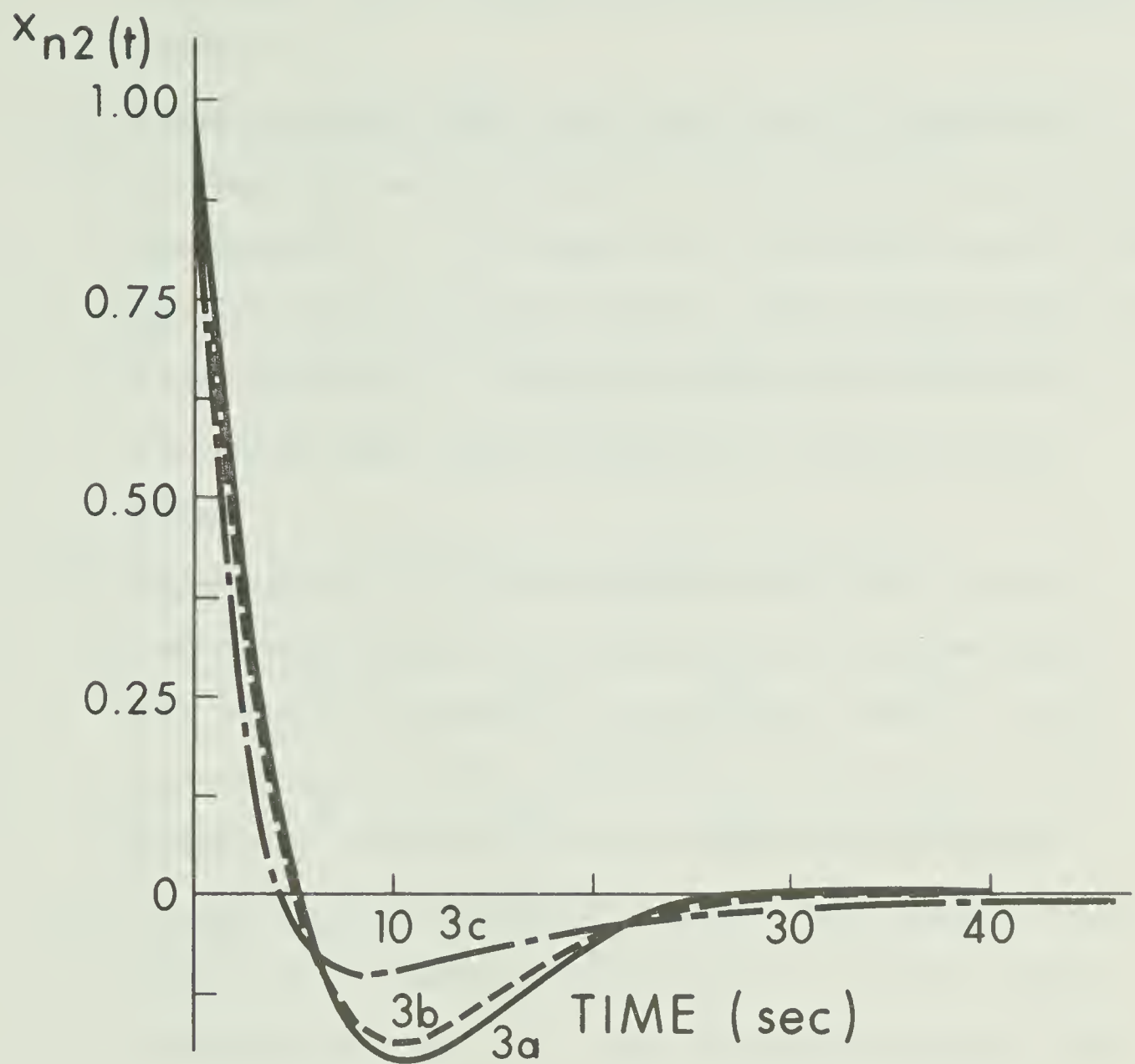


FIGURE 2.30 Velocity Error Response of the n th Vehicle (Systems 3a, 3b and 3c) to an Initial Offset in Position Error

functional. This is indeed true as indicated in the previous section.

2. The tests reported above only explore the local behaviour of the respective units and say little about the string behaviour (see Chapter 3). It is evident that both systems exhibit local stability of the controlled vehicle. This is true for all cost functionals and is a consequence of the inherent stability of the optimal state regulator used as the feedback control system.
3. Implementation of the three-vehicle system would require a communication system of approximately twice the capacity of that required to implement the two-vehicle system. That is, each vehicle in a string would receive velocity and position information from both the vehicle ahead and that behind.
4. It would seem that information received from a vehicle behind would be useful under some circumstances. One such case is illustrated in Figure 2.31. Here the position errors of the $(n+1)$ th and $(n-1)$ th vehicles have constant values of 1.0 and -0.5 units respectively. The control action of the n th vehicle results in a constant position error of +0.25 units as a steady-state condition. This results in equal spacing between the three vehicles. In the case of the two-vehicle system this type of behaviour would not be observed. Thus if a vehicle in a string had some positive position (or velocity) error, the vehicles ahead would show no change of state. This is an undesirable characteristic from the safety standpoint. The above-noted behaviour is closely tied in with the asymptotic

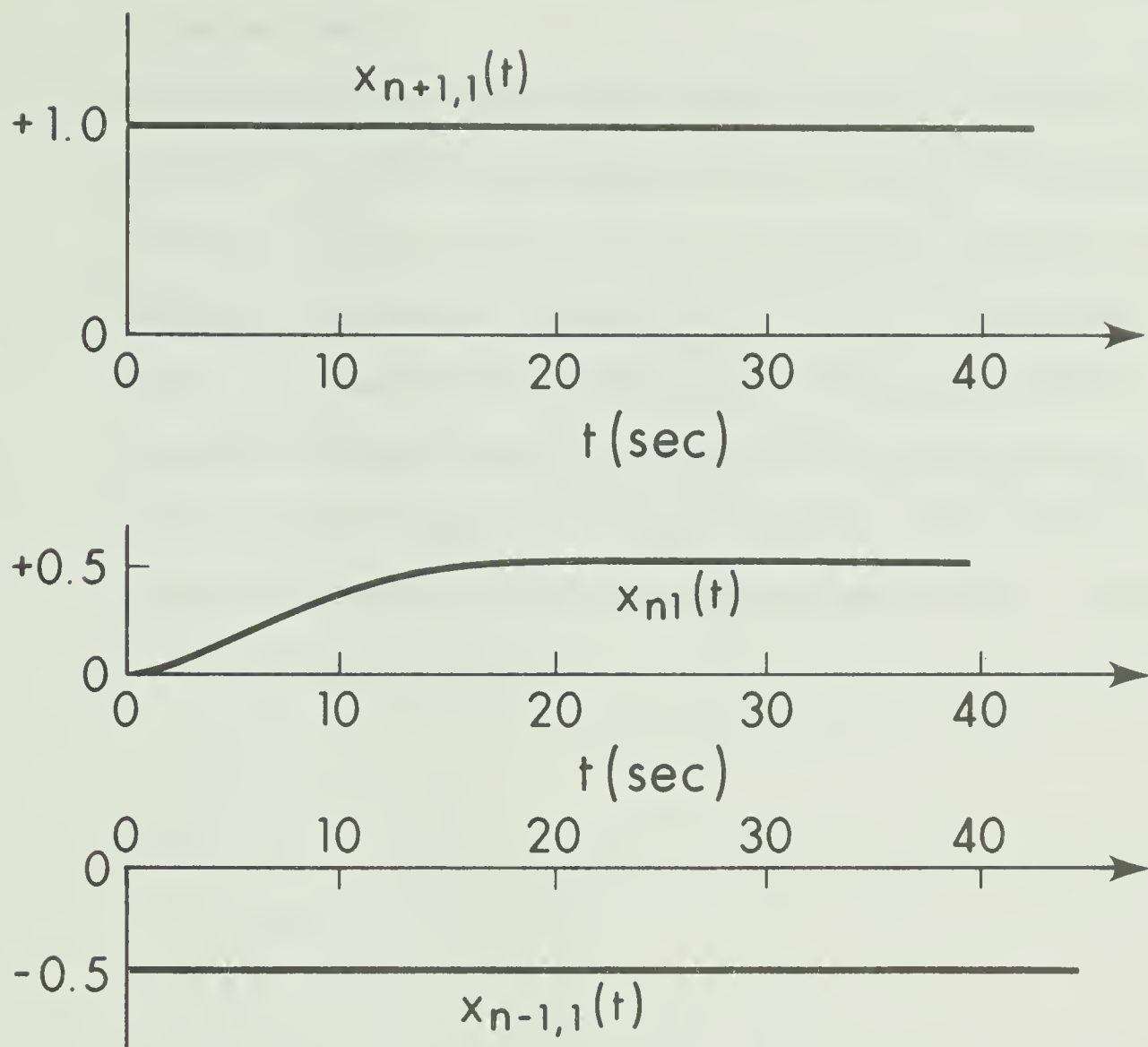


FIGURE 2.31 Position Error Response of the n th Vehicle to Offset in the Position Errors of the $(n-1)$ th and $(n+1)$ th Vehicles

behaviour of the two systems which will be discussed in the following chapter.

5. Both systems developed in this chapter could be modified to make use of optimal sampled-data control theory. The method used would parallel that of Levis and Athans^[8] who have investigated the optimal sampled-data control of high-speed trains. A sampled-data car-following system would have the advantage of being compatible with position-sensing devices placed on the roadway at discrete intervals. The continuous sensing of vehicle separation would require the use of radar or other similar technique.

REFERENCES

1. D.C. Gazis, R. Herman and R.B. Potts, "Car Following Theory of Steady-State Traffic Flow", *Ops. Res.*, Vol. 7, pp. 499-505, 1959.
2. R. Herman, E.W. Montroll, R.B. Potts and R.W. Rothery, "Traffic Dynamics: Analysis of Stability in Car Following", *Ops. Res.*, Vol. 7, pp. 86-106, 1959.
3. E. Kometani and T. Sasaki, "On the Stability of Traffic Flow", *J. Ops. Res. (Japan)*, Vol. 2, pp. 11-26, 1958.
4. R.E. Fenton and J.G. Bender, "A Study of Automatic Car Following", *I.E.E.E. Trans. Vehicular Technology*, Vol. VT-18, pp. 134-140, Nov. 1969.
5. W.S. Levine and M. Athans, "On the Optimal Error Regulation of a String of Moving Vehicles", *I.E.E.E. Trans. Auto Control*, Vol. AC-11, pp. 355-361, July 1966.
6. L.E. Peppard and V. Gourishankar, "Optimal Control of a String of Moving Vehicles", *I.E.E.E. Trans Auto. Control*, Vol. AC-15, pp. 386-387, June 1970.
7. M. Athans and P. Falb, "Optimal Control", Chapter 9, pp. 771-782, McGraw Hill, 1966.
8. A.H. Levis and M. Athans, "On the Optimal Sampled Data Control of Strings of Vehicles", *Transportation Science*, Vol. 1, pp. 362-382.

CHAPTER 3

ASYMPTOTIC STABILITY OF OPTIMALLY-CONTROLLED
STRINGS OF VEHICLES3.1 Introduction

In Chapter 2, the optimal controllers for two and three-vehicle basic car-following units were derived. The dynamic behaviour of the optimally-controlled units was studied by means of analogue computer simulation for a variety of cost functionals. It was pointed out that, in order to be useful in a practical situation, the optimal control strategies developed for the basic units must be applied to a string of many vehicles. This can be done by considering a string of vehicles to be made up of overlapping two or three-vehicle subsystems as the case may be.

A question which often arises in optimal control studies is concerned with the stability of the optimally-controlled systems. As is well known, there are several definitions of stability. In the present study, we will be concerned with the asymptotic stability of an optimally-controlled string of vehicles. It will be recalled from the discussion in Chapter 1 that asymptotic stability refers to the manner in which perturbations in the motion of one vehicle in a string are propagated down the string. A quantitative and more precise definition follows:

Defn: Consider a string of vehicles travelling along a roadway. Suppose one of the vehicles (say the n th) experiences a perturbation

in its motion. The string of vehicles is said to be asymptotically stable if the position of the $(n+1)$ th vehicle (the vehicle immediately behind the n th vehicle) does not exceed the position of the n th vehicle. In other words

$$z_{n+1}(t) \leq z_n(t) \quad \text{for all } t \quad (3.1)$$

where z indicates the position of a vehicle measured with respect to a fixed coordinate system.

In terms of position error, (3.1) can be written

$$x_{n+1,1}(t) + \hat{z}_{n+1}(t) \leq x_{n1}(t) + \hat{z}_n(t) \quad (3.2)$$

$$\text{or } x_{n+1,1}(t) - x_{n1}(t) \leq \hat{z}_n(t) - \hat{z}_{n+1}(t) \quad (3.3)$$

$$x_{n+1,1}(t) - x_{n1}(t) \leq \hat{h} \quad (3.4)$$

where \hat{z} is the scheduled position, \hat{h} is the scheduled headway and the position errors, $x_{.1}$, are as defined in Chapter 2. Theoretically, \hat{h} can approach zero although in practice it can never be less than the vehicle length.

In order to make the determination of the asymptotic stability of the optimally-controlled strings more convenient, analysis will be carried out in the frequency domain. Cosgriff^[1] has shown that a necessary and sufficient condition for asymptotic stability expressed in the frequency domain is

$$|G_{n+1}(j\omega)| = \left| \frac{X_{n+1,1}(j\omega)}{X_{n1}(j\omega)} \right| \leq 1 \quad \text{for all } \omega \text{ and } n \quad (3.6)$$

where $X_{n+1,1}(j\omega)$ and $X_{n1}(j\omega)$ are the Fourier transforms of the position errors of the $(n+1)$ th and n th vehicles respectively. Details of the proof of (3.6) are given in Appendix 3-1. If for a given string of vehicles, a general expression for the transfer function $G_{n+1}(j\omega)$, valid for all n , can be found, then the asymptotic stability of the string can be determined without actually simulating the vehicle string. When the string consists of a large number of vehicles this is an important advantage.

In Section 3.2 the asymptotic stability of three classical car-following feedback systems considered by other investigators will be reviewed in the light of the frequency domain definition given above.

In Section 3.3 the asymptotic stability of a string of four vehicles optimally controlled according to the strategy developed for the two-vehicle basic unit will be studied. Some preliminary results of this study are reported in [2]. The position error transfer function between any two vehicles in the string will be derived and the frequency response of the system examined for violation of the definition given in (3.6). The study will be carried out using the various cost functionals considered in Chapter 2.

In Section 3.4 a similar study will be carried out using the control strategy developed for the three-vehicle basic unit. The results for a given cost functional will be verified by simulation of a string of five vehicles.

In Section 3.5 the effects of a time delay in the control

loop on the asymptotic behaviour of an optimally-controlled vehicle string will be investigated by analogue computer simulation of a four-vehicle string based on the three-vehicle basic unit.

The chapter concludes with a discussion in Section 3.6 of the results reported in the preceding sections of the chapter.

3.2 Asymptotic Stability of Three Classical Car-Following Feedback Systems

In Chapter 1, three alternative classical feedback control systems for the automatic control of vehicle strings were discussed. In Chapter 2, the transfer functions relating the positions of successive vehicles in a string were developed. The conditions for which periodic disturbances in the motion of one vehicle would be attenuated as they propagated down the string were derived. It can easily be seen that these conditions are the same as those dictated by equation (3.6) to guarantee asymptotic stability of a string of vehicles. The control laws, transfer functions and asymptotic stability requirements for the three classical systems are presented below.

1. Relative Motion Car-Following System

(a) control law:

$$\ddot{z}_{n+1} = K_v(\dot{z}_n - \dot{z}_{n+1}) + K_d(z_n - z_{n+1} - \hat{h}) \quad (3.7)$$

(b) magnitude of transfer function:

$$|G_{n+1}(\omega)| = \frac{|Z_{n+1}(\omega)|}{|Z_n(\omega)|} = \left[\frac{K_d^2 + K_v^2 \omega^2}{(K_d - \omega^2)^2 + K_v^2 \omega^2} \right]^{\frac{1}{2}} \quad (3.8)$$

(c) criterion for asymptotic stability:

$$0 < \omega < (2K_d)^{\frac{1}{2}} \quad (3.9)$$

2. Relative Position Car-Following System

(a) control law:

$$\ddot{z}_{n+1} = K_v(v_s - \dot{z}_{n+1}) + K_d(z_n - z_{n+1} - \hat{h}) \quad (3.10)$$

(b) magnitude of transfer function:

$$|G_{n+1}(\omega)| = \left[\frac{K_d^2}{(K_d - \omega^2)^2 + K_v^2 \omega^2} \right]^{\frac{1}{2}} \quad (3.11)$$

(c) criterion for asymptotic stability:

$$\frac{K_v}{2(K_d)^{\frac{1}{2}}} \geq 0.7072 \quad (3.12)$$

3. Bender and Fenton^[3] Car-Following System

(a) control law:

$$\ddot{z}_{n+1} = K_v(\dot{z}_n - \dot{z}_{n+1}) + K_d(z_n - z_{n+1} - \hat{h} - k_1 \dot{z}_n - k_2 \dot{z}_{n+1}) \quad (3.13)$$

(b) magnitude of transfer function:

$$|G_{n+1}(\omega)| = \left[\frac{K_d^2 + (K_v - K_d k_1)^2 \omega^2}{(K_d - \omega^2)^2 + (K_v + K_d k_2)^2 \omega^2} \right]^{\frac{1}{2}} \quad (3.14)$$

(c) criterion for asymptotic stability:

$$\left[\frac{(K_v + K_d k_2)^2}{4K_d} - \frac{(K_v - K_d k_1)^2}{4K_d} \right]^{\frac{1}{2}} \geq 0.7072 \quad (3.15)$$

The criteria for asymptotic stability for the above systems were obtained by applying the requirement given by (3.6) to the transfer function magnitude equations (3.8), (3.11) and (3.14). Examination of the above criteria indicates that the relative motion feedback system

is not asymptotically stable according to (3.6) since $|G_{n+1}(\omega)|$ is not less than or equal to unity for all ω . The relative position and Bender and Fenton feedback systems are asymptotically stable providing the feedback gains satisfy the relations (3.12) and (3.15) respectively. Thus in designing a car-following system of either of these types, two factors would influence the choice of feedback gains. First, one would choose gains which would result in the desired dynamic behaviour of a two-vehicle component of the string and second, one would check whether or not this choice resulted in asymptotic stability of the entire vehicle string. Some compromise might be necessary to ensure both asymptotic stability and the desired dynamic behaviour of the string.

3.3 Asymptotic Stability of an Optimally-Controlled Vehicle String

Using the Two-Vehicle Basic Unit

The manner in which the control strategy developed for the two-vehicle unit can be applied to a multi-vehicle string will now be considered. The optimal feedback system for the two-vehicle unit is shown in Figure 2.4. It should be remembered that the control force on the leading vehicle must be made nearly equal to zero by choice of appropriate weighting factors in the cost functional for the system. The block diagram for the two-vehicle unit (in a simplified form) is shown in Figure 3.1. The feedback gain matrices are given by

$$\underline{L}_1^* = \begin{bmatrix} L_3^* & L_4^* \end{bmatrix} \quad \underline{L}_2^* = \begin{bmatrix} L_1^* & L_2^* \end{bmatrix} \quad (3.16)$$

where L_1^* , L_2^* , L_3^* and L_4^* are given by (2.43) and the vehicle state vectors by

$$\underline{x}_n = \begin{bmatrix} x_{n1} \\ x_{n2} \end{bmatrix} \quad \underline{x}_{n+1} = \begin{bmatrix} x_{n+1,1} \\ x_{n+1,2} \end{bmatrix} \quad (3.17)$$

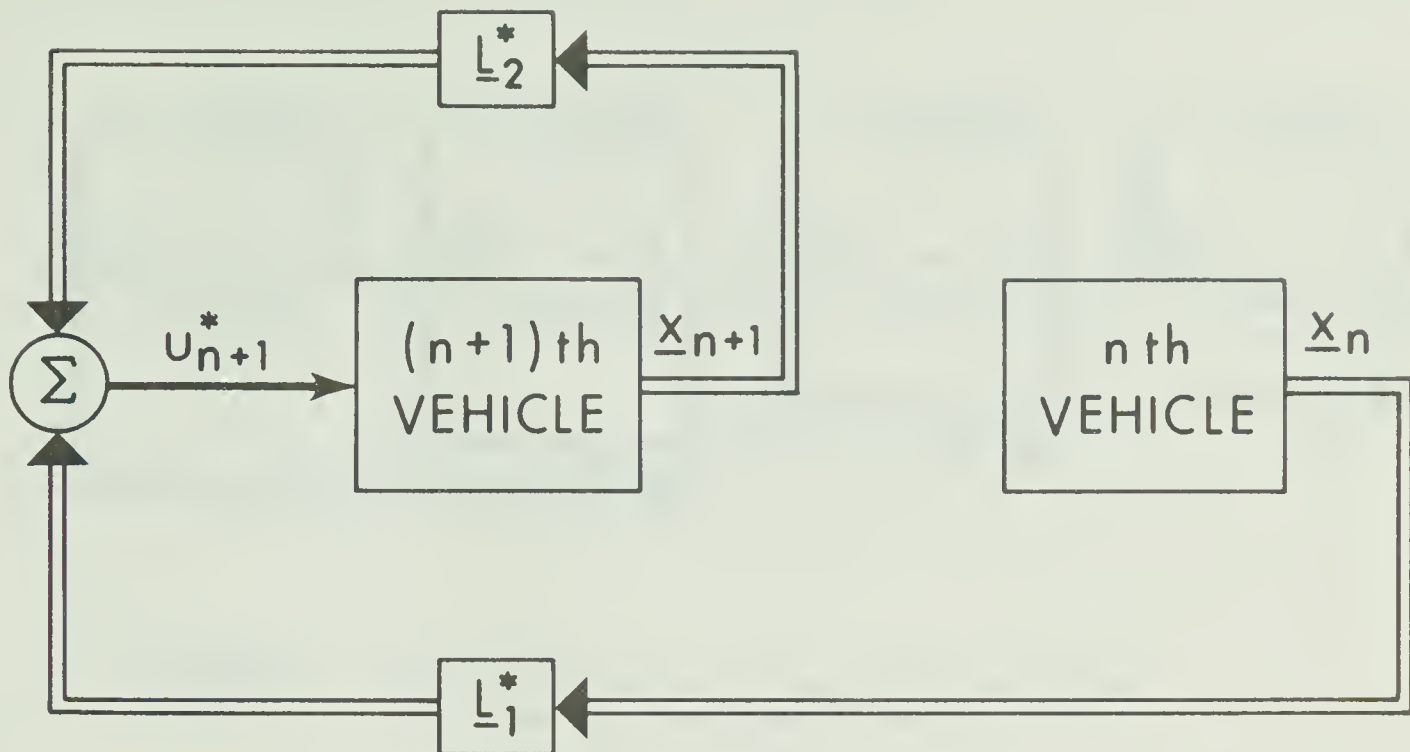


FIGURE 3.1 A Simplified Block Diagram of the Two-Vehicle Basic Unit

By overlapping three of the two-vehicle units shown in Figure 3.1, a four-vehicle string of optimally-controlled vehicles can be formed as shown in Figure 3.2. The control force for the first vehicle is dependent only on its own state (as if the vehicle ahead of it exhibited no error in position or velocity). Since each pair of vehicles in the string exhibits the car-following behaviour of the two-vehicle basic unit, the local stability of the system is assured. Knowing the vehicle dynamics and the optimal feedback gains, it is now possible to write a transfer function relating the position errors of any two successive vehicles. This transfer function will be identical between all pairs of vehicles. The signal flow graph for the two-vehicle unit of Figure 3.1 is shown in Figure 3.3. Using Mason's Rule,

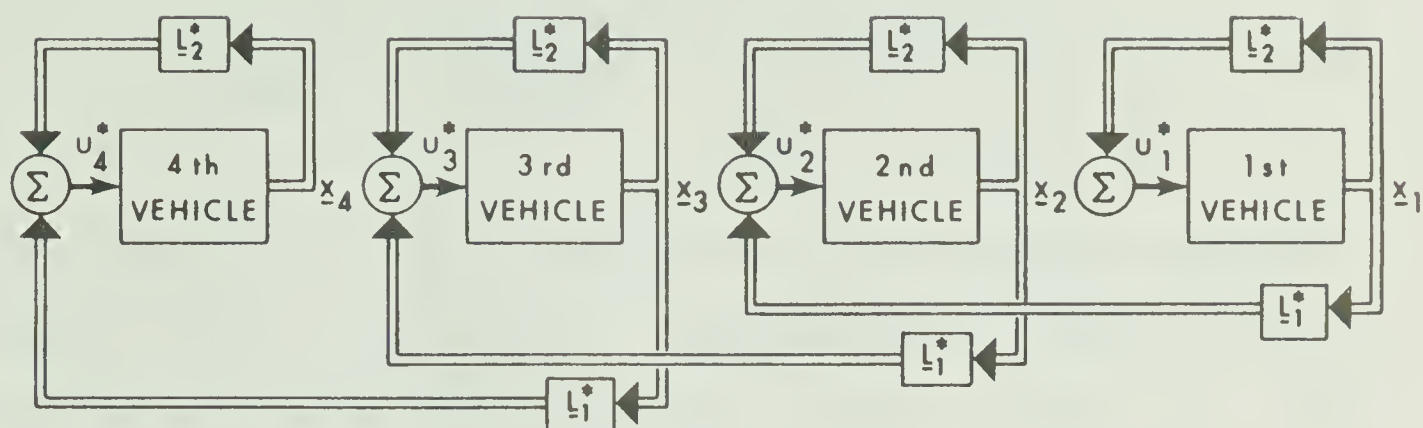


FIGURE 3.2 Block Diagram of a Four-Vehicle String Based on the Two-Vehicle Unit

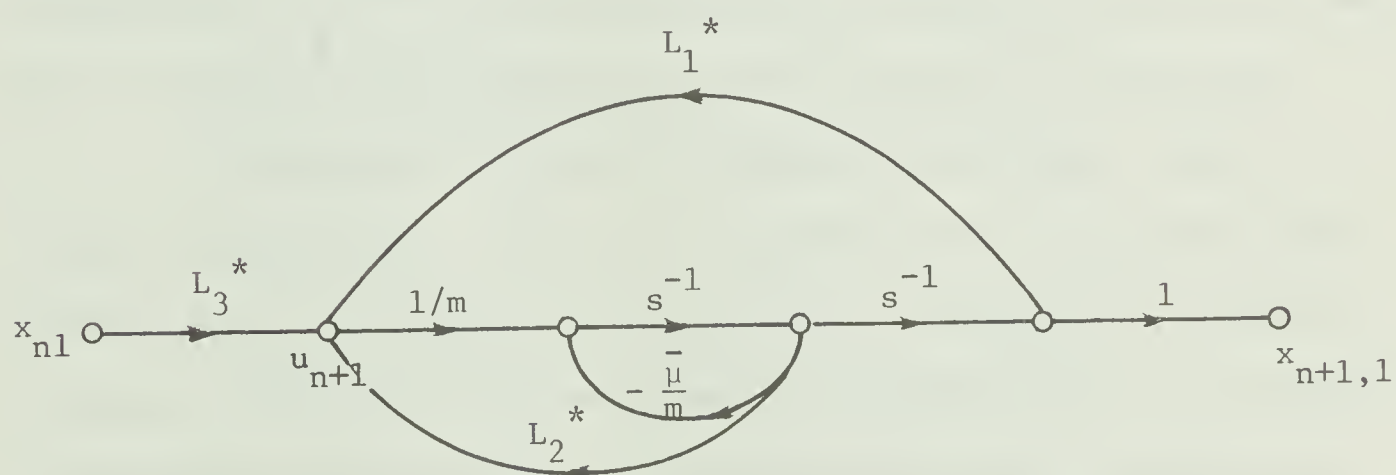


FIGURE 3.3 Signal Flow Graph for an Optimally-Controlled Two-Vehicle Unit

the transfer function $G_{n+1}(j\omega)$ can be written

$$G_{n+1}(j\omega) = \frac{X_{n+1,1}(j\omega)}{X_{n1}(j\omega)} = \frac{-L_3^*/m}{\frac{L_1^*}{m} + \omega^2 - j\omega(\frac{\bar{\mu}}{m} - \frac{L_2^*}{m})} \quad (3.18)$$

From Table 2.2, it can be seen that for all the systems considered, both L_1^* and L_2^* are negative. Hence the transfer function (3.18) is that of a second order system with resonant frequency $\omega_o = (\frac{-L_1^*}{m})^{1/2}$ and damping factor $\zeta = (\frac{\bar{\mu}}{m} - \frac{L_2^*}{m})/2(\frac{-L_1^*}{m})^{1/2}$. Equation (3.18) can then be written in the form

$$G_{n+1}(j\omega) = \frac{L_3^*/m}{\omega_o^2 - \omega^2 + j\omega(2\zeta\omega_o)} \quad (3.19)$$

Table 3.1 gives the values of $G(0)$, ζ and ω_o for the various systems corresponding to Table 2.2. Since system type 3 has no position error feedback ($L_1^* = L_3^* = 0$), the definition of asymptotic stability used here is not applicable and hence no data is given for this case.

From Table 3.1 it can be seen that the maximum value of $|G(j\omega)|$ evaluated at $\omega = 0$ for any system is unity. Also the lowest damping factor is 0.7072, the condition for maximally-flat frequency response. Hence it can be concluded that system types 1 to 7 satisfy requirement (3.6) and thus are asymptotically stable. It was concluded from the tests reported in Chapter 2 that system types 2 and 4 best met the requirements of an automatic car-following system. The remainder of the discussion in this section will therefore be confined to these two systems.

The magnitude of the transfer function $|G(j\omega)|$ for these two

System Type	$G(0)$	ζ	ω_o
1a($\alpha=1$)	1.0	0.707	0.178
2a($\alpha=1$)	1.0	0.707	0.178
2b($\alpha=5$)	1.0	0.707	0.266
2c($\alpha=10$)	1.0	0.707	0.316
2d($\alpha=100$)	1.0	0.707	0.564
2e($\alpha=500$)	1.0	0.707	0.840
2f($\alpha=1000$)	1.0	0.707	0.974
3a($\beta=1$)	—	—	—
3b($\beta=5$)	—	—	—
3c($\beta=10$)	—	—	—
3d($\beta=100$)	—	—	—
4a($\beta=1$)	1.0	0.707	0.178
4b($\beta=100$)	1.0	1.12	0.178
4c($\beta=1000$)	1.0	2.90	0.178
4d($\beta=1600$)	1.0	3.59	0.178
4e($\beta=10^5$)	1.0	37.7	0.133
5a($\alpha=\beta=1$)	1.0	0.707	0.178
5c($\alpha=\beta=10$)	1.0	0.725	0.316
5d($\alpha=\beta=100$)	1.0	0.760	0.562
5e($\alpha=\beta=1000$)	1.0	0.865	1.00
6a($\rho_4=0$)	1.0	0.707	0.178
6b($\rho_4=20$)	1.0	0.817	0.178
6c($\rho_4=100$)	1.0	1.14	0.177
6d($\rho_4=1000$)	1.0	3.28	0.166
7a($\rho_3=0$)	1.0	0.707	0.178
7b($\rho_3=0.5$)	0.656	0.707	0.197
7c($\rho_3=2$)	0.328	0.707	0.234
7d($\rho_3=10$)	0.090	0.707	0.324
7e($\rho_3=50$)	0.0195	0.707	0.475

Table 3.1 Tabulation of ζ and ω_o for a String of Vehicles Based on the Two-Vehicle Unit

systems is plotted vs. frequency ω in Figures 3.4 and 3.5 respectively. In Figure 3.4 the effects of varying α on the frequency response is illustrated. As was seen from test 1 in Chapter 2, the effect of increasing α for system type 2 was to shorten the response time to a step. This is reflected in Figure 3.4 as an increase in bandwidth for the transfer function $G(j\omega)$ when α is increased. It should be noted that in Table 3.1, varying α does not affect the damping factor. This is also evident from Figure 3.4. The effect of increasing β for system type 4 is shown in Figure 3.5. For $\beta \leq 1600$, the effect of increasing β is to increase the system damping without altering the bandwidth. For $\beta > 1600$, the system bandwidth decreases and the damping continues to increase with increasing β .

3.4 Asymptotic Stability of an Optimally-Controlled Vehicle String

Using the Three-Vehicle Basic Unit

3.4.1 Reasons for Using a Three-Vehicle Controller

Some discussion about the need for considering the three-vehicle concept especially with regard to the asymptotic behaviour of vehicle strings may be of interest. Consider the data for system type 7 in Table 3.1. The magnitude $|G(0)|$ increases as ρ_3 is decreased. This implies that for large values of ρ_3 , the propagation of disturbances down a string of vehicles would be highly damped which may at first appear to be highly desirable. However, since the controller is of the two-vehicle type, any vehicle in the string is unaffected by the motion of vehicles behind it. The danger of collision can be avoided if and only if the absolute value of any perturbation in position of a vehicle is less than the scheduled headway \hat{h} less the vehicle length, l . Thus

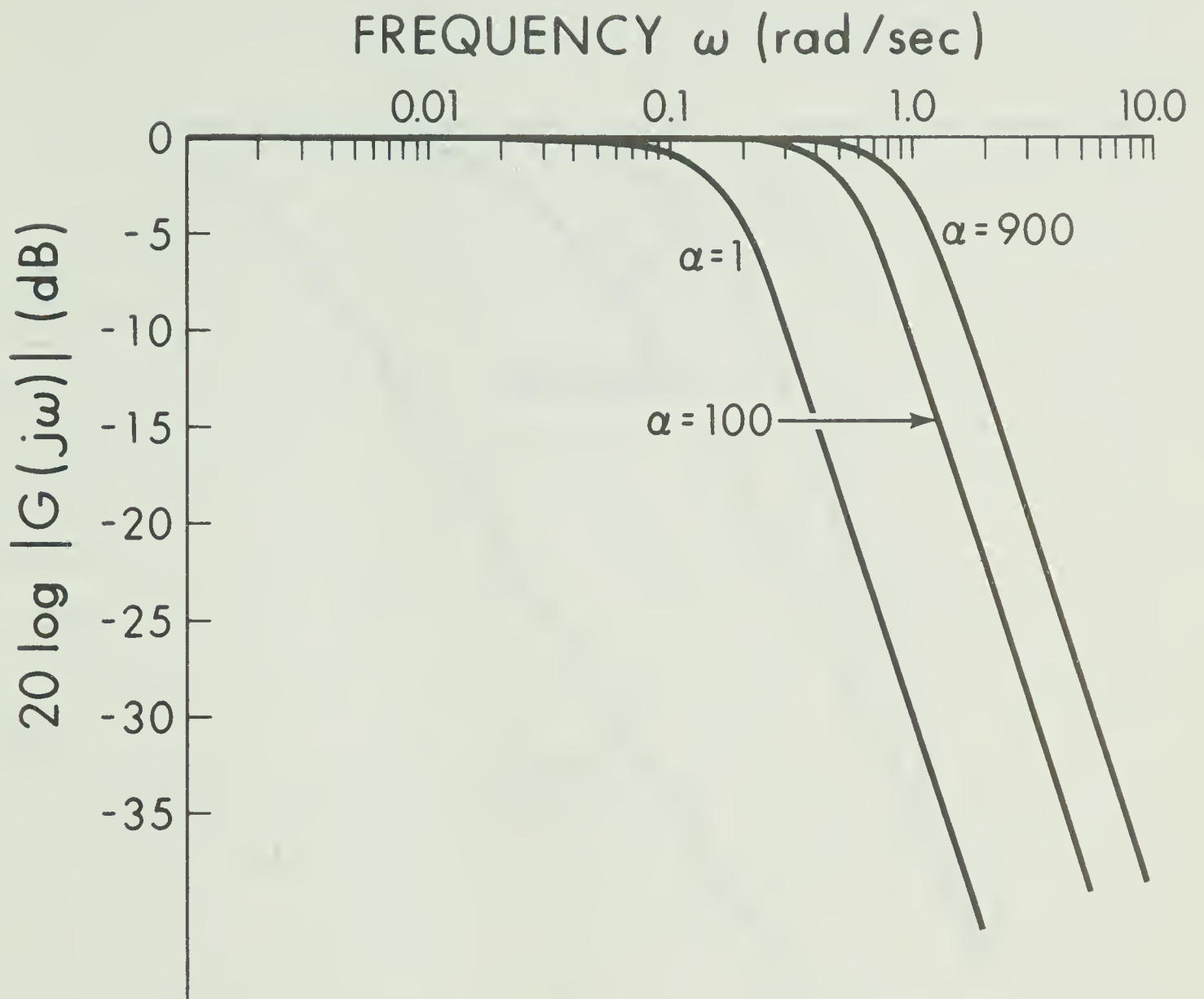


FIGURE 3.4 Magnitude of $G(j\omega)$ vs. Frequency for Two-Vehicle System Type 2

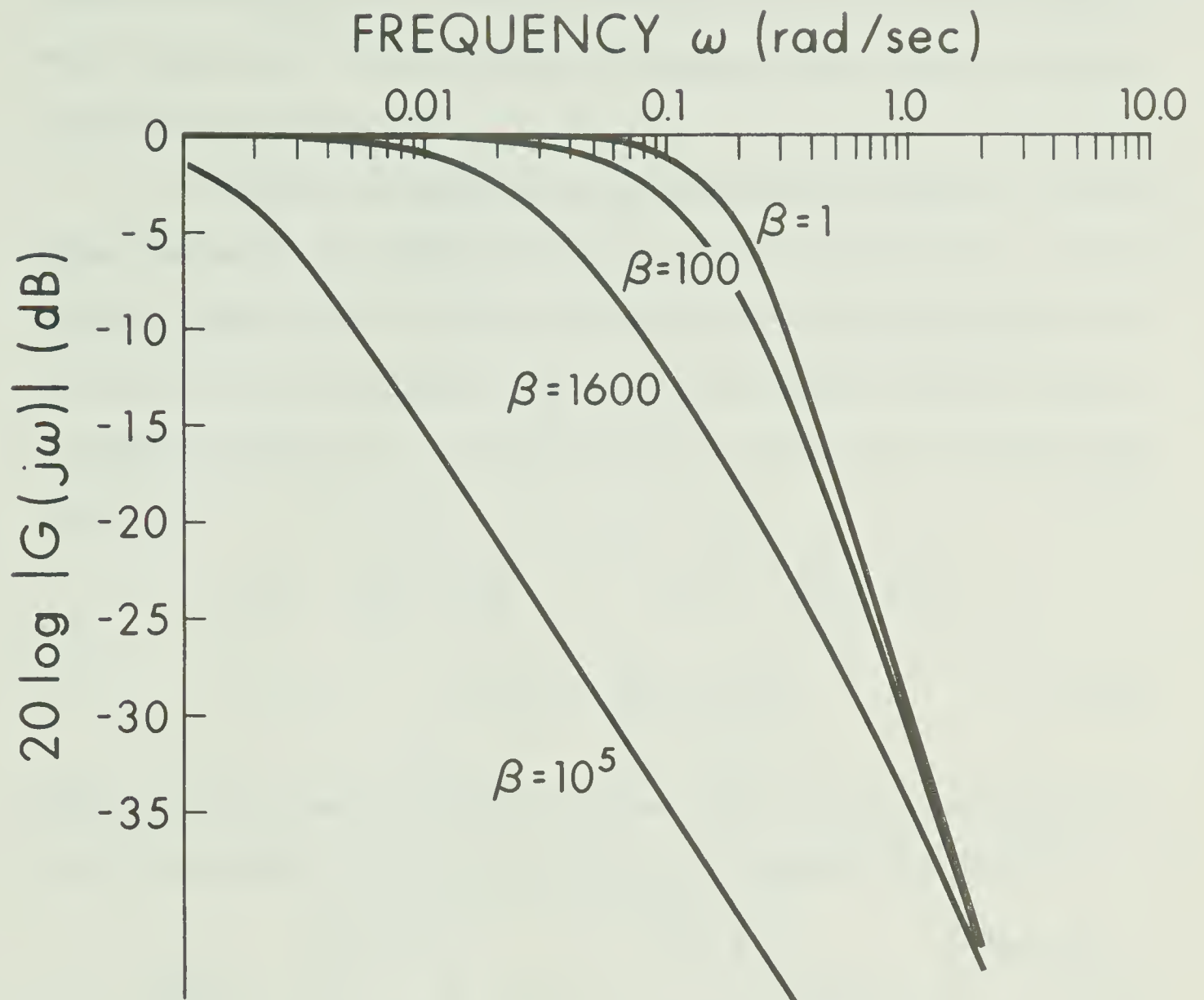


FIGURE 3.5 Magnitude of $G(j\omega)$ vs. Frequency
for Two-Vehicle System Type 4

high vehicle densities cannot be realized. This is an important reason for considering a string of vehicles based on the three-vehicle unit in which each vehicle receives information from both the vehicle ahead and that behind.

It will be recalled from the discussion in Chapter 2 that by proper choice of the weighting factors in the cost functional used, the optimal control $\underline{u}^*(t)$ for the three-vehicle unit was approximated to be $u_n^*(t)$. A block diagram of the resulting optimal feedback system is shown in Figure 3.6. In this figure the optimal gain matrices are given by

$$\begin{aligned} L_1^* &= \begin{bmatrix} L_5^* & L_6^* \end{bmatrix}, & L_2^* &= \begin{bmatrix} L_3^* & L_4^* \end{bmatrix}, \\ L_3^* &= \begin{bmatrix} L_1^* & L_2^* \end{bmatrix} \end{aligned} \quad (3.20)$$

where L_1^* to L_6^* are the optimal feedback gains for the three-vehicle unit as tabulated in Table 2.3 and the state vectors are given by

$$\underline{x}_{n-1} = \begin{bmatrix} x_{n-1,1} \\ x_{n-1,2} \end{bmatrix}, \quad \underline{x}_n = \begin{bmatrix} x_{n1} \\ x_{n2} \end{bmatrix}, \quad \underline{x}_{n+1} = \begin{bmatrix} x_{n+1,1} \\ x_{n+1,2} \end{bmatrix} \quad (3.21)$$

Using two overlapping three-vehicle units of this type, a four-vehicle string can be formed as shown in Figure 3.7. The first vehicle in the string behaves as if there were a vehicle ahead of it with a zero error state while the fourth vehicle behaves as if it sees a trailing vehicle with zero error state.

3.4.2 Derivation of the Transfer Function $G_{n+1}(j\omega)$

Since each vehicle in a string of vehicles based on the

three-vehicle unit receives information about the motion of the vehicle directly ahead and that directly behind, the transfer function $G_{n+1}(j\omega)$ relating the position errors of the n th and $(n+1)$ th vehicles in the string will depend on n and the total number of vehicles in the string, r . The following discussion will deal specifically with a four-vehicle string for which the signal flow graph is given in Figure 3.8. Using superposition, the block diagram for the string can be reduced to that shown in Figure 3.9 where

$$G'(j\omega) = \frac{L_5^*/m}{\frac{-L_3^*}{m} - \omega^2 + j\omega\left(\frac{\bar{\mu}}{m} - \frac{L_4^*}{m}\right)} \quad (3.22)$$

and

$$G(j\omega) = \frac{L_5^* + j\omega L_6^*}{\frac{-L_3^*}{m} - \omega^2 + j\omega\left(\frac{\bar{\mu}}{m} - \frac{L_4^*}{m}\right)} \quad (3.23)$$

The details of the derivation of the above are supplied in Appendix 3-2.

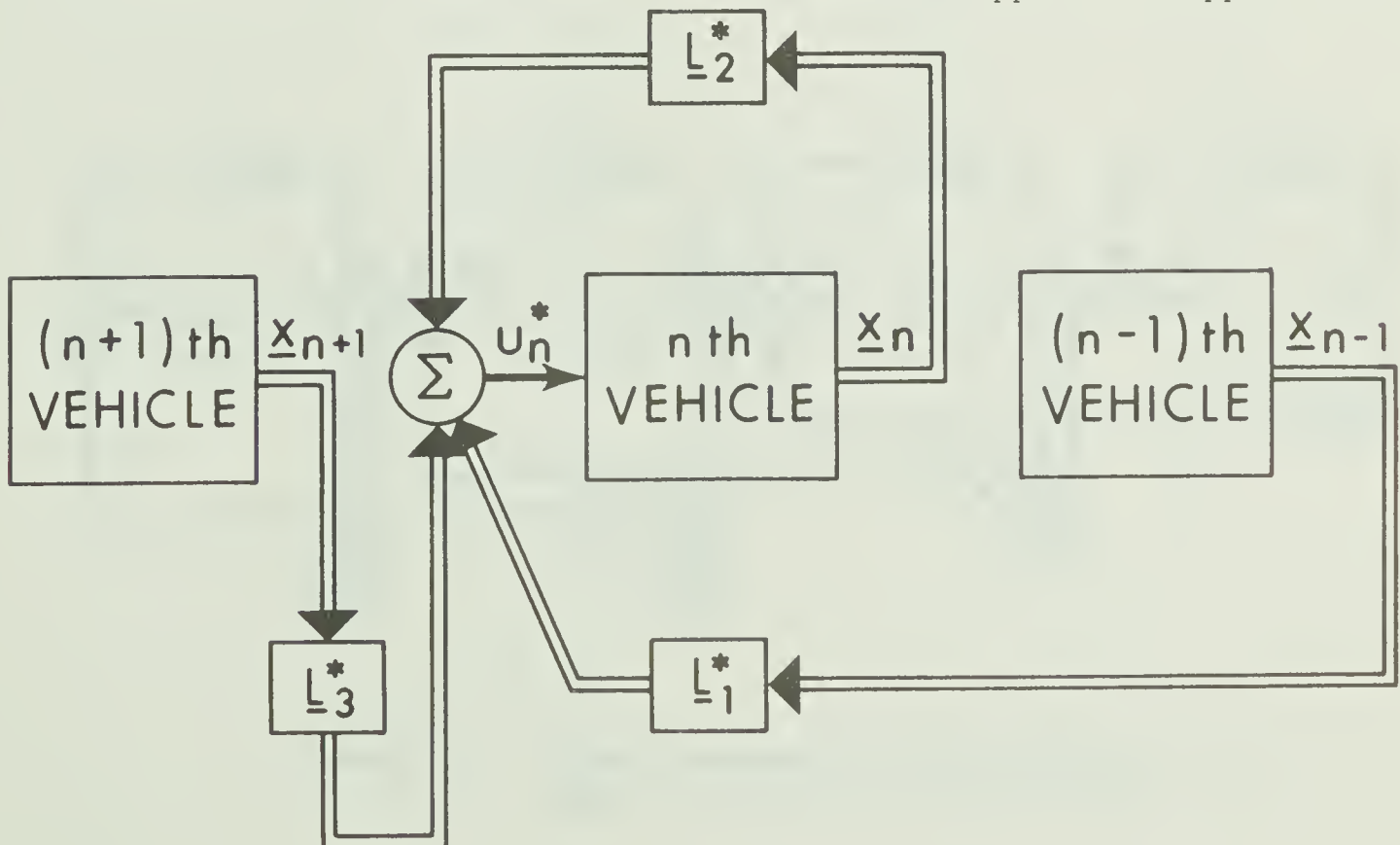


FIGURE 3.6 A Simplified Block Diagram of the Three-Vehicle Basic Unit

From (3.22) and (3.23) together with Figure 3.9, the transfer function $X_{i+1,1}/X_{i1}$ can be calculated for $i = 1, 2, 3$. As previously indicated, the value of this transfer function will depend on i . Hence for a string of r vehicles it is difficult to evaluate a general form for $G_{i+1}(j\omega)$. Some useful results can however, be obtained as outlined in the following subsection.

3.4.3 Some Steady-State Results on Asymptotic Stability

Consider the signal flow graph for a string of r vehicles as shown in Figure 3.10. Assume that the 1st vehicle exhibits a position error \bar{x}_{11} , this value being independent of the motion of the following vehicles. We would like to know the steady-state ($\omega = 0$) position errors of all the remaining vehicles in the string. We can calculate the values of $G'(0)$ and $G(0)$ from (3.22) and (3.23) together with the feedback gain values given in Table 2.3.

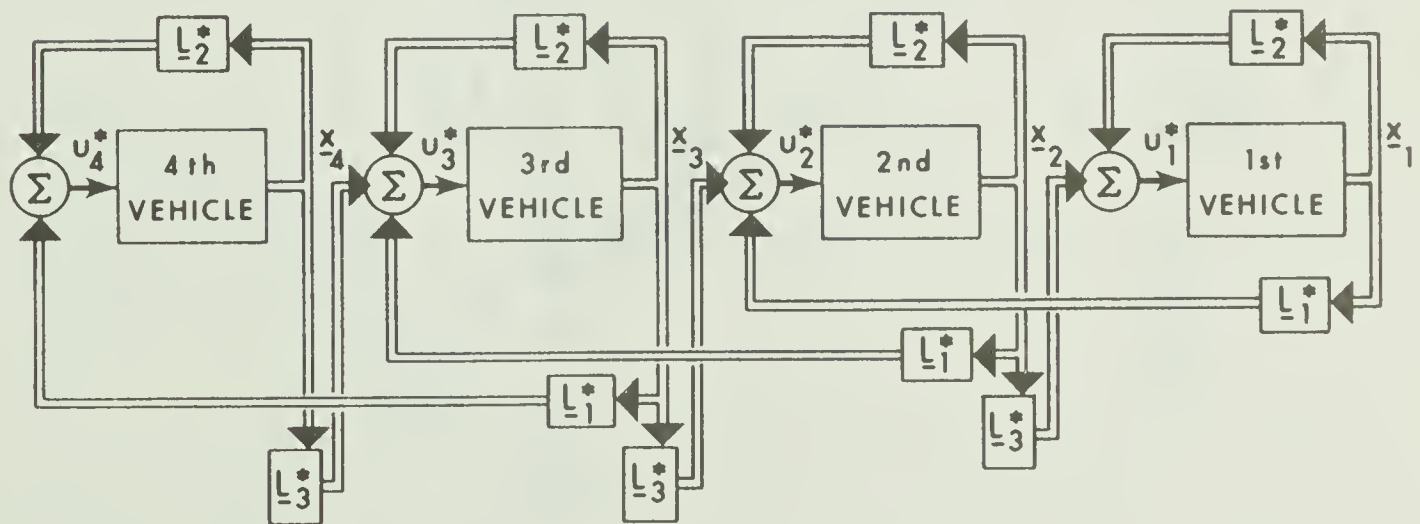


FIGURE 3.7 Block Diagram of a Four-Vehicle String Based on the Three-Vehicle Unit

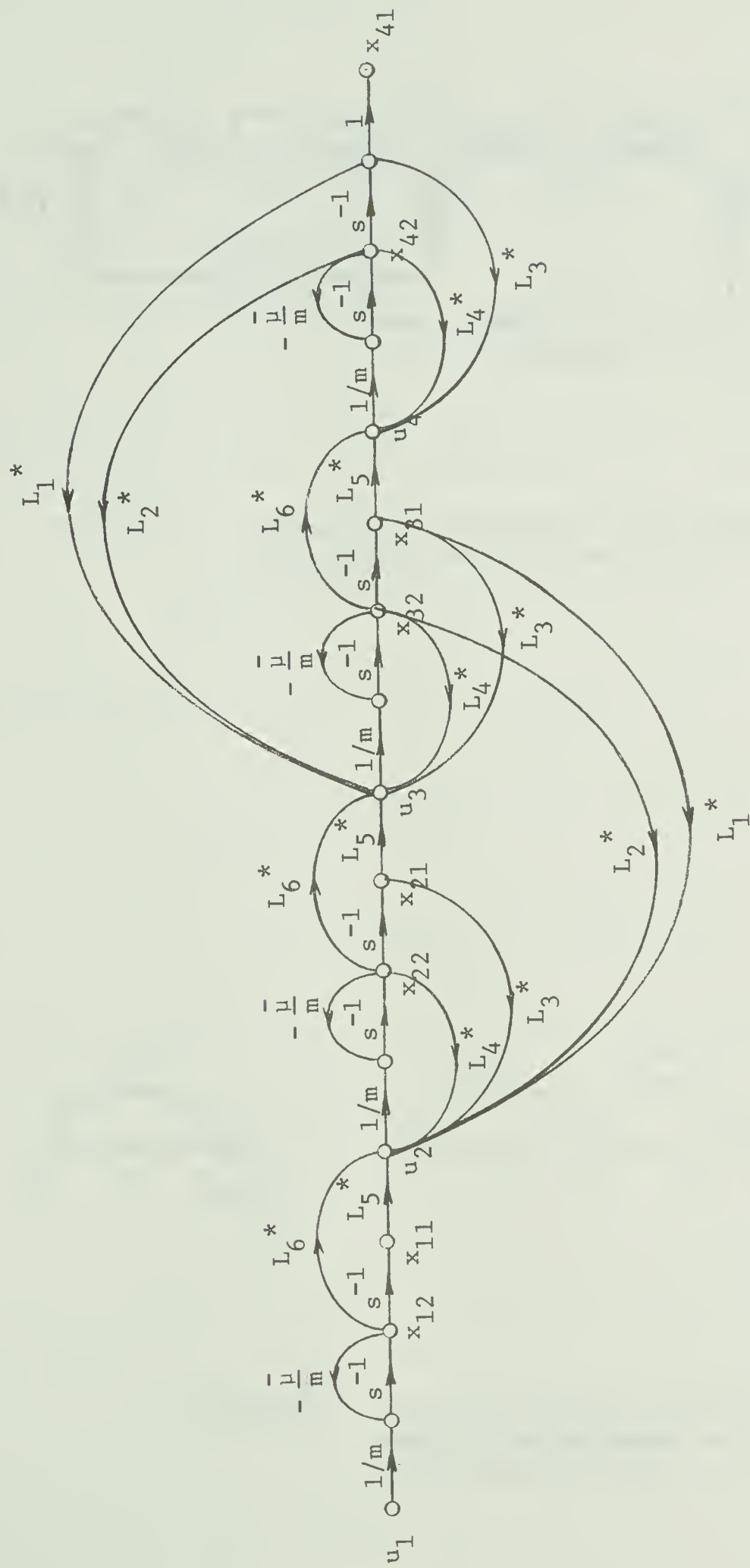


FIGURE 3.8 Signal Flow Graph for a String of Four Vehicles
Based on the Three-Vehicle Basic Unit

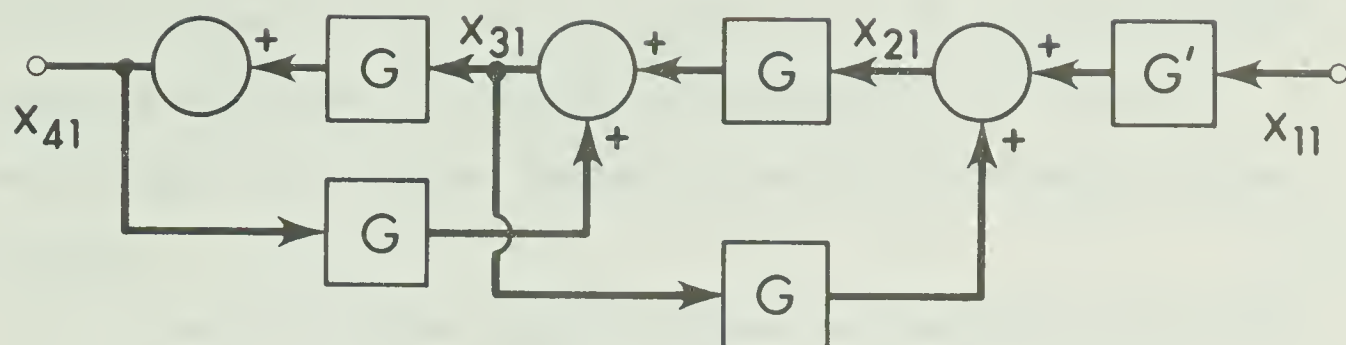


FIGURE 3.9 Reduced Block Diagram for the Four-Vehicle String Based on the Three-Vehicle Unit

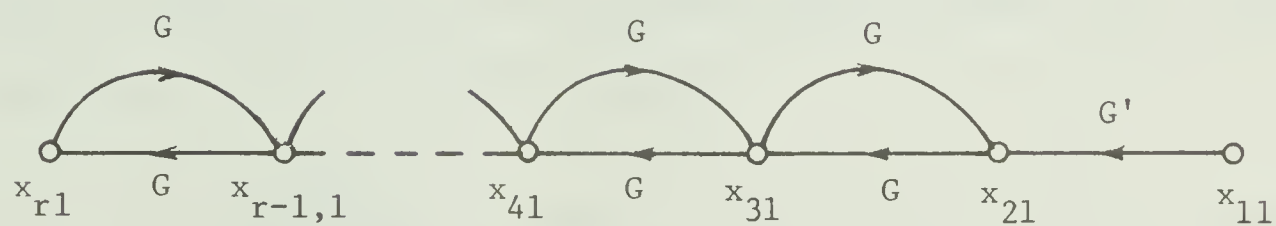


FIGURE 3.10 Signal Flow Graph for an r -Vehicle String Based on the Three-Vehicle Unit

$$G'(0) = G(0) = - \frac{L_5^*}{L_3^*} \quad (3.24)$$

which for system types 1 and 3 is equal to $\frac{1}{2}$. As in the two-vehicle case, the definition for asymptotic stability does not apply to system type 2 which has no feedback of position information between vehicles.

We will assume that for minimum cost at steady state, the headway, \bar{h} , between successive vehicles will be equal (but not necessarily equal to the scheduled headway, \hat{h}). This can be written as

$$\lim_{t \rightarrow \infty} [x_{i1}(t) - x_{i+1,1}(t)] = \bar{h} \quad \text{for all } i \quad (3.25)$$

We can now calculate the transfer functions

$$G_{r-2}(j\omega) = \frac{X_{r-1,1}(j\omega)}{X_{11}(j\omega)} = \frac{G^{(r-3)}(j\omega)G_1(j\omega)}{\Delta} \quad (3.26)$$

$$G_{r-1}(j\omega) = \frac{X_{r1}(j\omega)}{X_{11}(j\omega)} = \frac{G^{(r-2)}(j\omega)G_1(j\omega)}{\Delta} \quad (3.27)$$

where Δ is the determinant for the flow graph of Figure 3.10. We can now divide (3.27) by (3.26) to obtain

$$\frac{X_{r1}(j\omega)}{X_{r-1,1}(j\omega)} = G(j\omega) \quad (3.28)$$

Noting that $G(0) = \frac{1}{2}$, we can say from (3.25) and (3.28) that at steady state the last vehicle in the string will have a position error half that of the second-last vehicle and that all vehicles will be equally spaced. If the first vehicle moves \bar{x}_{11} , then each vehicle, i , must move $\frac{r-i+1}{r}$ of \bar{x}_{11} . That is,

$$\frac{x_{i1}(0)}{x_{11}(0)} = \frac{r-i-1}{r} = G_{i-1}(0) \quad (3.29)$$

Since we did not specify the scheduled headway, \hat{h} , the condition for asymptotic stability was reduced to

$$|G_{i-1}(j\omega)| \leq 1, \quad i = 2, 3, \dots, r \quad (3.30)$$

Neglecting the transient portion of the string motion, for a change in position of the first vehicle of \bar{x}_{11} , the maximum value of $G_{i-1}(0)$ will occur for $i = 2$. We can write

$$G_1(0) = \frac{x_{21}(0)}{x_{11}(0)} = \frac{x_{21}(0)}{\bar{x}_{11}} = \frac{r-1}{r} \quad (3.31)$$

As $r \rightarrow \infty$ the value of $G_1(0) \rightarrow 1$ and for all other r has a magnitude less than unity. Thus under steady-state conditions the three-vehicle system meets the requirement for asymptotic stability given by (3.30). (That is, (3.30) is satisfied for $\omega = 0$). In order to verify (3.30) for all ω it would be necessary to solve for $G_{i-1}(j\omega)$ for all i which would become very complex for multi-vehicle strings. In this thesis we have verified the three-vehicle system to be asymptotically stable by simulation of vehicle strings on the analogue computer and subjecting the first vehicle to a step change in position error. The results of this study are reported in the next subsection.

For a change in x_{11} of \bar{x}_{11} , we can calculate from (3.29) the new headway, \bar{h} , between vehicles at steady state to be

$$\bar{h} = \hat{h} + \frac{\bar{x}_{11}}{r} \quad (3.32)$$

The derivation of (3.32) is given in Appendix 3-3. From (3.32) it can be seen that the new headway is always greater than the original

scheduled headway for a positive change \bar{x}_{11} . For \bar{x}_{11} a negative change, collisions will occur for $\bar{x}_{11} > \hat{r}\hat{h} - \ell$ where ℓ is the vehicle length. This is clearly an improvement over the two-vehicle system for which collisions would occur for $\bar{x}_{11} > \hat{h} - \ell$.

3.4.4 Analogue Computer Simulation of a Vehicle String Based on the Three-Vehicle Unit

A string of five vehicles based on the three-vehicle optimal car-following unit was simulated on a PACE 231 analogue computer and the lead vehicle simulated to undergo a step change in position error $x_{11}(t)$. The position and velocity errors of the remaining four vehicles were plotted vs. time. Figures 3.11 - 3.16 show the results for system types 1a, 1b and 1c. It can immediately be seen that the steady-state position errors are as predicted by (3.29). That is, for a unit change in x_{11} , the steady-state values of the position errors for the 2nd, 3rd, 4th and 5th vehicles are 4/5, 3/5, 2/5 and 1/5 respectively. The effect of increasing α , the weighting on headway error in the cost functional, is to shorten the rise time of the system at the expense of slightly more oscillatory behaviour and greater velocity errors (and hence the need for greater forces to be applied to the vehicles). All three systems are asymptotically stable since $x_{i1}(t) < x_{i-1}(t)$ for all time t .

Figure 3.17 shows the effect of penalizing relative velocity between vehicles in the case of system type 3c. The damping on the system is increased and the overall performance is more desirable than that of system type 1. The velocity errors are also reduced as can be seen from Figure 3.18. Thus from the standpoint of achieving a damped, smooth response to a sudden change in the motion of some vehicle in a

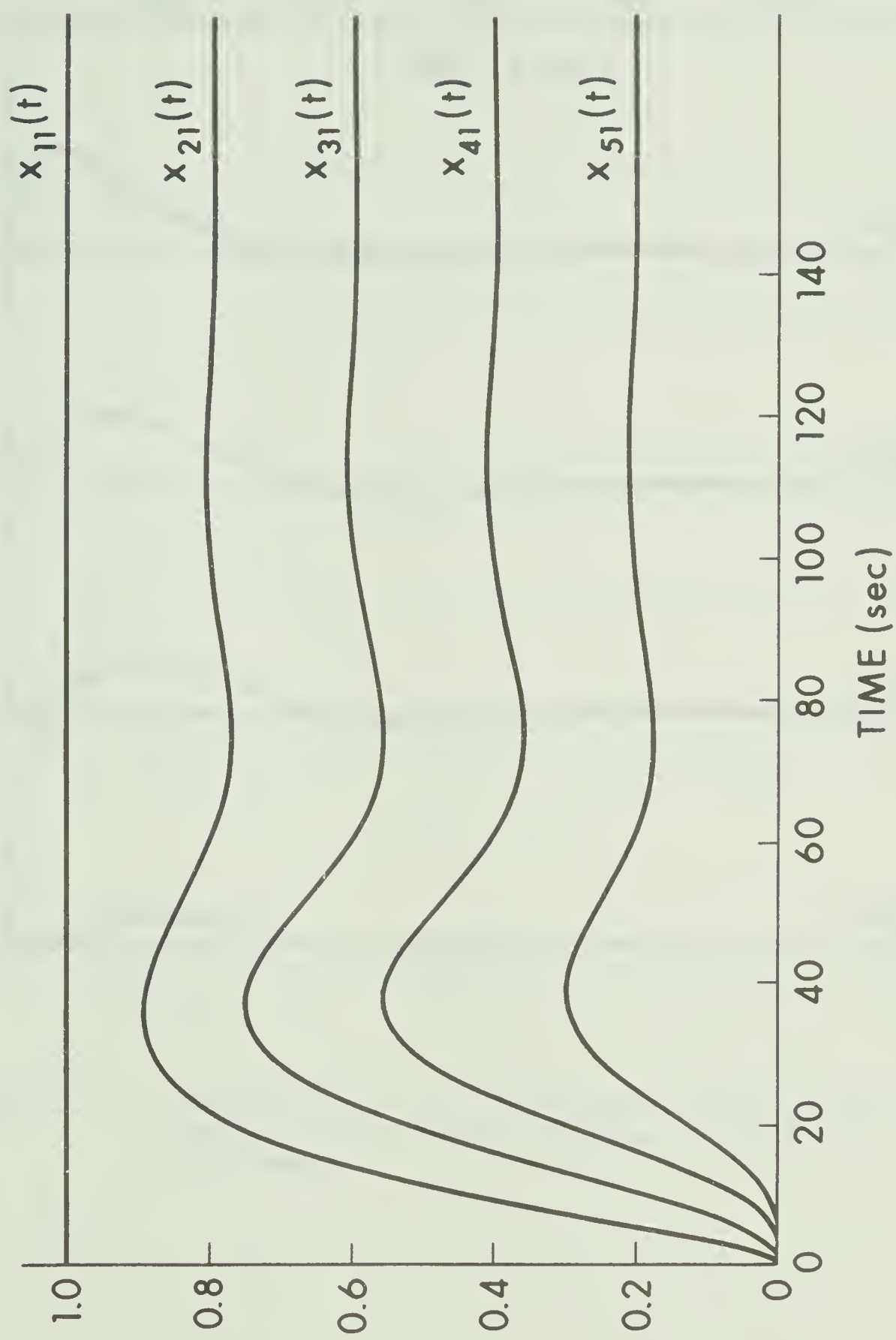


FIGURE 3.11 Position Errors for a Five-Vehicle String (System 1a)
When the Leading Vehicle Undergoes a Step Position
Error Change

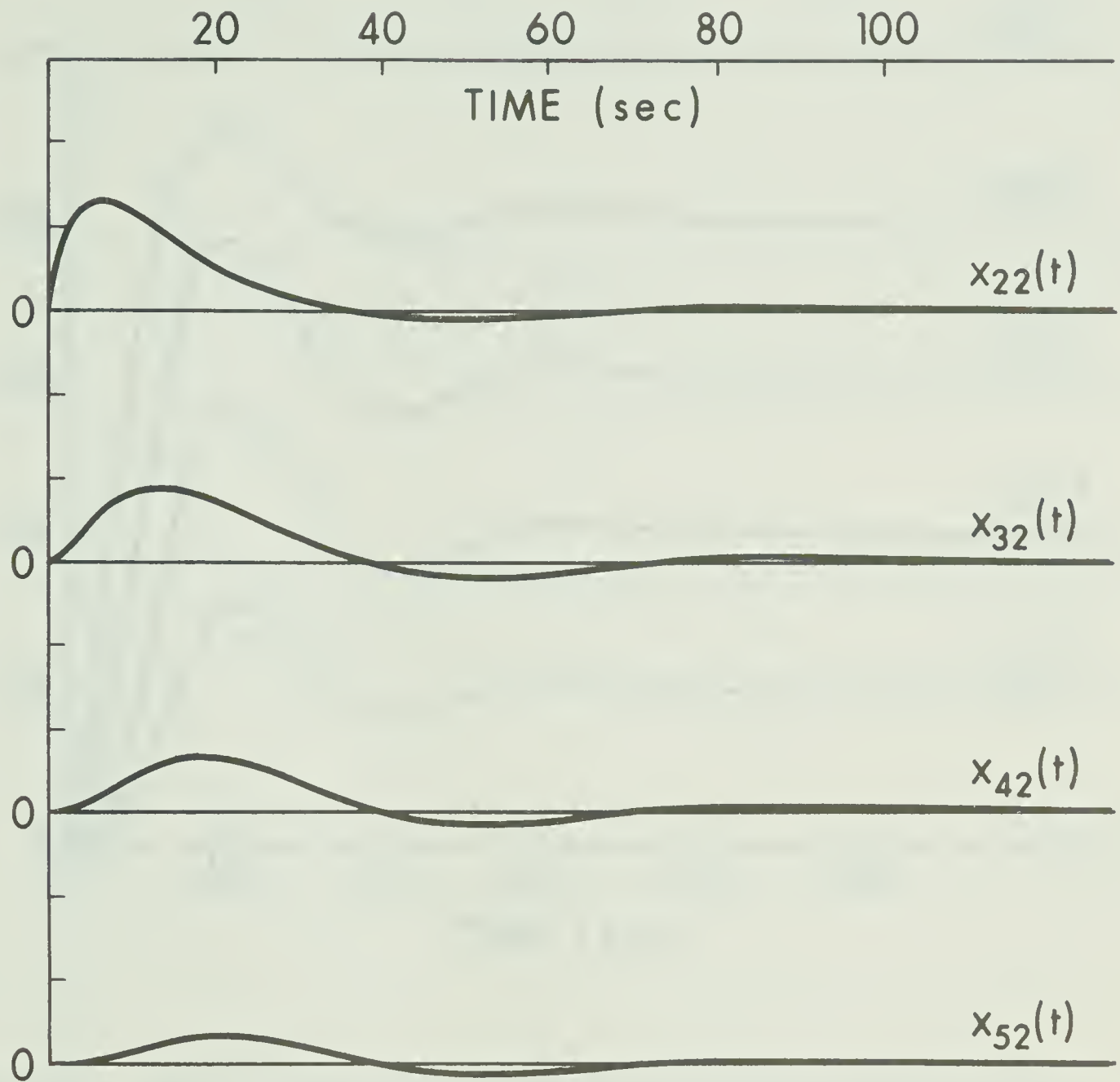


FIGURE 3.12 Velocity Errors for a Five-Vehicle String (System 1a) When the Leading Vehicle Undergoes a Step Position Error Change

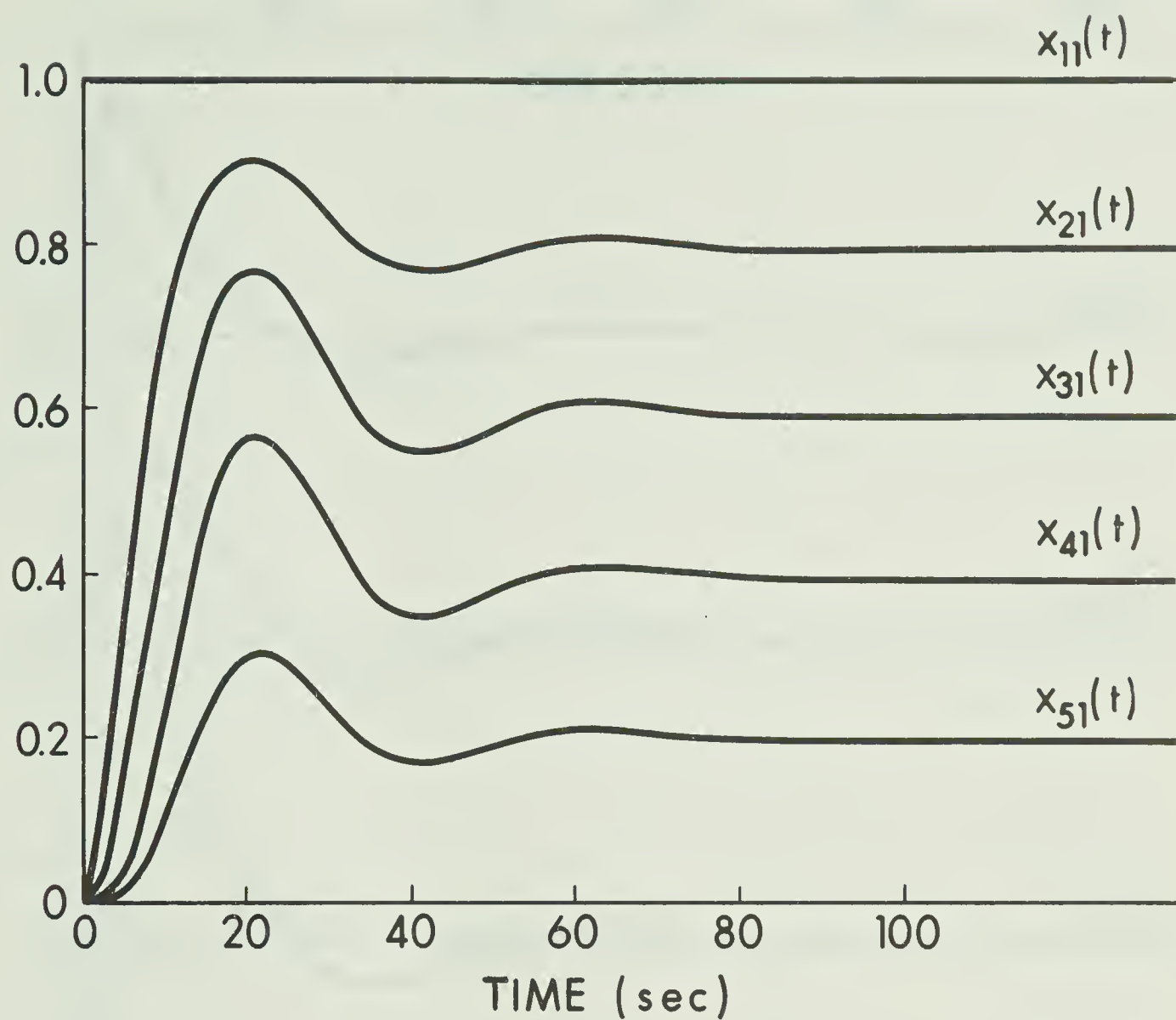


FIGURE 3.13 Position Errors for a Five-Vehicle String (System 1b) When the Leading Vehicle Undergoes a Step Position Error Change

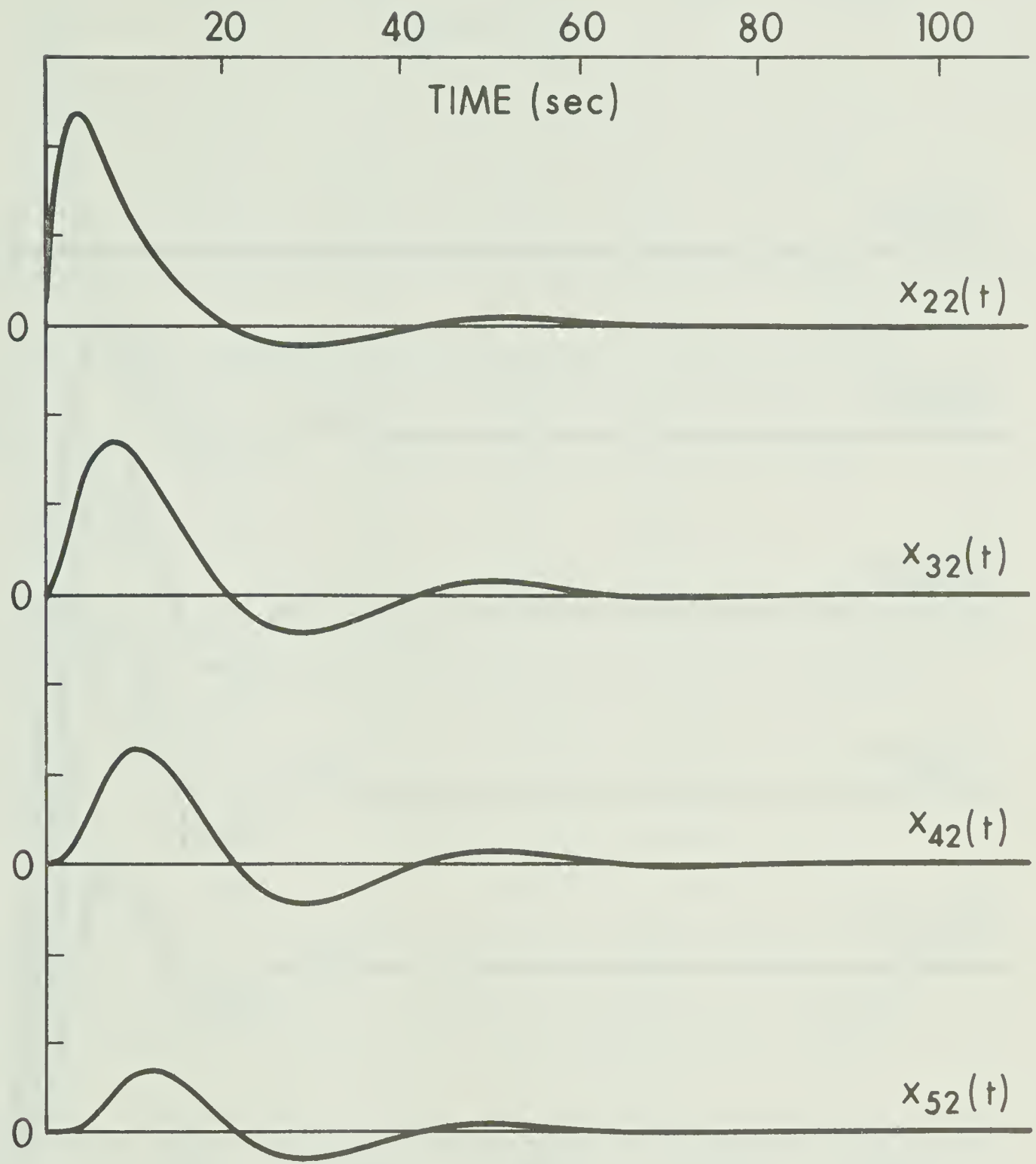


FIGURE 3.14 Velocity Errors for a Five-Vehicle String (System 1b) When the Leading Vehicle Undergoes a Step Position Error Change

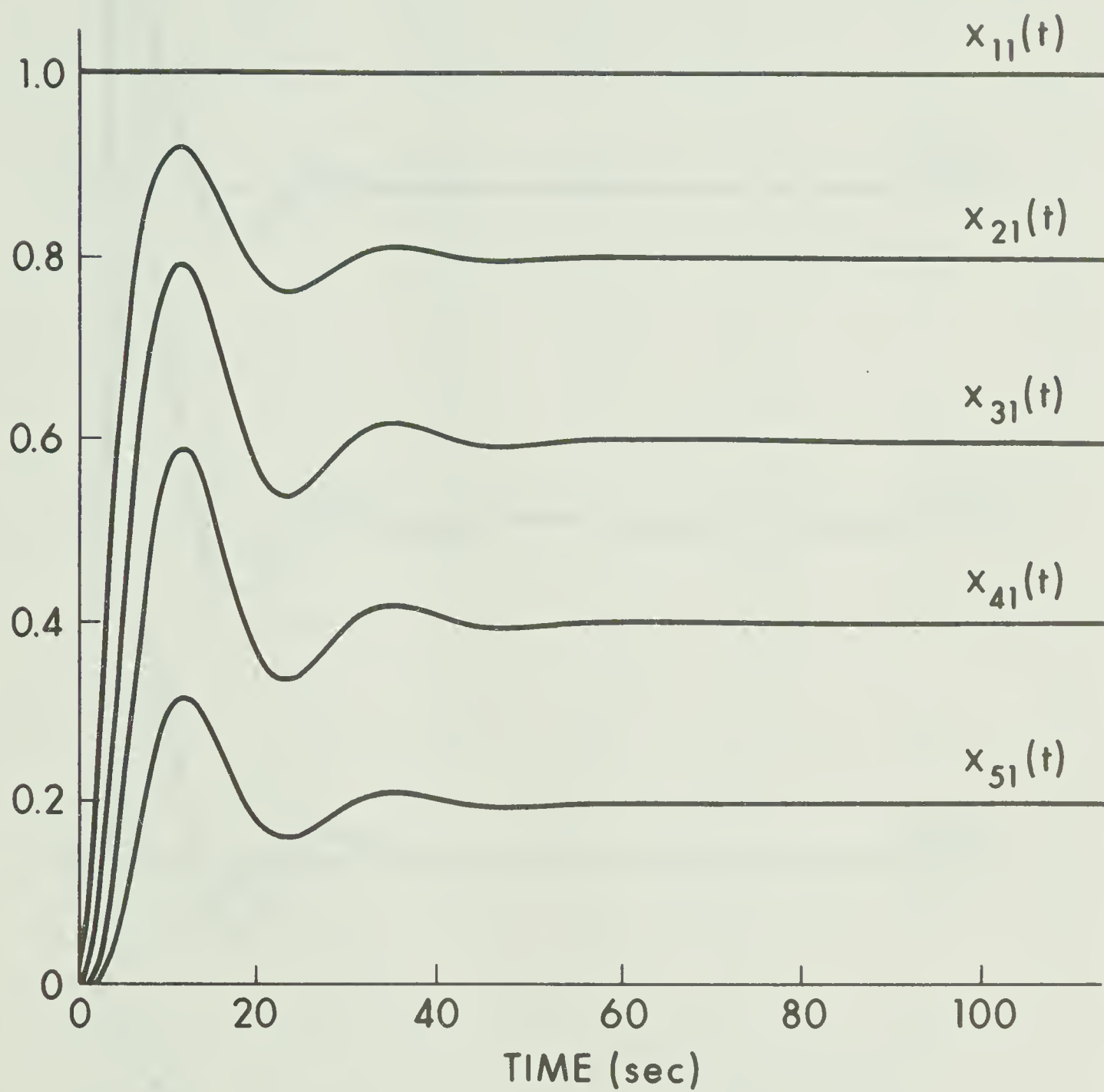


FIGURE 3.15 Position Errors for a Five-Vehicle String (System 1c) When the Leading Vehicle Undergoes a Step Position Error Change

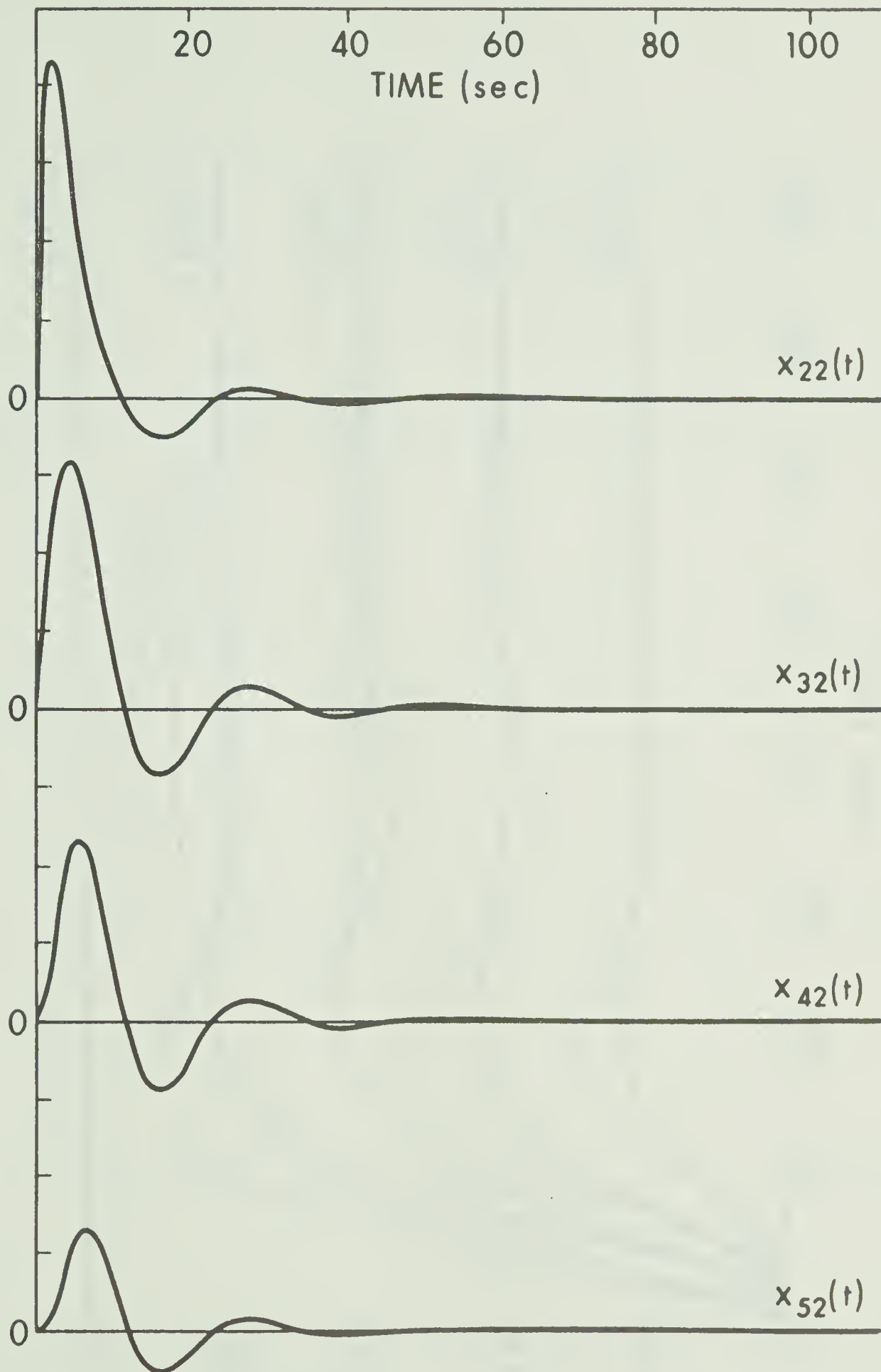


FIGURE 3.16 Velocity Errors for a Five-Vehicle String (System 1c) When the Leading Vehicle Undergoes a Step Position Error Change

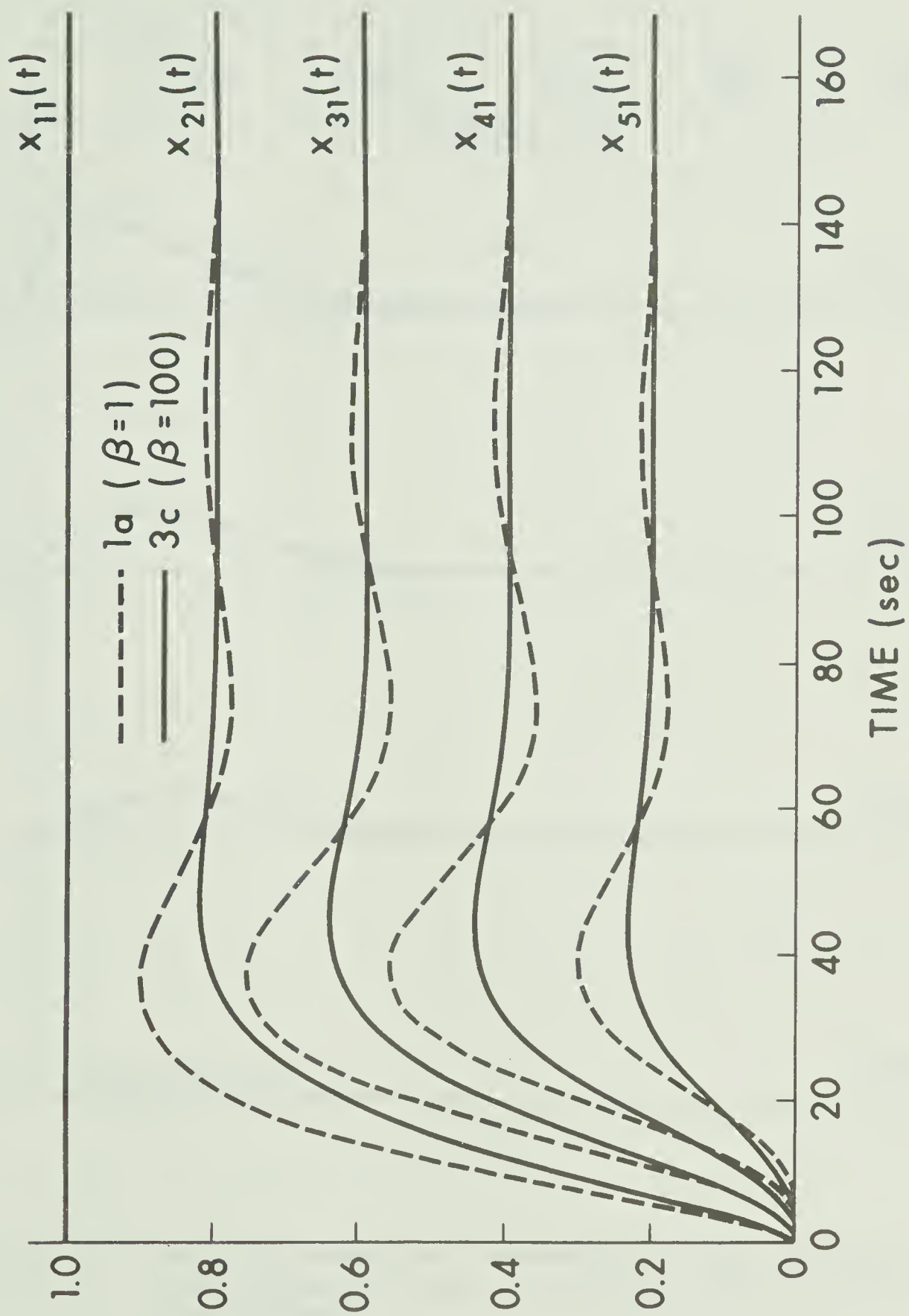


FIGURE 3.17 Position Errors for a Five-Vehicle String (Systems 1a and 3c) When the Leading Vehicle Undergoes a Step Position Error Change

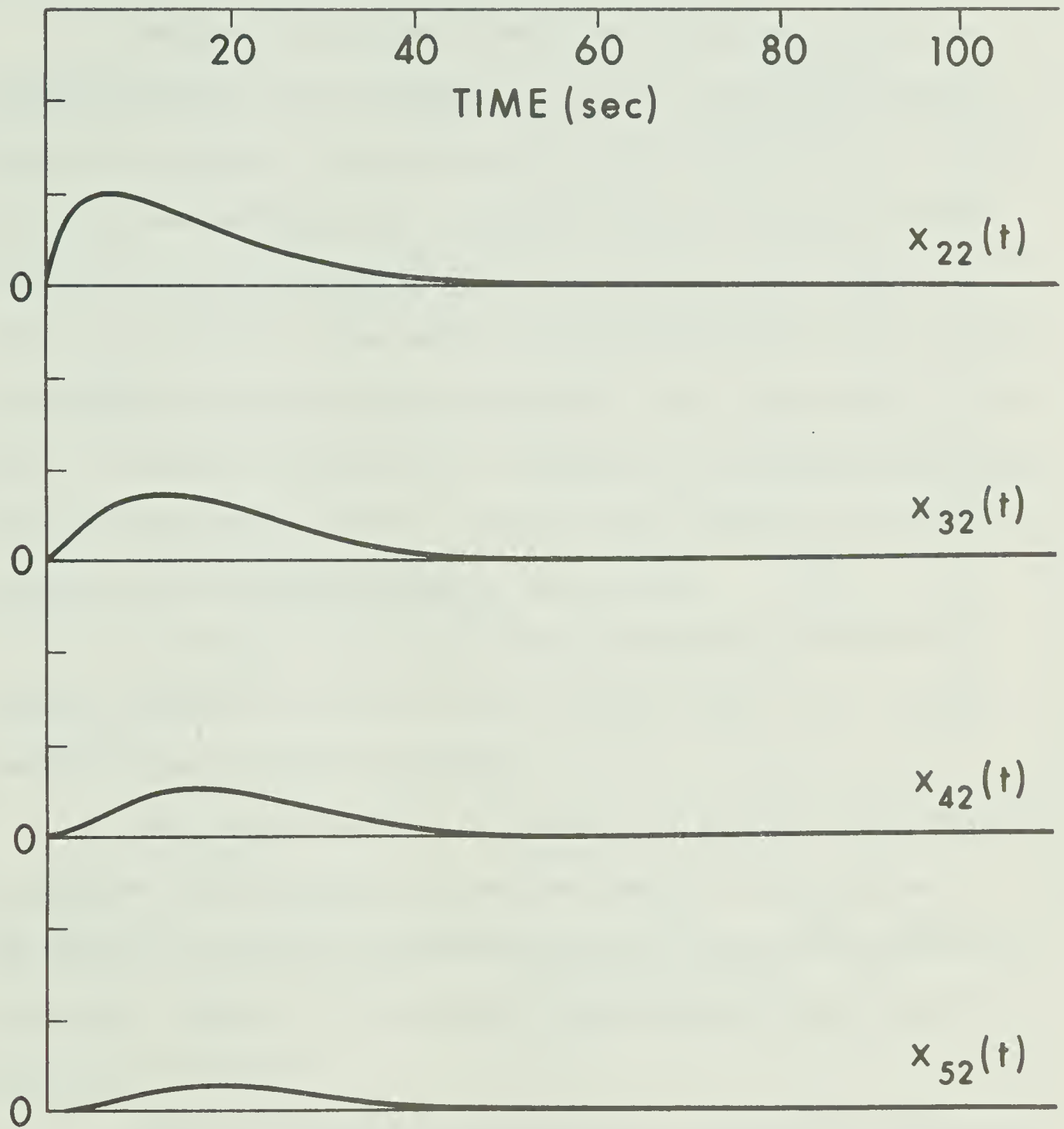


FIGURE 3.18 Velocity Errors for a Five-Vehicle String (System 3c) When the Leading Vehicle Undergoes a Step Position Error Change

string, the addition of a relatively large weighting on relative velocity in the cost functional seems desirable.

3.5 Effects of a Time Lag on Asymptotic Behaviour

The above discussion assumes that the error states from adjacent vehicles can be transmitted accurately and instantaneously between each vehicle. In actual practice this would not be the case. Both noise contamination and a time delay would be experienced upon receiving an error state by some vehicle from another. We will consider the effects of a time delay on the asymptotic behaviour of the three-vehicle system discussed previously. This time delay is a net result of sensing, transmission, receiving, processing and mechanical delays in the control system. The delay thus appears in the control inputs to the vehicles as shown in Figure 3.19.

A string of four vehicles was simulated on a PACE TR-48 analogue computer and the time delay obtained using a PDP-8 digital computer interfaced with the TR-48.

The leading vehicle was simulated to undergo a step change in position error at time $t = 0$ and the position error response of the remaining three vehicles was recorded for various time delays in the control inputs. The two systems considered were system type 1a and system type 3c.

Figure 3.20 shows the position error response of the second vehicle for various time delays in the control paths of system type 1a. It can be seen that for a delay, τ_d , of 2 seconds, the response is nearly normal (refer to Figure 3.11). The system becomes unstable for time delays greater than about 2.5 seconds. Figure 3.21 shows the

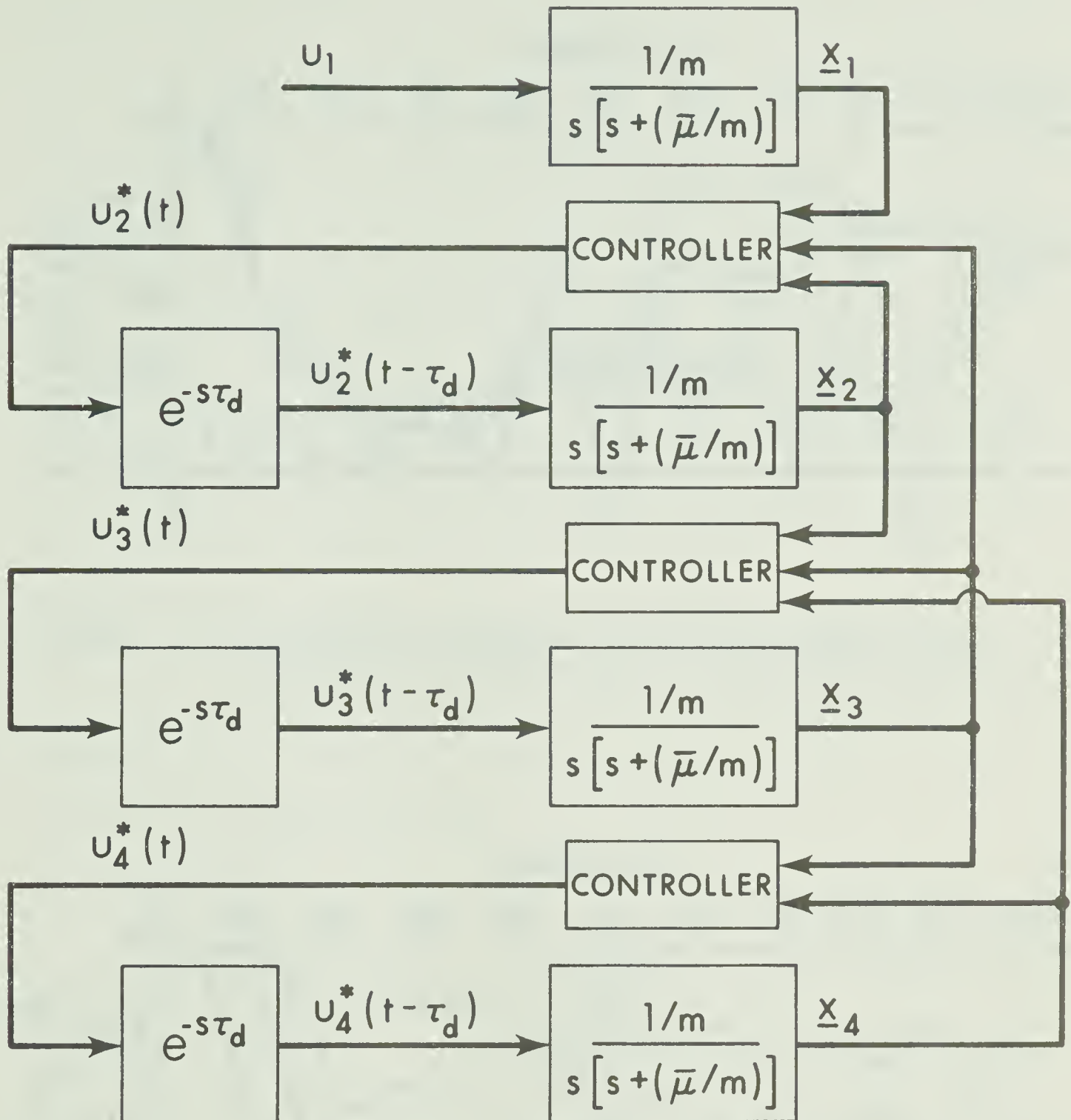


FIGURE 3.19 Block Diagram of Four-Vehicle String with Time Delays in the Control Paths

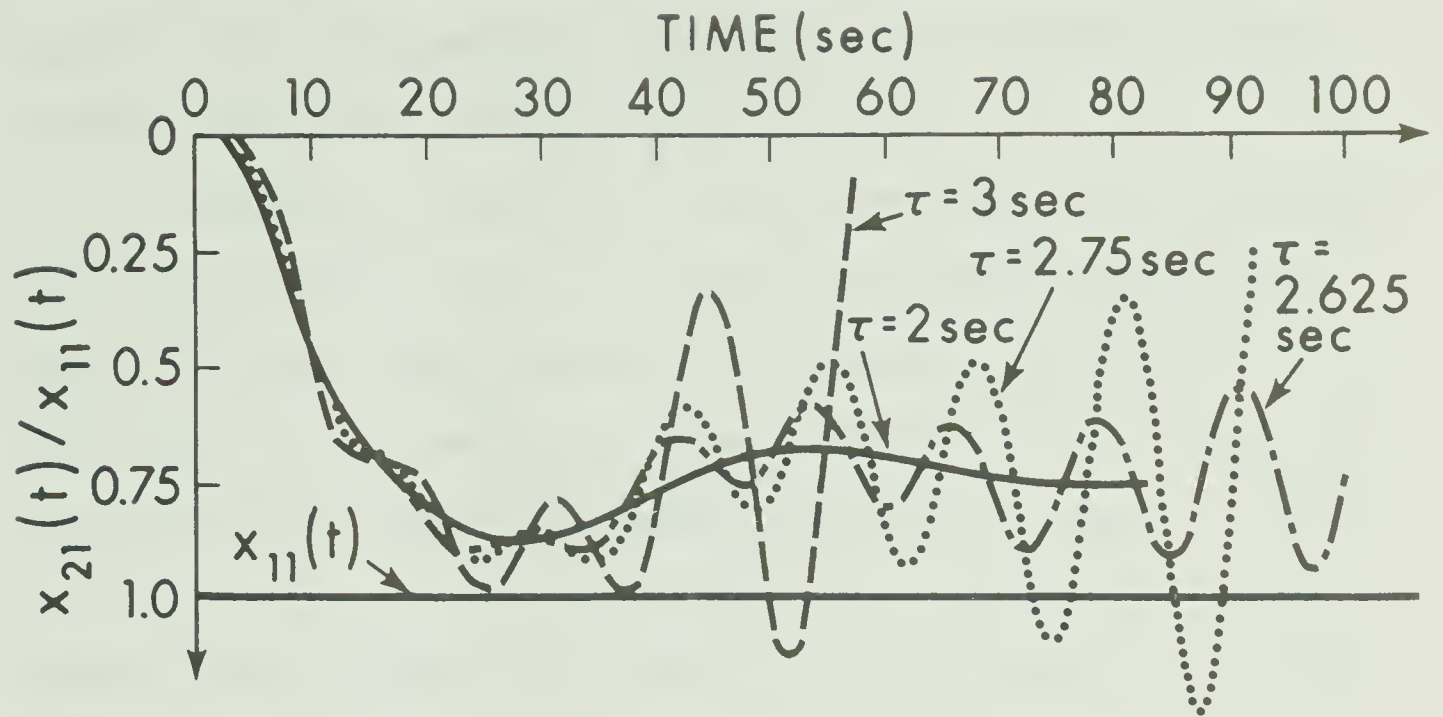


FIGURE 3.20 Position Error Response of the Second Vehicle in a Four-Vehicle String for Various Time Delays (System 1a)

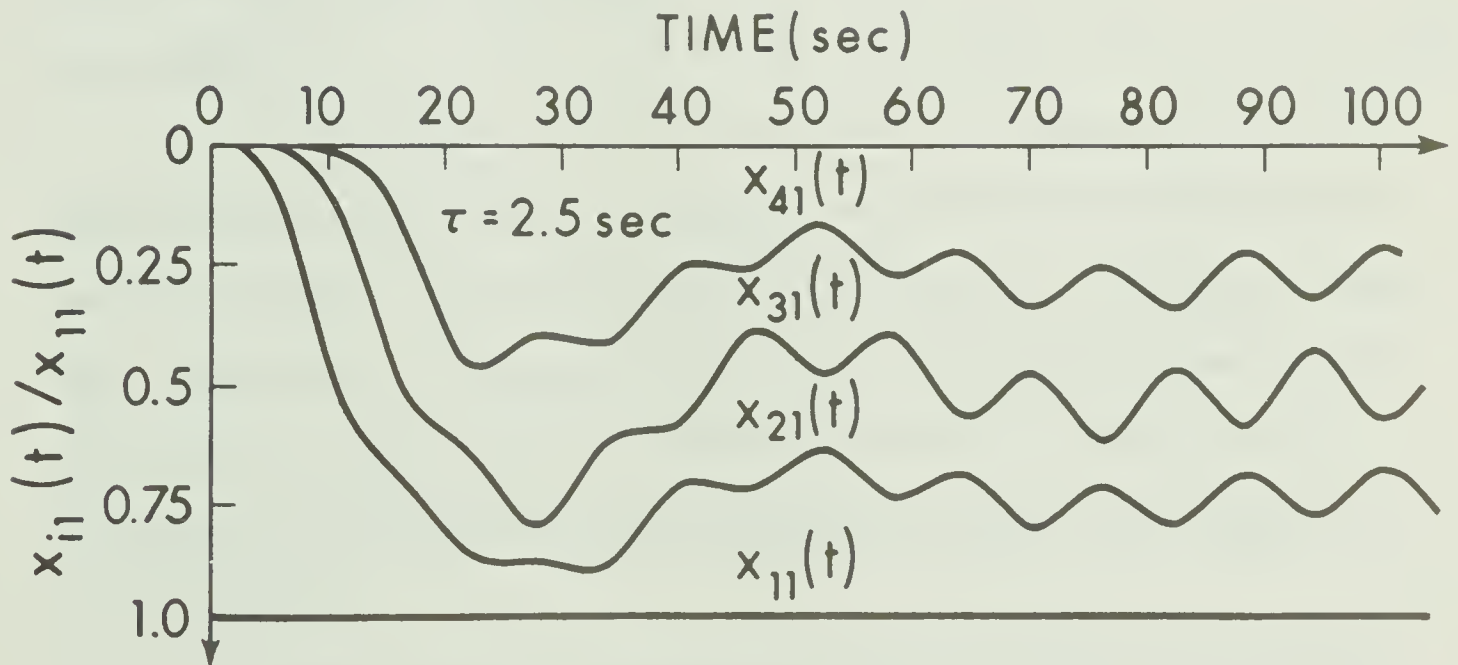


FIGURE 3.21 Position Error Response of a Four-Vehicle String for a 2.5 Second Time Delay (System 1a)

position error response for all vehicles in the string for $\tau_d = 2.5$ seconds. It can be seen that the error states of adjacent vehicles are 180° out of phase with one another.

Figure 3.22 shows the position error response of the second vehicle for system type 3c. It should be recalled that this system appeared to exhibit more desirable behaviour than did system type 1a (see Figure 3.17). However, it appears that system type 3c will not remain stable for time delays greater than about 1.6 seconds although performance at $\tau_d = 1.5$ seconds is near normal. Figure 3.23 shows the position error response of all vehicles in the string for $\tau_d = 1.625$ seconds.

From the above, it appears that the three-vehicle systems can operate satisfactorily with relatively large time delays in the feedback loops. It is unlikely that the total delay in an automatic system would exceed 1.5 seconds.

3.6 Summary

In this chapter we have discussed the asymptotic stability characteristics of strings of vehicles controlled by several types of control systems. It was shown that for two types of "classical" feedback controllers, the feedback gains must be carefully chosen according to the relations given by (3.12) and (3.15). A third system (relative velocity and position feedback) was shown to be asymptotically unstable.

In the case of the two-vehicle type optimal car-following system of Figure 3.2, it was found that the transfer function relating the position error of any vehicle to that of the vehicle directly

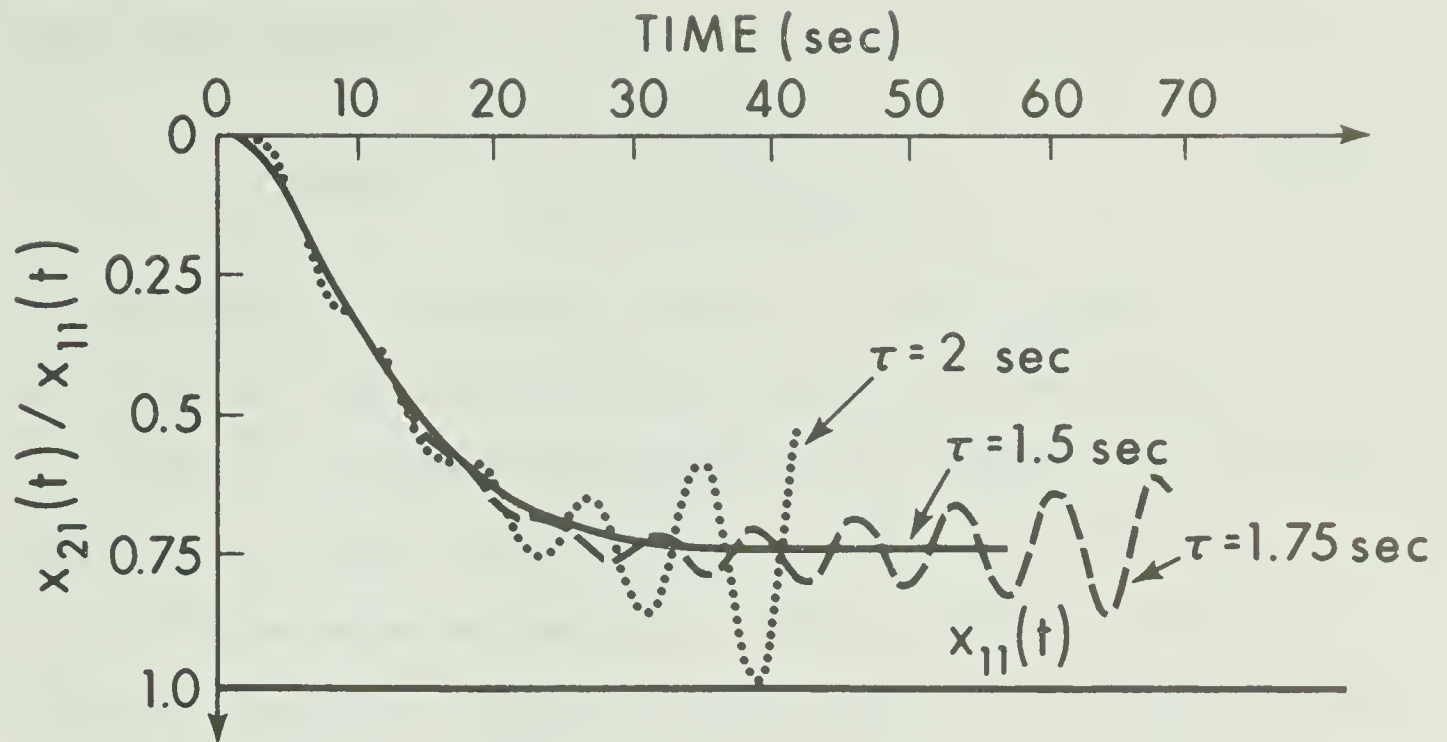


FIGURE 3.22 Position Error Response of the Second Vehicle in a Four-Vehicle String for Various Time Delays (System 3c)

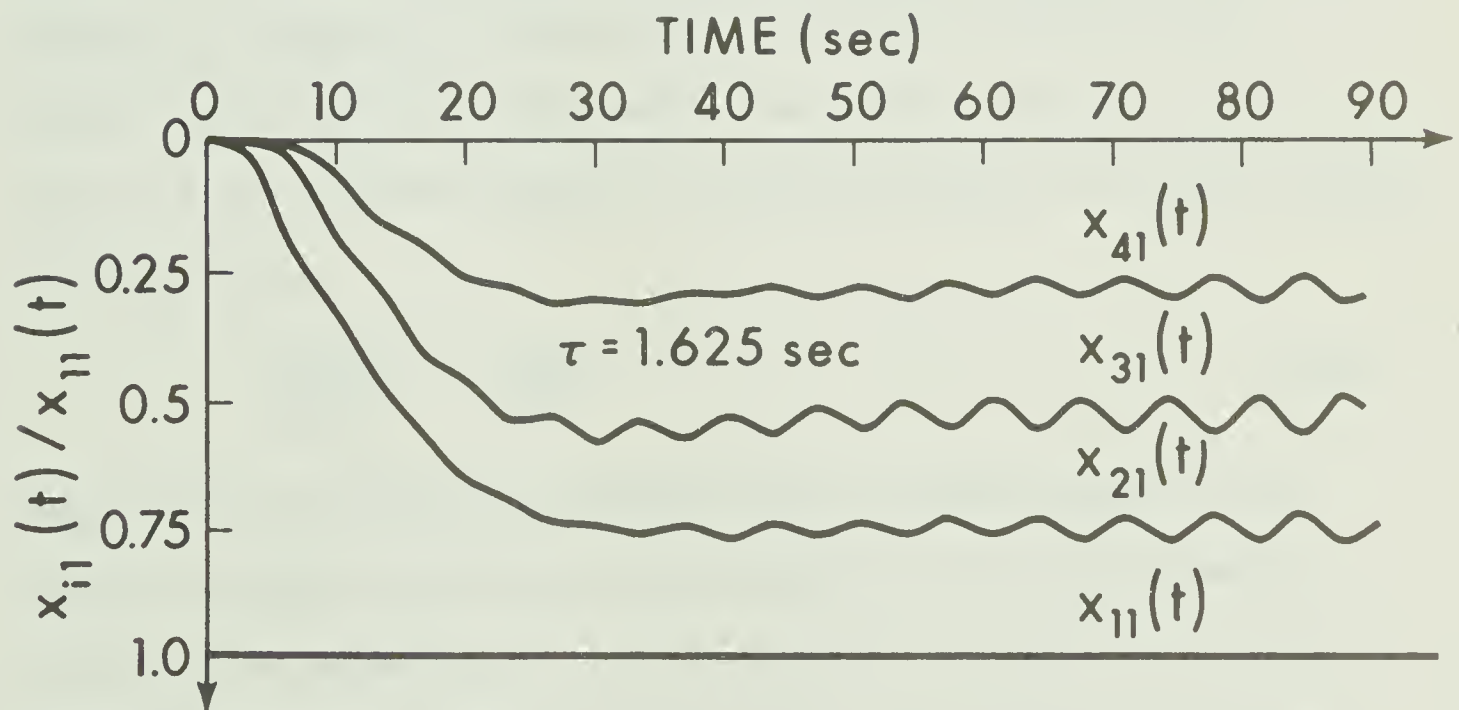


FIGURE 3.23 Position Error Response of a Four Vehicle String for a 1.625 Second Time Delay (System 3c)

ahead was of the form

$$G_{n+1}(j\omega) = \frac{L_3^*/m}{\omega_o^2 - \omega^2 + j\omega(2\zeta\omega_o)} \quad (3.33)$$

The requirement for asymptotic stability is that $G_{n+1}(j\omega) \leq 1$ for all frequency ω and hence the optimal system would be stable for $\zeta \geq 0.7072$ (the condition for maximally flat response). It was shown (see Table 3.1) that for all the cost functionals examined that $\zeta \geq 0.7072$ and hence the two-vehicle optimal systems all exhibited asymptotic stability. This is a useful result in that one is free to choose the relative weighting of the terms within the cost functional without fear of creating an unstable vehicle string.

In the case of the three-vehicle type optimal system of Figure 3.7, it was found that the transfer function $G_{n+1}(j\omega)$ was dependent on n and on the total number of vehicles in the string. A general result relating the steady-state position error of the i th vehicle in an r vehicle string to the position error of the 1st vehicle was shown to be

$$\frac{x_{i1}(0)}{x_{11}(0)} = \frac{r-i+1}{r} \quad (3.34)$$

Hence for a perturbation in position error of some vehicle in the string, the remaining vehicles will only move a fraction (given by (3.34)) of the magnitude of this perturbation. This is in contrast with the majority of the two-vehicle type optimal systems which had $G_{n+1}(0) = 1$. It should be pointed out that a step change in position error of a vehicle resulting in a steady-state offset in that variable is not a realistic situation. In practice, variations in the position

error of any vehicle will be random in nature and probably zero-mean. Hence we can say that the three-vehicle type system would react less strongly to random fluctuations in the motion of some vehicle than would the two-vehicle system. This is desirable when a group of vehicles sees a positive change in the position error of a vehicle at the end of the group. If the change is negative then collisions can occur if the magnitude of the change is large enough. This is illustrated mathematically by equation (3.32). Note however that vehicles ahead of a vehicle which exhibits a positive perturbation in position error see a "negative" change in that variable. In the three-vehicle system, these preceding vehicles react to the perturbation while in the two-vehicle system they do not. Hence we can conclude that, while requiring a more complex communications system, the three-vehicle automatic car-following system is more desirable from the standpoint of asymptotic behaviour.

REFERENCES

1. R.L. Cosgriff, "Dynamics of Automatic Longitudinal Control Systems for Automobiles", pp. 235-351 in "Theory and Design of Longitudinal Control Systems for Automobiles", Communication and Control Systems Laboratory, Ohio State University, Columbus, Ohio, Report No. EES 202A-8, September 1965.
2. L.E. Peppard and V. Gourishankar, "Asymptotic Stability of Optimally-Controlled Vehicle Strings", Proc. Fourth Hawaii Int. Conf. on System Sciences, pp. 287-289, January 1971.
3. R.E. Fenton and J.G. Bender, "A Study of Automatic Car-Following", I.E.E.E. Trans. Vehicular Technology, Vol. VT-18, pp. 134-140, November 1969.

APPENDIX 3-1

A Necessary and Sufficient Condition for
Asymptotic Stability of Vehicle Strings

In Section 3.1, the necessary and sufficient condition for asymptotic stability of a string of vehicles is stated as

$$|G_{n+1}(j\omega)| = \left| \frac{X_{n+1,1}(j\omega)}{X_{n1}(j\omega)} \right| \leq 1 \quad (\text{A3-1.1})$$

where $X_{n+1}(j\omega)$ and $X_n(j\omega)$ are the Fourier transforms of the position errors $x_{n+1}(t)$ and $x_{n1}(t)$ of the $(n+1)$ th and n th vehicles in the string respectively and $G_{n+1}(j\omega)$ is called the transfer function. Throughout this discussion we will be concerned with the motion of the $(n+1)$ th vehicle which is the "controlled vehicle" in the two-vehicle basic unit discussed earlier. The proof of (A3-1.1) is outlined in this appendix. It is based on that by Cosgriff given in [1].

If the transfer function $G_{n+1}(j\omega)$ is identical for all n , then

$$X_{n+1,1}(j\omega) = [G_{n+1}(j\omega)]^n X_{11}(j\omega) \quad (\text{A3-1.2})$$

The magnitude of the transfer function, namely $|G_{n+1}(j\omega)|$, will have one or more peaks and will approach zero as $\omega \rightarrow \infty$. As n increases, the values $|G_{n+1}(j\omega)|^n$ will be concentrated around the peaks of $|G_{n+1}(j\omega)|$.

Initially, it will be assumed that $|G_{n+1}(j\omega)|$ has a peak at $\omega = 0$ (which is generally the case) and then it will be assumed that a peak exists at $\omega = \omega_1 \neq 0$. The transfer function $G_{n+1}(j\omega)$ can

be approximated by an exponential series around each of its peaks.

For a peak occurring at $\omega = 0$, this approximation is

$$\frac{G_{n+1}(j\omega)}{G_{n+1}(0)} = [e^{-\eta_2\omega^2 - \eta_4\omega^4 - \dots}][e^{-j\eta_1\omega - j\eta_3\omega^3 - \dots}] \quad (\text{A3-1.3})$$

$\omega \text{ near } 0$

where the first factor is the amplitude $|G_{n+1}(j\omega)/G_{n+1}(0)|$ and the second is the phase shift of $G_{n+1}(j\omega)/G_{n+1}(0)$. For n sufficiently large Cosgriff^[1] has shown that the n th power of this ratio can be approximated by

$$\left[\frac{G_{n+1}(j\omega)}{G_{n+1}(0)} \right]^n = e^{-\eta_2\omega^2} e^{-j\eta_1\omega} \quad (\text{A3-1.4})$$

For a peak occurring at $\omega = \omega_1 \neq 0$, this approximation can be written

$$\left[\frac{G_{n+1}(j\omega)}{G_{n+1}(j\omega_1)} \right]^n = e^{-\eta_2(\omega - \omega_1)^2} e^{-j\eta_1(\omega - \omega_1)} e^{j\theta} \quad (\text{A3-1.5})$$

where θ is the phase of $G_{n+1}(j\omega_1)$. A similar approximation exists for the corresponding peak at $\omega = -\omega_1$.

For asymptotic stability, the perturbation in the position of the $(n+1)$ th vehicle must be bounded when the disturbance affecting the first vehicle is bounded. The time response of the $(n+1)$ th vehicle can be written by means of a convolution integral as

$$x_{n+1,1}(t) = \int_{-\infty}^{\infty} x_{11}(\tau) g_{n+1}(t-\tau) d\tau \quad (\text{A3-1.6})$$

where $g_{n+1}(t)$ is the inverse transform of $[G_{n+1}(j\omega)]^n$.

If the peak of $G_{n+1}(j\omega)$ occurs at $\omega = 0$, the peak value of $x_{n+1}(t)$ will occur when $x_{11}(t)$ is equal to its bound and is of long duration. This peak value is given by

$$(x_{n+1,1})_{\max} = (x_{11})_{\max} \int_{-\infty}^{\infty} g_{n+1}(t) dt = (x_{11})_{\max} [G_{n+1}(0)]^n \quad (\text{A3-1.7})$$

From (A3-1.7) it is immediately obvious that for $(x_{n+1,1})_{\max}$ to be bounded as $n \rightarrow \infty$, $G_{n+1}(0)$ must be less than or equal to unity. For a peak occurring at $\omega = \omega_1$ it can similarly be shown that the condition for $(x_{n+1,1})_{\max}$ to be bounded as $n \rightarrow \infty$ is $|G_{n+1}(j\omega_1)| \leq 1$.

Thus the condition for asymptotic stability can be written

$$|G_{n+1}(j\omega)| \leq 1 \quad \text{for all } \omega. \quad (\text{A3-1.8})$$

APPENDIX 3-2

In this appendix, the analysis of the signal flow graph for a string of four vehicles based on the three-vehicle basic unit (Figure 3.8) will be presented in detail.

The branch functions of Figure 3.8 are expressed in terms of the complex frequency s . We would like to obtain the transfer function

$$G_{n+1}(s) = \frac{X_{n+1,1}(s)}{X_{n1}(s)} \quad (\text{A3-2.1})$$

for each pair of vehicles (the n th and $(n+1)$ th) in the string where X_{n1} and $X_{n+1,1}$ are the position errors in the frequency domain for the two adjacent vehicles. Referring to the four-vehicle string of Figure 3.8 the following transfer function can be defined.

$$G'(s) = \left. \frac{X_{21}(s)}{X_{11}(s)} \right|_{X_{31} = X_{41} = 0} \quad (\text{A3-2.2})$$

The signal flow graph required to calculate $G'(s)$ is given in Figure A3-2.1.

Also define

$$\Gamma_1(s) = \left. \frac{X_{31}(s)}{X_{21}(s)} \right|_{X_{11} = X_{41} = 0} \quad (\text{A3-2.3})$$

$$\Gamma_2(s) = \left. \frac{X_{41}(s)}{X_{31}(s)} \right|_{X_{11} = X_{21} = 0} \quad (\text{A3-2.4})$$

The signal flow graph required to calculate the above two transfer functions is given in Figure A3-2.2. (The graph for Γ_1 is shown and $\Gamma_1 = \Gamma_2$).

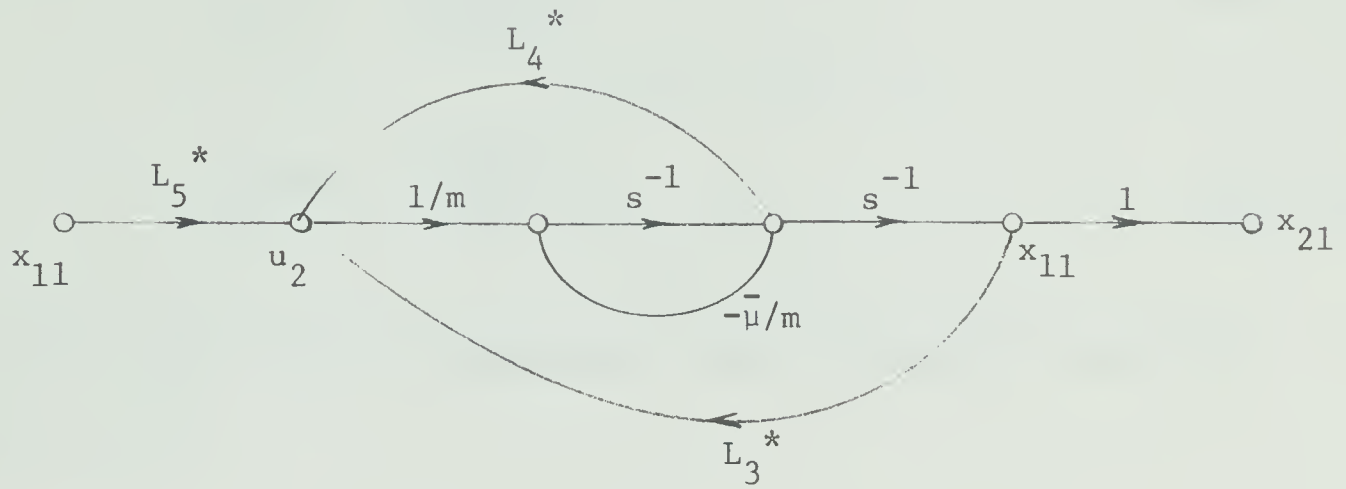


Figure A3-2.1 Signal Flow Graph Required to Calculate $G'(s)$

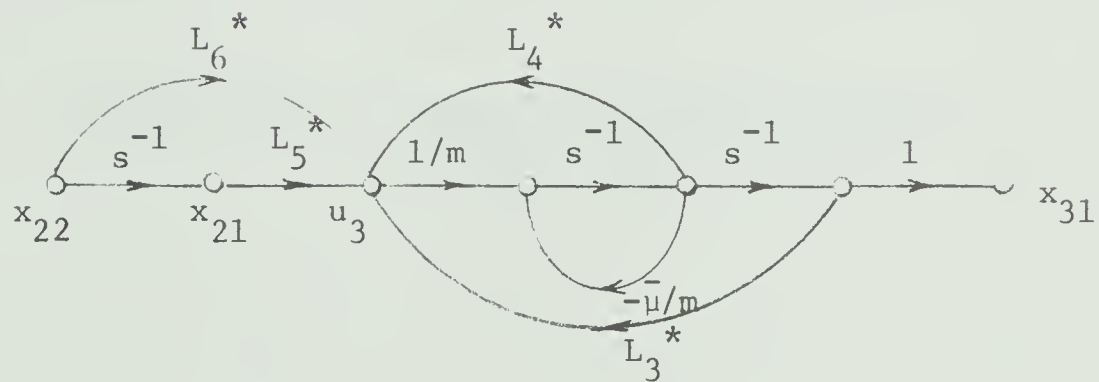


Figure A3-2.2 Signal Flow Graph Required to Calculate $\Gamma_1(s)$ and $\Gamma_2(s)$

Now define

$$\Gamma_3(s) = \frac{X_{21}(s)}{X_{31}(s)} \quad \left| \quad X_{11} = X_{41} = 0 \right. \quad (\text{A3-2.5})$$

$$\Gamma_4(s) = \frac{X_{31}(s)}{X_{41}(s)} \quad \left| \quad X_{11} = X_{21} = 0 \right. \quad (\text{A3-2.6})$$

$\Gamma_3(s) = \Gamma_4(s)$ and the corresponding signal flow graph is given in Figure A3-2.3.

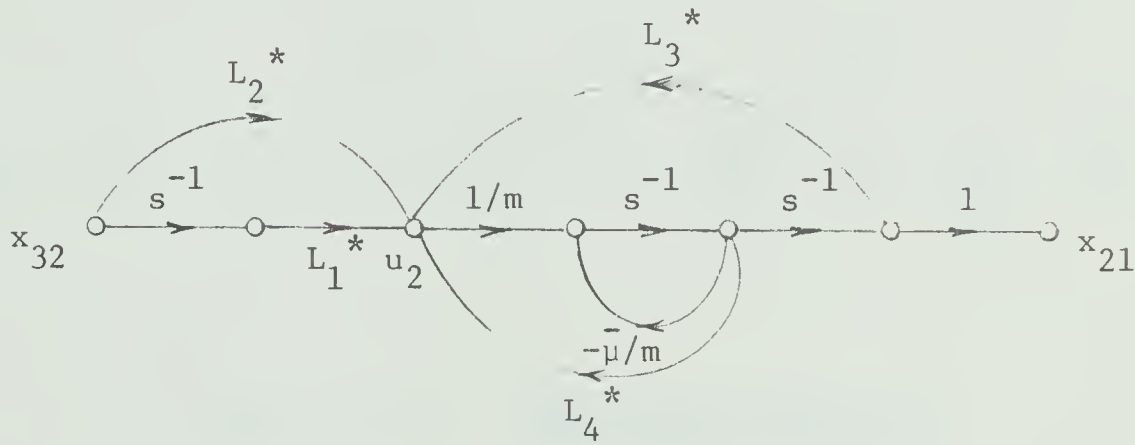


Figure A3-2.3 Signal Flow Graph Required to Calculate $\Gamma_3(s)$ and $\Gamma_4(s)$

The above five transfer functions when taken together completely describe the motion of any vehicle in the string for a perturbation in the motion of the first vehicle. The motion of the first vehicle is assumed to be unaffected by the motion of the following

vehicles and hence $X_{11}(s)/X_{21}(s) = 0$. Noting that for the three-vehicle unit, $L_1^* = L_5^*$ and $L_2^* = L_6^*$ (see Table 2.3), we can write

$$\Gamma_1(s) = \Gamma_2(s) = \Gamma_3(s) = \Gamma_4(s) = G(s) \quad (\text{A3-2.7})$$

Using superposition, the signal flow graph for the four-vehicle string can be redrawn as shown in Figure A3-2.4.

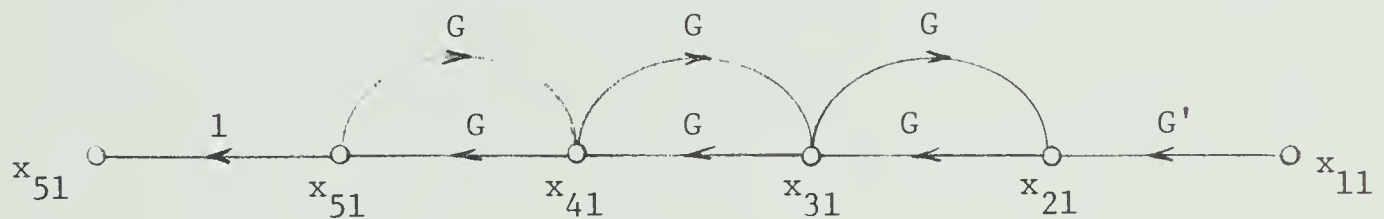


Figure A3-2.4 Signal Flow Graph for a Four-Vehicle String

Using Mason's Rule $G'(s)$ and $G(s)$ can be found to be

$$G'(s) = \frac{L_5^*/m}{s^2 + \left(\frac{\mu}{m} - \frac{L_4^*}{m}\right)s - \frac{L_3^*}{m}} \quad (\text{A3.28})$$

$$G(s) = \frac{L_5^* + L_6^* s}{s^2 + \left(\frac{\mu}{m} - \frac{L_4^*}{m}\right)s - \frac{L_3^*}{m}} \quad (\text{A3-2.9})$$

Knowing $G'(s)$ and $G(s)$, the transfer function $G_{n+1}(s)$ given by (A3-2.1) can be derived for $n = 1, 2, 3$. In the case of an r -vehicle string, the signal flow graph becomes that shown in Figure 3.10.

APPENDIX 3-3

In this appendix, the relationship between the scheduled headway, \hat{h} , resulting from a change in the position error of the 1st vehicle of \bar{x}_{11} will be derived. In subsection 3.4.3 it was shown that for a string of r vehicles, each vehicle, i , in the string will move the fraction $\frac{r-i+1}{r}$ of \bar{x}_{11} . We can now write

$$\hat{h} - \bar{h} = \hat{z}_{i-1} - \hat{z}_i - (z_{i-1} - z_i) \quad (\text{A3-3.1})$$

$$\text{or } \hat{h} - \bar{h} = \hat{z}_{i-1} - z_{i-1} - (\hat{z}_i - z_i) = x_{i-1,1} - x_{i1} \quad (\text{A3-3.2})$$

Since at steady-state $x_{i-1,1} - x_{i1}$ is equal for all i , let $i = 1$ and write

$$\bar{h} = \hat{h} - (x_{11} - x_{21}) = \hat{h} + \bar{x}_{11} \left(1 - \frac{r-1}{r}\right) \quad (\text{A3-3.3})$$

$$\text{or } \bar{h} = \hat{h} + \frac{\bar{x}_{11}}{r} . \quad (\text{A3-3.4})$$

CHAPTER 4

THE ROLE OF THE HUMAN OPERATOR IN A SEMI-
AUTOMATIC CAR-FOLLOWING SYSTEM4.1 Problems Associated with the Implementation of the Automatic
Optimal Car-Following System

The automatic optimal car-following system described earlier in this thesis was designed to meet the requirements of a longitudinal control system for a string of vehicles as outlined in Chapter 1. It has subsequently been demonstrated that the optimal system meets these requirements. It nevertheless must be pointed out that implementation of this system in a one-step manner is not economically or practically feasible. Some of the problems involved in implementing the automatic car-following system are:

1. The automatic system is not compatible with the present-day highway-automobile-driver system. The vehicles required for the automatic system would probably be electrically propelled, receiving power from the guideway. This would enable the construction of smaller, lighter vehicles. The vehicles would be equipped with receiving and transmitting apparatus as well as the necessary running-gear for automatic lateral control. Communication between vehicles would probably be handled by waveguides or similar devices associated with the guideway. Devices for position sensing as well as for automatic lateral control would also be associated with the guideway. From the above it can be concluded that implementation of the automatic system would require replacement of the conven-

tional automobiles now used on existing highways and extensive modification of the highways themselves.

2. Emergency situations cannot be handled by the optimal automatic control system. When an emergency condition develops in a string of vehicles proceeding in steady state along a guideway (for example, one vehicle may suddenly accelerate or decelerate at a high and uncontrolled rate), it may be necessary to apply the maximum available corrective force to the other vehicles in the string in order to minimize the number of collisions. This cannot be done by the optimal controller for two reasons. First, each vehicle in the optimal system receives motional information from, at most, the vehicles directly ahead and behind. Thus an emergency situation will not be immediately detected by all vehicles in the string. Second, the optimal controller will not apply the maximum available force to a vehicle since it is designed to minimize the expenditure of control energy. Hence, an overriding control system (which would monitor the states of all vehicles in the string) would be required to handle emergency situations.
3. The automatic longitudinal car-following system cannot handle merging and exiting operations. A merging scheme such as that suggested by Athans^[1] for use with high-speed trains might be incorporated into the automatic system only at the cost of a more elaborate sensing and communication system. The problem of exiting from a vehicle string might perhaps be more easily handled.

Most of the problems mentioned above could be solved by the inclusion of the human operator as a link in the automatic system. The

role of the human operator would be that of an "inexpensive" but at the same time adaptive overriding controller in an otherwise "automatic" system. Such a system, in which the human operator would handle merging and exiting, emergency situations and possibly lateral control of the vehicle, would be economically feasible since it could make use of existing highways and automobiles. The details of such a system will be discussed later in this chapter.

In Section 4.2, two main qualities of the human operator, namely adaptation and optimization, which enhance his usefulness as a link in an automatic control system will be discussed. In Section 4.3 the tracking performance of the human operator with two types of displays and two types of controllers will be investigated. Section 4.4 will present the results of a simulated car-following experiment in which the human operator in the control loop is supplied with information about the difference between the states of his vehicle and those of an optimally-controlled vehicle. In Section 4.5 the general form of a semi-automatic car-following system based on the experimental results is proposed.

4.2 Adaptive and Optimization Characteristics of the Human Operator

The human operator possesses two main qualities which enable him to extend and improve upon the performance of a control system. These are *adaptation* and *optimization*.

Adaptation: The human has long been recognized as an adaptive control system, that is, a system which will maintain control in the face of change. The human operator adapts by becoming aware of some change which requires an alteration in his response pattern. The

information which he receives about this change can be either *direct* or *inferred*. Direct information is gathered either by the unaided senses or through sensing instruments. Inferred information is obtained by observing deviation of the system output from that expected. Normally the operator will employ a combination of both direct and inferred information. The advantage of direct information is that it can be predictive. That is, the operator can learn about changes which will affect control before they actually do so. Since no feedback from the system output is required, direct information is said to be open loop in nature. On the other hand, inferred changes in the system require closed-loop adjustments often made on a trial basis. As a consequence, this type of adaptation can never be made before the change being adapted to has affected the system output. When using a combination of direct and inferred information, the operator will usually infer a change from the behaviour of the controlled element and then use direct information to explain the change and so choose a course of action.

Optimization: Optimization, either by an automatic system or the human operator, implies the existence of some performance criterion which influences the nature of the control. For the human operator behaving as an adaptive system, some criterion must exist if he is to know whether or not he has successfully adapted to a change. As Kelley^[2] has pointed out, the optimality of the human operator does not imply the finding of a solution to a mathematically defined criterion function but rather the exercising of judgement with respect to the many different criteria relevant to human action.

4.3 Effects of Display and Controller Characteristics on Human Operator Tracking Performance

4.3.1 Display and Controller Types

Two different types of displays and two different types of controllers were tested in order to determine a suitable display-controller combination for achieving good tracking performance. The displays considered are:

1. Scope display (SD) - The difference between the operator's controller output and the driving function (for a compensatory tracking task) is displayed by the horizontal displacement of an oscilloscope beam. This is illustrated in Figure 4.1(a).
2. Meter display (MD) - The difference between the operator's controller output and the driving function is displayed by the displacement of a meter needle from a zero-centre position. The meter was adjusted to exhibit approximately critical damping. The meter display is illustrated in Figure 4.1(b).

The controllers considered are:

1. Knob-actuated potentiometer controller (KC) - This controller is shown in Figure 4.2(a). The controller output is proportional to the angle of rotation from top centre.
2. Lever-actuated potentiometer controller (LC) - This controller is shown in Figure 4.2(b). It is attached to the operator's arm rest and is operated by the fingers of the left or right hand.

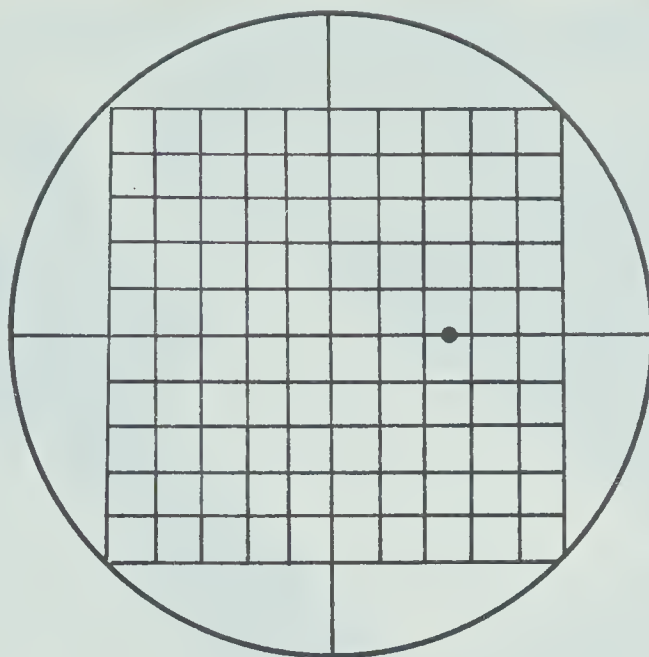


FIGURE 4.1(a) Scope Display in Which Tracking Error is Proportional to Displacement of Dot From Zero (Hughes Model 106 "Memo-Corder")

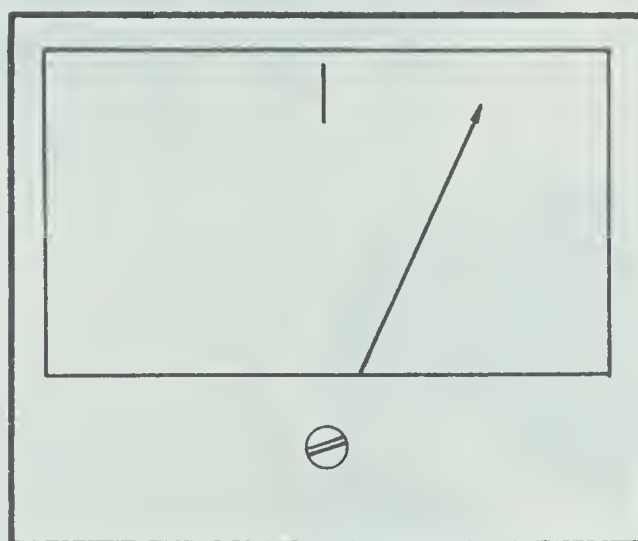


FIGURE 4.1(b) Meter Display in Which Tracking Error is Proportional to Displacement of Needle From Zero

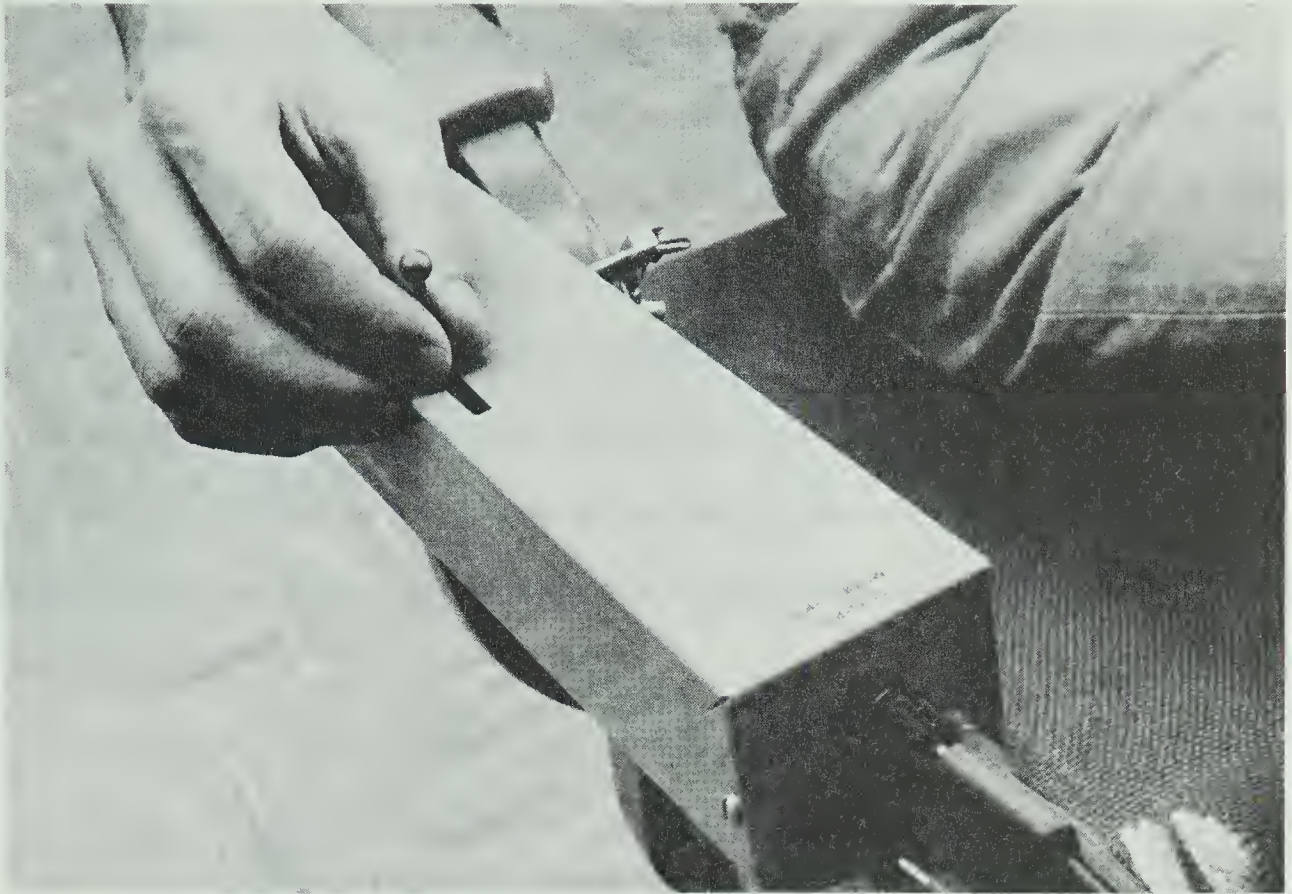


FIGURE 4.2(a) Lever Controller

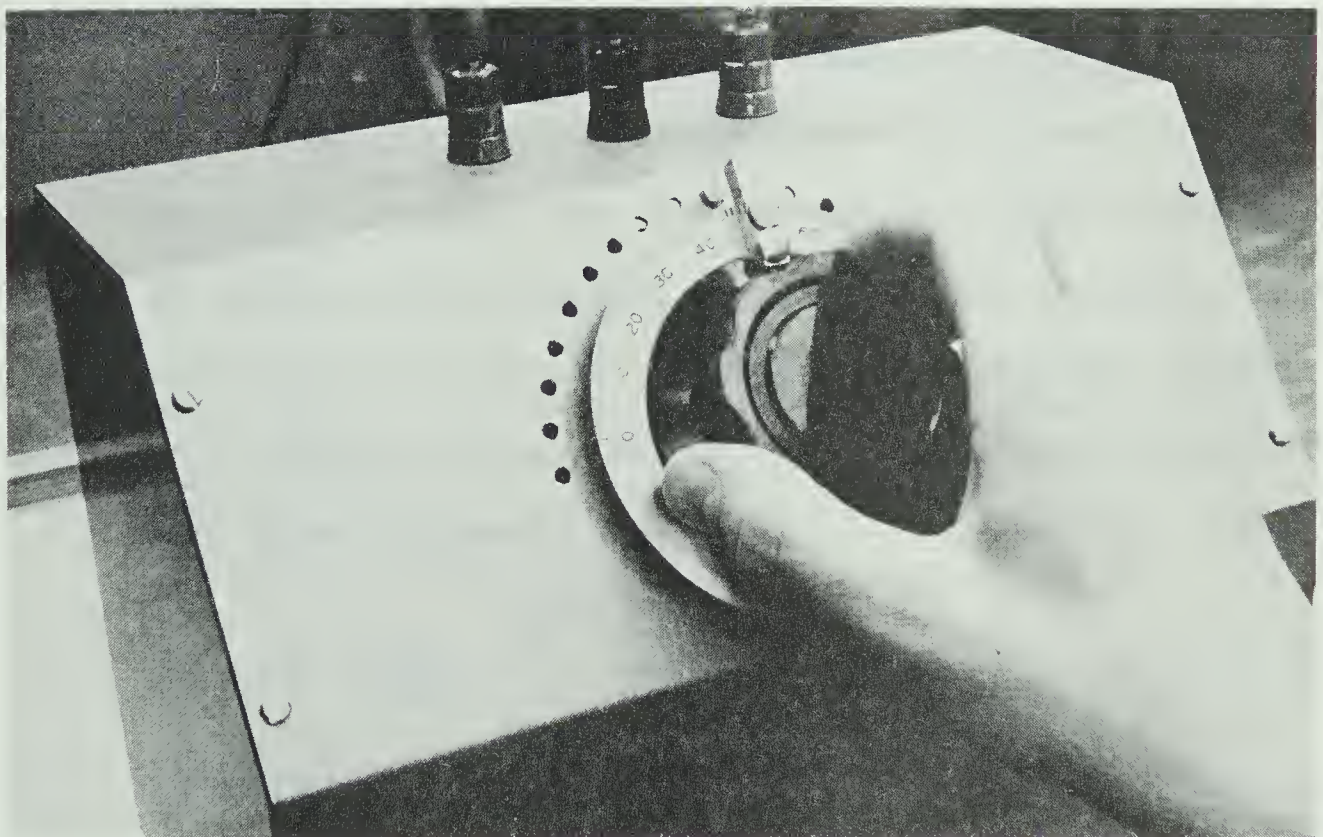


FIGURE 4.2(b) Knob Controller

4.3.2 Display Type and Magnification vs. Tracking Performance

For a particular controller sensitivity, it would be expected that the gain associated with the display device (the display magnification) would have a significant effect on human tracking performance. In order to determine the form of the dependence of tracking performance on display magnification and on display type, the following compensatory tracking experiments were performed: (The configuration of these experiments is indicated in block diagram form in Figure 4.3).

1. KC-SD: The sensitivity of the KC was fixed and the magnification of the SD varied. For each magnification setting, four 200 second compensatory tracking runs were made. The forcing function used was the output of a SERVOMEX Model R.G. 77 Random Noise Generator band-limited by a second-order, maximally-flat filter with an upper break-point of 0.0625 Hz. The resulting signal has essentially uniform power output to very low frequencies and an amplitude distribution approximating Gaussian with zero-mean. The measure of tracking performance was taken to be the value of the mean squared tracking error over the 200 second run. That is, the tracking performance index is given by

$$P = \frac{1}{200} \int_0^{200} [w(t) - u(t)]^2 dt \quad (4.1)$$

where $w(t)$ is the forcing function and $u(t)$ is the output of the controller. Two test subjects (male, ages 26 and 27) were instructed to maintain, as near as possible, zero error on the

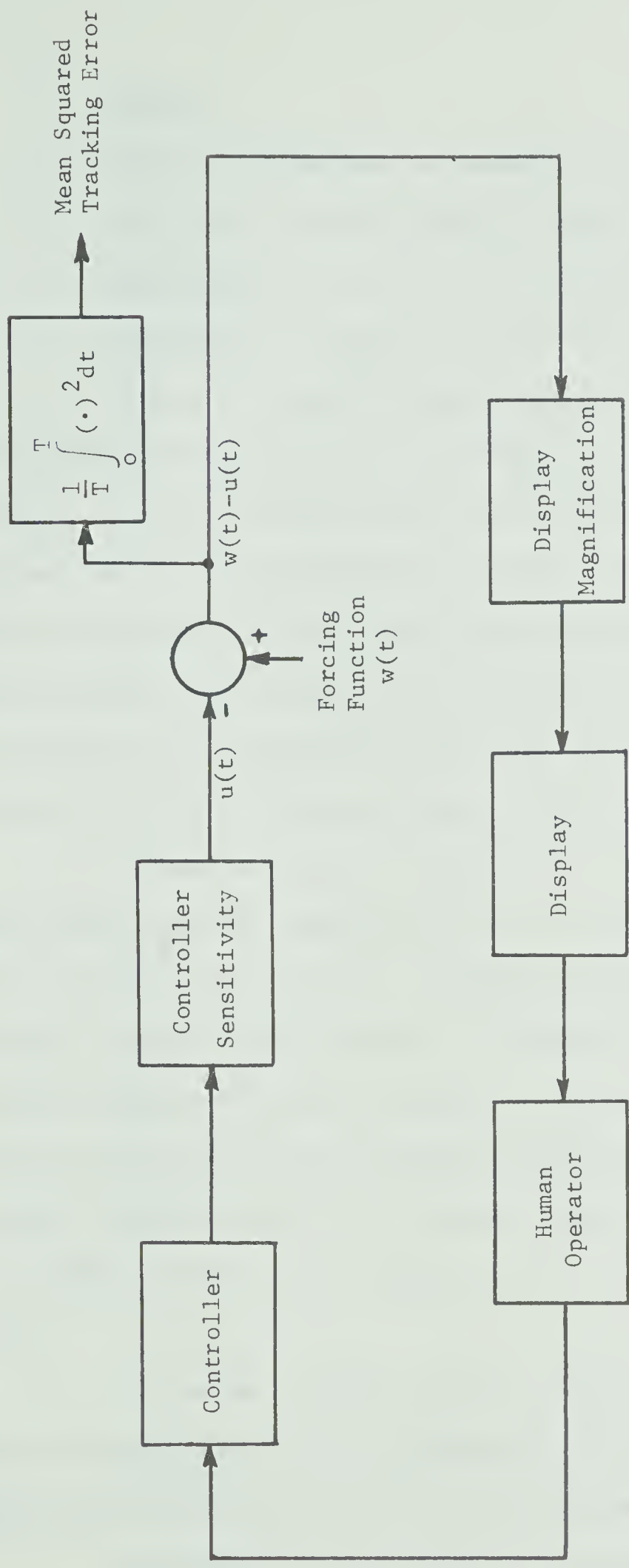


FIGURE 4.3 Block Diagram for the Tracking Experiments Described in Section 4.3

display.

2. KC-MD: For the same KC sensitivity as used in the SD experiment above, the same series of runs was made using the MD.

Equal magnification on the two displays was taken to be equal percentage of full-scale indication for a given input.

Figure 4.4 shows the mean value of P for the four runs at each magnification using the SD plotted vs. magnification. The mean squared tracking error and magnification scales are arbitrary but consistent for all the experiments reported in this chapter. Figure 4.5 shows the mean values of P using the MD normalized with respect to the corresponding values using the SD plotted vs. magnification. Figure 4.6 shows the forcing function $w(t)$ and the tracking error $[w(t) - u(t)]$ plotted vs. time for typical runs at various SD magnifications (subject B).

It can be seen from Figures 4.4, 4.5 and 4.6 that tracking performance improves significantly for an increase in magnification of either display from X1 to X5. Further performance improvement with increased magnification is minimal. In addition, both test subjects found tracking to be more fatiguing at higher magnifications. This might possibly show up as a reduction in tracking performance if runs longer than 200 seconds were required. Hence it was concluded that, for either display type, a magnification of from X2 to X5 was most useful.

It can be seen from Figure 4.5 that tracking performance using the MD was superior at all magnifications to that using the SD. Hence the MD was used for all further experiments.

Tabulation of the values of P obtained for each run of the above experiments is presented in Appendix 4-1.

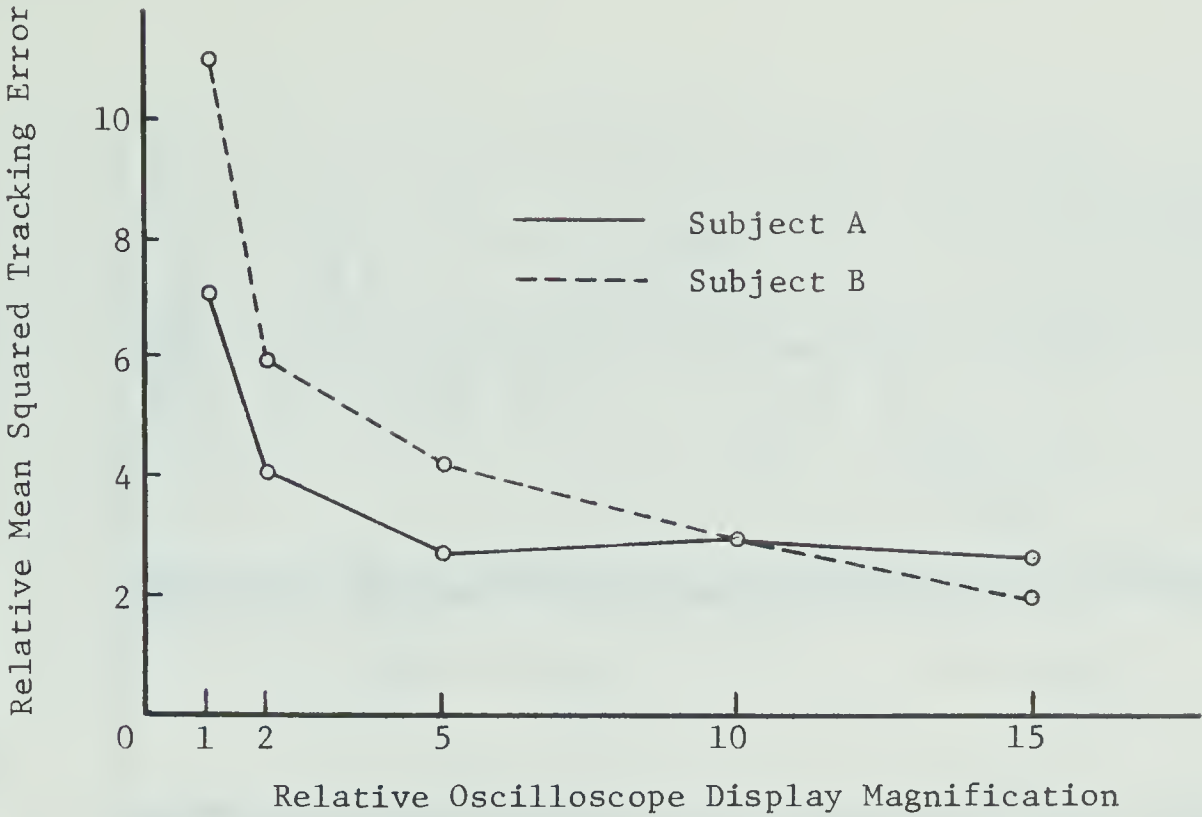


FIGURE 4.4 Tracking Performance of Subjects A and B Using the Oscilloscope Display and Knob Controller

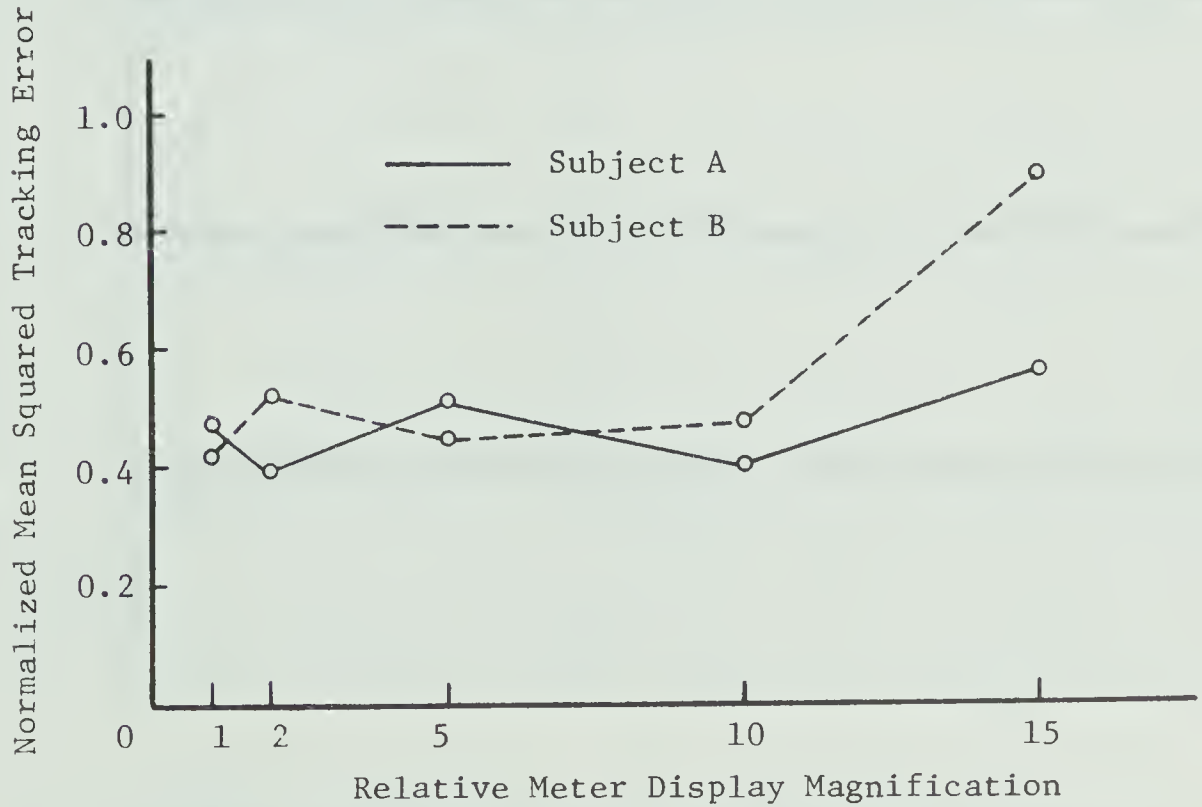


FIGURE 4.5 Tracking Performance of Subjects A and B Using the Meter Display and Knob Controller

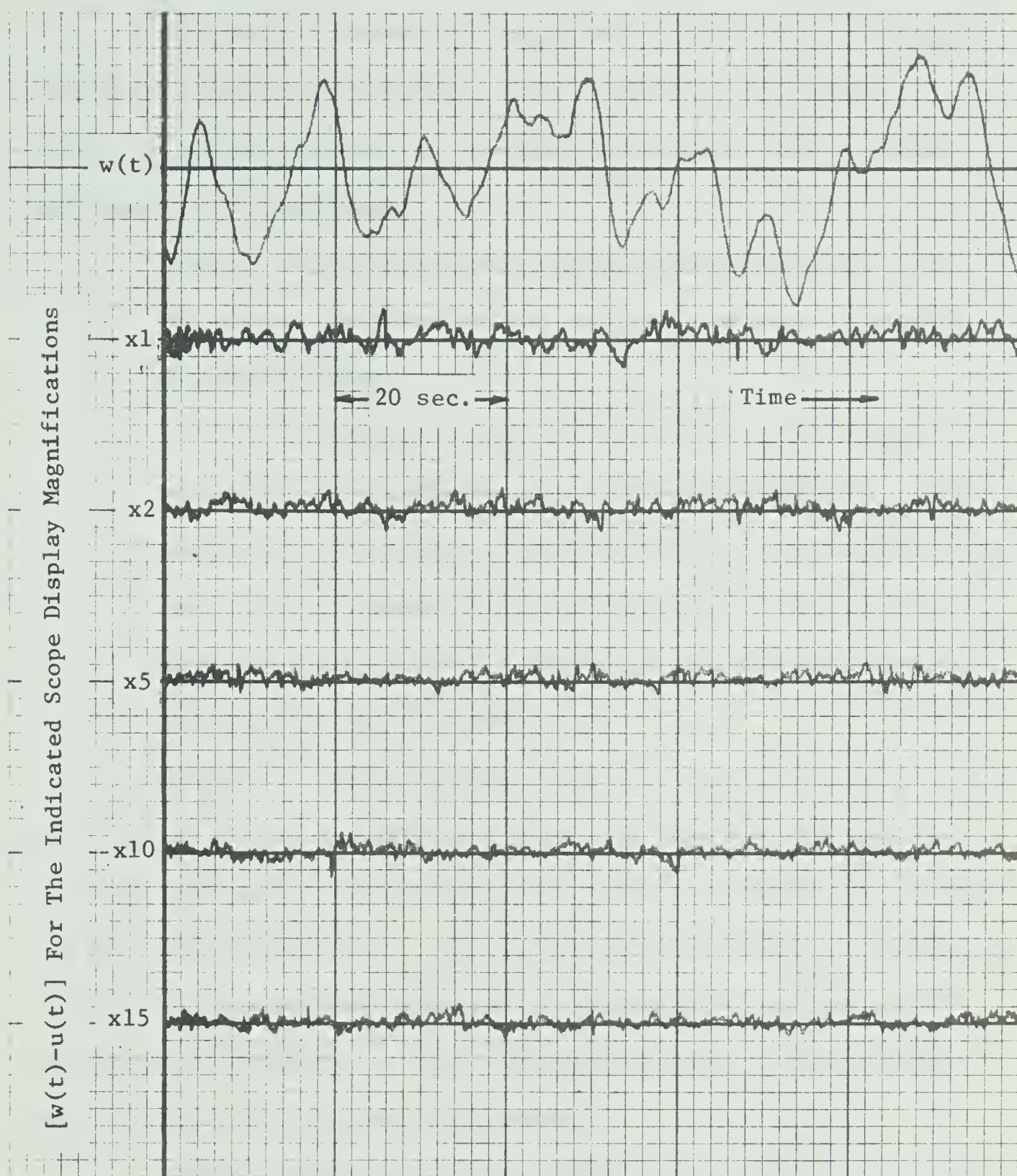


FIGURE 4.6 Tracking Error Time Response of Subject B
For Various Oscilloscope Display Magnifications

4.3.3 Controller Type and Sensitivity vs. Tracking Performance

In order to assess the relative merits of the two types of controllers previously described and to determine the effect of controller gain (sensitivity) on tracking performance, the following experiments were performed:

1. KC-MD: For an MD display magnification fixed at X2, two 200 second runs were made by subject A at each of several KC sensitivities.
2. LC-MD: An experiment similar to that above but using the LC at various sensitivities was performed by subject B. In addition, for a fixed LC sensitivity of X1, MD magnification was varied to assess the relative merits of the LC and KC at each magnification. Four 200 second runs were made to each magnification by subject B.

Figure 4.7 shows the mean values of P for each set of two runs plotted vs. KC sensitivity. From this figure there appears to be an optimum sensitivity for achieving the best tracking performance (in this case, about 0.5). The test subject reported that tracking was difficult at low sensitivities due to the necessity of large knob rotations and difficult at high sensitivities due to the tendency to over-correct for a display displacement.

Figure 4.8 shows the mean values of P for each set of two runs plotted vs. LC sensitivity. Less degradation in tracking performance at low sensitivities is apparent possibly due to the ease of moving the LC large distances compared to the KC.

Figure 4.9 shows the mean values of P for each set of four runs using a X1 LC sensitivity plotted vs. MD magnification. Values

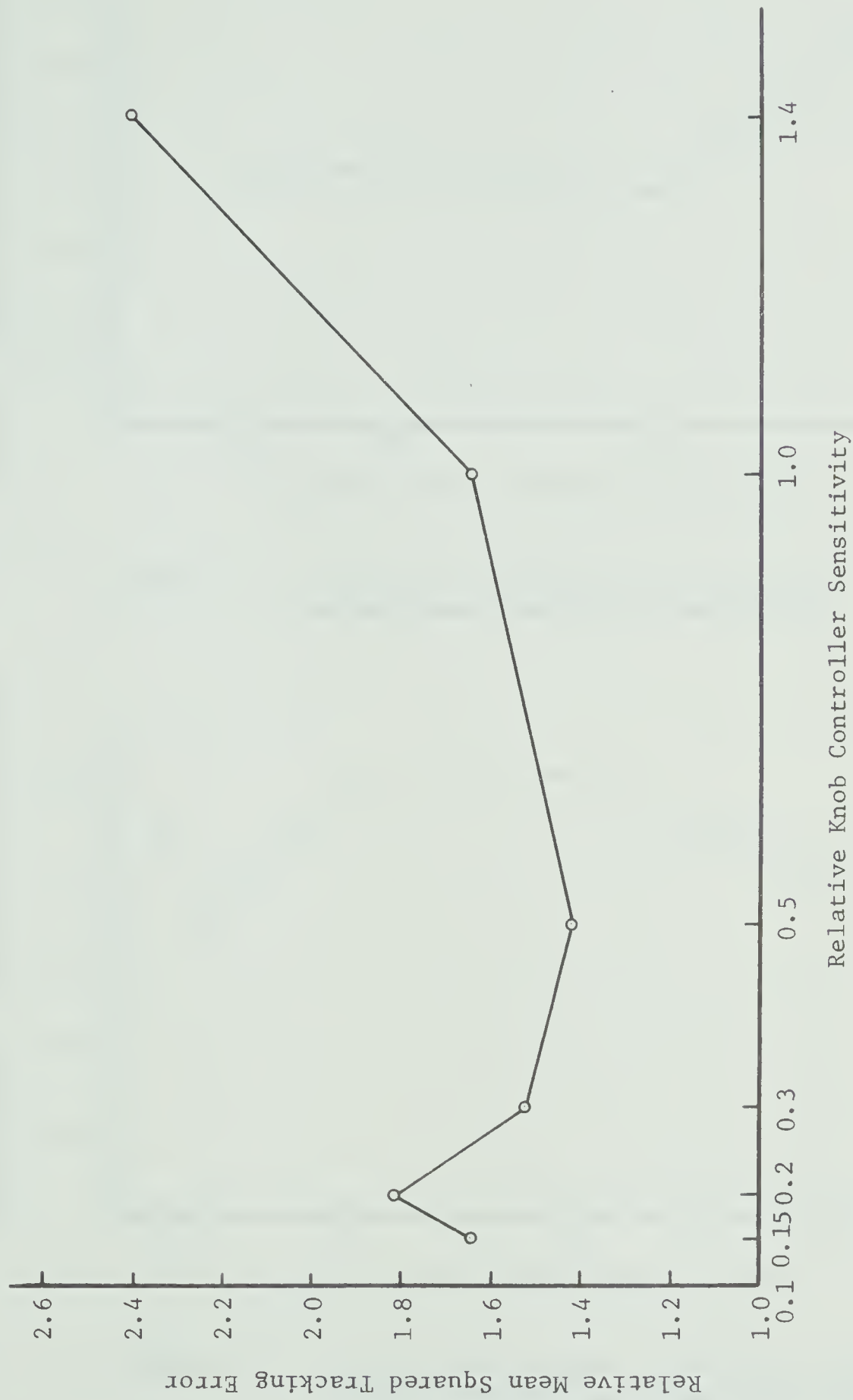


FIGURE 4.7 Tracking Performance of Subject A For Varying Knob Controller Sensitivity

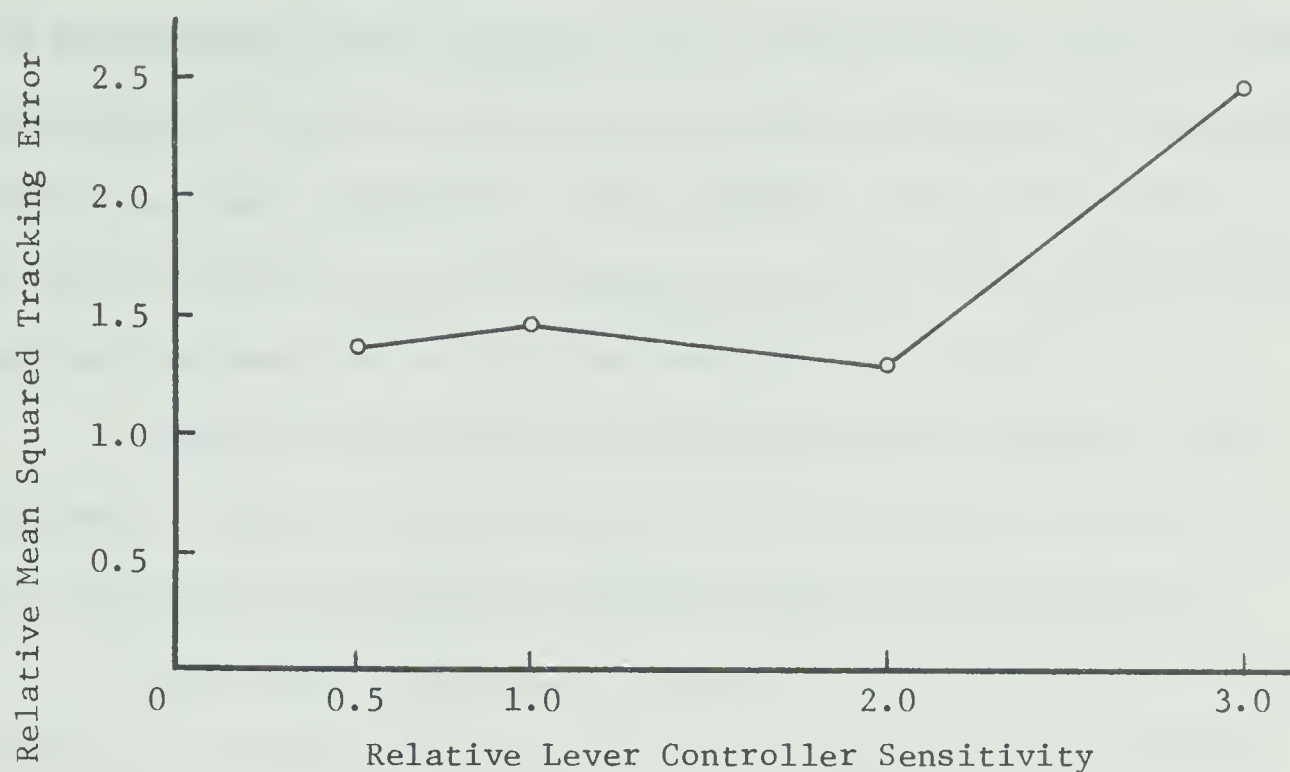


FIGURE 4.8 Tracking Performance of Subject B For Varying Lever Controller Sensitivity

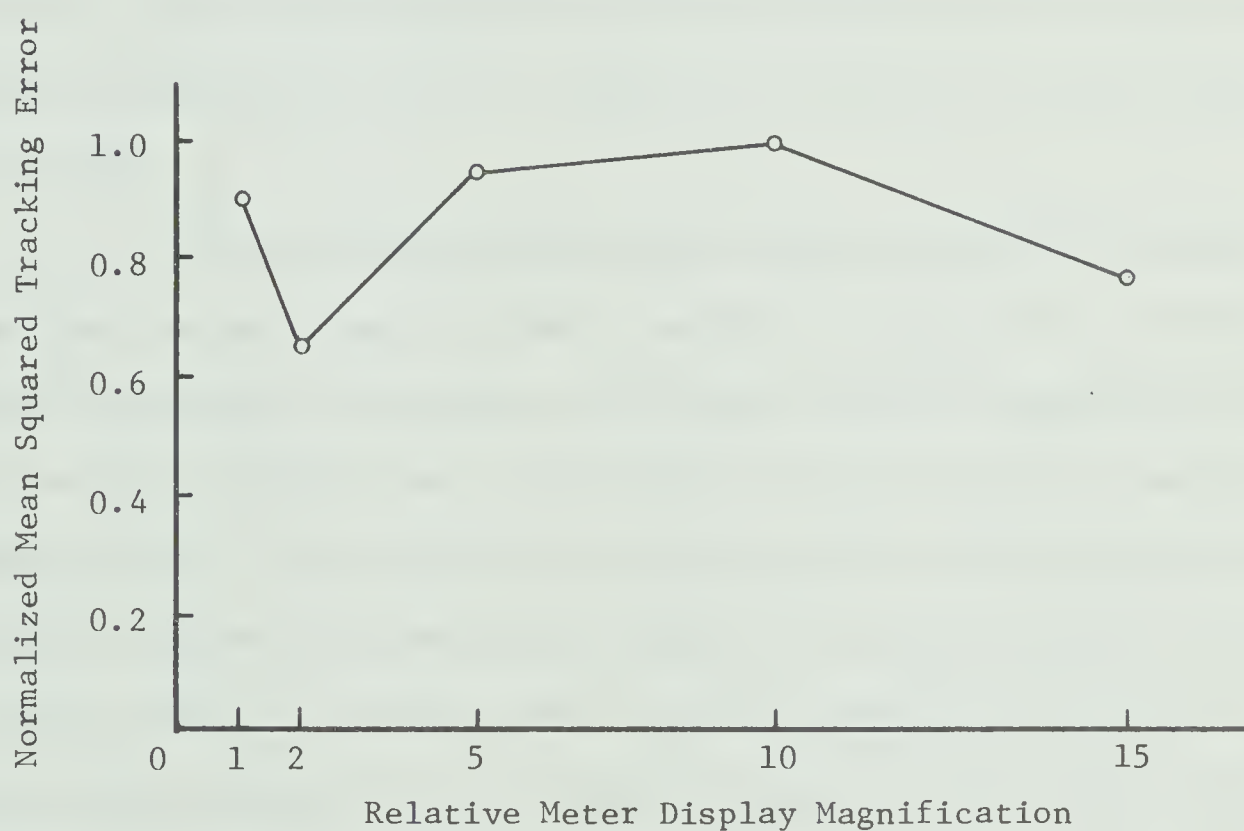


FIGURE 4.9 Tracking Performance of Subject B Using the Meter Display and Lever Controller

of P are normalized with respect to the corresponding values obtained using the KC. It can be seen that performance using the LC is slightly better than that using the KC. Both subjects expressed a preference for the LC due to its ease of operation and thus this controller was used for the remainder of the experiments in this chapter.

Values of mean squared tracking error for each run of the experiments reported in this subsection are tabulated in Appendix 4-1.

4.4 A Simulated Car-Following Experiment with the Human Operator

The results reported in the previous section indicate that the MD-LC configuration results in the best combination of tracking performance and ease of operation. This display-controller combination can now be used in a simulated car-following experiment. Also keeping in mind the results of the previous experiments, MD magnification was adjusted to be in the range of X2 to X5 and LC sensitivity to be near X1.

The car-following experiment can be described as follows:

The human operator was required to perform a compensatory tracking task which would result in headway and relative velocity regulation between his vehicle [(n+1)th] and a lead vehicle (nth) simulated to undergo random motion. The velocity error was simulated by the output of the SERVOMEX Random Noise Generator, filtered as described in the previous section, while the position error was the integral of the velocity error. It was also desired that the operator supply a control to the (n+1)th vehicle which was optimal with respect to some performance index such as those used for the two-vehicle optimal control system discussed in Chapter 2. To achieve this goal, the information displayed to the operator was chosen to be a linear combination of the difference between

the optimal control (for a particular cost functional) and the operator's control and the difference between the optimal position error of the (n+1)th vehicle and the position error of the operator's vehicle. This is shown in Figure 4.10 which is a block diagram of the car-following experiment.

The displayed information can be written as

$$D = u_{n+1}^*(t) - u_{n+1}(t) + \phi[x_{n+1,1}^*(t) - x_{n+1,1}(t)] \quad (4.2)$$

where ϕ is a non-negative weighting factor. For $\phi = 0$, the operator receives no feedback of information as to the state of his vehicle. He will thus attempt only to minimize the difference between his control and the optimal control.

For values of ϕ of 0, 2, 5, 10 and 20, four 100 second runs were made by subject B and the mean squared values of $(x_{n1} - x_{n+1,1})$, $(x_{n1} - x_{n+1,1}^*)$, $(x_{n2} - x_{n+1,2})$, $(x_{n2} - x_{n+1,2}^*)$ and $(u_{n+1} - u_{n+1}^*)$ recorded for each run. Tabulation of these results can be found in Appendix 4-1. The optimal control scheme chosen was that of two-vehicle system 2d derived in Chapter 2. The average mean squared values of $(x_{n1} - x_{n+1,1})$, $(x_{n2} - x_{n+1,2})$ and $(u_{n+1} - u_{n+1}^*)$ for each set of four runs are plotted vs. ϕ in Figures 4.11, 4.12 and 4.13 respectively. Table 4.1 gives the corresponding numerical results. Figures 4.14, 4.15 and 4.16 show the quantities $(x_{n1} - x_{n+1,1}^*)$, $(x_{n1} - x_{n+1,1})$, $(x_{n2} - x_{n+1,2}^*)$, $(x_{n2} - x_{n+1,2})$, and $(u_{n+1}^* - u_{n+1})$ plotted vs. time using a BRUSH 8-channel recorder for $\phi = 0, 2$ and 16 respectively.

It can be seen from Figure 4.14 that for $\phi = 0$, the quantity $(x_{n1} - x_{n+1,1})$ is not kept near zero but is allowed to drift as the

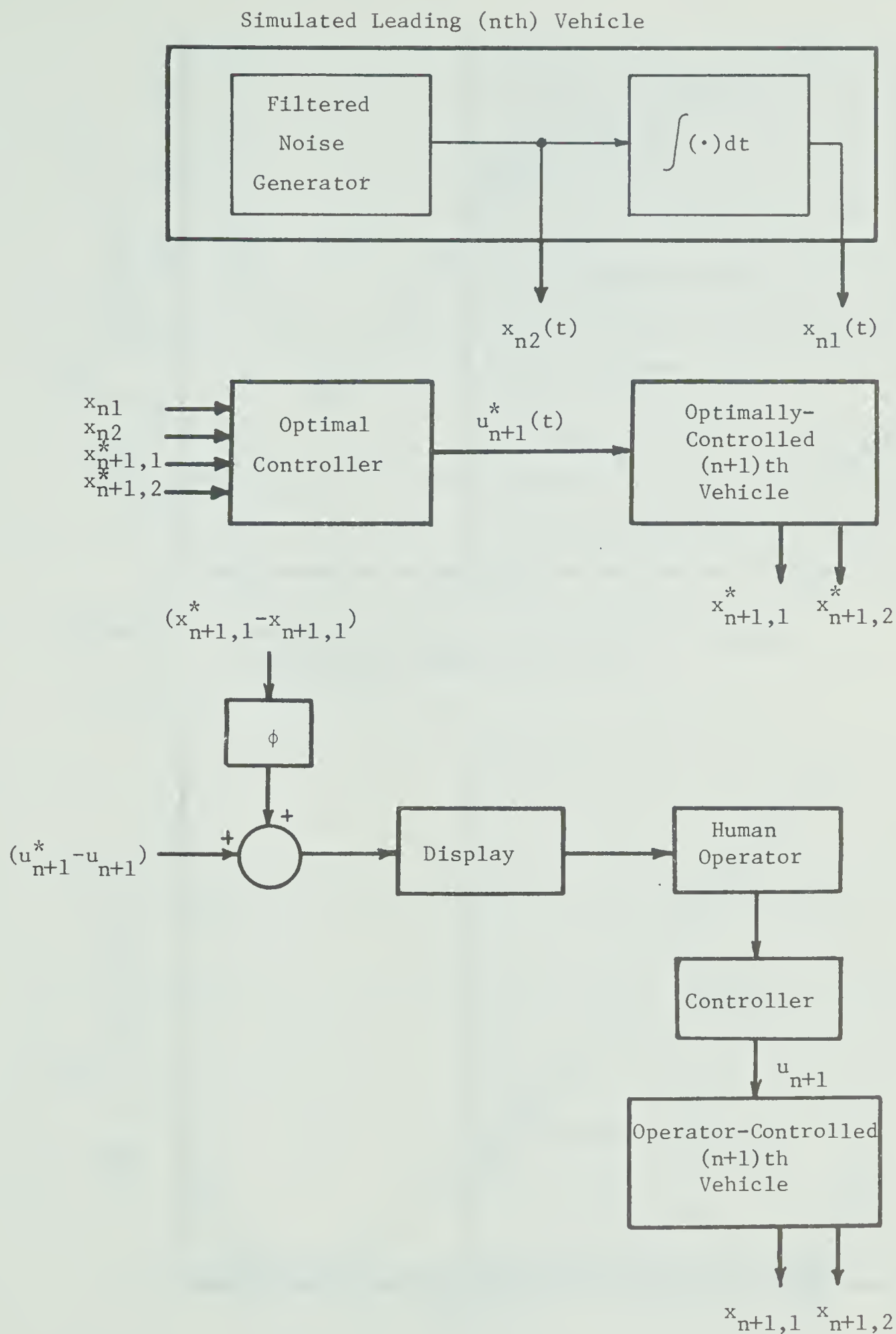


FIGURE 4.10 Block Diagram of the Simulated Car-Following Experiment Described in Section 4.4

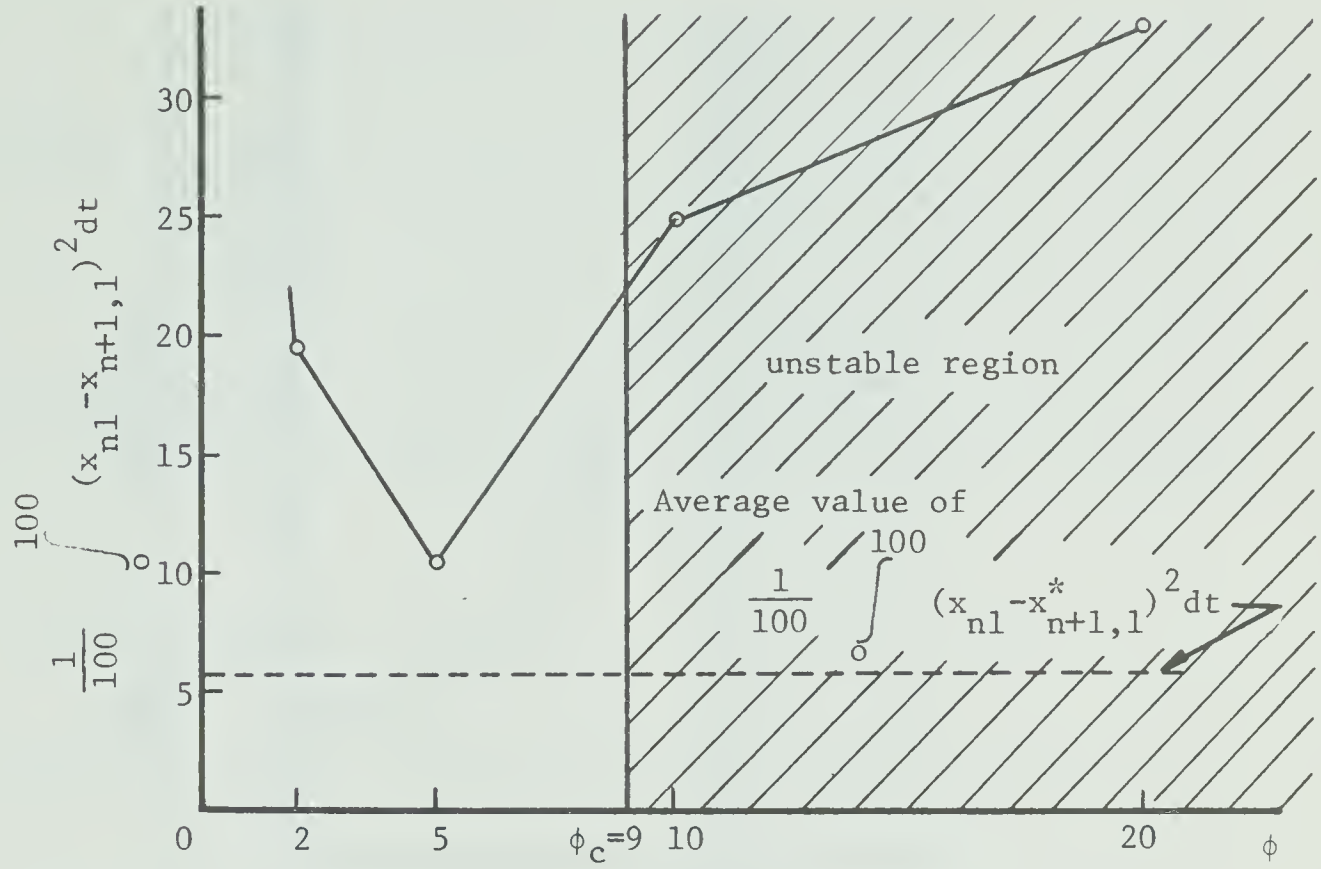


FIGURE 4.11 Variation in Mean Squared Headway Deviation with Display Weighting Factor ϕ

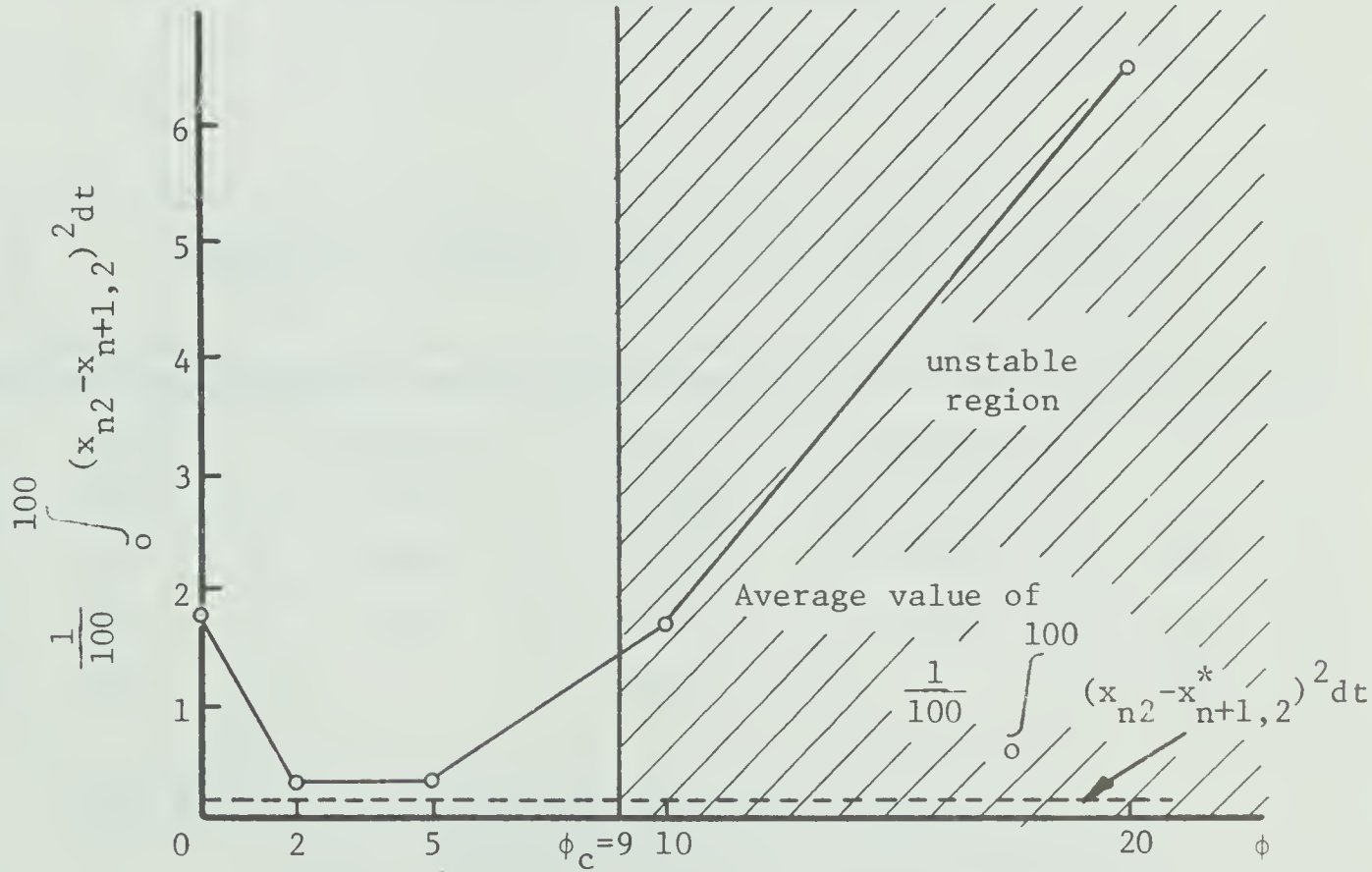


FIGURE 4.12 Variation in Mean Squared Relative Velocity with Display Weighting Factor ϕ

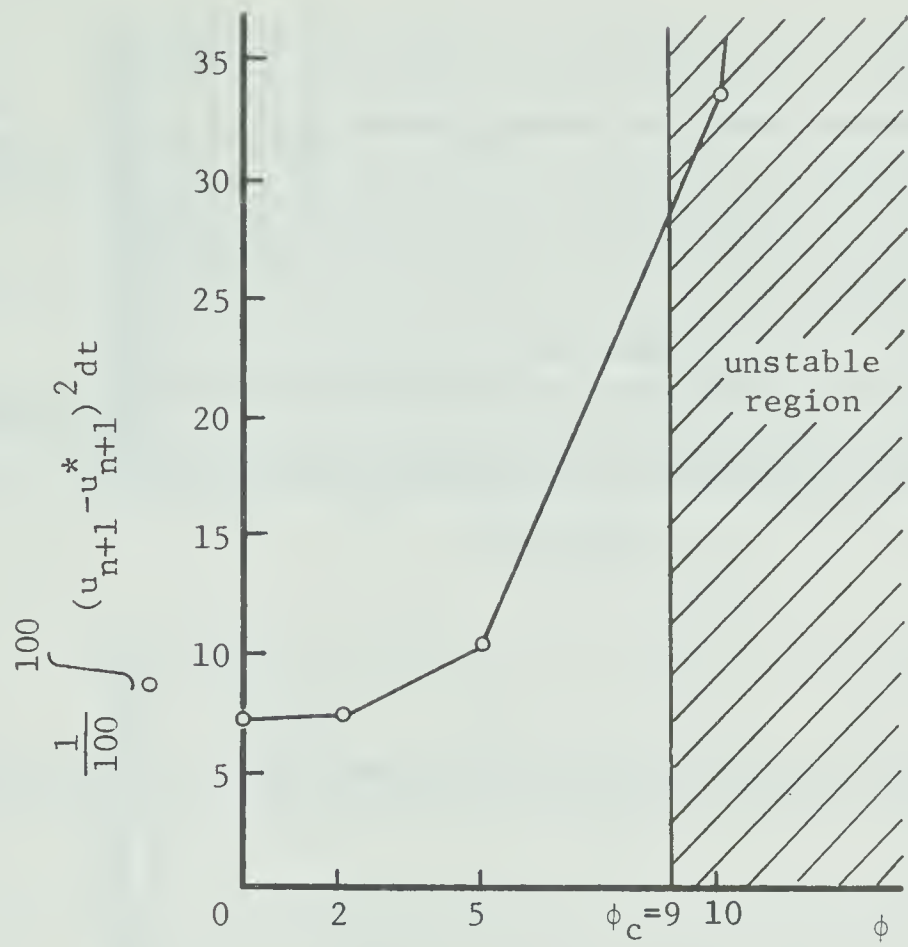


FIGURE 4.13 Variation in Mean Squared Control Error With Display Weighting Factor ϕ

ϕ	Average Mean Squared Value of the Indicated Quantity				
	$(x_{n1} - x_{n+1,1})$	$(x_{n1} - x_{n+1,1}^*)$	$(x_{n2} - x_{n+1,2})$	$(x_{n2} - x_{n+1,2}^*)$	$(u_{n+1}^* - u_{n+1})$
0	5170	Average	1.77	Average	7.12
2	19.4	For 20	0.295	For 20	7.37
5	10.5	Runs =	0.302	Runs =	10.4
10	25.0	5.79	1.74	0.190	33.7
20	33.2		6.49		123.0

Table 4.1 Average Relative Mean Squared Errors For Each Set of Four Runs Taken For a Particular Value of ϕ . Values Correspond to Those Plotted in Figures 4.11, 4.12 and 4.13.

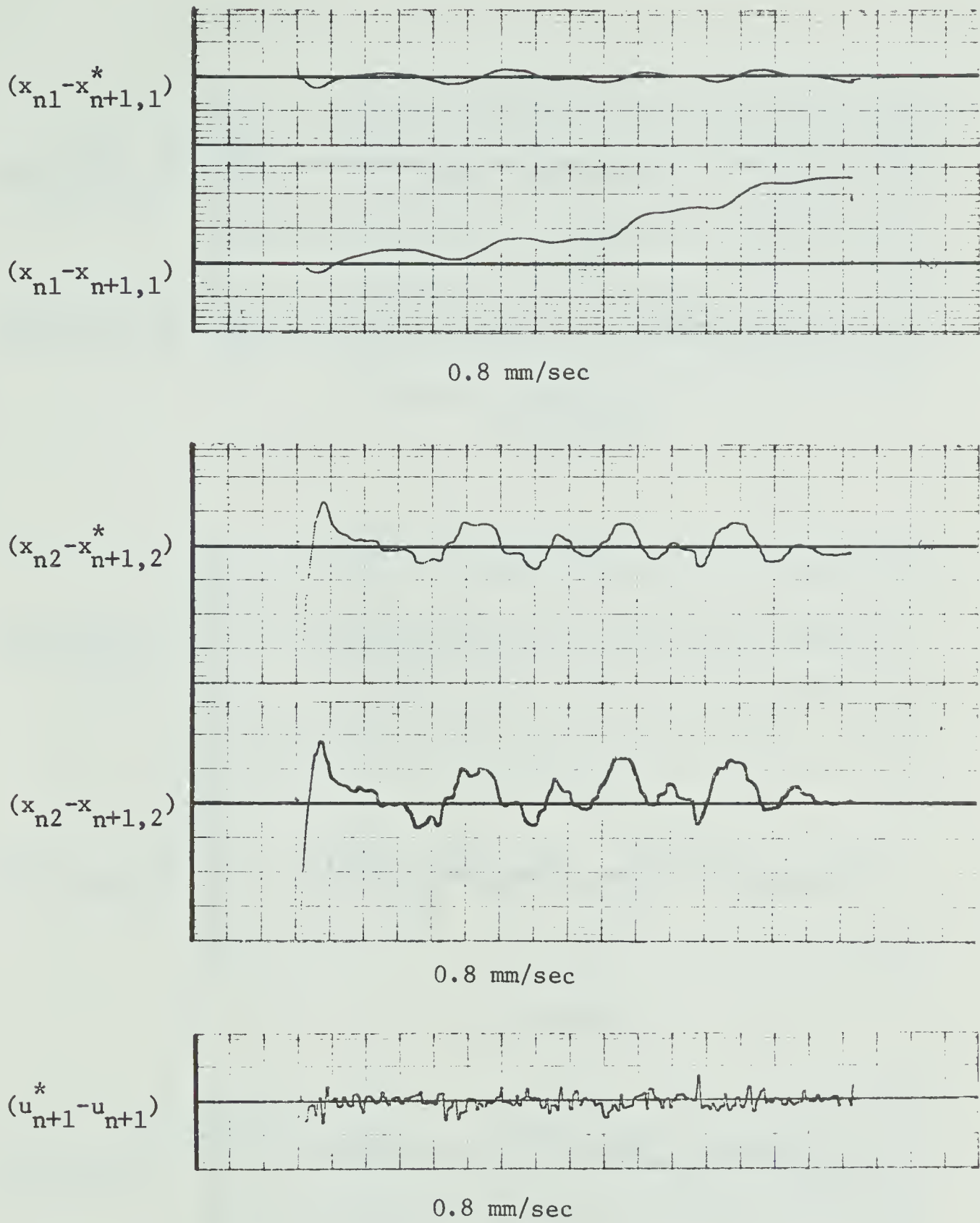


FIGURE 4.14 Operator and Optimal Controller Performance for $\phi = 0$

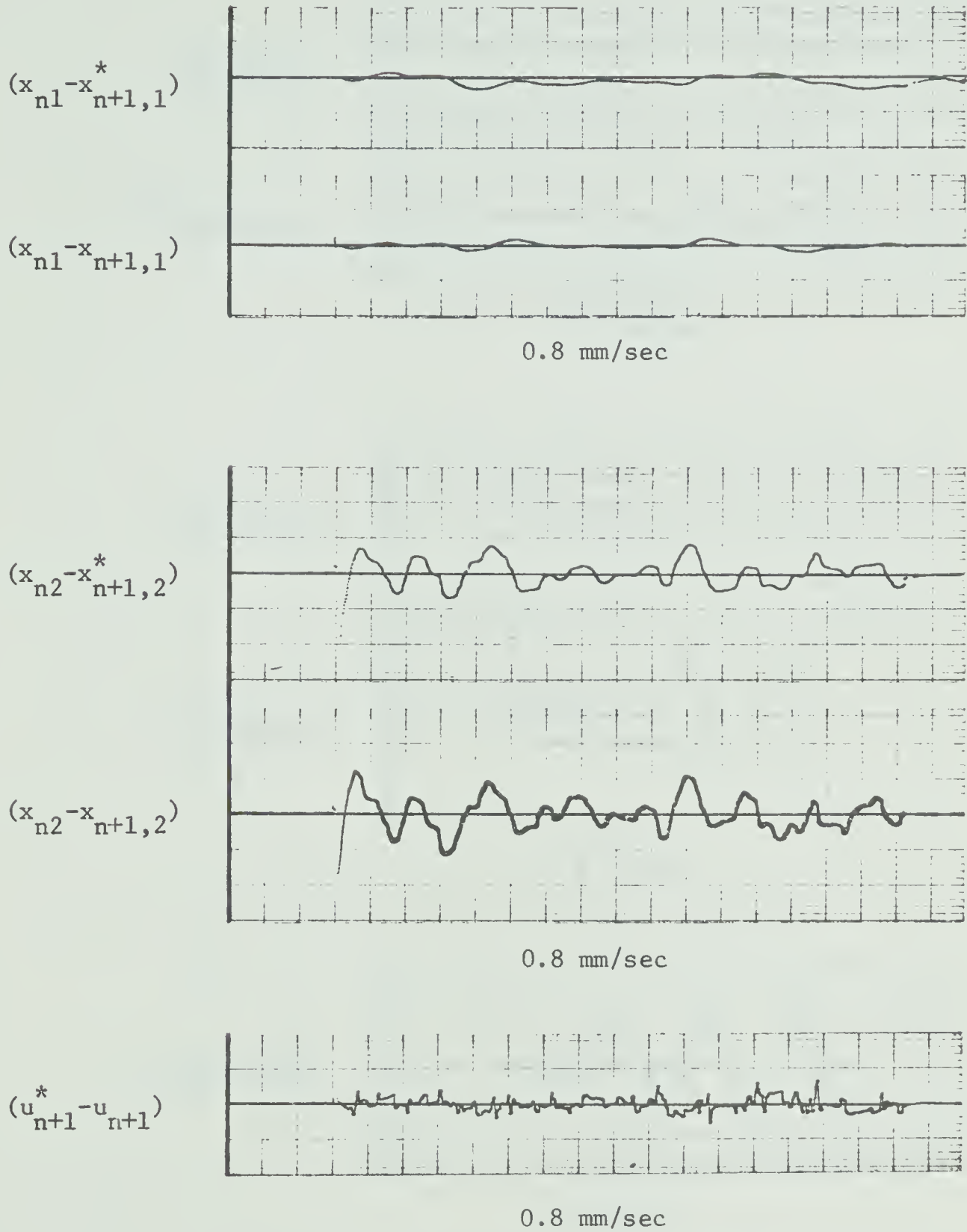


FIGURE 4.15 Operator and Optimal Controller Performance for $\phi = 2$

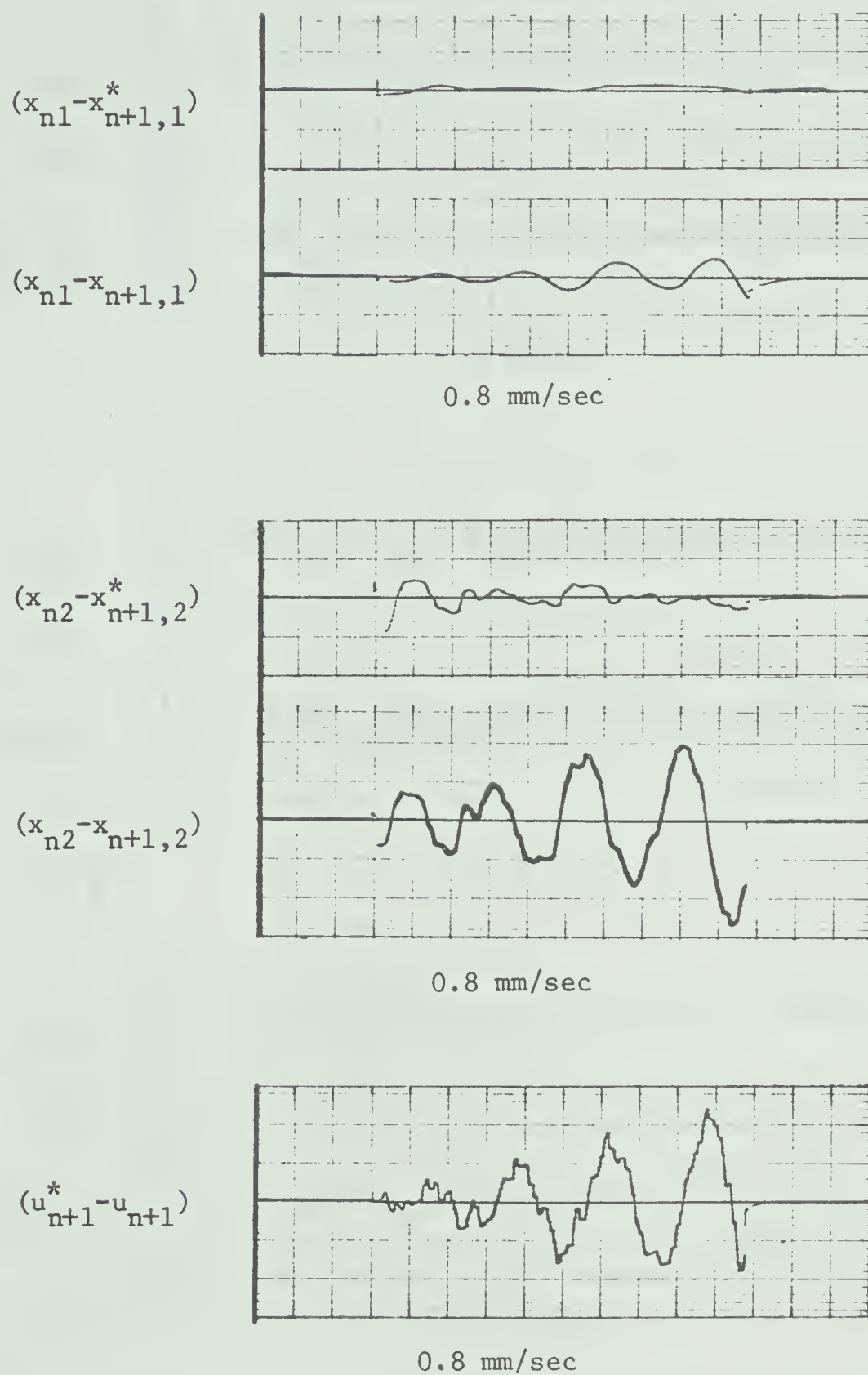


FIGURE 4.16 Operator and Optimal Controller Performance for $\phi = 16$

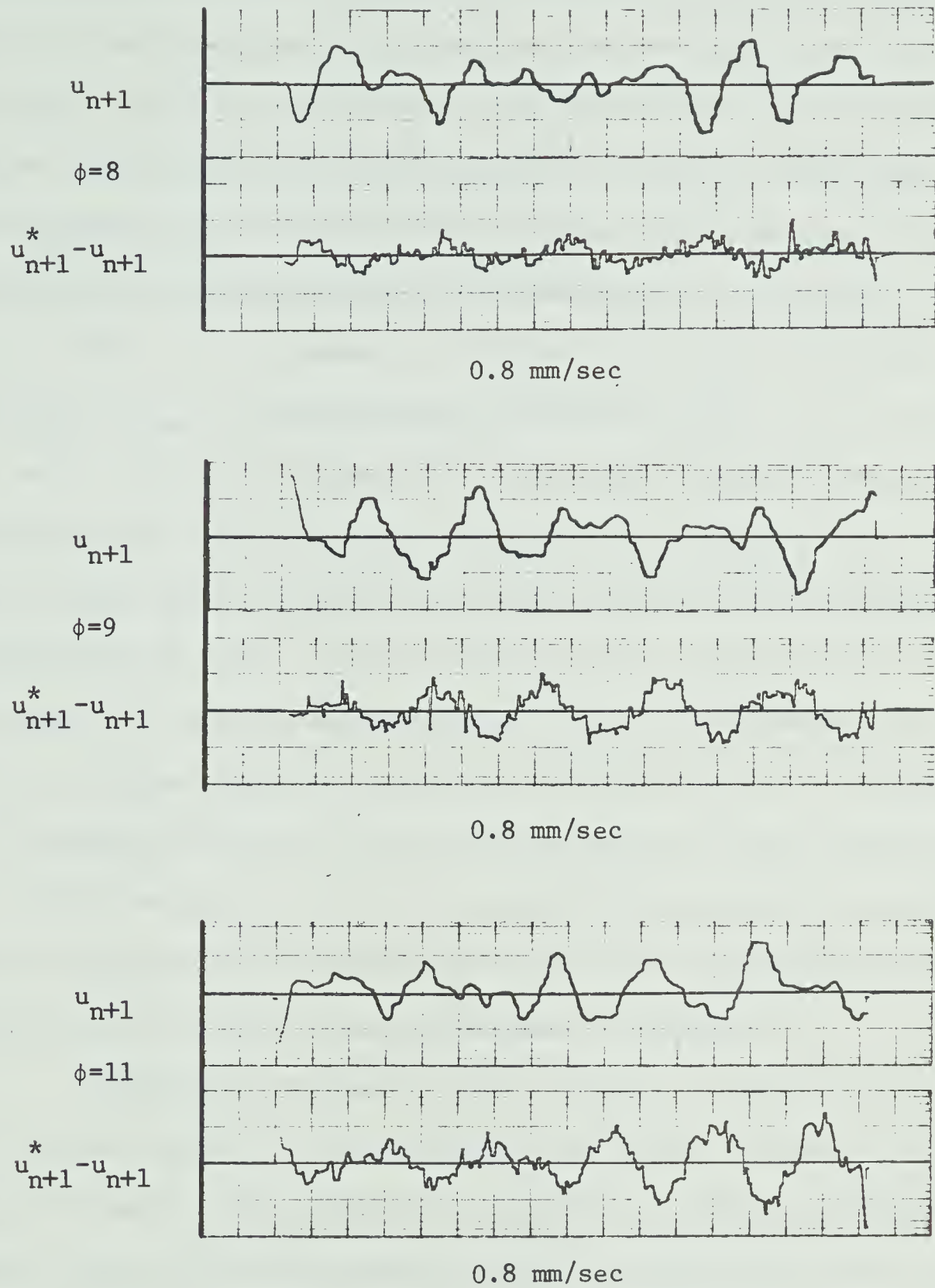


FIGURE 4.17 Control Errors as a Function of Time Near the Critical Value of ϕ

run progresses. This is because no information is supplied to the operator about the state of his vehicle. It can also be seen from this figure that the operator tracks the optimal control very closely. However, since the control of the operator's vehicle is open-loop, any variation in his control from the optimal will cause $(x_{n1} - x_{n+1,1})$, and hence the headway error, to drift from zero.

When ϕ is increased to 2 (Figure 4.15), both the headway error $(x_{n1} - x_{n+1,1})$ and the control difference $(u_{n+1}^* - u_{n+1})$ are kept near zero. For $\phi = 16$ (Figure 4.16), the vehicle-operator system is unstable and the quantities $(x_{n1} - x_{n+1,1})$, $(x_{n2} - x_{n+1,2})$ and $(u_{n+1}^* - u_{n+1})$ are in the form of sinusoidal oscillations increasing in amplitude with time. For the particular test subject used in this experiment, the system becomes unstable for $\phi > 9$ (approximately). Figure 4.17 shows $(u_{n+1}^* - u_{n+1})$ plotted vs. time for $\phi = 8, 9$ and 11. We can define the value of ϕ for which the system becomes unstable as the critical value, ϕ_c . It is to be expected that since ϕ_c is dependent to a large extent on the operator's inherent gain and time delay, variations in ϕ_c would occur from operator to operator.

Examination of Figures 4.11, 4.12 and 4.13 would indicate that the best value of ϕ for achieving near-optimal control of the operator's vehicle lies between $\phi = 2$ and $\phi = 5$. The exact value would depend on the relative importance assigned to each of the three quantities $(x_{n1} - x_{n+1,1})$, $(x_{n2} - x_{n+1,2})$ and $(u_{n+1}^* - u_{n+1})$. That is, one could write a performance index of the form

$$I = \int [\theta_1(x_{n1} - x_{n+1,1})^2 + \theta_2(x_{n2} - x_{n+1,2})^2 + \theta_3(u_{n+1}^* - u_{n+1})^2] dt \quad (4.3)$$

where θ_1 , θ_2 , and θ_3 are non-negative weighting factors. The value of ϕ chosen for a particular operator would of course have to be less than ϕ_c .

The above experiment could be repeated for a different optimal control scheme (i.e. any of those derived in Chapter 2). It could also be carried out using a three-vehicle type unit with similar results.

4.5 Proposal of a Semi-Automatic Car-Following System

In this section, a semi-automatic personal-vehicle car-following system will be proposed based on the results of the experiments reported in Sections 4.3 and 4.4. A general description of the system is as follows:

1. The vehicles are conventional automobiles with internal combustion, turbine or electric propulsion systems. Lateral control is accomplished automatically or by the human operator.
2. The vehicles would be operated in the normal manner except on special sections of roadway where steady-state longitudinal control is desirable to increase the traffic flow rate while maintaining safety of travel.
3. On the special sections, the human operator would be responsible for longitudinal control aided by some form of display (such as the meter display described previously).

From this display, augmented by his normal sense-inputs, the driver would supply a control force to the vehicle.

If the displayed information is of the form studied in Section 4.4, that is, in the case of a two-vehicle type system, the displayed information is given by Equation 4.2, then each vehicle in

the string will receive information as to the state of the vehicle directly ahead as well as its own. An on-board analogue computer calculates the error states for the two vehicles, that is, the deviations in position and velocity from scheduled values. The analogue computer also generates an optimal control with respect to a performance criterion of the form discussed in Chapter 2. This optimal control is the desired force to be applied to the vehicle in a fully-automatic system. In the proposed semi-automatic system, the difference between the optimal control and that supplied by the driver is displayed together with the difference between optimal position error and that of the operator's vehicle. The human operator thus attempts to maintain this difference equal to zero (compensatory tracking) and thus exert the optimal force on the vehicle. As in Chapter 2, the dynamics of the propulsion system are assumed negligible. At any time the driver is free to apply whatever control he desires to his vehicle. This feature enables the operator to make use of his adaptive abilities in emergency situations. Exiting and merging operations would also be handled by the driver. After leaving the special section of roadway, normal operation would resume. In this system, the driver would not necessarily be aware of the performance criterion being used. As was seen in Chapter 2, the nature of the optimal control strategy is strongly influenced by the values of the weighting factors in the cost functional. For a quadratic cost functional, the optimal control is a linear function of the vehicle states. That is, for the case of the two-vehicle system,

$$\underline{u}^*(t) = -\underline{L}^* \underline{x}^*(t) \quad (4.4)$$

The constant matrix \underline{L}^* is the matrix of optimal feedback gains corresponding to a particular cost functional. This would be built in to the on-board analogue computer and could be changed depending on the traffic conditions. For example, a roadside signalling device at the start of the special section could set the feedback gains of all vehicles as they entered the section. The choice of gains (i.e. performance criterion) would be a function of the traffic conditions and could be made by a digital computer. The driver would then supply the appropriate optimal force to his vehicle by performing a compensatory tracking task. A simplified representation of the proposed semi-automatic system is shown in Figure 4.18.

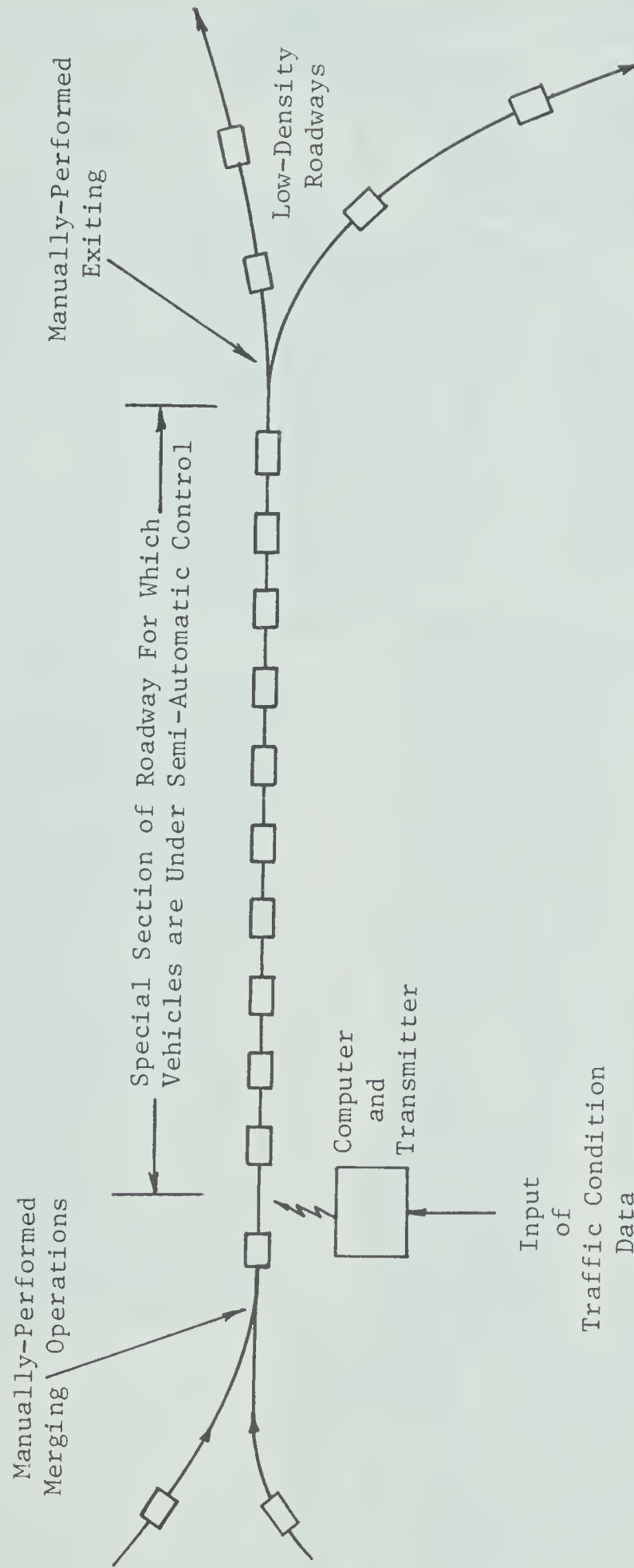


FIGURE 4.18 Diagram of Proposed Semi-Automatic Car-Following System

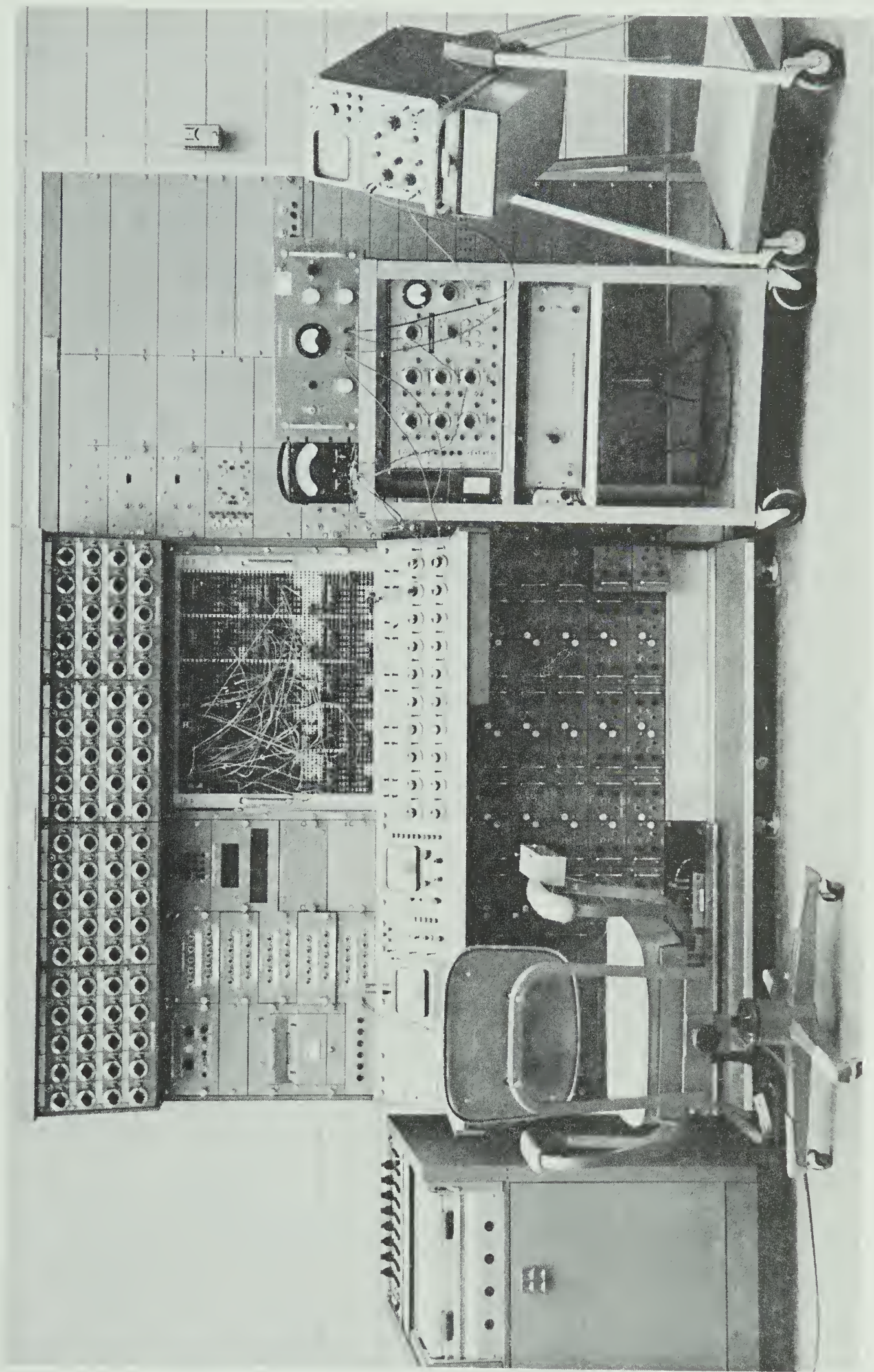


FIGURE 4.19 Overall View of Equipment Used in Tracking Experiments Reported in This Chapter

REFERENCES

1. M. Athans, "Applications of Optimal Control to High-Speed Ground Transportation Problems", Sixth Allerton Conference on Circuit and System Theory, Monticello, Ill., October 1968.
2. C.R. Kelley, "Manual and Automatic Control", John Wiley and Sons Inc., 1968.

APPENDIX 4-1

Tabulation of Experimental ResultsReported in Sections 4.3 and 4.4

Run	$\frac{1}{200} \int_0^{200} [(w-u)^2] dt$ for the indicated magnifications				
	X1	X2	X5	X10	X15
1	6.64	3.43	3.15	2.79	2.37
2	6.90	4.13	2.28	3.40	2.75
3	8.56	4.14	2.19	2.67	2.44
4	6.29	4.96	2.26	2.72	2.25
Mean	7.10	4.16	2.47	2.89	2.45

Table A4-1.1 Mean Squared Tracking Errors for Subject A
Using the KC and SD at Various Magnifications (Corresponding to Figure 4.4)

Run	$\frac{1}{200} \int_0^{200} [(w-u)^2] dt$ for the indicated magnifications				
	X1	X2	X5	X10	X15
1	11.19	4.71	4.18	2.84	2.09
2	11.06	6.54	4.12	3.00	-
3	13.78	6.11	4.17	3.35	-
4	8.19	6.63	4.87	2.95	-
Mean	11.0	6.00	4.34	3.04	2.09

Table A4-1.2 Mean Squared Tracking Errors for Subject B
Using the KC and SD at Various Magnifications (Corresponding to Figure 4.4)

Run	$\frac{1}{200} \int_0^{200} [(w-u)^2] dt$ for the indicated magnifications				
	X1	X2	X5	X10	X15
1	3.78	1.66	1.08	0.934	1.41
2	3.88	1.71	1.10	1.28	-
3	2.54	1.73	1.52	1.18	-
4	2.75	1.49	1.47	1.38	-
Mean	3.37	1.65	1.29	1.19	1.41

Table A4-1.3 Mean Squared Tracking Errors for Subject A
Using the KC and MD at Various Magnifications
(Corresponding to Figure 4.5)

Run	$\frac{1}{200} \int_0^{200} [(w-u)^2] dt$ for the indicated magnifications				
	X1	X2	X5	X10	X15
1	4.87	3.22	2.35	1.63	1.86
2	4.77	2.86	1.77	1.15	-
3	4.61	3.54	1.63	1.32	-
4	4.75	3.01	1.96	1.59	-
Mean	4.75	3.16	1.93	1.42	1.86

Table A4-1.4 Mean Squared Tracking Errors for Subject B
Using the KC and MD at Various Magnifications
(Corresponding to Figure 4.5)

Run	$\frac{1}{200} \int_0^{200} [(w-u)^2] dt$ (X2 display magnification)					
	X.15	X.2	X.3	X.5	X 1	X1.U
1	1.63	1.59	1.55	1.40	-	2.21
2	1.66	2.04	1.51	1.43	-	2.60
Mean	1.65	1.81	1.53	1.42	1.65	2.41

Table A4-1.5 Mean Squared Tracking Errors for Subject A
Using the MD and KC at Various Sensitivities
(Corresponding to Figure 4.7)

Run	$\frac{1}{200} \int_0^{200} [(w-u)^2] dt$ (X2 display magnification)			
	X.5	X1	X2	X3
1	1.25	1.35	1.36	2.10
2	1.48	1.58	1.23	2.80
Mean	1.37	1.47	1.30	2.45

Table A4-1.6 Mean Squared Tracking Errors for Subject B
Using the MD and LC at Various Sensitivities
(Corresponding to Figure 4.8)



Run	$\frac{1}{200} \int_0^{200} [(w-u)^2] dt$ for the indicated magn.				
	X1	X2	X5	X10	X15
1	4.40	1.90	1.75	1.28	0.846
2	4.23	2.24	2.04	1.28	1.21
3	4.41	2.04	1.81	1.69	1.36
4	3.99	2.06	1.80	1.37	2.30

Table A4-1.7 Mean Squared Tracking Errors for Subject B
Using the LC and MD at Various Magnifications
(Corresponding to Figure 4.9)

ϕ	$\frac{1}{100} \int_0^{100} [(\cdot)^2] dt$ for the indicated quantity				
	$X_{n1} - X_{n+1,1}$	$X_{n1} - X_{n+1,1}^*$	$X_{n2} - X_{n+1,2}$	$X_{n2} - X_{n+1,2}^*$	$U_{n+1}^* - U_{n+1}$
0	2529	3.94	0.830	0.181	7.63
	1731	6/78	0.388	0.170	6.20
	4493	8.43	2.194	0.159	8.32
	11920	3.82	3.637	0.154	6.33
2	33.0	8.91	0.394	0.161	9.28
	27.18	6.31	0.255	0.166	7.83
	11.16	4.69	0.261	0.171	6.83
	6.40	6.57	0.268	0.177	5.54
5	10.51	7.31	0.268	0.169	9.32
	13.23	5.61	0.262	0.164	11.67
	14.28	6.84	0.407	0.157	12.60
	4.03	5.74	0.270	0.179	7.97
10	32.12	4.97	2.637	0.172	39.16
	13.89	4.95	0.398	0.175	22.73
	33.95	5.15	2.565	0.361	43.30
	20.15	4.30	1.361	0.191	29.48
20	30.54	5.06	6.277	0.176	125.07
	36.70	6.75	7.521	0.164	134.63
	44.35	4.72	8.743	0.201	144.36
	21.29	4.92	3.421	0.354	89.30

Table A4-1.8 Tabulation of Experimental Results of Simulated Car-Following Experiment Reported in Section 4.4

CHAPTER 5

CONCLUSIONS AND SUGGESTIONS FOR FUTURE RESEARCH

5.1 Summary of Results and Conclusions

In Chapter 1, a review of previous research done in the areas of high-speed ground transportation systems, traffic flow models, automatic car-following systems and human operator characteristics was presented. From this review, it was apparent that a possible solution to the traffic congestion, air pollution and high accident rate now prevalent in urban areas would be the development of an automated personal-vehicle system using electric propulsion. It was shown that conventional automobile-driver traffic flow rates are limited by the inherent limitations of the human operator, namely reaction time delay and sensitivity to relative velocity variations. It was seen that a string of driver-controlled automobiles could become asymptotically unstable when the average intervehicular spacing was small. Hence it was determined that the objectives in the development of a fully-automatic car-following system must be to increase traffic flow rates as well as to increase safety of travel.

The control requirements for a personal-vehicle car-following system were also outlined in Chapter 1. Briefly, these are: the maintenance of a specified headway between adjacent vehicles, the maintenance of zero relative velocity between adjacent vehicles, the existence of local and asymptotic stability of the vehicle string and the limitation of the forces applied to each vehicle in the system.

In Chapter 2, the development of an automatic car-following system based on state-regulator theory of optimal control was presented. The state equation (equation of motion) for each vehicle was written in terms of the error state vector, that is, the difference in that vehicle's state and the scheduled state. The drag force on each vehicle was linearized about the scheduled operating velocity. Two types of car-following systems were developed - a two-vehicle type system in which each vehicle in the string bases its motion on that of the vehicle directly ahead and a three-vehicle system in which each vehicle in the string bases its motion on that of both the vehicle directly ahead and that directly behind.

For both types of systems, a performance criterion (reflecting the control requirements) was written in terms of a quadratic cost functional. In its most general form, this functional was devised to penalize the system for deviations from desired headway between vehicles, non-zero relative velocity between adjacent vehicles, the application of large forces (and hence large expenditure of control energy) to the vehicles and the deviation of all vehicle states from the desired values. For a particular cost functional, it was shown that the optimal control for each vehicle is a linear function of the vehicle states. In the case of a string based on the two-vehicle basic unit, each vehicle was found to require the feedback of velocity and position errors from the preceeding vehicle while in the case of a string based on the three-vehicle basic unit, additional feedback of velocity and position errors was required from the trailing vehicle.

The dynamic behaviour of both basic units was studied by simulating the respective optimal feedback systems on an analogue

computer. The results of these simulations indicated that the basic units exhibit local stability for all forms of the general cost functional. Generally, it was found that the weighting associated with the headway deviation term in the cost functional affects the response time bandwidth of the system while the weighting associated with the relative velocity term affects the damping factor. It was concluded that the desired dynamic behaviour for a specific application could be obtained by suitable choice of these weighting factors.

The two and three-vehicle units appeared to exhibit similar local behaviour and it was felt that the advantages of the three-vehicle design would lie in the area of string behaviour. This topic, which is closely related to that of asymptotic stability of the vehicle string, was investigated in Chapter 3. The requirement for asymptotic stability of a string of vehicles was found in terms of the frequency-domain transfer function relating the position of successive vehicles. The asymptotic stability characteristics of several "classical" feedback car-following systems were presented which indicate that these systems can be unstable for improper choice of feedback gains. For the two-vehicle optimal system it was shown that the requirement for asymptotic stability is met for all forms of the general cost functional. For the three-vehicle system, the requirement was shown to be met under steady-state conditions and string simulations indicated that this system also exhibits asymptotic stability for all forms of the general cost functional. It was shown that for the three-vehicle type system, a perturbation in the motion of a vehicle in the string causes less disturbance in the motion of the following vehicles than for the two-vehicle type system. In addition, each vehicle in the three-vehicle

type string reacts to disturbances in the motion of trailing vehicles. These two factors combine to make the three-vehicle system more desirable from the standpoint of travel safety. It was also shown that the optimal feedback system can operate satisfactorily with time delays of greater than one second in the control loop.

In Chapter 4 it was pointed out that the automatic optimal system, while exhibiting desirable characteristics, was not implementable in a one-step manner to replace the present automobile-roadway systems. Hence, it was concluded that a necessary intermediate step in automating the private automobile would be the inclusion of the human driver as a link in a feedback car-following system. By proper choice of displayed variables, it was shown that the human operator can control the longitudinal motion of a vehicle in a near-optimum manner with respect to the motion of the vehicle directly ahead.

In short, the main contributions of this thesis lie in two areas. First, it was shown that the problem of controlling the longitudinal motion of a string of personal vehicles can be solved by the application of optimal control theory. The resulting control system was found to be linear, time invariant, and to exhibit desirable local and asymptotic characteristics. Second, the feasibility of using the human operator as a link in the car-following feedback system was investigated. The preliminary results of simulated car-following experiments indicate that this is a useful concept which should be studied at greater length under actual traffic conditions.

5.2 Suggestions for Future Research

The communication system requirements imposed by the automatic and driver-controlled optimal car-following systems must be carefully

investigated in order to determine the technological feasibility of implementing such systems.

Since position sensing devices placed along the guideway will probably be discrete in nature, it would be useful to examine the performance of sampled-data optimal car-following systems corresponding to the continuous-time systems derived in this thesis. In considering the implementation of the optimal system, it would also be necessary to consider the effects of state measurement noise and vehicle nonlinearities on system performance.

An analytical study of the effects of a time delay on the performance of the optimal system would also be useful.

As previously indicated, while the experiments reported in this thesis indicate that the human operator is capable of near-optimum control of a vehicle in a simulated car-following situation, experiments under actual road conditions would have to be undertaken in order to evaluate the performance of such a system. The asymptotic stability of a string of automobiles controlled by operators in the above manner would be of prime consideration.

In the interest of safety, it would be useful to study the performance of the human operator in handling an emergency situation such as a sudden stop of the preceding vehicle.

B30007